Sapienza Università di Roma

Facoltà di Ingegneria

Dipartimento di Ingegneria Strutturale e Geotecnica

Dottorato di ricerca – XXV Ciclo

Multi-physics modelling for the safety assessment of complex structural systems under fire.

The case of high-rise buildings

Candidate: Filippo Gentili

Advisor: Prof. Franco Bontempi

Co-Advisor: Prof. Luisa Giuliani

Dissertazione presentata per il conseguimento del titolo di

Dottore di ricerca in Ingegneria delle strutture

A.A. 2011/2012

Alla mia famiglia

Acknowledgements

I would like to express my deepest gratitude to Prof. Franco Bontempi, for his indispensable scientific contribution as well as for his valuable human advices and his support.

Thanks are also due to the coordinator of Ph.D. activities Prof. Rega.

I would like to offer my special thanks to Prof. Luisa Giuliani, for the contribution given to this research and for all the support she gave me.

I wish to thank Prof. Torero (University of Edinburgh) and Prof. Kristian Hertz (Technical University of Denmark) for their valuable contribution and for the warm hospitality at their departments.

The suggestions by Professors Domenico Liberatore, Maurizio De Angelis and Luca Grossi and by Engineers Fabio Dattilo and Gianni Longobardo are gratefully acknowledged.

I thank my colleagues and friends Francesco, Pierluigi, Konstantinos, Chiara, Francesca, and Stefania for the continuous help and the friendship.

Finally, I would like to thank my family.

SYNTHESIS OF THE WORK

TABLE OF CONTENT

SYNTHESIS

ABSTRACT

Among all structures, high-rise buildings pose specific design challenges with respect of fire safety for a number of reasons, in particular the evaluation of both the fire development (fire action) and response of the structural system to fire (structural behaviour).

In relation to the fire action, large compartments and open hallways often present in modern high-rise buildings don't let themselves to be designed within compliance to current codes and standards. A comprehensive analysis of the fire environment is required to understand the fire dynamics in these cases. A Computational Fluid Dynamic (CFD) model allows a quite accurate representation of realistic fire scenarios, because it takes into account the distribution of fuel, the geometry, the occupancy of individual compartments and the temperature rise in structural elements that are located outside the tributary area of fire scenario.

In relation to the structural behaviour under fire, the passive fire resistance of structural elements and the intrinsic robustness of the system are the only measures to rely on in order to maintain the structural integrity of the building during and after the fire and avoid major economic losses due to structural failures and prolonged inoperability of the premises. Disproportionate damages induced by fire can be avoided with a proper design of the structure, aimed at reducing the vulnerability of the elements to fire (i.e. their sensitivity to fire) or at increasing the robustness of the structural system (i.e. its sensitivity to local damages).

The topic of this thesis is the evaluation of the structural safety in case of fire by means of advanced multi-physics analyses with direct reference to the modern Performance-Based Fire Design (PBFD) framework. A fundamental aspect is how some basic failure mechanisms can be triggered or modified by the presence of fire on a part of a structural system, such as three hinge mechanism, bowing effects, catenary action, thermal buckling and snap-through, sway and non-sway collapse. High rise buildings, which are expected to be susceptible to fire-induced progressive collapse, will be investigated. Critical elements will be identified in the system and countermeasure for enhancement of structural integrity will be suggested. The investigation of the response of such a

complex structures subjected to fire scenarios requires the use of CFD and Finite Element (FE) models for a realistic evaluation of the fire action and of the structural response respectively.

Figure 0.1 shows the main topics covered in the thesis.

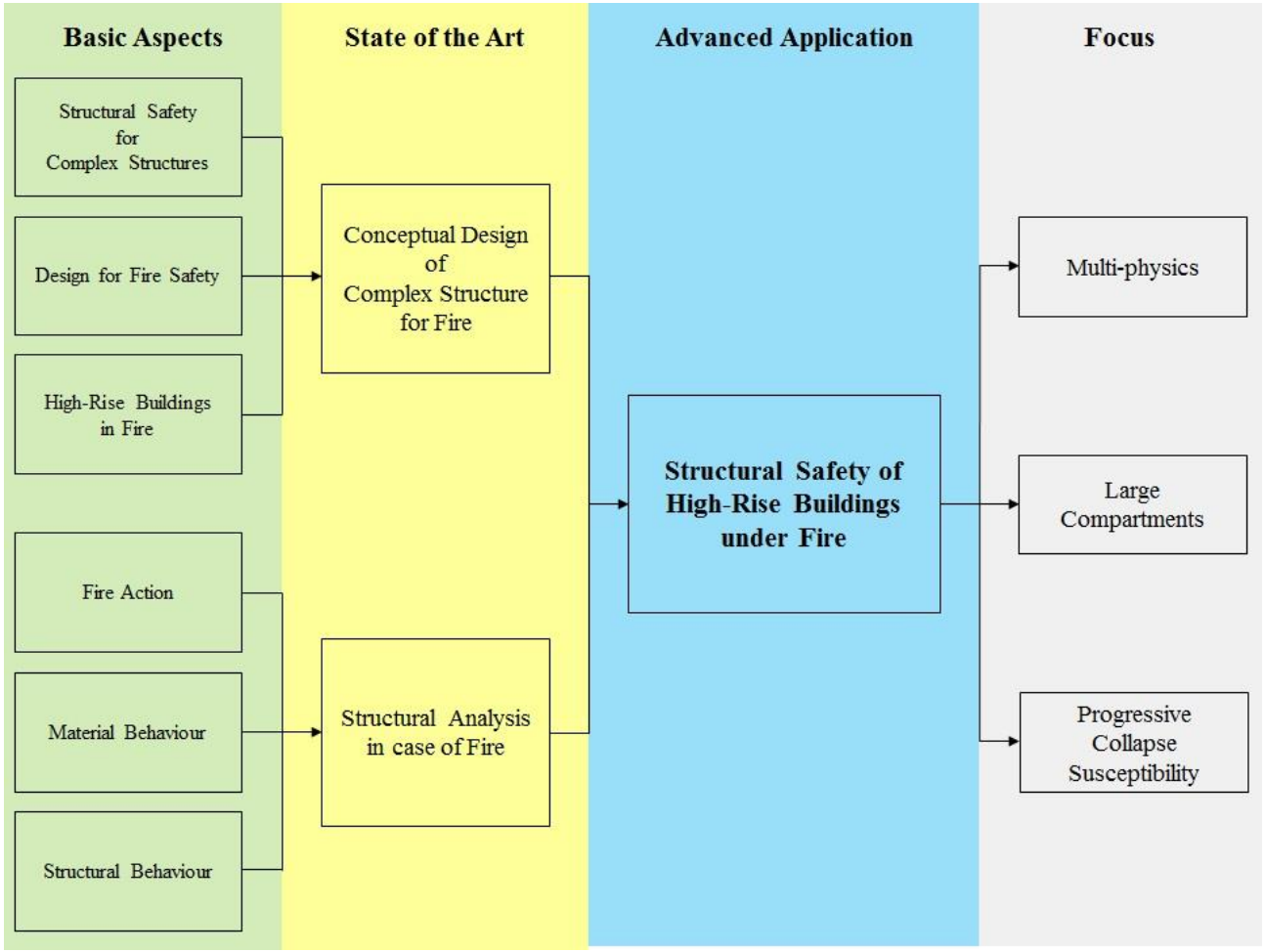

Figure 0.1 - Thesis Scheme

KEYWORDS

Structural fire safety; high-rise buildings; collapse mechanisms; hindered thermal expansion; thermal buckling; material degradation; numerical analysis; fire-induced collapse; nonlinearities; fire model; snap through; CFD modelling; steel industrial hall; fire propagation; distribution of combustible; ventilation conditions.

SELECTED PUBLICATIONS

JOURNAL PAPERS

1. Gentili F, Giuliani L, Bontempi F. *Structural response of steel high rise buildings to fire: system characteristics and failure mechanisms*, Journal of Structural Fire Engineering, in press (March 2013).
2. Gentili F, Giuliani L, Bontempi F. *Effects of combustible stacking in large compartments, Journal of Structural Fire Engineering*, in press (September 2013).
3. Gentili F. *Advanced numerical analyses for the assessment of steel structures under fire*, International Journal of Lifecycle Performance Engineering, Special Issue on Fire Safety Design and Robustness Considerations in Structural Engineering, Inderscience, in press.
4. Gentili F, Carstensen JV, Giuliani L. *Comparison of the performances of two concrete floor slabs in the case of fire*, in preparation.

CONFERENCE PAPERS

5. Gentili F, Petrini F. *Evaluation of structural risk for bridges under fire*, Proceeding of 6th International Conference On Bridge Maintenance, Safety And Management (IABMAS 2012), Stresa, Lake Maggiore, Italy, 8-12 July 2012.
6. Crosti C, Olmati P, Gentili F. *Structural response of bridges to fire after explosion*, Proceeding of 6th International Conference On Bridge Maintenance, Safety And Management (IABMAS 2012), Stresa, Lake Maggiore, Italy, 8-12 July 2012.
7. Gentili F, Giuliani L, Petrini F. *Numerical investigation of fire induced collapse of a single storey two span frame*, Proceedings of Eurosteel, 6th European Conference on Steel and Composite Structures, Budapest (Hungary), 31 August - 2 September 2011.
8. Gentili F, Grossi L, Bontempi F. *Role of CFD in the quantitative assessment of structural performance in fire scenarios*, Proceedings of Applications of Structural Fire Engineering (ASFE), Prague (Czech Republic), 29-30 April 2011.
9. Gentili F, Crosti C, Giuliani L. *Performance based investigations of structural systems under fire*, Proceedings of The Fourth International Conference on Structural Engineering, Mechanics and Computation (SEMC2010), Cape Town (South Africa), 6-8 September 2010.

ESSENTIAL LITERATURE

Arangio S & Bontempi F. Basis of the analysis and design for fire-induced collapses in structures. *International Journal Lifecycle Performance Engineering*, 2012.

Buchanan A H. *Structural Design for Fire Safety.* Chichester (England), Wiley, 2002.

Drysdale D. *An Introduction to Fire Dynamics.* 2nd ed. Chichester, West Sussex, England, Wiley, 1999.

Duthinh D, McGrattan K & Khashkia A. Recent advances in fire-structure analysis. *Fire Safety Journal,* 43(2), pp. 161-167, 2008.

Franssen JM, Kodur V & Zaharia R. *Designing steel structures for fire safety.* London: CRC Press, 2009.

Giuliani L & Budny I. Different design approaches to structural fire safety. *International Journal Life-Cycle Performance Engineering*, 2012.

Hertz KD. Parametric Fires for Structural Design. *Journal of Fire Technology,* 2001.

ISO/TR 13387-1. *Fire safety engineering - Part 1: Application of fire performance concepts to design objectives,* 1999.

La Malfa A & La Malfa S. *Approccio ingegneristico alla sicurezza antincendio (in Italian).* 5th ed., Legislazione Tecnica, 2009.

Moss P, Dhakal R, Bong M. & Buchanan, AH. Design of steel portal frame buildings for fire safety. *Journal of Constructional Steel Research Research,* Volume 65, pp. 1216-1224, 2009.

Petrini F. Performance-based fire design of complex structures. *International Journal Life-Cycle Performance Engineering,* 2012.

Petterson, O, Magnusson SE & Thor J. *Fire Engineering design of steel structures.* Sweden: Bulletin 52, 1976.

Purkiss, JA. *Fire Safety Engineering Design of Structures.* Burlington (USA), Butterworth-Heinemann, 2007.

Rein Guillermo, Zhang Xun, Williams Paul, Hume Ben & Heise Alex. *Multi-storey fire analysis for high-rise buildings.* London, 11th Interflam, 2007

Starrosek U. *Progressive Collapse of Structures.* London: Thomas Telford Publishing, 2009.

Usmani A, Chung Y & Torero J. How did the WTC collapse: a new theory. *Fire Safety Journal,* 38(6), 2003.

Vassart O, Cajot LG, Franssen JeanMarc, O'Connor M & Zhao B. *3D simulation of industrial hall in case of fire. Benchmark between ABAQUS, ANSYS and SAFIR.* Edinburgh, 10th International Fire Science & Engineering Conference INTERFLAM, 2004.

INTRODUCTION

1. STRUCTURAL SAFETY OF HIGH-RISE BUILDINGS UNDER FIRE

Chapter 1

1. STRUCTURAL SAFETY OF HIGH-RISE BUILDINGS UNDER FIRE

1.1. FIRE SAFETY STRATEGIES

Structural integrity of buildings and safety of people in urban areas have been often endangered in the past by malevolent or accidental fires. Fires cause many hundreds of deaths and millions of dollars of property loss each year (Hall, 2011). Unfortunately, fires can occur in almost any kind of building, often when least expected. The safety of the occupants depends on many factors in the design and construction of buildings, including the expectation that certain buildings and parts of buildings will not collapse in a fire or allow the fire to spread (Buchanan, 2002).

Fire safety engineering can be defined as the application of scientific and engineering principles to the effects of the fire in order to reduce the loss of life and damage to property by quantifying the risks and hazards involved and provide an optimal solution to the application of preventive or protective measures (Purkiss, 2007).

Fire safety is a rapidly expanding multi-disciplinary research topic. It requires the integration of many different fields of science and engineering (Buchanan, 2002).

The objectives of the fire safety strategies are to limit to acceptable levels the probability of death, injury and property loss. The balance between life safety and property protection varies in different countries, depending on the type of building and its occupancy.

In order to contrast an exceptional action as fire, different strategies are possible:

a) reduce the probability that the action occurs or reduce its intensity, implementing specific measures of event control, such as forbidding smoke and storage of combustible material in premises, shutting down electric equipment during the night or when the premises are not used, etc. (prevention);

b) reduce the effects of the action on the structure e.g. by installing a sprinkler system or by changing the properties of the fire compartment, so that the fire will be milder or shorter (protection);
c) avoid or reduce the damages that may be caused on the structural system by the fire, by insulating the elements or by increasing the dimension or the mechanical properties of their section or material resistance;
d) reduce the effects of a local damage, by reducing the susceptibility of the structure to progressive collapse (mitigation) (Crosti, et al., 2012).

With the term prevention it is intended measures aimed at reducing the possibility of the occurrence of the event, while the term protection is referred to measures aimed at limiting the damage resulting from fire. The latter can be active (all the measures that are taken in order to obtain extinguish fire during its initial phase) and passive (the set of measures that are taken in order to minimize damage building during fire generalized). Of course, their effectiveness is shown at different times during the evolution of fire.

Prevention (strategy a) concerns the limitation of ignition sources, the training and information of staff and customers and the compliance with specific regulation on systems. The strategies a) and b) are based on non-structural measures. Active protective measures include both the use of technological systems, such as automatic detection systems, alarm systems, smoke, ordinary extinguishing systems (hydrants and fire extinguishers), automatic extinguishing systems (sprinklers) and the adoption of decisions planning and appropriate organizational planning that makes it quick and safe evacuation of the building and the timely intervention of rescue teams.

The strategies c) and d) are structural measures, also called passive protection measures. The c) provides for a nominal behaviour and reversible under the action of the structure, while d) allow the development of local crises and proportional to the intensity of the fire: this positive correlation between effect (damage) and cause (fire) is linked the requirement of structural strength.

The passive protection is achieved through the consideration of three main aspects:

- Reaction to fire which depends on the characteristics of combustibility and flammability of materials used.
- Fire Resistance. Mainly, it is estimated by the *stability or load-bearing capacity R* (capacity of the structure or of a steel member to withstand the specific actions), the *integrity E* (capacity of the elements of separation to prevent the passage of hot gases or the ignition

beyond the exposed surface), *the thermal insulation I* (capacity of a member of separation to prevent excessive transmission of heat).

– Compartmentalization. The compartment is realized through the use of elements of predetermined resistance to fire and allows achieving some of the goals of safety such as the limitation of the maximum area involved by the fire, the reduction of the impact on structures, the separation of the spaces, the isolation of the hazard, the protection of the escape routes.

Figure 1.1 summarizes the main possible strategies against fire in relation with the evolution in time.

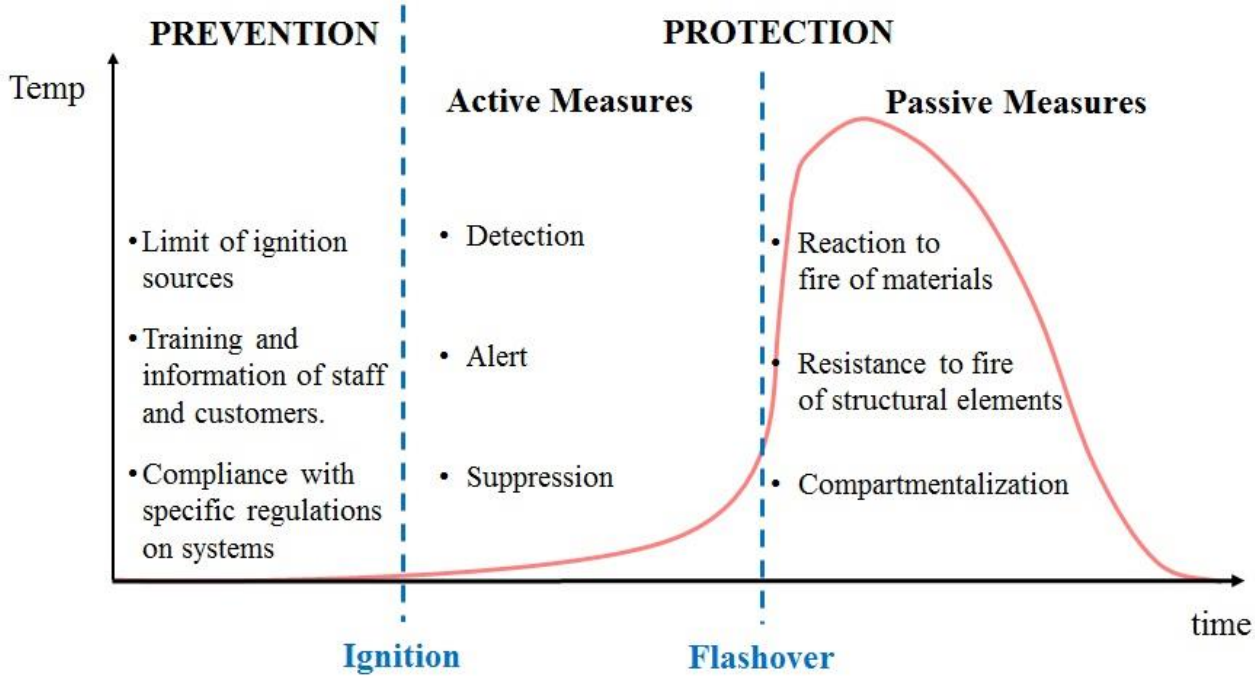

Figure 1.1 - Strategies against fire during the evolution of the fire.

Robustness is the last barrier before the structural collapse. Under some circumstances, the passive fire resistance of structural elements and the intrinsic robustness of the system are the only measures to rely on, in order to maintain the structural integrity of the building during and after the fire and avoid major economic losses and additional casualties due to collapsing members (Franssen, et al., 2009). Figure 1.2 shows a tree of events that emphasizes the role played by the robustness in the safety assessment.

1.2. AIM OF THE THESIS

The topic of the thesis is the structural safety of a high-rise building in case of fire. In order to highlight some of peculiar aspects of the fire design of high-rise buildings, the work is subdivided into three sections (Figure 1.3).

In the first section, attention is paid to the following ideas:

- a high-rise building is a complex structure, with consequences thereof. Given the high economic impact that would result from an eventual collapse of the structure, it is not sufficient to ensure the safety of people, but large damage to structures should be avoided as the collapse of the structure represent an unacceptable economic loss;
- the evaluation of structural safety of a complex structure, such as a high-rise building, can be consistently implemented in framework focused on a global vision of the structural system as the dependability;
- fire is considered in the Eurocodes with the framework of the accidental situation design together with other Low-Probability High-Consequences (LP-HC) actions (Arangio & Bontempi, 2012) such as explosions, and impacts. The classic semi-probabilistic approach used in standard conditions is not suitable for this type of events. Different strategies are possible in order to prevent or mitigate the effects of the event (exposure), to prevent or mitigate the effects of the action (vulnerability) prevent or mitigate of the effects of the damage (progressive collapse susceptibility);
- the prescriptive approach is often not suitable for high-rise building, because it require to comply with limitations on the geometry, materials, size of the premises, etc., that are far from the design needs and from the real layout of tall building. The advance in technology of the past few decades has led to the use of innovative materials that did not exist at the time these regulations were formed. In addition, new architectural requirements push towards the presence of atria and open spaces, which require on one side the use of longer and lighter elements and on the other side implies additional difficulties in the prediction of the fire development.

The second section of the thesis wants to underline some aspects related to the structural analysis in case of fire. Three essential models for calculating the structural fire behaviour are discussed: a fire model for the study of the fire development, a heat transfer model for the assessment of the internal temperature of the elements, and a structural model for evaluating the structure load bearing capacity, which takes the temperatures obtained from the heat transfer

model as input. For each of the three problems (design fire, heat transfer, structural response), different levels of simplification are possible.

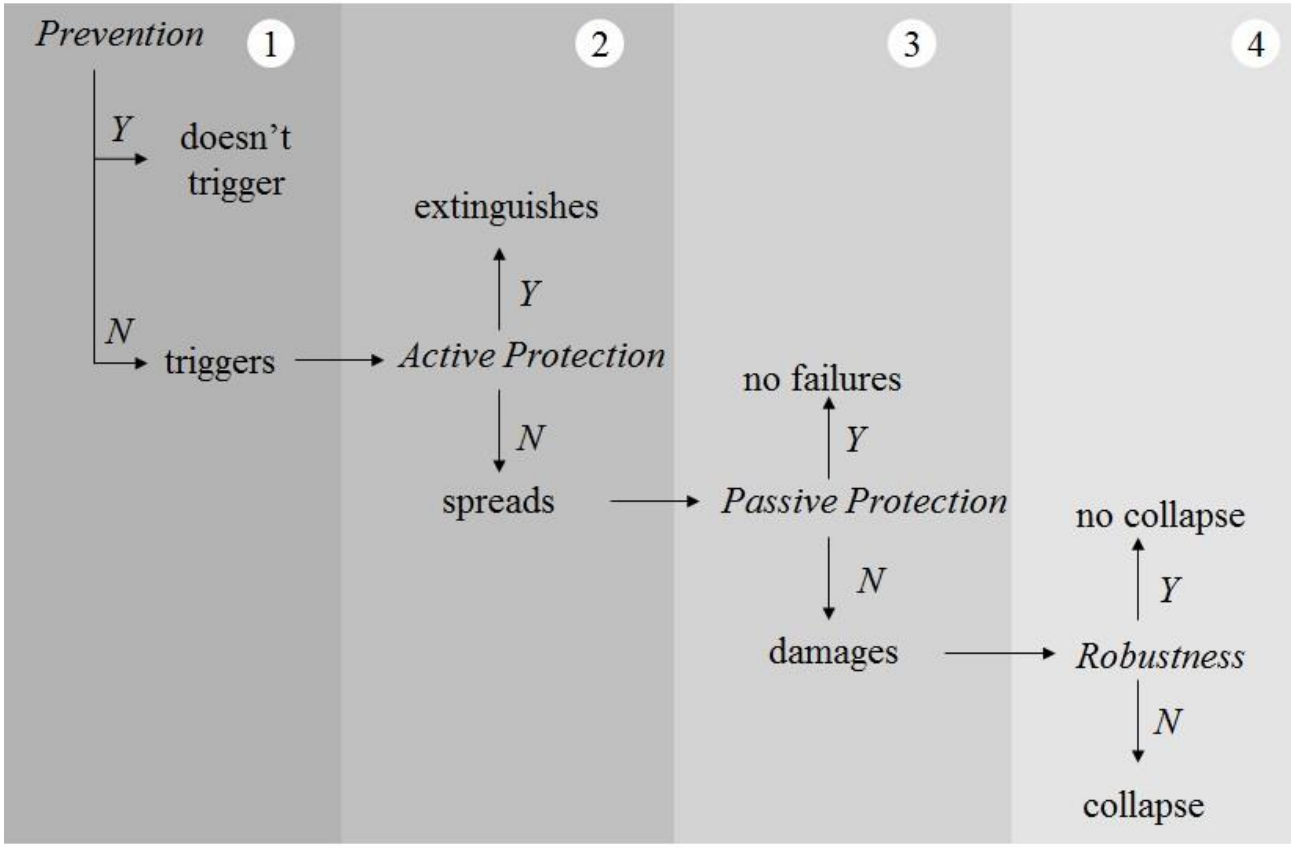

Figure 1.2 - Effectiveness of measures against fire (Giuliani, 2011)

With regard to the definition of a design fire for example, the simplest model is represented by monotonically increasing curves that refer to the post-flashover phases. This model is used for a given required time of resistance (nominal curves). When the level of detail increases, characteristics related to the fuel (fuel load) and to the compartment (ventilation and thermal inertia of the enclosure) can be taken into account (parametric curves). Finally CFD simulations represent the most advanced solution, capable of accounting for possible modification of the ventilation or of other fire properties during the fire, as well as of modelling both the pre and post-flashover phase. The modelling of the fire with a parametric curve may not be sufficiently adequate for large compartments, where the occurrence of flashover is not frequent and the distribution of the combustible is not uniform, being large spaces generally less densely furnished than small rooms. The study of the degradation of the material and the behaviour of some simple structural elements under fire provides a preliminary idea on the possible failure mechanisms found in a structure.

The third section of the thesis shows three applications for emphasizing the following issues:

- the study of the mechanical response to the fire of a single storey steel structure showed that: i) a reliable evaluation of collapse mechanisms requires the consideration of the full three-dimensional structure; ii) since the deformed configuration of the structure under fire must be investigated, an efficient numerical algorithm is needed for solving the finite element problem; iii) the interaction of the heated elements with the rest of the structure can trigger different mechanisms of collapse depending on the mutual position of the elements; iv) the natural fire approach represents the most conducive solution in order to evaluate realistic fire scenarios. The results show the need to conduct multi-physics analysis when the structure presents reasons of complexity;
- large compartments often represent a challenge for structural fire safety, because of lack of prescriptive rules to follow and difficulties of taking into account the effect of non uniform distribution of the combustible materials and of the fire propagation. These aspects are discussed with reference to an industrial steel building taken as case study. Fires triggered by the burning of wooden pallets stored in the premises are investigated with respect to different stacking configurations of the pallets with the avail of a CFD code. The results in term of temperatures of the hot gasses and of the steel elements composing the structural system are compared with simplified analytical model of localized and post-flashover fires, with the aim of highlighting limitations and potentialities of different modelling approaches;
- the response of a steel high rise building is investigated up to the crisis of the structure with respect to a standard fire in a lower and in a higher storey: the comparison of the failures induced by a fire triggered at the different heights in the building allows highlighting the role played in the collapse by the beam-column stiffness ratio and a possible propagation of the initial failures to zones of the structure not directly involved in the fire. It has to be pointed out that the focus of this study is on the behaviour of the steel components. The investigations take into account a full nonlinear response of the structure, influenced by material degradation at high temperatures, possibility of buckling, large displacements and deformations and exploitation of plastic reserve by the elements. In the presentation of the performed investigations and in the discussion of the outcomes, a focus is done on methodological aspects concerning the definition of fire scenarios and collapse criteria, the modelling of substructure and the identification of failure modes. Critical elements will be identified in the system and countermeasure for enhancement of structural integrity will be suggested.

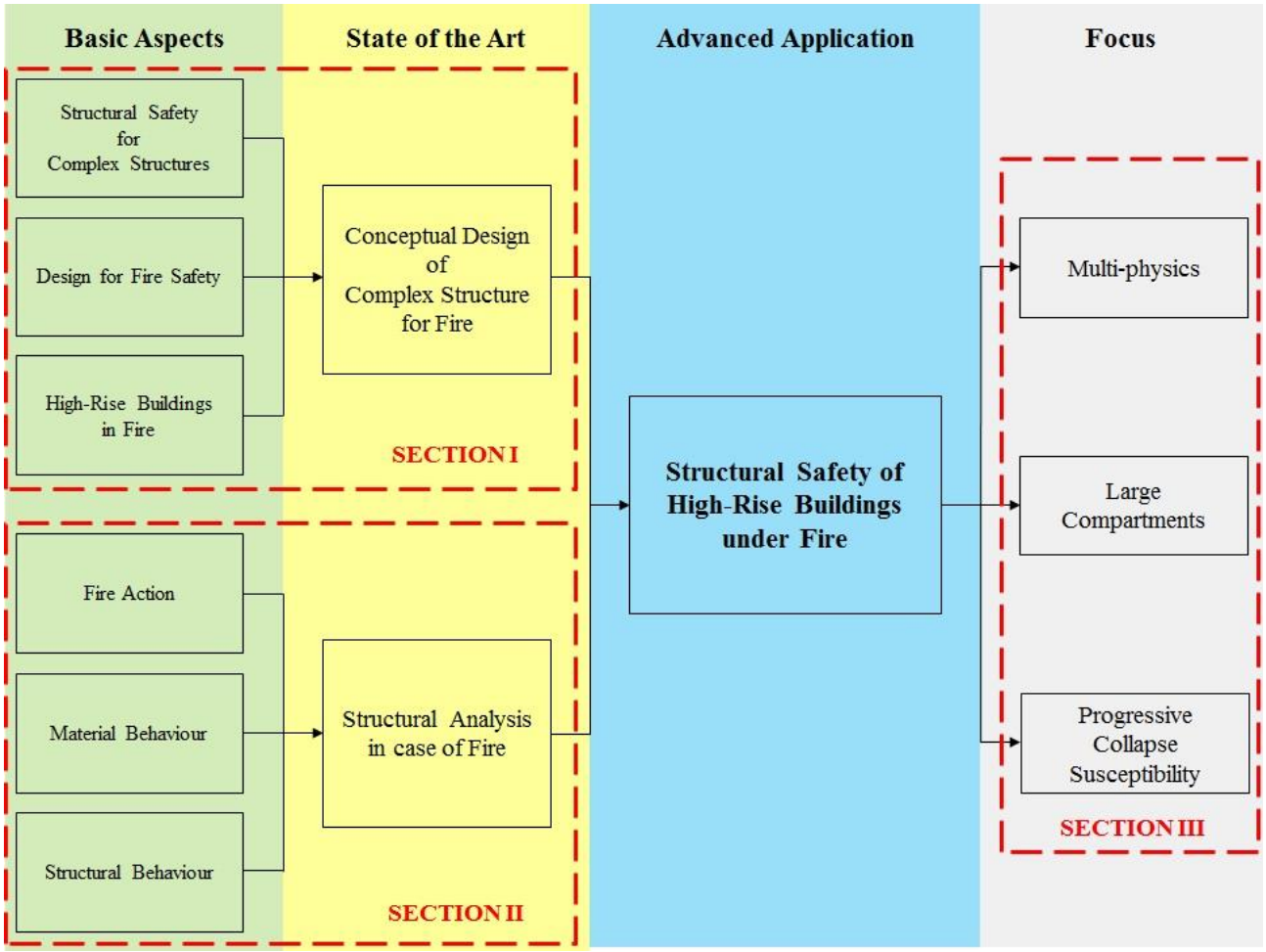

Figure 1.3 - Thesis Scheme

SECTION 1:

COMPLEX STRUCTURES IN FIRE

2. STRUCTURAL SAFETY
3. DESIGN FOR FIRE SAFETY
4. HIGH-RISE BUILDINGS IN FIRE

Chapter 2

2. STRUCTURAL SAFETY

2.1. ESSENTIAL REQUIREMENTS OF CONSTRUCTIONS

In Europe, the Directive 89/106/CEE (Construction of European Community, 1988) has set the essential requirements for construction. This code, concerning the products used in the construction of buildings and civil engineering works, was abrogated in 2011 and replaced by Regulation 305-2011 (Construction of European Community, 2011). The requirements must, for a construction subject to normal maintenance, be satisfied for an economically reasonable working life. The requirements generally concern actions which are foreseeable.

The essential requirements are:

- *Mechanical resistance and stability*

The construction works must be designed and built in such a way that the loadings that are liable to act on it during its constructions and use will not lead to collapse of the whole or part of the work, to major deformations to an inadmissible degree, to damage to other parts of the works or to fittings or installed equipment as a result of major deformation of the load-bearing construction or to damage by an event to an extent disproportionate to the original cause.

- *Safety in case of fire*

The construction works must be designed and built in such a way that, in the event of an outbreak of fire, the load-bearing capacity of the construction can be assumed for a specific period of time, the generation and spread of fire and smoke within the works are limited, the spread of the fire to neighbouring construction works is limited, occupants can leave the works and the safety of rescue teams is taken into consideration.

- *Hygiene, health and the environment*

The construction work must be designed and built in such a way that it will not be a threat to the hygiene or health of the occupants or neighbours.

- *Safety in use*

The construction work must be designed and built in such a way that it does not present unacceptable risks of accidents in service or in operation such as slipping, falling, collision, burns, electrocution, injury from explosion.

- *Protection against noise*

The construction works must be designed and built in such a way that noise perceived by the occupants or people nearby is kept down to a level that will not threaten their health and will allow them to sleep, rest and work in satisfactory conditions.

- *Energy economy and heat retention*

The construction works and its heating, cooling and ventilation installations must be designed and built in such a way that the amount of energy required in use shall be low, having regard to the climatic conditions of the location and the occupants.

2.2. STRUCTURAL SAFETY

Safety is an important topic in structural engineering. It includes protection of people (SIA 260 Building Code, 1982) and of properties (ISO/FDIS 2394, 1988).

The first code states that: *A structure can be declared safe if during a critical event, such as impact, fire, downfall, safety of people assured*, while the latter states that: *Structures and structural elements should be designed, built and maintained in such a way as to serve properly and economically their intended use during their design life. Particularly they should satisfy, with proper levels of reliability: i) serviceability state requirements, ii) ultimate load state requirements, iii) structural integrity requirements*.

2.3. STRUCTURAL REQUIREMENTS

The "EN 1990: Basis of structural design" (EN 1990, 2002) provides comprehensive information and guidance on the principles and requirements for safety, serviceability and durability that are normally necessary to consider in the design of buildings and civil engineering structures.

The EN 1990 affirms that the structures and structural elements should be designed, built and maintained in such a way that they fulfil their function during the whole life of exercise or project

and in economic way. For this purpose the structures and structural elements must comply with the following structural requirements (Figure 2.1).

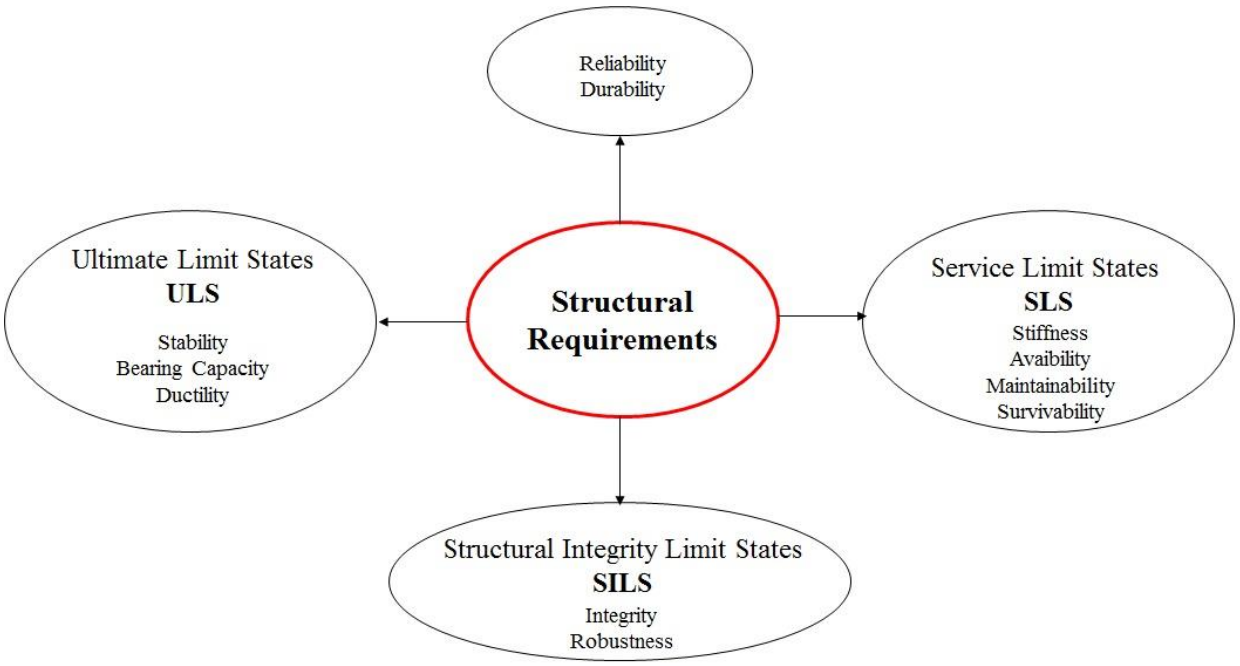

Figure 2.1 – Structural requirements

Some of these such as reliability and durability must be evaluated for each limit state, the others refer to specific states limits.

- Durability

It is the ability of a structure of not maintaining the required safety level in time. This requirement may be taken into account in the following ways: i) using materials which, if well maintained, do not degrade their physical and mechanical properties during the life of the project (routine maintenance); ii) increasing the size of the elements constituting the structure, so as to compensate for the degradation during the life of the project; iii) do not adopt any special measure on the element design, but provide for their replacement during the design life of the entire structure, in accordance to a maintenance plan defined beforehand; iv) providing appropriate levels of inspections and maintenances, at given time points (extraordinary maintenance).

- Reliability

According to (ISO/FDIS 2394, 1988), it is the ability of a structure or structural element to fulfil the specified requirements, including the working-life, for which it has been designed. It represents the grade of confidence on the structure with respect to environmental or human actions and can be quantitatively measured as the probability that structural failures don't occur during the required

service life. The reliability of a structural system is obtained from the reliability of each structural element that constitutes the system. A logical assessment defines which and how many and elements should work properly in order to ensure a correct performance of the structure for its entire service life. The purpose of this requirement is to introduce a safety factor which is a function of the dispersion of the values of resistance (R) and those of stress (S). The comparison between these distributions indicates what the probability that R> S (Catallo, 2005).

2.3.1. Serviceability state requirements

The requirements related to the functional efficiency are taken into account by means of the verification of an appropriate number of serviceability limit states (SLS). The serviceability limit states correspond to conditions beyond which the specific service requirements for a structure or a structural element are no longer met. The functional efficiency is the ability of the structure to provide adequate performance for its entire nominal life (Arangio, et al., 2010).

The focus is mainly on:

- the operation of the constructed works or any part thereof;
- personal comfort;
- the aesthetics of the structure.

The serviceability performances of the structural system are related to the following aspects:

- Stiffness

It represents the ability that a structure has to counteract to the deformations imposed by a load level content.

- Availability

It is intended as readiness for correct serviceability. This is a very important property for structures with varied serviceability levels (e.g. a long span bridge).

- Survivability

It is intended as the ability of the structural system to provide basic services in presence of a failure. It is particularly important for critical infrastructures and for special structures such as military constructions, power generation plants, etc.

- Maintainability

It is the ability to undergo repairs and modifications. It can be intended as the ease taken for the maintenance, to be performed in accordance with prescribed requirements.

2.3.2. Ultimate load state requirements

These requirements are related to the mechanical efficiency and are taken into account in the design phase by means of the verification of an appropriate number of ultimate limit states (ULS). The ultimate limit states correspond to conditions beyond which the specific resistance requirements for a structure or a structural element are no longer met. These performances relate mainly to (Crosti, 2011):

- Stability

It is the capacity of a compression member or element to remain in position and support load, even if forced slightly out of line or position by an added lateral force. In the elastic range, removal of the added lateral force would result in a return to the prior loaded position, unless the disturbance causes yielding to commence (Galambos, 1998) .

- Bearing capacity or resistance

It represents the maximum reaction that a given structural entity is able to oppose, before reaching the collapse, to an increase external load acting on it.

- Ductility

It is the ability of a structure, or part of it, to offer a suitable degree of resistance beyond the domain of elastic response.

2.3.3. Structural integrity requirements

- Integrity

It refers to the absence of structural failure. This requirement concerns therefore the structural state, in the sense that the maximum grade of structural integrity is related to the nominal configuration of the structure, i.e. the undamaged one. In the design phase, it is taken into account by means of the verification of an appropriate number of structural integrity limit states (SILS). A recent Italian code (Ministero delle Infrastrutture e dei Trasporti, 2005) explicitly require considering the structure also in a damaged configuration, where a lack of structural elements can for any reason reduce the integrity level of the system.

- Robustness

According to (EN 1991-1-7, 2006), the robustness is the ability of a structure to withstand actions due to fires, explosions, impacts or consequences of human errors, without suffering damages disproportionate to the triggering causes. In a robust structure the damage remains bounded in a limited portion of the structure and the entity of the collapse is proportional to the initial failed

elements directly affected by the accidental actions. Several qualitative definition of the term robustness can be found in literature and regulations: It is defined as the structural insensitivity to local failure by SEI (2007) and Starrosek (2008). According to this definition, the structural robustness is a property that does not depends on the particular triggering cause, but is inherent to the structural system. According to Faber (2007) the robustness is defined as the ratio between the indirect and direct consequences of an action. Hence, robustness could be increased also by reducing the exposure of the structure (i.e. reducing the probability for the structure of being affected by a potentially damaging event) or its vulnerability (i.e. the probability for the structure of being damaged by a force acting on the some structural elements as a consequence of the critical event) (Giuliani, 2008).

2.4. COMPLEX STRUCTURAL SYSTEMS

The complexity of a structural system may be related to the type of behaviour and the coupling level of different parts that compose it. In this perspective, Perrow (1984) proposes a matrix having on one axis the behaviour and on other the coupling (Figure 2.2).

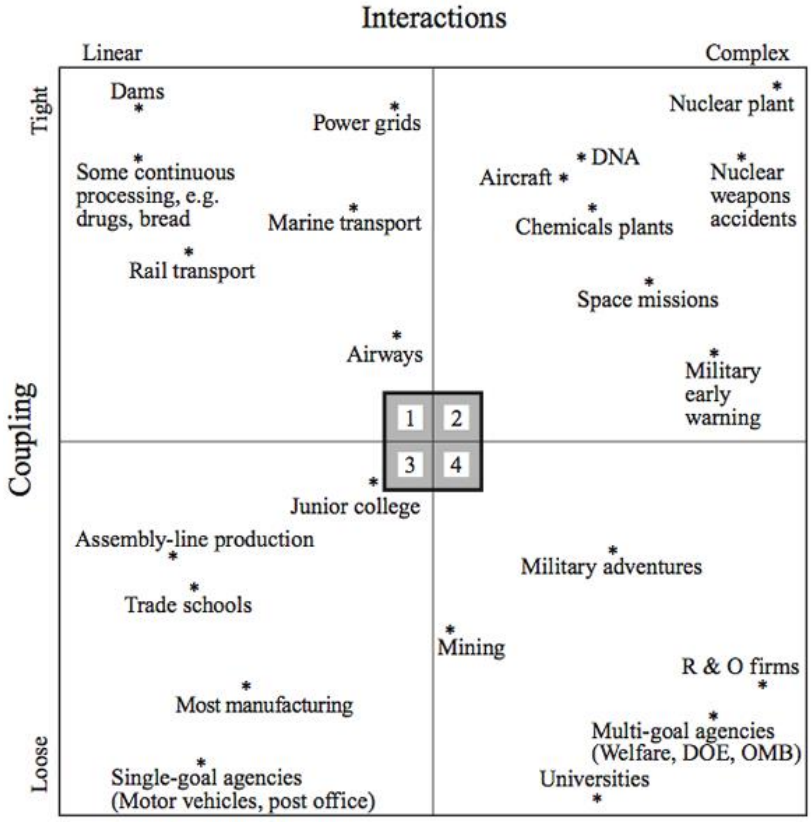

Figure 2.2 - Structural complexity (Perrow, 1984)

The intrinsic behaviour of parts (and then the whole system) can be linear or nonlinear. Parts can have slack among them or tight couplings; the degree of coupling reflects both the time factor (how quickly changes are propagated) as well the extent of propagation (the grade of interdependence). Simple systems are characterized by linear behaviour and loose couplings, while complex systems have nonlinear behaviour and tightly couplings.

In addition, the role of uncertainty must be taken into account. Generally the complex structures are characterized by the high level of uncertainty of some parameters.

2.5. PERFORMANCE-BASED DESIGN

The Performance-Based Design (PBD) is a modern approach that allows designers to consistently take into account all the aspects related to the serviceability and safety of both existing and new structures without enforcing any limitation to the available design solutions. PBD has been mainly formalized and specialized for earthquake engineering applications. Extensions to other design situations, like blast (Hamburger & Whittaker, 2003), wind (Petrini & Ciampoli, 2011), tsunami (Riggs , et al., 2008) scenarios, have been recently proposed. PBD is practically required in case of complex structures due to the fact that prescriptive approach is inadequate in dealing with non-ordinary configurations.

In general, a PBD approach must consider the whole life-cycle of the structural system (SEAOC, 1995). It is possible schematizing the PBD approach for complex structures in two main steps:

- Conceptual organization of the design

The first step regards: i) the qualitative definition of the performance requirements (generally related with structural safety, serviceability and robustness); ii) the conceptual organization of the structural system in its different parts and their reciprocal connections and, iii) the individuation of the acting hazards and their intensities. At this stage, the performances requirements and limit states have to be taken into account in defining a suitable initial design configuration and in discriminating unfeasible configurations that are expected to being not able to fulfil the performance requirements. This task is particularly challenging for two reasons: i) the main choices in this preliminary design are essentially founded on the personal expertise of the designer and on the historical cases regarding similar structures; ii) in case of complex structures, mechanisms for stress transmissions and stiffness couplings between different structural elements and/or structural parts are really complex to predict, especially for safety of robustness evaluations. A suitable tool to

govern the complexities arising in carrying out this phase is given from the structural system decomposition, represented by the design activities related with the classification and the identification of the structural system components, and by the hierarchies (and the interactions) between these components.

- Performance investigation of a structural design configuration

After an initial structural design configuration has been defined in elements and in its system behaviour and the performance requirements, the quantitative definitions of some structural performance indicators and the respective limit states need to be carried out. The structural performance indicators are proper response parameters that have to be quantified under different loads with various intensities; the attaining of fixed thresholds for these parameters defines the limit states of the related performance, while the overcrossing of these thresholds is assumed as the failure in fulfilling the performance requirements. The different limit states are usually associated with so-called damage states expressed in terms of proper damage parameters, which can be also assumed as structural performance indicators. The performances of the structural configuration must be quantified and eventually optimized by exploring alternative design configurations. Traditionally, two main philosophies can be adopted in assessing the performance: i) Probabilistic approach, or ii) Heuristic approach. The probabilistic approach is usually feasible in case of performances investigation of structural configurations and actions whose can be statistically characterized by the avail of databases with a satisfying amount of data, while the heuristic approach may be preferable when the designer must deal with accidental actions and/or structures with raw statistical data (Petrini, in press).

Figure 2.3 shows a diagram of multi-level code format, that many countries have adopted.

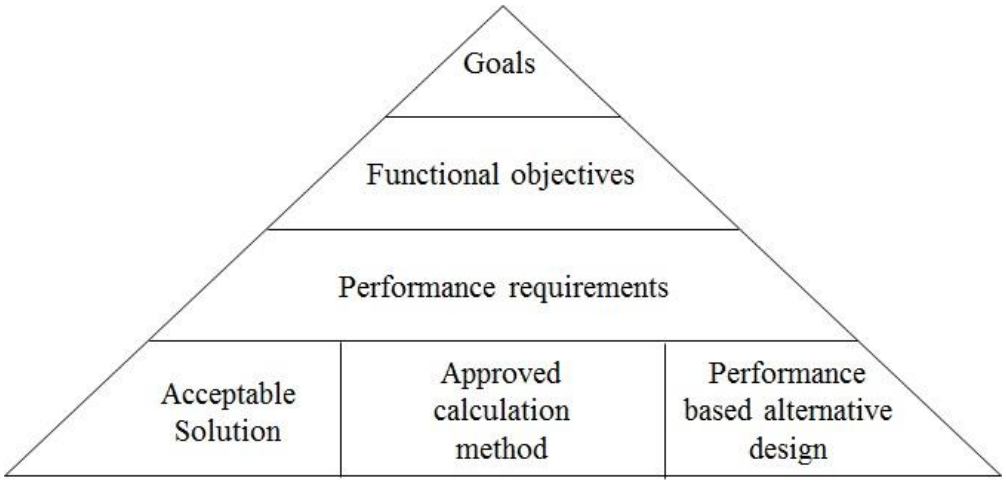

Figure 2.3 - Hierarchical relationship for performance-based design (Buchanan, 2002).

At the highest levels, there is legislation specifying the overall goals, functional objectives and required performance which must be achieved in all buildings. At the lower level, there are three common means of achieving those goals: a prescriptive acceptable solution, an approved standard calculation method or a performance-based design.

2.6. STRUCTURAL DEPENDABILITY

For complex structural systems, or large scale projects where there are significant dependencies between elements or sub-systems, it is important to have a solid knowledge on how the system works as a whole, and on how the elements behave singularly. The goal is to achieve established limits of the acceptable service and safety levels. Therefore, it becomes important to define a global concept that groups the relevant attributes together. Dependability can be defined as the collective term used to describe the availability performance and its influencing factors. The dependability of a system can be defined as the grade of confidence on the safety and on the performance of a structural system. This is a qualitative definition that has been originally developed in the field of Computer Science (Avižienis, et al., 2004).

The structural dependability can be described by dividing it in three different conceptual blocks: the first group concerns the requirements presented above, that are referred as dependability attributes; the second group concerns the external or internal threats that can mine the dependability of the structure; the third group eventually includes the dependability means, i.e. the strategies and methods that can be followed in order to achieve and maintain a dependable system.

The threats for system dependability are faults (defects or anomalies in the system behaviour that represents a potential cause of error), errors (the cause for the system being in an incorrect state) and failures (permanent interruption of the system ability to perform a required function under specified operating conditions).

The means for dependability assurance embrace different strategies and methods. Particularly, it seems useful to distinguish between the prevention and the presumption of the possible threats. In the first case the aim is to avoid the occurrence of threats that may cause damage in the structure, in the second case instead these threats are assumed possible and the consequences on the structure are investigated.

Arangio (2012) relates the aspects introduced above with the concept of dependability as Figure 2.4 shows.

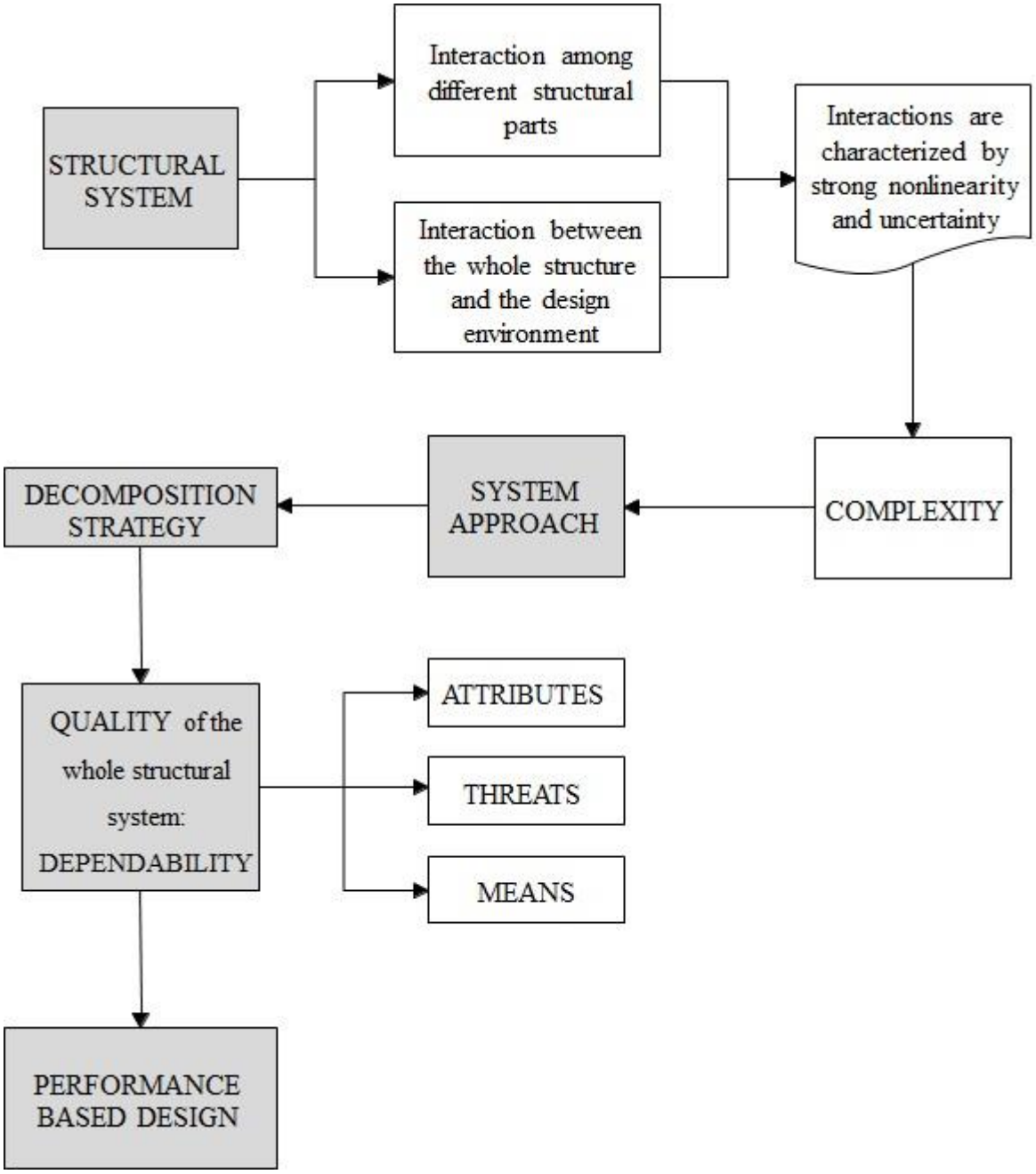

Figure 2.4 - Roadmap for the analysis and design of complex structural systems (Arangio, 2012)

Chapter 3

3. DESIGN FOR FIRE SAFETY

3.1. SAFETY IN CASE OF FIRE

The Interpretative Document No. 2 (The Council of the European Communities, 1994) related to Council Directive 89/106/EEC (Construction of European Community, 1988) provides an explanation of the second essential requirement of the construction concerning the safety in case of fire.

As mentioned in the previous chapter, great attention is paid to the following aspects:

- Load-bearing capacity of the construction for a specific period of time

The stability of the main structure provides for the safety of the occupants, increases the safety of rescue teams and fire-fighters, guards against collapse of a building, causing injury to people, and allows the construction products involved in fire safety to carry out their functions for the necessary time. The required period of stability, usually expressed in terms of conventional fire resistance times, depends on the goals of regulators.

- Limitation of generation and spread of fire and smoke within the construction works

The prevention of the initial ignition and the limitation of spread of fire within and then beyond the room of origin allow retarding the speed of fire development and spread of fire and smoke in the works so as to enable occupants near and/or remote from the origin of fire to have sufficient time to escape and the fire brigade/rescue teams to control the fire before it has grown too large.

- Limitation of spread of fire to neighbouring construction works

The problem of fire spread between construction works which are entirely separate, as in buildings facing each other across a street for example and of fire spread between different construction works joined together, but with a fire-separating wall between them has to be considered through limitation of radiation, through the limitation of radiation, the control of the penetration of the fire to the inside of the building and using fire resistant materials.

- Evacuation of occupants

The goal can be achieved through design of escape routes in order to ensure safe evacuation of occupants to a place of safety, separation of escape routes from the surroundings by means of fire and smoke-separating elements, smoke control measures, limitation of fire and smoke generation from wall and ceiling linings and floor coverings in escape routes.

- Safety of rescue teams

The resistance time of the construction must take into account the time necessary to work of the rescue teams with a reasonable level of safety through such measures as the design of access/space for fire-fighting appliances outside/inside the building, water supply installations serving fire safety installations and fire-fighting or safety staircases.

3.2. THE SUBSYSTEMS OF THE DESIGN

Fire safety must take into account three different aspects such as building and fire people that are interrelated and influence one another (Figure 3.1).

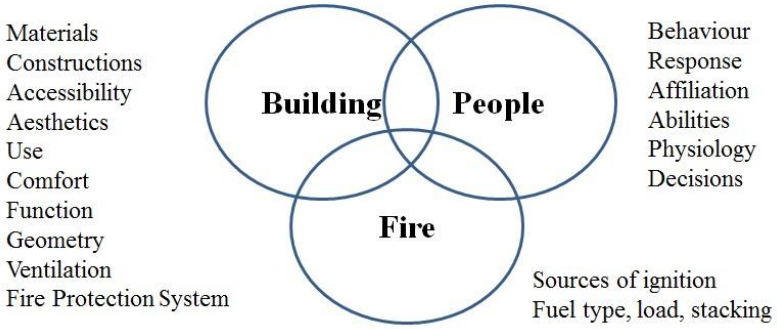

Figure 3.1 - Building life safety design framework related to fire event adapted from (Alvarez & Meacham, 2010)

Given the complexity of the problem, ISO/TR 13387-1 (1999) proposes the division of fire safety design in some separate components of the systems. Arangio & Bontempi (2012) adapt the approach in the Figure 3.2

- SS0 - Design constraints and possibilities (blue),
- SS1 / SS2 - Action definition and development (red),
- SS3 / SS4 - Passive system and active response (yellow),
- SS5 / … SS9 - Safety and performance (purple).

Specifically:

A. Design is connected with parameters that can be considered fixed (SS0a) and others that are modifiable (SS0b);

B. Action is modelled both at the beginning (SS1) and during its development (SS2);

C. System response originates both from passive characteristics (SS3) and active measures (SS4);

D. Safety is related fundamentally with human life (SS5); after that, performance can be progressively associated with loss of property (SS6), interruption of business (SS7), contamination of the environment (SS8) and destruction of heritage (SS9).

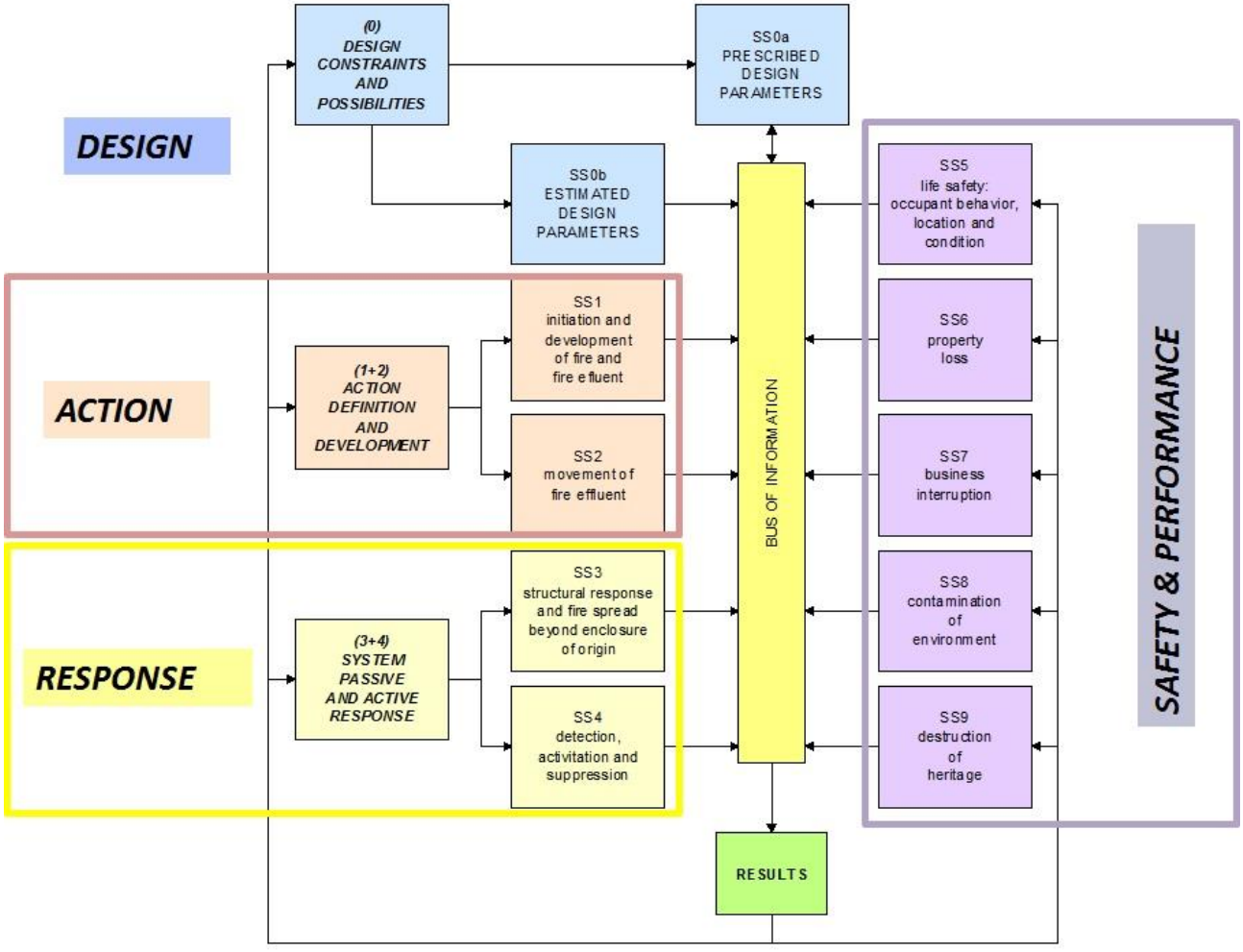

Figure 3.2 - General framework of analysis of fire safety (Arangio & Bontempi, 2012)

In the central part of the chart of Figure 3.2 there is a yellow rectangle that symbolizes the crossing point of information arising from the various parts From this sort of bus of information (in the Computer Science language), the various results are collected and the decisions are taken in a

performance-based design framework (Petrini, 2012; Gentili et al, 2010). Of course, iterative corrections are not only possible but often necessary; various lines of feedback connect the items that can be modified.

3.3. SAFETY STRATEGIES AGAINST EXTREME ACTIONS

A structure can experience during its design life two kind of events:

- High Probability – Low Consequences (HPLC) events, where small releases of energy, a small numbers of breakdowns and only a few people are involved;
- Low Probability – High Consequences (LPHC) events, which generally involve very large releases of energy, large numbers of breakdown and large numbers of people.

Natural events (like storm, earthquakes…) characterized by usual return period of return belong to the first class of events while accidental events fit in the second class (Handling Exceptions in Structural Engineering, 2008). Terroristic attacks, too, are intended to be in the right place in this second class.

HPLC and LPHC events have generally very different characteristics both from the design and the analysis point of view. From the codes or standard point of view, design loads were determined on the basis of frequent to rare values of the actions, depending on the limit state considered. Very severe values of the actions were disregarded, being associated to very low probability of occurrence. Design situations connected with HPLC events are well established and usually founded on probabilistic or semi-probabilistic based safety formats (ISO/FDIS 2394, 1988).

Looking at the example in Figure 3.3 (Bontempi, et al., 2009), the verification can be carried out at a global level (called 4^{th} level in the Figure), at the level of the single structural element (3^{rd} level), on the section of the element (2^{nd} level), and at the material level (1^{st} level). For each level appropriate methods and tools are available. Level 1 corresponds to the allowable stresses verification, Level 2 and Level 3 correspond to the classical limit state checks, Level 4 is required for such an assessment of the robustness of the structure.

For HPLC, the check of a structure is usually conducted with a conceptual disaggregation of the structure itself, considering an element by element procedure (EN 1990, 2002) and this type of approach seems reasonable and, effectively, has conducted over the years to the realization of large part of the constructions. Recent very large or very impressive structural failures have posed some doubts about the applicability of this approach, not only in case of innovative concepts, as defined

above, but also in structures facing LPHC events (Starrosek, 2009). In all these situations, it is not more satisfactorily to consider the structure as simply composed by elements, but it is required to deal with the whole structure characterized as a system, with cooperative and emergent behaviours.

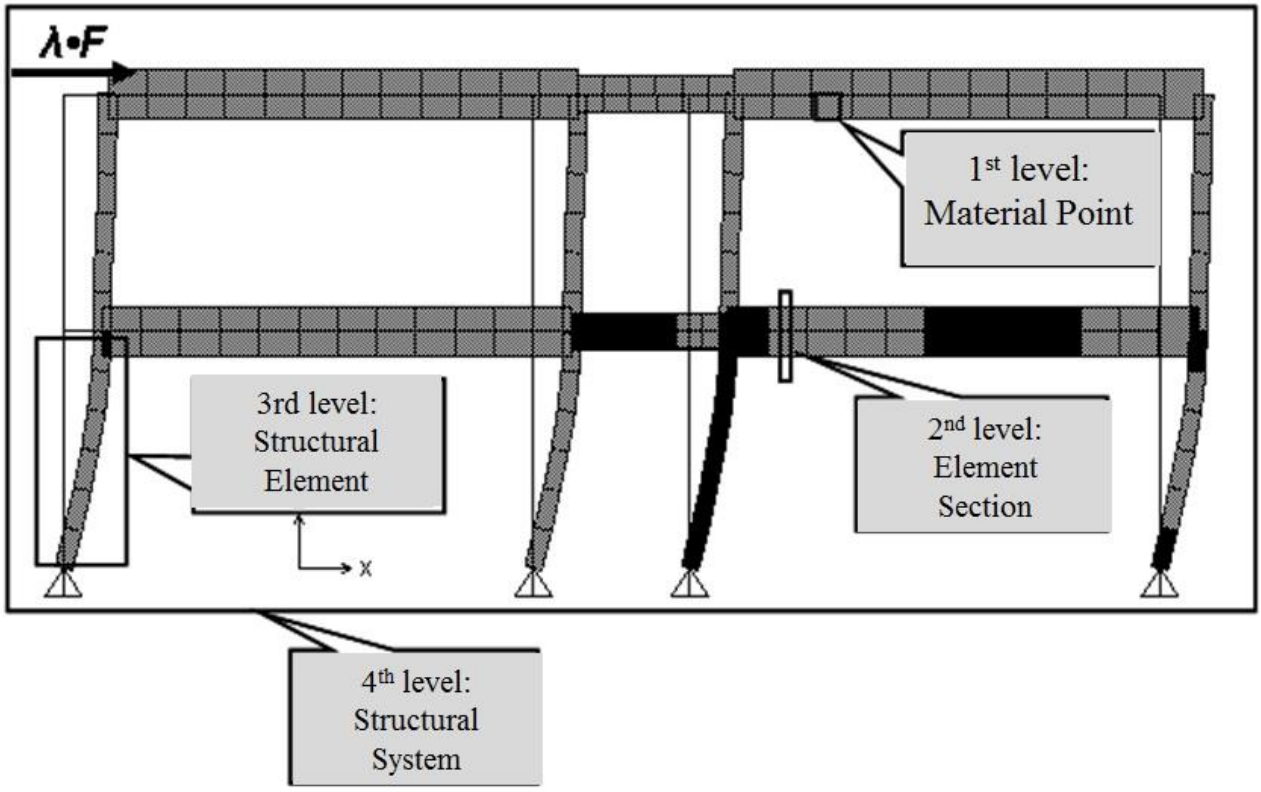

Figure 3.3 – Level of check (Bontempi, et al., 2009)

To start solving the structural problem, in the case of possible LPHC events, Arangio & Bontempi (2012) consider Figure 3.4.

Here, it is represented, in an ideal form, the possible problem framework as function of the complexity of the problem itself (Perrow, 1984). Of course, problem complexity increases passing from usual to innovative designs but it also in-creases passing from HPLC to LPHC events. This appears clear when one thinks that, by definition, HPLC events are frequently observed (and then statistically describable), being LPHC events only rarely experienced and, above all, more variable in nature.

As shown in Figure 3.4, one can adopt two different frameworks to solve the problem:

- a deterministic approach;
- a stochastic approach.

It means that with the first approach one fixes all the aspects of the problem in a definite way, while with the second approach one allows some stochastic to enter in the description.

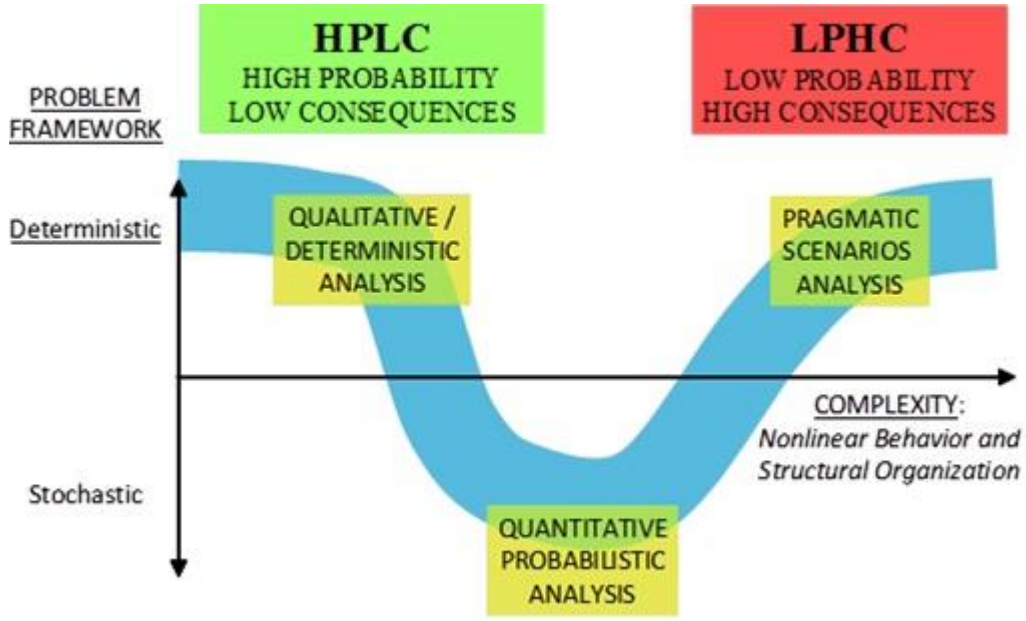

Figure 3.4 - HPLC vs. LPHC situations and corresponding analysis strategies (Arangio & Bontempi, 2012)

Now, one recognizes essentially three regions:

- the first one is a region connected with low complexity, i.e. temporary designs or HPLC events, where even direct qualitative analysis finds place; usually, here, true deterministic analysis are conducted;
- the second region is found where the complexity of the problem has grown and aspects of the problem can be usefully considered adding stochastic in the formulation;
- finally, it appears that as the complexity of the problem has reached some critical size, the only way to face and to solve the problem is turning back to some ad-hoc deterministic approach; it means that, with an act of force, the problem is posed and solved by the so-called heuristic way of thinking.

When an unexpected or critical event occurs, the consequences of this event on a structure can be classified in the following three groups:

- the extreme action associated to the event hits the structure;
- the structure is damaged in the area directly affected by the action;
- the local damage causes failures of the other structural elements and leads to the collapse of a significant part of the structure.

For each of these groups, (Giuliani, 2012) identifies a classification of strategies to increase safety. The aim of design strategies can be:

- prevention or mitigation of the effects of the event (increase collapse resistance);
- prevention or mitigation of the effects of the action (increase structural integrity);
- prevention or mitigation of the effects of the damage (increase structural robustness).

Figure 3.5 summarizes these possibilities.

The first aim is the most general one and this could be accomplished by trying to avoid the critical event whenever possible (e.g. by means of deterrence or other security measures against malevolent attacks) or by reducing the exposure of the construction to the extreme action associated to the event (e.g. by moving the location of the premises or protecting the structural system with physical barriers).

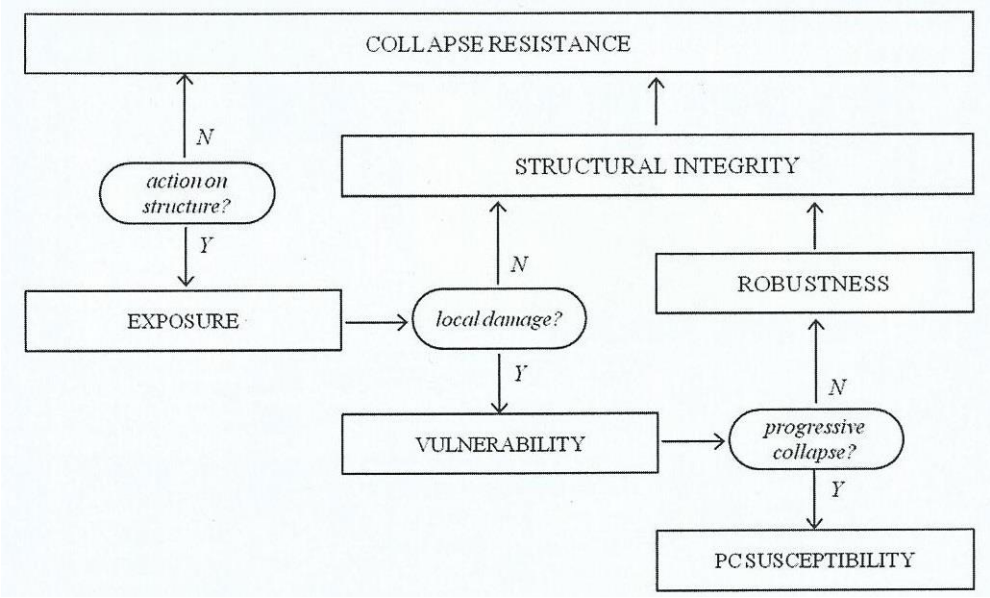

Figure 3.5 - Strategies for safety against extreme events and corresponding requirements (Giuliani, 2012)

In relation to the second group, the structure should be made less vulnerable to the action by increasing the specific local resistance of the single elements (by increasing their section or using a more resistant material), as well as by favouring a higher redistribution of stresses among the elements (redundancy), so that the action won't determine the overloading and failure of elements directly to it. The easiness of triggering damage in a system is referred to structural vulnerability, according to the definitions given by Faber (2006) and used in Giuliani (2008). It is related both to structural choices and characteristic of the action.

In relation to the third aim, the reduction of the sensitivity or the structural system to local failures is referred to the progressive collapse susceptibility and in this case the robustness doesn't depend on the action, but only on the structural system.

3.4. ENGINEERING METHODS

ISO/TR 13387-1 (1999) considers four types of analysis procedures:

- Simple calculation;
- Computer-based deterministic analysis;
- Probabilistic studies;
- Experimental methods.

3.4.1. Deterministic design

Deterministic procedures exist to quantify ignition, fire growth, flame spread, the movement of combustion products, the movement of people, the reaction to fire and effect on fire of building systems and features, and the consequences of fire for the building and its occupants. A deterministic study using comparative criteria will generally require far fewer data and resources than a probabilistic approach and is likely to be the simplest means of arriving at a design solution.

The treatment of uncertainty is usually conducted through several safety factors in a conservative approach

3.4.2. Probabilistic design

Probabilistic procedures are based on fire incident and field survey data, as well as a variety of techniques for producing best subjective estimates. These procedures are based on the following basic principles:

- Risk

Risk is considered simply as the product between extent of negative consequences and probability of occurrences

Arangio & Bontempi (2012) synthesize in Figure 3.6 from an engineering point of view all the activities connected to risk. Fundamentally, one has different actions related to risk, nested one inside the other, which can be arranged from the more specific to the broader one in the following order:

- Risk Analysis;
- Risk Assessment;
- Risk Management.

The last one, Risk Management defines the Context of the engineering enterprise, covering the social, individual, political, organizational, and technological features; develops the Risk Assessment; decides the Risk Treatment, meaning what to do in terms of risk; there are four possibilities: avoidance, reduction, transfer and acceptance.

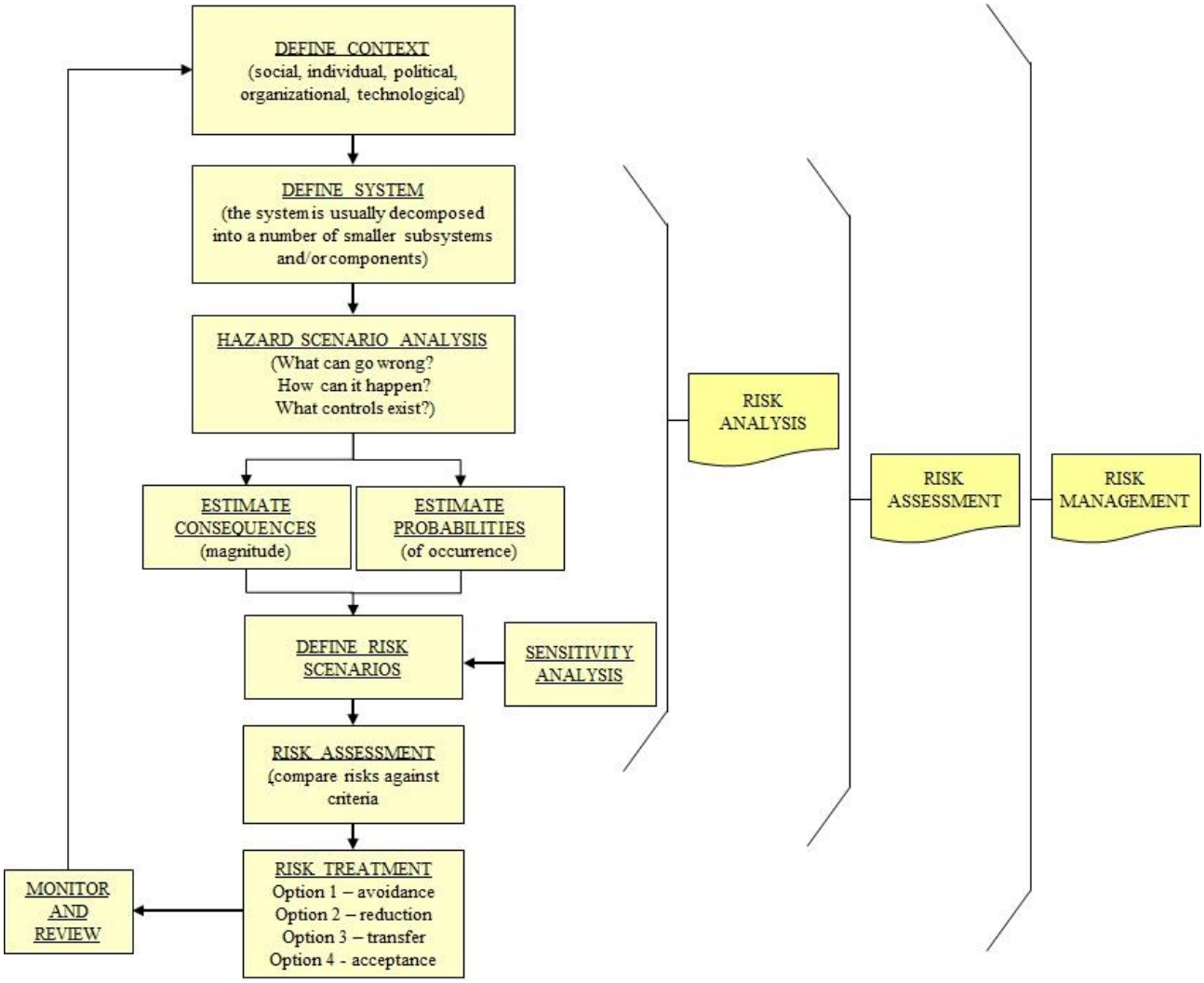

Figure 3.6 - Risk and relevant processes (Arangio & Bontempi, 2012)

Risk Assessment is the part specifically devoted to the judgment of the risk in comparison with specified criteria or in relation with historical cases: by the way, in the case of Fire Safety, just case histories are a strong source of knowledge. The phase of risk assessment puts the qualitative and the quantitative basis for the decisions to be taken to treat risk.

The engine of the whole process is anyway Risk Analyis. Here: i) one defines the system and its boundary; the system is usually decomposed in smaller subsystems or parts easily to be described; ii) for the system identified in this way, one develops the hazard scenarios analysis that recognizes which negative events can happen; iii) the qualitative aspects of the previous point are quantitatively fixed by estimating the consequences (magnitudes), and the probabilities of occurrences.

The intrinsic nature of LPHC events, discussed in paragraph 3.3, usually leads to deterministic problem solving approaches, strongly undermines the possibility of developing accurate risk analyses because they necessitate the computation of the probability of occurrence. Practically, as explained before, this part must be reverted to a heuristic assessment. Even if the probabilistic part of the analyses mentioned in Figure 3.6 is not easily applicable in the case of fire risk, it is widely accepted that the general framework proposed in the plot is a useful tool for describing the activities connected to fire risk because it is able to clearly point out all the necessary aspects of the problem.

- Fire Safety Concepts Tree

A useful tool for fire hazard and consequence analysis is the fire safety concepts tree. It is a graphical representation of the deliberations and professional judgments of the NFPA Technical Committee on Systems Concepts for Fire Protection in Structures, and represents one way in which building fire safety can be viewed. It is divided into two primary branches, “prevent fire ignition” and “manage fire impact,” with the concept being that one or the other must be accomplished in order to meet one’s fire safety objectives. One can use the tree as a guide to evaluate potential fire impacts in those cases where a building fails to meet the criteria of one or more branches (e.g., if ignition is not prevented, one can evaluate the ability of the building’s systems to manage the fire impact). One can also modify the fire safety concepts tree into the form of an event tree or a decision tree for risk analysis. Also, an event tree allows one to identify and assess the number of safety barriers in a system and what happen if each is successful or fails. It allows probabilities to be applied to the successes and failures to develop an estimate of the risk.

3.5. DESIGN APPROACHES TO STRUCTURAL FIRE SAFETY

Modern codes endorse two different ways for the design of structures subjected to fire: either by means of a prescriptive approach or with a performance-based approach. A prescriptive code provides for fire safety by prescribing some combination of specific requirements, without referring

to the desired safety level or how it is achieved. In comparison, a performance-based code allows any solution that can lead to an a priori imposed safety level. In some cases, for example when dealing with complex structures where it is impossible to comply with all the architectonical prescriptions of a prescriptive code, a performance-based approach is more appropriate in obtaining the optimal structural behaviour under fire, and a prescriptive code proves to be inadequate. Giuliani (2012) highlights the main differences between two approaches.

3.5.1. Prescriptive approach to structural fire safety

The fully-developed fire method (Petterson, et al., 1976) and further parametric curves described by analytical expressions (Wickstrom, 1985; Hertz, 2005) was based on the parameter dependency on property of the fuel and of the compartment. The idea of these methods consists in the prevention of any failure in the structure during the whole development of a fire that can trigger in a given compartment. Even if parametric curves are a quite realistic modelling of the fire action, some uncertainties are present in the knowledge of compartment and fuel properties and in the main assumptions adopted for the analytical description of the compartment fire. Nominal fires are not meant to model the fire action in a realistic way but are aimed at providing conventional curves for describing the gas temperature (ISO, 1975). When standard fire is used, the fire action does not depend on the actual fire load or on the properties of the compartment and the temperature increases monotonically with the time without any cooling phase. As a consequence, the resistance of structural elements has to be referred to a specific and limited time of the fire, depending on a certain class of resistance defined for the elements. The classes of resistance depend on the type of occupancy of the building, which ideally relates the resistance time of the structure to the safety of the people in the premises. The safety of people however appears as the main goal of this design approach, whereas the behaviour of the structure after that time remains undefined.

3.5.2. Performance-based fire design (PBFD)

A performance-based approach to fire safety design can be followed, by defining a set of safety and performance goals. A design goal could be for example to design a structure capable of withstanding a compartment fire without any damage Additionally, a lower safety level could be required under more infrequent but critical circumstances, and local structural damages could be accepted, provided that the failure propagation is prevented and a major collapse is avoided under all circumstances. As a matter of fact, even in case the structural elements are designed for resisting a compartment fire without failing, unexpected critical events may lead to an underestimation of the

actual fuel load (e.g.: arson, misuse of the structure) or to an overestimation of the structural capacity (e.g. human errors in the design or execution phases of the construction); other critical situations could be triggered by the unfortunate occurrence of errors or defects (Bontempi & Petrini, 2010), which are not critical for the structure when triggering one at a time, but may not be absorbed within the usual safety coefficients in case of simultaneous occurrence with a fire; finally, fires can also occur as a consequence of other critical events such as an earthquake or an explosion (Wald, et al., 2002): in this case the fire would affect a structure already partially damaged, leading most likely to greater consequences than expected. PBFD lend itself to be effectively used to this aim: however, due to the lack of a well-established methodology and the complexity of this kind of investigations, where material degradation, large displacements and local mechanisms should be accounted for, the performance-based approach to structural fire safety have been hardly used in the daily practice and is mostly limited to research studies or design of special constructions.

In the view of a performance-based fire design (PBFD) two different steps may be considered to assess the structural performance: the first step is a qualitative analyses, the second one is a quantitative analyses.

The overall structure of the process involves the definition of the design fire exposure, the thermal/mechanical response of the structural assembly (including any fireproofing materials), and the structural response of the structural system (Beyler, et al., 2007).

The assessment of structural performance is based on a multi-physics analysis. Assessment of safety in case of fire requires several skills. The judgment grounds on fire risk analysis, on fire dynamics, on heat transfer and structural behaviour. The Figure 3.7 represents the flowchart of this analysis. At the beginning, through a qualitative judgment, safety objective and general requirements are decided. The main safety objectives are the protection of life and the protection of property (Buchanan, 1994). In addition another major objective of fire safety is the maintenance of function (Schleich, 2006).

The basic elements of a performance based design framework are defined in such a way to allow the user to freely choose any solution to the problem, favouring in this way the design flexibility and the use of new techniques and technology as they become available (Torero, 2011). The objectives must be clearly stated at the outset of the design process, and any design solution should be permitted, which fulfils these objectives whilst still adhering to the performance targets of the design framework. The specific objectives should reflect the maximum acceptable level of damage to people, the building and its contents, damage to equipment or critical processes in the building,

interruptions, increases in risk or environmental damage caused by fire or protective measures (Grosshandler, 2002). They should be exactly identified in relation to the matter, even in relation to the objectives already laid down by the ISO/TR 13387-1 (1999). In order to achieve these objectives a measurable quantity (performance), a method of measure (performance criteria) and an acceptable limits (performance limits) are established.

The performance criteria represent a link between the definition of the objective and a quantitative evaluation. The performance criteria are threshold values, ranges of threshold values, or distributions that are used to develop and evaluate test projects for a specific project ideas. They have the form of indicators of damage and constitute one of the basic parameters of design, which should be carefully evaluated. These values have to be checked in some remarkable scenarios of fire. The document ISO/PDTS 16773 (2005) defines design fire scenario as "a qualitative description of the development of a fire in time with the identification of specific events that characterize the fire and that differentiate it from other scenarios". The choice of fire scenarios constitutes the basis of the process of PBFD. In most cases it is a choice based on experience, by pragmatically considering the fire that may have the most severe effects on the structure.

For the evaluation of fire safety in case of any quantitative approach, it is necessary not only to recognize the relevant factors but also to quantify and ranking them, referring to their contributions to fire damage and their importance in relation to the fire safety.

The quantitative assessment of structural performance is based on a multi-physics analysis, including: fire risk analysis, fire dynamics, heat transfer and structural behaviour. In this context, three different numerical models have to be implemented (Buchanan, 2002): i) a fire model for the study of the fire development; ii) a heat transfer model for the assessment of the internal temperature of the elements; iii) a structural model for evaluating the structure load bearing capacity, which takes as input the temperatures obtained from the heat transfer model. The fire engineering begins with the development of a design fire exposure to the structure. This normally takes the form of a time-temperature curve based upon the fire load, ventilation, and thermal properties of the bounding surfaces. Design fire loads are dependent upon the occupancy and other fire protection features of the building. Detailed design involves the use of thermal/mechanical models to assess the performance of each design configurations, resulting in trial protection thicknesses based upon tentative thermal failure criteria. The final analysis process concerns the prediction of structural performance under design loads with the structural elements heated according to the heat transfer analysis (Petrini, in press). This analysis can be performed for

individual elements, for the substructure in the fire area, or for the whole structural system. The structural analysis has to take into account the effects of thermal expansion, loading and unloading, large deformations and thermo-plastic behaviour of materials (Giuliani, 2012; Crosti, 2009).

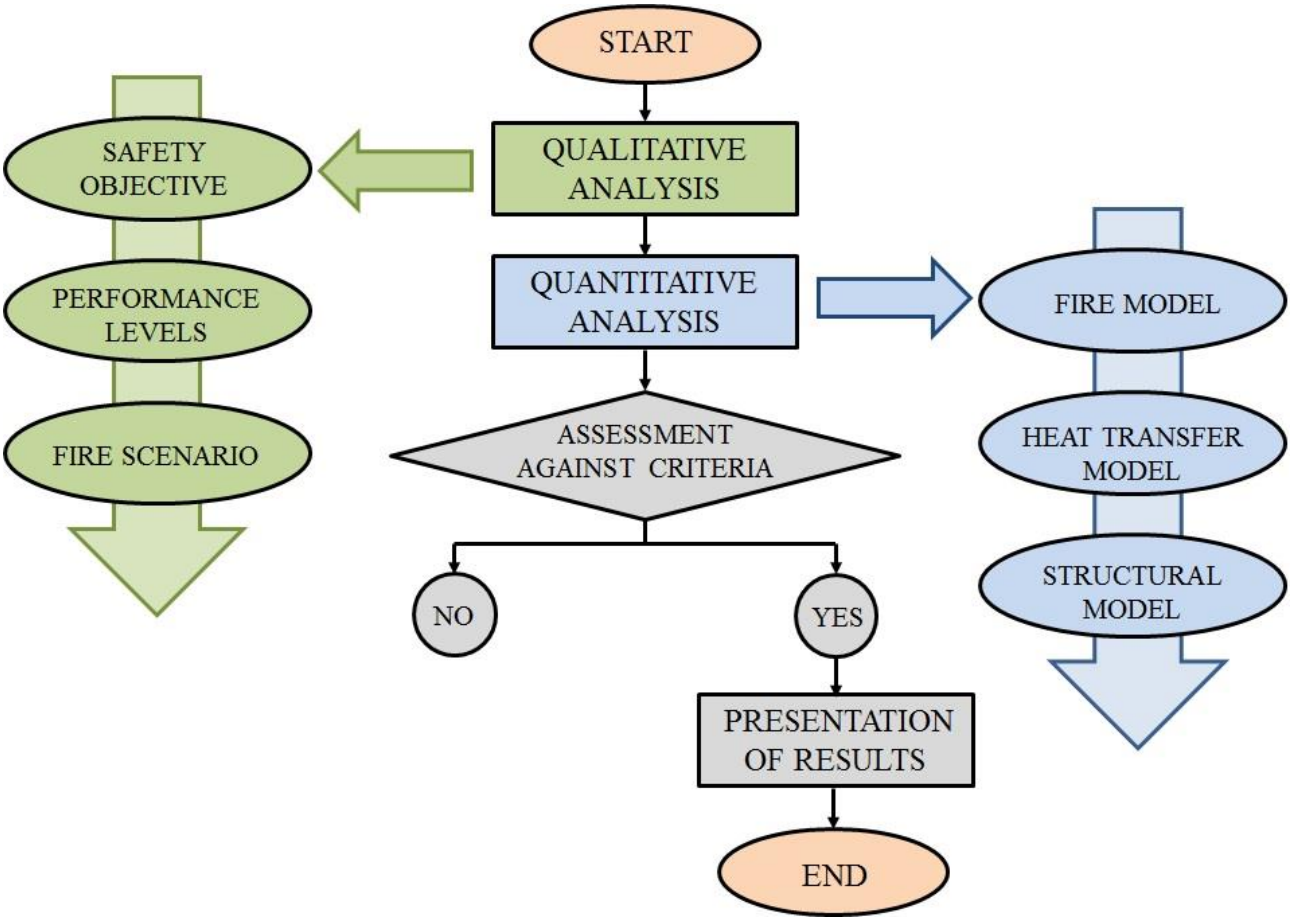

Figure 3.7 - Flowchart of Performance-Based Fire Design

3.5.3. Special issues in the PBFD of complex structures

In case of PBFD of complex structures, Petrini (2012) underlines some special issues:

1. Methods for performance investigation. Probabilistic approaches are more suitable in case of PBFD of simple structures due to the relatively low number of variables;

2. Scale level for performance investigations. In simple structures the fire performance investigation can be usually conducted with reference to the structural key elements, which are limited in number, on the other hand for complex structures the fire resistance of single elements is not significant while the fire resistance of the system as whole is more relevant.

3. Performance thresholds and collapse definition. In simple structures the thresholds applied to proper response parameters to define the lack of performance are easily definable referring to the

single structural elements, on the contrary for high redundant structures the collapse of a limited number of secondary elements do not necessarily imply the lack of performance.

4. Adopted models. Advanced structural models are needed in PBFD of complex structures due to the necessity of assessing global collapses rather than local ones, and advanced fire model are usually needed in order to assess the fire propagation.

5. Difficulties in determining proper fire scenarios. The fundamental fire scenarios are usually easily identifiable and limited in number for ordinary structures, while for complex structures this step is not so trivial.

6. Complexity of fire compartments. Beside the structural complexity, another parameter playing a prominent role is the configuration of the fire compartments; in fact the compartmentalization determines the size and the geometry of structure directly engaged by the fire. In case of simple structures, compartments are usually well defined and with simple geometries. In addition, complex geometries for fire compartments increase the uncertainty regarding the effectiveness of the compartments.

In Table 3.1 LP-HC events (like fires) are compared with ordinary events and in Table 3.2, where complex structures are compared with ordinary structures.

Table 3.1 - LP-HC versus ordinary events.

	Ordinary events	LP-HC events
Approach for Performance investigation	Probabilistic	Heuristic
Statistics	Complete	Incomplete
Uncertainties	Low	High
Models	Ordinary	Advanced
Load scenarios	Simple	Complex

Table 3.2 - Complex versus ordinary structures.

	Ordinary structures	Complex structures	Notes
Design approach	Prescriptive - PBD	PBD	
Minimum check level	Element	Element – Global	Investigations at a global level for robustness assessment
Models	Simple-Ordinary	Advanced	Models are intended having same complexity both for structure and actions
Approach for Performance investigations	Probabilistic (Performance = structural risk with respect to a specific limit sate)	Heuristic (Performance = "impact", identified with the consequences if the risk occurs)	Also Semi-Heuristic (Performance = structural risk with respect to a specific limit sate and to a specific scenario)
Fire scenarios	Easily identified and limited in number	Not trivial to define and great in number	
Definition of performance thresholds and collapse	Simple-Ordinary	Not trivial	e.g. for high redundant structures the collapse of a limited number of secondary elements do not necessarily imply the lack of performance
Compartmentation	Simple	Complex	

Chapter 4

4. HIGH-RISE BUILDINGS IN FIRE

4.1. FACTORS OF COMPLEXITY

Among all building typology, the fire design of high-rise buildings is particularly challenging with respect to both non-structural and structural design aspects: the enhanced design difficulties in providing i) a safe and prompt vertical evacuation of the building, ii) an effective vertical compartmentalization for avoiding vertical fire spread, refer both to non-structural aspects (architectural design choices and active measures) and iii) the enhanced susceptibility of high-rise buildings to disproportionate collapse, due to the significant vertical elevation of the structural system and to the complex and often untraditional design. Figure 4.1 highlights the main issues for high-rise buildings.

4.1.1. Evacuation

The time necessary for full building evacuation increases with building height. In the case of very tall buildings, full building evacuation via stairways might be impractical. A "defend-in-place" strategy has been employed in many building designs by i) designing compartments allowing people to remain in place, e.g., residential units; ii) temporarily evacuating people to areas of refuge on a floor; or, iii) moving people to dedicated refuge floors elsewhere in the building. Recently, times for full building evacuation have been reduced by employing elevators specifically designed to supplement the egress system of a building. Buildings employing assembly occupancies with large occupant loads on the upper floors of a tall building require special consideration.

4.1.2. Fire spread

The presence of large compartments is often required in high-rise buildings and is nowadays also a desired characteristic of many offices and residential premises as well. Nevertheless, prescriptive design and verification methods for structural fire safety can only be applied to compartments not exceeding specific dimensions and design of larger compartments often represent a challenge for

architects and structural engineers. Rein et al. (2007) underline the most important limitation of the current nominal approaches for this type of structure in their range of validity.

The application domain of the standard fire curve, the parametric curves and the natural fires are strongly linked to the experimental compartments that gave origin to these curves, i.e. simple, rectangular and of relatively small size. For example, Eurocode (EN 1991-1-2, 2004) states that the design equations are only valid for compartments with floor areas up to 500 m^2 and heights up to 4 m. The enclosure must have no openings on the ceiling, and the compartment linings were also restricted to thermal inertia between 1000 and 2200 $J/m^2s^{½}K$, which meant that highly conductive lining, like glass facades, and highly insulated materials could not be taken into account. As a result, common features in modern construction like large enclosures, high ceilings, atria, large open spaces, connected multiple floors and glass facades are excluded from the range of applicability of current methodologies.

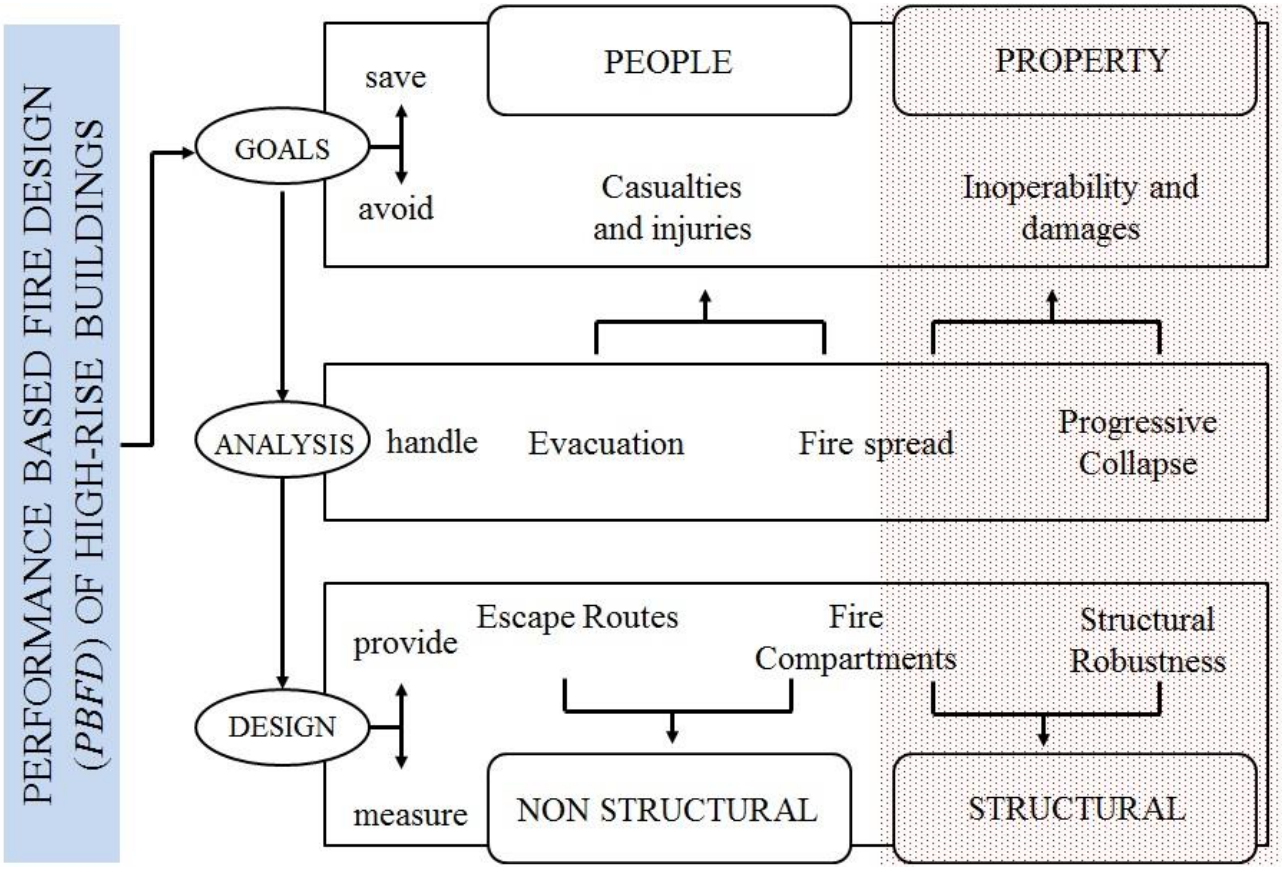

Figure 4.1 - Goals, challenges and safety measures for the design of high-rise buildings against fire

Moreover stack effect is a natural physical phenomenon which occurs in high rise buildings which experience a pressure difference throughout their height as a result of temperature differentials

between outside air temperature and inside building temperatures. The effect is pronounced in tall buildings because of their greater height. Stack effect causes air to move vertically, either upward or downward in a building. It can cause smoke from a fire to spread in the building if it is not controlled. Finally, the water supply needs in tall buildings can be beyond water supply capability of public mains and fire department pumpers. Above the height achievable by the local fire authority pumps, buildings must have the capability to supply its water independent of the fire department appliances.

4.1.3. Structural behaviour

The consequences of a fire-induced collapse are enormous in term of safety of people and integrity of the structure and the risk associated to the event can be significant, even if the occurrence of a structural fire is very low. Tall buildings generally are considered iconic because they are generally unusual in height, design or other feature. They are recognizable as unique. Therefore, in case active measures cannot prevent the development of a structural fire (such in case of arson or of a fire during a construction stage or a faulty maintenance of the sprinkler system), structural damages should be avoided or limited to a localized area.

The organization of the structural system and in particular the ratio of strength and stiffness of adjacent elements can influence the progressive collapse susceptibility of the system. Another consideration concerning the propagation of failures is that a particularly dangerous situation is represented by a possible spread of failures to elements not directly involved in the fire, i.e. element that due to their location or because of greater insulation have still a relatively low temperature at the time of failure.

4.2. CASE HYSTORY

For centuries, fires have been a threat to buildings. Some have led to the devastations of all or major portion of cities (for example, the burning of Rome in 64 AD; the great fire of London in 1666; the fire of Moscow in 1571 and 1812, the Hamburg, Germany, fire in 1842; the great fire in Quebec, Canada, 1845; the great fire in Shanghai in 1894; the great earthquake and fire of San Francisco, USA, in 1906).

Table 4.1lists significant fires in high-rise office buildings, hotel buildings, residential and apartment buildings, and mixed-use buildings.

Table 4.1 - Significant High-Rise Building Fires

Date	Type of building	Incident	Persons killed/Injuried
March 25, 1911	Factory	Asch Building Triangle Shirtwaist Factory Fire, New York City, New York, USA	146 workers killed
June 5, 1946	Hotel	Hotel LaSalle, Chicago, Illinois	61 killed
December 7, 1946	Hotel	Hotel Winecoff, Atlanta, Georgia	119 killed, 90 injured
January 26, 1969	Hotel	Victoria Hotel, Dunnville, Ontario, Canada	13 killed
December 25, 1971	Hotel	Tae Yon Kak Hotel, Seoul, South Korea	163 killed
Febraury 24, 1972	Office	Andraus Building, Sao Paulo, Brazil	16 killed, 330 injured
September 1, 1973	Hotel	Hafnia Hotel, Copenhagen, Denmark	35 killed
February 1, 1974	Office	Joelma Building, Sao Paulo, Brazil	179 killed, 300 injured
July 12, 1974	Hotel	Zaragoza, Spain	76 killed
November 21, 1980	Hotel	Prince Hotel, Kawaji, Japan	44 killed
November 21, 1980	Hotel	MGM Grand Hotel, Las Vegas, Nevada, USA	85 killed, 600 ca. injured
February 10, 1981	Hotel	Las Vegas Hilton Hotel, Las Vegas, Nevada, USA	8 killed, 350 injured
March 6, 1982	Hotel	Westchase Hilton Hotel, Houston, Texas, USA	12 killed
October 18, 1984	Hotel	Alexander Hamilton Hotel, Paterson, New Jersey, USA	15 killed, and more than 50 injured
December 31, 1986	Hotel	Dupont Plaza Hotel, Puerto Rico	97 killed and more than 140 injured
November 29, 1987	Hotel	Hotel Concorde, Margarita, Venezuela	11 killed
January 1, 1988	Hotel	First Hotel, Bangkok, Thailand	13 killed
January 11, 1988	Mixed use	East 50th Street Apartment Building, Mahnattan, New York, USA	4 killed, 16 injured
May 4, 1988	Office	First Interstate Bank Building, Los Angeles, California, USA	1 killed, 40 injured
June 30, 1989	Office	Peachtree 25th Building, Atlanta, Georgia, USA	5 killed, 26 injured
December 24, 1989	Residential	John Sevier Center, Johnson City, Tennessee, USA	16 killed, 50 injured
March 1, 1990	Hotel	Sheraton Hotel, Cairo, Egypt	18 killed, 70 injured
February 23, 1991	Office	One Meridian Plaza, Philadelphia, Pennsylvania, USA	3 killed
January 6, 1995	Residential	Residential High-Rise, North York, Ontario, Canada	6 killed
November 20, 1996	Office	Garley Office Building, Hong Kong, China	40 killed, 81 injured
July 11, 1997	Hotel	Royal Jomtien Resort, Pattaya, Thailand	91 killed, 51 injured
September 11, 2001	Office and hotel	World Trade Center, New York, USA	2749 killed and thousands injured
March 5, 2003	Hotel	Rand Inn International Hotel, Johannesburg, South Africa	6 killed, 67 injured
October 17, 2003	Office	69 West Washington, Chicago, Illinois, USA	6 killed, several injured
October 17, 2004	Office	Parque Central, Caracas, Venezuela	-
February 12, 2005	Office	Windsor Building, Madrid, Spain	-
May 13, 2008	Office	Technical University, Delft, Netherlands	-
February 9, 2009	Hotel	Mandarin Oriental Hotel, Beijing, China	1 killed, 7 injured

4.2.1. Fires without structural damages

– Andraus Building, Sao Paulo, Brazil, 1972 (Figure 4.2)

The Andraus Building is a well-known building in the city centre of São Paulo, Brazil which is located in Republic district, on the corner of avenida São João with rua Pedro Américo. It is 115 metres tall and has 32 floors, and its construction ended in 1962. The building was constructed of reinforced concrete. Its façade had extensive floor to ceiling glazed areas, with a spandrel of only 350mm in height and projecting 305mm from the face of the building. It has significant architectural value, being one of the best-known skyscrapers of São Paulo, of considerable prominence in the skyline with its unmistakable geometric shape (Wikipedia, 2012).

Figure 4.2 – Andraus Building before (wikipedia, 2008) and during fire (urbanity.es, 2009)

On February 24, 1972, the building suffered a great fire which caused the deaths of 16 persons trapped inside the building. 330 others were also injured. The fire began on the second floor and consumed the entire building, which contained several corporate offices, among them the Henkel multinationals and Siemens. Wind and combustible interior finishes and contents contributed to the fire spread. After the fire broke through the windows, three to four floors above the department store floors were exposed to a flame front. The front increased in height as more floors became

involved. At its peak the mass of flame over the external façade was 40m wide and 100m high and projecting at least 15m over the street (The Institution of Structural Engineers, 2002).

The building was renovated after the fire, and currently houses municipal and federal government offices (Wikipedia, 2012).

- Joelma Building, Sao Paulo, Brazil, 1974 (Figure 4.3)

The Joelma fire occurred on Friday February 1, 1974, in the Joelma Building, a 25 story building of reinforced concrete situated in downtown São Paulo, at 225 Avenue Nine of July (Craighead, 2009). It is one of the most notable tragedies to have occurred in Brazil. The *in situ* concrete floor slabs projected 900mm on the north wall and 600mm on the south wall. The exterior facade was made of hollow tiles rendered with cement plaster on both sides and aluminium-framed windows (The Institution of Structural Engineers, 2002).

Figure 4.3 - Joelma Building before (triposo, 2012) and during fire (dominio sfantasticos, 2012)

A short-circuit in a faulty air-conditioner on the 12th floor near to a window ignited the fire at 8:50 AM. The large amount of combustible materials, including paper, plastics, electrical equipment and wooden walls and furniture, contributed to the fire spreading rapidly. Most importantly, the building had no emergency exits, fire alarms or fire sprinkler systems installed (wikipedia, 2012).

The fire spread externally up 13 storeys on two of the facades to the top of the building, readily igniting combustible finishes inside the windows of the floors above, enabling the vertical spread of the fire to continue. There were 179 fatalities.

4.2.2. Fire with structural damages

- MGM Grand Hotel, Las Vegas, Nevada, USA, 1980 (Figure 4.4)

A fire at the MGM Grand Hotel on November 21, 1980, resulted in the deaths of 85 guests and hotel employees, injury to about 600 (Society of Fire Protection Engineers, 2012) and more than $30 million in property damage (Craighead, 2009). The high-rise building, constructed in the early 1970s, consisted of twenty-one stories of guest rooms situated above a large, ground-level complex comprised of a casino, showrooms, convention facilities, jai alai fronton, and mercantile complex. The hotel was partially sprinklered, but major areas including the Main Casino and The Deli, the area of fire origin, were not sprinklered. The most probable cause of the fire was heat produced by an electrical ground fault within a combustible concealed space in a serving station for waitresses of The Deli. Openings in vertical shafts (elevators and stairwells) and seismic joints allowed toxic smoke to spread to the top floor (wikipedia, 2012).

Figure 4.4 – MGM Grand Hotel before (University of Nevada Las Vegas, 2012) and during fire (PBS, 2012)

On the one hand, the disaster led to the general publicizing of the fact that, during a building fire, smoke inhalation is a more serious threat than flames, on the other part it stressed the need for several precautions in the fire design such as:

- seismic joints need to be protected against fire and smoke spread between floors;
- concealed spaces in fire resistive and non-combustible buildings should have few combustibles;
- vertical openings, including stairways and elevator shafts, need to be protected to limit smoke and fire spread between floors;
- large assembly buildings need a pre-fire emergency plan.

– First Interstate Bank, Los Angeles, California, USA, 1988 (Figure 4.5)

The First Interstate Bank building was located in Los Angeles, California (Society of Fire Protection Engineers, 2012). The tower has a structural steel frame with lightweight concrete slab on profiled steel deck. The external cladding system was made of glass and aluminium. The building had a structural steel frame with sprayed fire protection and steel floor pans and lightweight concrete decking (The Institution of Structural Engineers, 2002). It was 62 stories high and was in the process of being retrofitted with automatic sprinkler protection for a cost of $3.5 million at the time of the fire.The installation was not required by codes at the time the owners decided to provide increased fire protection for the building. However, the system was inoperative, awaiting the installation of water flow alarms. It had sprinkler protection only in the basement, garage and underground pedestrian tunnel. The sprinkler system was, however, not operational at that time. The fire began at 10:25 p.m. on May 4, 1988 on the 12th floor. Flames spread vertically in the building through a return air-shaft and in the space in between the exterior curtain walls and the edges of the floors. Flames also penetrated behind the spandrel panels around the ends of the floor slab where there was sufficient deformation of the aluminium mullions to weaken the fire stopping allowing the flames to pass through, even before the windows and mullions had failed. Flames were estimated to be lapping 10m up the face of the building. The curtain walls including windows, spandrel panels and mullions were almost completely destroyed by the fire. However, the building structure as a whole did not collapse. The total burnout of four and a half floors did not cause damage to the main structural members due to a good application of spayed fire protection on all steelwork. There was only minor damage to one secondary beam and a small number of floor decks. The non-structural damages included:

- Virtually all external cladding from the 12th to 16th floors was destroyed and fell to the ground.
- The heat of the fire caused some aluminium alloy valves in the occupant hose cabinets to fail, creating water leaks and causing water damage on floors below the fire.

The property loss was estimated at over $200 million, excluding the business interruption loss.

The main factors leading to the rapid fire growth and the fire spread to five floors included:

- the lack of effective fire fighting measures, such as automotive sprinklers;
- the delayed reporting of the fire (Craighead, 2009);
- the open-plan floors with a floor area of over 1600m^2;
- the failure of vertical compartmentalization measures, in the façade system and the floor openings.

The open-plan floors with large quantity of combustible office contents without any internal fire barriers contributed to quick fire growth within a fire floor. In addition, the gaps between the external cladding and the floors were not fire stopped and the fire could easily spread to floors above. Without the effective fire fighting on the 16th floor by the fire brigade, the fire could have spread to all floors above.

Figure 4.5- The First Interstate Bank Building before (FireFighter EMT, 2009) and during fire (Los Angeles Fire Department, 1999)

In fact, minor fire spreads also occurred through the floor service openings for electricity and communications. This highlights the importance of applying effective fire stopping system to all floor and wall openings to ensure the effectiveness of fire compartmentalization. It was also shown that if fire protection to structural members is adequately designed and applied with quality control, fire damage to fire exposed members will be minimised and structural collapse can be prevented (University of Manchester, 2012). There was one fatality. Because of the fire, Los Angeles building codes were changed, requiring all high-rises to be equipped with fire sprinklers.

– One Meridian Plaza, Philadelphia, Pennsylvania, 1991 (Figure 4.6)

One Meridian Plaza was a 38 story office building in Philadelphia, Pennsylvania. The building used structural steel with concrete floors on metal decking and protected with spray-on fire protection. The exterior of the building was covered by granite curtain wall panels with glass windows attached to perimeter floor girders and spandrels. Only the below-ground services floors were fitted with sprinklers at the time of construction. Subsequently sprinklers had been installed on the 30th, 31st, 34th, and 35th floors and to parts of the 11th to 15th floors, but no sprinklers were installed on the floor of fire origin (Society of Fire Protection Engineers, 2012).

Figure 4.6 – One Meridian Plaza before (wikipedia, 2012) and during fire (skyscrapercity, 2004)

Fire broke out on the 22nd floor, due to spontaneous combustion of rags left by painters, penetrated through the windows and heat exposure from the fire plumes ignited materials on the seven floors above. The fire was stopped as it approached the 30th floor which had sprinklers. Although the fire burned for 19 hours, the structure did not collapse (The Institution of Structural Engineers, 2002). Three firemen lost their lives. The fire destroyed eight floors (Craighead, 2009), causing an estimated $100 million in direct property loss and an equal or greater loss through business interruption. Litigation resulting from the fire amounts to an estimated $4 billion in civil damage claims. Twenty months after the fire this building, one of Philadelphia's tallest, situated on Penn Square directly across from City Hall, still stood unoccupied and fire-scarred, its structural integrity in question (http://911research.wtc7.net/, 2011).

- Parque Central, Caracas, Venezuela, 2004 (Figure 4.7)

The tallest building in Caracas, Venezuela is a 56 story, 220 meter tall office tower. A fire started on the 34th floor around midnight on October 17, 2004 and spread to more than 26 floors. It burned for more than 17 hours (The Institution of Structural Engineers, 2002).

The cause of triggering is not clear, but the most realistic hypotheses are the storage of flammable material in the aviation administration, a short-circuit, and arson.

Figure 4.7 – Paque Central before (flickr, 2012) and during fire (zetatalk, 2012)

Although the original designers took extraordinary care to design a building that included state-of-the-art high-rise fire safety for the 1970s, designing fire detection and alarm systems, fire hose cabinets, pressurized stairs and a wet-pipe sprinkler system the sprinkler system had not been properly tested or maintained, thus it wasn't in a working condition (Society of Fire Protection Engineers, 2012). Investigation determined that fire pumps malfunctioned, exits were blocked and elevators were not accessible. The fire was finally brought under control by a combination of military helicopters dropping water on the building and fire fighters, who laid 40 stories of fire hose (Craighead, 2009). The event has not caused casualties because the building was empty at the moment of the fire. Between 2005 and 2007 the entire building was renovated by the Ministry of Infrastructure at cost of ca. $30 millions (NFPA Journal, 2005).

– The Mandarin Oriental Hotel, Beijing, China, 2009 (Figure 4.8)

On February 9, 2009, the nearly-completed 160 meter, 40-story Mandarin Oriental hotel in Beijing's Television Cultural Centre (TVCC) in Beijing caught fire around 8:00 pm, was engulfed within 20 minutes, and burned for at least 3 hours until midnight.

Figure 4.8 – The Mandarin Oriental Hotel before (wikipedia, 2007) and after fire (NBC news, 2009)

The fire was started by fireworks display authorized by CCTV itself, without the permission or participation from Beijing police, the Beijing Fire Department, Beijing City government, or any

other governmental department, ignited in the building around the tower's top and preceded downward around the tower's sides while fireworks continued to burst dramatically above the blaze. The propagation has been allowed by the lack of sprinklers system, not installed yet. Despite the fact that the fire extended across all of the floors for a period of time and burned out of control for hours, no large portion of the structure collapsed (Society of Fire Protection Engineers, 2012).

4.2.3. Fires with structural collapse

– Seven World Trade Center, New York, USA, 2001 (Figure 4.9)

The 47-storey building, known as Seven World Trade Center (WTC7) was a 47 story building, clad in red exterior masonry (wikipedia, 2012). The original structure was completed in 1987. An elevated walkway connected the building to the World Trade Center plaza. The building was 190 m tall, with a trapezoidal footprint that was 100 m long and 43 m wide (NIST, 2008).

Figure 4.9 – World Trade Center 7 before (wikipedia, 2012) and during fire (911 Myths, 2012)

The final design for 7 World Trade Center was for a much larger building than originally planned when the substation was built (Lew, 2005). The structural design of 7 World Trade Center therefore included a system of gravity column transfer trusses and girders, located between floors 5 and 7, to transfer loads to the smaller foundation. Existing caissons installed in 1967 were used, along with

new ones, to accommodate the building. The 5th floor functioned as a structural diaphragm, providing lateral stability and distribution of loads between the new and old caissons. Above the 7th floor, the building's structure was a typical tube-frame design, with columns in the core and on the perimeter, and lateral loads resisted by perimeter moment frames. It was set on fire by debris from the WTC towers (WTC1 and WTC2) when they collapsed on 11 September 2001. WTC7 collapsed totally about seven hours later. The collapse appears to have been due primarily to the effects of fire, and not to impact damage from the collapsing WTC towers (http://911research.wtc7.net, 2012). Because of the structural damage and because the collapse of WTC 1 & 2 interrupted the public water supply to WTC 7, automatic sprinklers in the building were rendered inoperable. Fires burned in the building for nearly seven hours before it collapsed. The mechanisms causing the total collapse of WTC7 have not yet been confirmed. Loss of structural integrity in one of the load transfer systems caused by fire has been suggested as the 'trigger' event.

– Windsor Tower, Madrid, Spain, 2005

The Windsor Tower, built in Madrid in 1979, was a 32-storey concrete office building with a reinforced concrete core and an height of 106 m. The structure had two technical floors without windows in the middle. Originally, the perimeter columns and internal steel beams were left unprotected and vertical openings were not protected. There was no fire stopping between the floor slabs and the exterior wall. At the time of the fire, the building was undergoing a multi-year fire protection improvement program consisting of protecting steel structural members, upgrading the curtain wall and installing automatic sprinklers, except for the 9th and 15th floors. Some of the curtain wall fire stopping and vertical opening protection had not been completed. The fire started on the 21st floor and spread rapidly throughout the entire building, leading to collapse of the outermost steel parts of the upper floors. Fire fighters needed almost 24 hours to extinguish it (University of Manchester, 2012).

The main factors leading to the rapid fire growth and the fire spread to almost all floors included:

- the lack of effective fire fighting measures, such as automotive sprinklers;
- the "open plan" floors with a floor area of 1000 m^2;
- the failure of vertical compartmentalization measures, in the façade system and the floor openings.

It was believed that the multiple floor fire, along with the simultaneous buckling of the unprotected steel perimeter columns at several floors, triggered the collapse of the floor slabs above the 17th floor (Craighead, 2009), (Fletcher, et al., 2006). When the fire spread below the 17th floor, those

protected perimeter columns survived, except for the unprotected columns at the 9th and 15th floors which all buckled in the multiple floor fire However, they did not cause any structural collapse, because the applied loads supported by these buckled columns had been redistributed to the remaining reinforced concrete shear walls (NILIM, 2005). After the fire, the building was demolished.

Figure 4.10 – Windsor Tower before and after fire (Photo: Fernando Lamarca)

- Technical University, Delft 2008

The Faculty of Architecture building of Technical University of Delft was a reinforced concrete and steel structure completed in 1970. It is a combination of six 3-storeys structures with a 13 storeys tower located above (Meacham, et al., 2010). There was a different floor-slab, joist and beam configuration on even-numbered versus odd-numbered floors. The building is divided in three wings and characterized by large open studio spaces and large window openings.

In the morning of May 13, 2008 a fire started in the southern wing of the building for a breakdown of a coffee machine. The fire propagates throughout the building very rapidly, even if the fuel load has been calculated to be not particularly high and caused the collapse of the northern wing of the building. Although all building occupants evacuated safely, without injured, damages were significant enough that the building had to be demolished.

Researchers of National Science Foundation from United States with researcher from TNO and Efectis in the Netherlands are conducting out studies not only in order to identify the "trigger" event that lead to the particular collapse mechanism and the reasons that limited the propagation of the damages to the vertical direction, but also in order to establish a mechanism for data collection and archiving for future fires of significance.

Figure 4.11 - Technical University of Delft before and after fire (Meacham, et al., 2010)

4.3. STRUCTURAL SYSTEM CHARACTERISTIC AND WEAKNESS

The above cases show that the progression of a fire accident in high-rise buildings is a really complex phenomenon with possibly unexpected developments. Figure 4.12 shows what is considered here as the most useful model for the comprehension of the accident, from the hazard chance to the final catastrophe possibility (Reason, 1990). By this vision, the construction is considered as composed by a series of firewalls (in the Computer Science meaning) that block the progression of the hazard into a collapse. These firewalls are of different nature: at the beginning, they are connected with the conception of the structure, and so they are of logical type; some ones are connected with the specific action; others are related to intrinsic, passive, properties of the structure (ability to sustain temperature damages, …), while some others are associated with active

safety measures (sprinklers, …). Realistically, each of these firewalls has imperfections and deficiencies: in the graphical representation of Figure 4.12, these are represented by holes in the firewalls. The model predicts that, also if the single shortage is not critical, when an alignment of these weaknesses arises, this can lead to the development of a crisis.

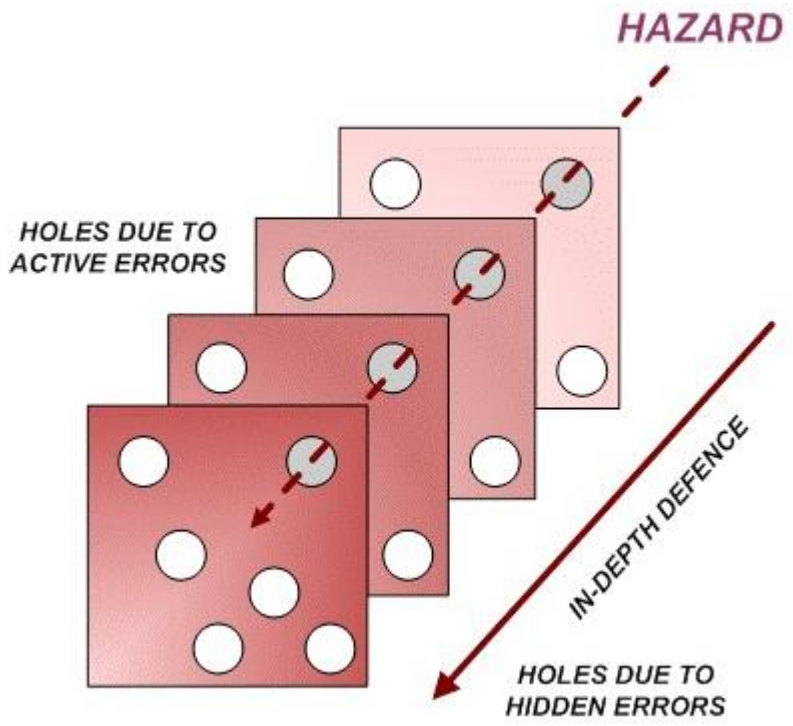

Figure 4.12 - Model of development of fire accidents (adapted from Reason, 1990)

In relation to the fires in tall buildings, the previous model can be detailed as shown in Figure 4.13 - Detailed model for Fire Safety Engineering: structural system characteristics and weaknesses. This plot represents a reference model for the activities of Fire Safety Engineering: on the left there are the system characteristics while on the right there are the weaknesses of the system represented as holes in the firewalls.

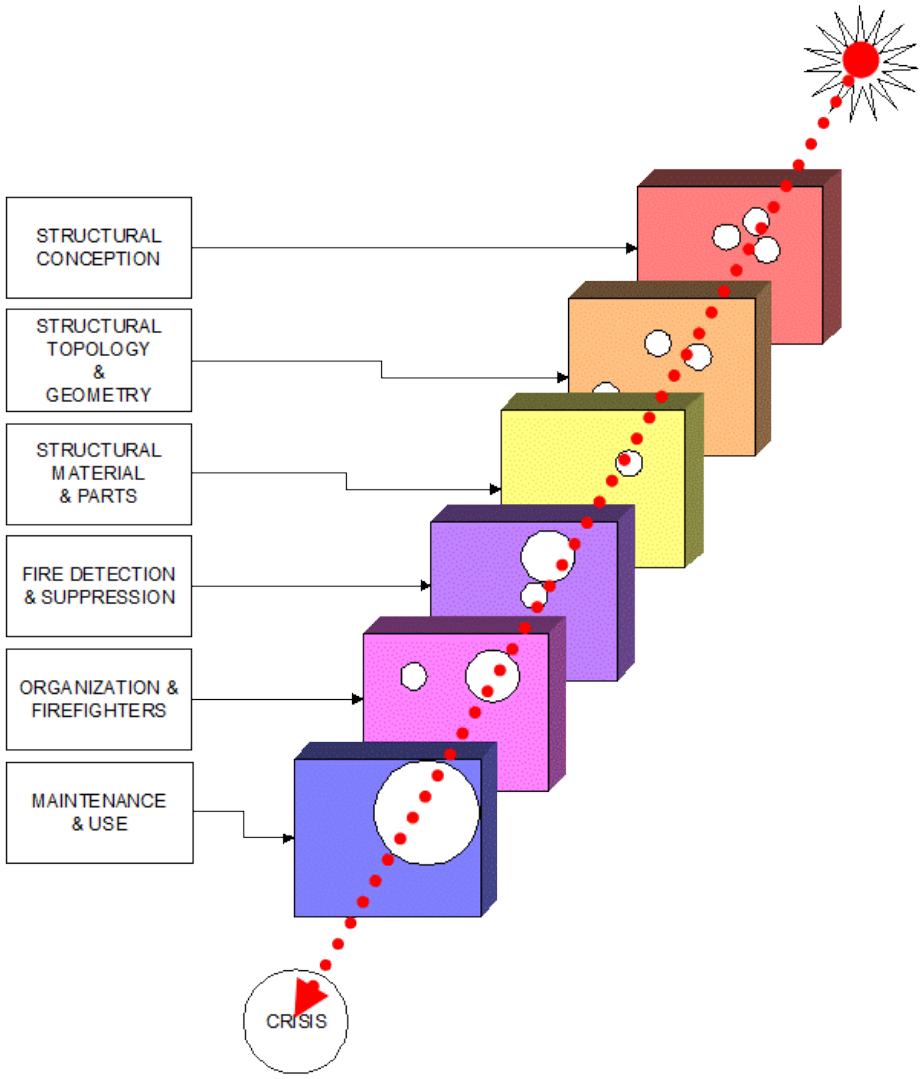

Figure 4.13 - Detailed model for Fire Safety Engineering: structural system characteristics and weaknesses.

SECTION 2:

BACKGROUND ASPECTS FOR STRUCTURAL FIRE SAFETY

5. FIRE ACTION
6. MATERIAL BEHAVIOUR
7. STRUCTURAL BEHAVIOUR

Chapter 5

5. FIRE ACTION

5.1. FIRE COMPARTMENT

The equilibrium equation is written with reference to the heat power and not to the heat energy, as the fire is a transient phenomenon and even though the energy balance is maintained at each time, the composing quantities vary with time.

$$\dot{Q}_C = \dot{Q}_B + \dot{Q}_R + \dot{Q}_L + \dot{Q}_W \tag{5.1}$$

where:

$\dot{Q}_C$ [W] is the heat produced per unit time by combustion;

$\dot{Q}_B$ [W] is the heat accumulated per unit time in the hot gasses (can be neglected);

$\dot{Q}_R$ [W] is the heat radiated per unit time to the outside through the openings;

$\dot{Q}_L$ [W] is the heat dissipated per unit time by the air flow through the openings;

$\dot{Q}_W$ [W] is the heat absorbed per unit time by the enclosure (walls, ceiling, floor);

The terms $\dot{Q}_W$, $\dot{Q}_L$ and $\dot{Q}_R$ depend on the properties of the compartment, i.e. the enclosure material and the size and geometry of the room and of the openings.

The heat power $\dot{Q}_C$ depends instead on the properties of the combustible such as the calorific value and the maximum rate of combustion. However, in case the oxygen for supporting combustion is not sufficient for the fuel to reach its maximum the rate of combustion (ventilation-controlled fire), the combustion rate will be governed by the air income and therefore will also be dependent on the size of the opening.

The expressions of the four heat powers terms of Eq. 5.1 will be given in the following and the role of the main compartment and fuel properties in the definition of each term will be discussed in

detail. In particular, the heat power $\dot{Q}_R$ dissipated by radiation through the openings will be obtained by means of the Stefan-Boltzmann's equation. The heat power $\dot{Q}_L$ lost to the outside by the replacement of hot gasses with fresh air will by calculated by means of Bernoulli's equation. The heat power $\dot{Q}_W$ that is absorbed by the enclosure will be found by specializing Fourier's equation of conduction for the case of a mono-dimensional heating flux trough the walls. The heat power $\dot{Q}_W$ will be calculated and the expression will be specialized to the case of a ventilation-controlled fire. Under this assumption, the temperature of the hot gas in the compartment will be then obtained as a numerical solution of the heat power balance expressed in Eq. 5.1.

5.1.1. Fire parameters: compartment and fuel properties

In the previous section it has been shown that all heat power term of Eq. 5.1 are governed by parameters, which depend either on the properties of the compartment or of the fuel.

In particular, the heat power $\dot{Q}_R$ that can be dissipated by radiation through the openings resulted to be proportional to the opening area A.

The heat power $\dot{Q}_L$ lost to the outside by the replacement of hot gasses with fresh air depends instead not only on the area of the opening A, but also on the squared root of its height h. It can be expressed by a relation of proportionality to a parameter named opening factor O and better defined in the following.

The heat power $\dot{Q}_W$ that is absorbed by the enclosure is governed by the wall property and particularly the density, the specific heat capacity and the thermal conductivity of the walls. As better explained below, these three quantities can be combined in a single parameter, called thermal inertia b, which is defined and better discussed below.

The heat power $\dot{Q}_C$ depends instead on the properties of the combustible and in particular on the effective calorific value of the combustion H and on the mass burning rate $\dot{m}$. However, in case the oxygen for supporting combustion is limited, the mass burning rate $\dot{m}$ won't reach the maximum allowable by the fuel but will be also governed by the air income and therefore the heat power $\dot{Q}_C$ will also depend on the opening factor O.

- Opening factor

This parameter, indicated with the symbol is called opening factor and is measured in [$m^{1/2}$]:

Opening factor: $O = A\sqrt{h}/A_t$ [$m^{1/2}$] (5.2)

where the total area of the enclosure can be calculated in case of a rectangular room of length L, width W, and height H as:

Total area of the enclosure: $A_t = 2 \cdot (LW + LH + WH)$ [m^2] (5.3)

If several vertical openings are present in the compartment, the opening factor can be calculated by considering an equivalent window, which has the area of the sum of the areas of the openings and an average height, weighted on the basis of the area of each opening.

Opening factor (n openings): $O = \sum_i^n A_i \sqrt{h_{av}} / A_t$ [$m^{1/2}$] (5.4)

where:

Averaged height: $h_{av} = \sum_i^n A_i h_i / \sum_i^n A_i$ [m] (5.5)

– Thermal inertia

The heat loss outside of the compartment is an important factor for the determination of the evolution of temperatures inside of the compartment. Heat transfer to the compartment boundaries occurs by convection and radiation. The thermal properties of the walls have to be known in order to evaluate the heat transfer by conduction through the walls (Leonardo Da Vinci Project, 2005).

The three main parameters characterising the thermal properties of a material are the density ρ [kg/m^3], the specific heat c [J/kg·K] and the thermal conductivity λ [W/m·k]. Their product provides an estimate of the thermal inertia

$$b = \sqrt{p \cdot c \cdot l} \quad [J/m^2 s^{1/2} K] \quad (5.6)$$

– Effective calorific value

The calorific value is the heat developed by the combustion of a mass unit of the combustible material. It is indicated with the symbol H and it is measured in [J/kg].

Determination of calorific values is done by burning a determined amount of the combustible material in a calorimeter and measuring the products of combustion. The gross calorific value can be calculated as the heat released during the combustion. Hence, the effective (net) calorific value is calculated by subtracting the heat of vaporization of the water produced in the combustion process, as the energy required to vaporize the water is not realized as heat. Net calorific values are therefore

also referred to as lower heating values (*LHV*) as opposed to gross calorific values, which represent instead the higher heating values (*HHV*).

Lists of net calorific values of most common combustibles can be found in Tab. 3.1 of the Swedish bulletin (Petterson&al., 1976) and in Tab. E.3 of Eurocode 1 (EN1991-1-2, 2002). These values refer to dry materials, so effective calorific values can be calculated from here by subtracting the heat of vaporization of the moisture content of the combustible, which should be known. The following formula, reported in the annex E.2.4 of Eurocode 1 (EN1991-1-2, 2002) can be used:

$$H = H_0 \cdot (1 - 0.01 \cdot u) - 0.025 \cdot u \tag{5.7}$$

where:

H_0 [MJ/kg] is the net calorific value of the dry material

u [%] is the moisture content expressed as a percentage of the dry weight

– Fuel load density

The fuel load represents the energy which is released during a fire, which depends on the amount of combustible and on its effective calorific value. It is indicated with the symbol Q and measured in [MJ].

In usual compartments, where more than one combustible material is present, the fuel load can be calculated as the sum of each distinct fuel load.

$$Q = \sum_j m_j H_j \qquad [\text{MJ}] \tag{5.8}$$

Since not all the material generally burns out during a fire, a combustion factor $\mu < 1$ can be applied to the combustible mass, which is typically of the order of 0.8-1. In addition to this, the Annex E of the Eurocode 1 considers also an optional reductive factor for the calculation of the fire load, in presence of combustible material in containments against fire. This is however not allowed by the Danish regulation and won't be further discussed here.

It can be useful to refer to the fuel load density q [MJ/m^2], defined as the fuel load per unit area of the enclosure At.

$$q = Q / A_t \qquad [\text{MJ/m}^2] \tag{5.9}$$

This choice is motivated by the two following considerations:

- the same fuel load has a different effect on compartments of different size;

- in usual compartments, the combustible materials are mostly represented by the furniture, which can be considered uniformly spread along the floor surface.

The fuel load density is sometime referred not to the area A_t of the whole enclosure (sum of the wall, ceiling and floor surface, as described above), but to the area A_f of the floor only and in this case it is indicated with the symbol q_f.

$$q_f = Q/A_f \qquad [\text{MJ/m}^2 \text{ of floor area}] \qquad (5.10)$$

Characteristic fire load densities q_{kf} referred to floor area are reported in Tab. E.4 of the annex E of Eurocode 1 (EN1191-1-2: 2002) for different type of occupancy. In the same annex is specified that the design value can be derived from the characteristic one by means of a set of partial coefficients, according to a formula, which is here reported:

$$q_{f,d} = \mu \cdot q_{f,k} \cdot \delta_{q1} \cdot \delta_{q2} \cdot \delta_{qn} \qquad [\text{MJ/m}^2 \text{ of floor area}] \qquad (5.11)$$

where:

μ [ad.] is the combustion factor;

$q_{f,k}$ $q_{f,k}$ [MJ/m2]is the characteristic fire load density, taken from Tab. E.1 or, in case of variable fuel content, calculated as ratio between the 80% fractile value of the fire load and the floor area of the compartment;

δ_{q1} [ad.] is a safety factor for fire activation risk, which increases from 1.1 to 2.13 with the size of the compartment (Tab. E.1 of EN1991-1-2:2002);

δ_{q2} [ad.] is a reductive or safety factor for fire activation risk, which increases from 0.78 to 1.66 depending on the type of occupancy (Tab. E.1 of EN1991-1-2:2002);

δ_{qn} [ad.] is a cumulative factor for fire activation risk in presence of active protection measures, which is calculated as the products of different reductive or safety coefficients accounting for fire detection and suppression measures (Tab. E.2 of EN1991-1-2:2002).

The Eurocodes annexes are however only informative and each country can limit their use or substitute them with different national rules. This formula, as in general most part of annex E, is not accepted by several countries, as Denmark, Finland, France, and United Kingdom.

5.1.2. Rate of Heat Release

The fire load defines the total available energy, but the maximum gas temperature in a fire depends also on the rate of the heat release. The Figure 5.1 shows how same fire load either burning very quickly or smouldering may lead to completely different gas temperature curves. The two *RHR* curves corresponding to the same amount of fire load, because the surface beneath both curves is the same.

The *RHR* is the source of the gas temperature rise. Two different events may occur, depending whether or not during the growth process there is always enough oxygen to sustain combustion. Either the *RHR* reaches a maximum value without limitation of oxygen to sustain combustion.

If the *RHR* reaches a maximum value without limitation of oxygen to sustain combustion, it is limited by the available fire load (FUEL CONTROLLED FIRE). Otherwise the available oxygen limits the *RHR* (VENTILATION CONTROLLED FIRE).

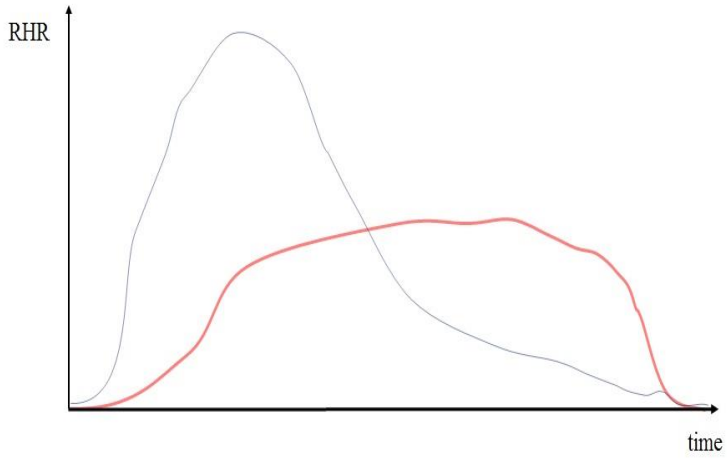

Figure 5.1 – Two RHR curves corresponding to the same amount of fire load.

5.2. PRE-FLASHOVER FIRES MODELS

In a localised fire, there is an accumulation of combustion products in an upper layer beneath the ceiling, with a horizontal interface between this hot layer and the lower layer where the temperature of the gases remains much colder (Leonardo Da Vinci Project, 2005).

The thermal action of a localised fire can be assessed by using the expression given in the annex C of (EN 1991-1-2, 2004). This action depends on the horizontal distance of structural elements from the fire. The annex shows two methods developed by (Heskestad, 1995) and (Hasemi & Tokunuga, 1984).

The two methods are valid under the following conditions:

- The diameter of the fire is limited by $D \leq 10\ m$
- The rate of heat release of the fire is limited by $Q \leq 50\ MW$

5.2.1. Flame not impacting the ceiling (Heskestad's method)

An empirical method, based on experiments, has been developed to determine the thermo-dynamic data of an open fire (Heskestad, 1995). These data are mainly temperature and velocity according to radial and axial distance along the flame and the plume of the open fire.

The flame lengths L_f of a localised fire Figure 5.2 is given by:

$$L_f = -1.02 \cdot D + 0.0148 \cdot Q^{2/5} \quad \text{[m]} \tag{5.12}$$

When the flame is not impacting the ceiling of a compartment (L_f < H;) or in case of fire in open air, the temperature Θ(z) in the plume along the symmetrical vertical flame axis is given by :

$$\Theta_{(z)} = 20 + 0.25 \cdot Q_c^{\,2/3} \cdot \left(z - z_0\right)^{-5/3} < 900 \quad \text{[°C]} \tag{5.13}$$

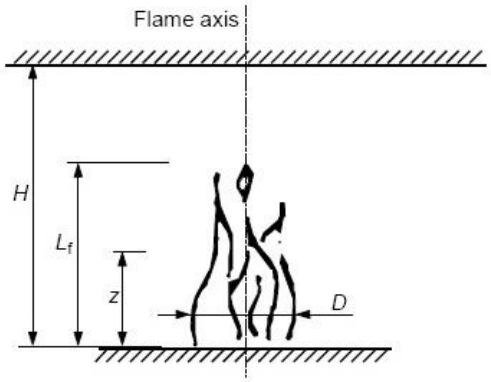

Figure 5.2 – Heskestad model

where

D is the diameter of the fire [m];

Q is the rate of heat release [W] of the fire according to E.4 of Annex E (EN 1991-1-2, 2004);

Q_c is the convective part of the rate of heat release [W], with Q_c = 0,8 Q by default;

z is the height [m] along the flame axis;

H is the distance [m] between the fire source and the ceiling;

The virtual origin z_0 of the axis is given by:

$$L_0 = -1.02 \cdot D + 0.00524 \cdot Q^{2/5} \quad [\text{m}] \tag{5.14}$$

5.2.2. Flame impacting the ceiling (Hasemi method)

Hasemi's method is a simple tool for the evaluation of the localised effect on horizontal elements located above the fire. It is based on the results of tests made at the Building Research Institute in Tsukuba, Japan (Hasemi & Tokunuga, 1984).

When the flame is impacting the ceiling ($L_f \geq H$; see Figure 5.3) the heat flux $\dot{h}\left[W/m^2\right]$ received by the fire exposed unit surface area at the level of the ceiling is given by :

$$\begin{aligned} \dot{h} &= 100000 && \text{if} && y \leq 0.30 \\ \dot{h} &= 136300 - 121000 \cdot y && \text{if} && 0.3 \leq y < 1.0 \\ \dot{h} &= 15000 \cdot y^{-3,7} && \text{if} && y \geq 1.0 \end{aligned} \tag{5.15}$$

where

y is a parameter [-] given by : $$y = \frac{r + H + z'}{L_h + H + z'} \tag{5.16}$$

r is the horizontal distance [m] between the vertical axis of the fire and the point along the ceiling where the thermal flux is calculated;

H is the distance [m] between the fire source and the ceiling;

L_h is the horizontal flame length given by the following relation:

$$L_h = \left(2.9 \cdot H \cdot {Q_H}^{*0.33}\right) - H \quad [m] \tag{5.17}$$

${Q_H}^*$ is a non-dimensional rate of heat release given by :

$${Q_H}^* = Q / \left(1.11 \cdot 10^6 \cdot H^{2.5}\right) \quad [-] \tag{5.18}$$

z' is the vertical position of the virtual heat source [m] and is given by:

$$z' = 2.4 \cdot D \cdot \left({Q_D}^{*2/5} - {Q_D}^{*2/3}\right) \quad \text{when} \quad {Q_D}^* < 1.0 \tag{5.19a}$$

$$z' = 2.4 \cdot D \cdot \left(1.0 - {Q_D}^{*2/5}\right) \quad \text{when} \quad {Q_D}^* < 1.0 \tag{5.19b}$$

where

$$Q_D^{*} = Q/\left(1.11\cdot 10^{6}\cdot D^{2.5}\right) \qquad [-] \qquad (5.20)$$

Q $[m]$

D $[W]$

The net heat flux $\dot{h}_{net}$ received by the fire exposed unit surface area at the level of the ceiling, is given by:

$$\dot{h}_{net} = \dot{h} - \alpha_c\cdot\left(\Theta_m - 20\right) - \Phi\cdot\varepsilon_m\cdot\varepsilon_f\cdot\sigma\cdot\left[\left(\Theta_m + 273\right)^4 - \left(293\right)^4\right] \qquad \left[W/m^2\right] \qquad (5.21)$$

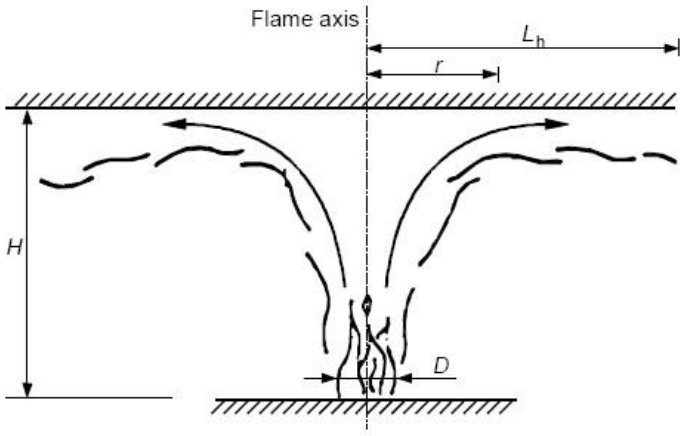

Figure 5.3 – Hasemi model

5.3. POST-FLASHOVER MODELS

A post-flashover fire within a compartment means that this compartment is completely engulfed in fire: all combustible materials are simultaneously burning (Leonardo Da Vinci Project, 2005). There are many simplified and advanced fire models. The most commons are:

5.3.1. Nominal Fire

The first represent only the post-flashover phase and are constituted by a monotone increasing curve (ISO, 1975). A standard formula is applicable for each compartment.

The standard temperature-time curve (Figure 5.4) is given by:

$$T_g = 345\cdot\log_{10}\left(8\cdot t + 1\right) + 20 \qquad [°C] \qquad (5.22)$$

where

t is time [min]

T_g is gas temperature in the fire compartment [°C]

$h = 25\,W/\left(m^2 K\right)$ is the coefficient of heat transfer by convection

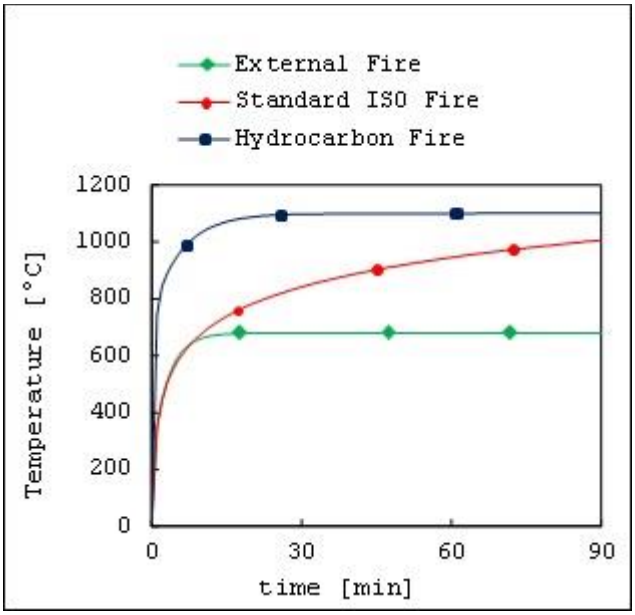

Figure 5.4 – Nominal Fire Curve

The external fire curve (Figure 5.4) is given by:

$$T_g = 660 \cdot \left(1 - 0.687 e^{-0.32 \cdot t} - 0.313 e^{-3.8 \cdot t}\right) + 20 \qquad [°C] \qquad (5.23)$$

where

t is time [min]

T_g gas temperature near the member [°C]

$h = 25\,W/\left(m^2 K\right)$ is the coefficient of heat transfer by convection

The hydrocarbon temperature-time curve (Figure 5.4) is given by

$$T_g = 1080 \cdot \left(1 - 0.325 e^{-0.167 \cdot t} - 0.675 e^{-2.5 \cdot t}\right) + 20 \qquad [°C] \qquad (5.23)$$

where

t is time [min]

T_g gas temperature near the member [°C]

$h = 50\ W/\left(m^2 K\right)$ is the coefficient of heat transfer by convection

5.3.2. Natural Simplified Fire Model

The parametric fire curves belong to the natural simplified models. The natural models are models that take into account a fire evolution more in line with real expected to occur in buildings. Annex A of the Eurocode **(EN 1991-1-2, 2004)** provides a simplified formula for parametric fire curves that is function of the opening factor, the fire load and the thermal inertia of the surrounding walls of the compartment. They have a cooling phase and a distinction is made between a fuel controlled and ventilation controlled fire.

5.3.3. Natural Advanced Fire Model

Two kinds of numerical models are available to model the real fires: multi zone models and field models. In the multi zone models, the fire compartment is divided into a hot zone, with a uniform temperature, above a fresh air zone and a fire plume that feeds the hot zone just above the fire. For each of the zones, the heat and mass balance is solved. Semi-empirical relations govern plume entrainment, irradiative heat exchange between zones and mass flow through openings to adjoining compartments. The application of this model is mainly in pre-flashover conditions, in order to know the smoke propagation in buildings.

Field models are also called Computational Fluid Dynamics (CFD) models. These models are based on two or three dimensional heat and mass transport, solving the equations of conservation of mass, momentum and energy for discrete points in the enclosed compartment. In this model, material properties and boundary conditions may be defined as the function of temperatures. Field models will provide accurate information about temperatures from the pieces of the fire room.

The complexity and the CPU time needed with field models allow few applications of such model in respect to fire resistance particularly for fully developed fire. In fire domain the use of field model is often reduced to the application of smoke movement.

Chapter 6

6. MATERIALS BEHAVIOUR

6.1. STEEL BEHAVIOUR UNDER FIRE

Steel has excellent strength properties at ambient temperature, however, like other materials, it changes its properties and loses its strength and stiffness at elevated temperature. The choice of an appropriate model of the stress-strain relationships is very important in the numerical analysis in the framework of the performance-based fire engineering (Crosti & Bontempi, 2008), (Gentili, et al., 2010).

The simplest models of stress-strain relationships are based on multi-linear approximations of the steel $\sigma-\varepsilon$ behaviour. However, multi-linear approximation tends to be somewhat coarse in representing the complex shape of the curve. Therefore, in order to more closely represent the steel behaviour usually a combination of linear and smooth curves is used, as for example the curves proposed by (Poh, 2001), (Anderberg, 1988), (EN 1993-1-2, 2005). Other curves are obtained by the fitting of experimental data. For example, Luecke et al. of the National Institute of Standards and Technology (NIST) (Luecke, et al., in press) proposed a stress-strain relationship based on the fitting of high-temperature tensile constitutive data for nine steel recovered from the collapse of the World Trade Center in 2001.

The temperature dependent properties that are important for modelling the fire response of steel structures include (a) thermal, (b) mechanical, and (c) deformation properties.

6.1.1. Thermal properties

The main thermal properties that influence the temperature rise are specific heat and thermal conductivity. Thermal properties determine the temperature profile in the steel sections resulting from the fire exposure. Eurocode, the ASCE manual and the report NIST NCSTAR 1-3D specify empirical relationships for thermal conductivity and specific heath as function of temperature (for details, see (ASCE, 1992), (EN 1993-1-2, 2005), (NIST, 2008). In these models, thermal

conductivity decreases with temperature in an almost linear fashion. On the contrary, the specific heat of steel increases with an increase in temperature with a large spike occurring around 750 °C.

- Specific heat

The specific heat capacity (also referred to just as specific heat) is the heat that a unit mass of a material should receive in order to increase its temperature of one degree. Specific heat capacity of a material can be calculated at a constant pressure or at a constant volume and is indicated as c_p or c_v respectively and is measured in [J/(kg·K)].

$$c_p = \frac{Q}{(m \cdot \Delta T)} \qquad [\mathrm{J \cdot kg^{-1} \cdot K^{-1}}] \qquad (6.1)$$

where

Q [J] is the heat energy

m [kg] is the mass of the material

ΔT [K] is the temperature of the material

The temperature of 735°C is called "Curie-temperature" and corresponds to the magnetic phase transition (Figure 6.1).

$$c_p = 425 + 7.73 \times 10^{-1} \cdot \Delta T - 1.69 \times 10^{-3} \cdot \Delta T^2 + 2.22 \times 10^{-6} \cdot \Delta T^3 \quad 20°C \le \Delta T < 600°C \quad (6.2a)$$

$$c_p = 666 - \left(\frac{13002}{\Delta T - 738} \right) \quad 600°C \le \Delta T < 735°C \quad (6.2b)$$

$$c_p = 545 - \left(\frac{17820}{\Delta T - 731} \right) \quad 735°C \le \Delta T < 900°C \quad (6.2c)$$

$$c_p = 650 \quad 900°C \le \Delta T < 1200°C \quad (6.2d)$$

In simple calculation models the specific heat may be considered to be independent of the steel temperature with the following average value

$$c_p = 600 \qquad [\mathrm{J \cdot kg^{-1} \cdot K^{-1}}] \qquad (6.3)$$

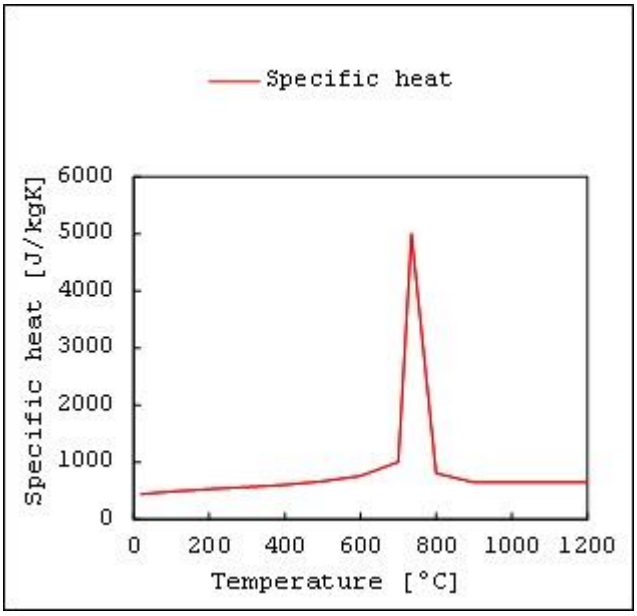

Figure 6.1 - Variation of the specific heat capacity of carbon steel (adapted from (EN 1993-1-2, 2005))

- Thermal conductivity

The thermal conductivity is a property of the materials, which describes their ability to conduct heat. It is defined as the heat that crosses in one second a unit of thickness of a given material, due to a unit difference of temperature along the thickness. It is indicated in the following with the symbol λ and has the unit of measure of a thermal power per meter per Kelvin [W/(m·K)].

$$\lambda = \frac{Q}{(d \cdot \Delta T \cdot \Delta t)} \qquad \text{[W/(m·K)]} \qquad (6.4)$$

where:

Q *[J]* is the heat energy;

d [m] is the thickness of the material;

ΔT *[K]* is the temperature of the material surface;

Δt *[s]* is the time.

The higher the conductivity, the shorter the time needed for the heat to penetrate the element. This time is not only affected by the conductivity of the material, but also by the thickness of the element to be penetrated. This is described by the thermal conductance α_c (for conductivity), which can be obtained by the ratio between the conductivity and the element thickness and which is measured in [W/K].

$$\alpha_c = \frac{\lambda}{d} \tag{6.5}$$

Steel has a quite high conductivity in comparison with other construction materials (eg. concrete), so that when one side of a steel element is exposed to fire, the opposite side is quickly heated. Furthermore, steel elements used in construction have typically quite slender profiles, so that thickness to be crossed by the heat flow for heating the profile is quite low. The low thermal conductance, which is the result of a high conductivity and a small thickness, is the reason why the temperature of a steel element exposed to fire can be considered to be constant along the profile. The discontinuity in the variation of the conductivity is due to a modification of the lattice of the steel, which moves from the ferritic to austenitic phase around this temperature (Figure 6.2).

The thermal conductivity of steel may be determined from the following:

$$\lambda_a = 54 - 3.33 \times 10^{-2} \cdot \Delta T \qquad 20°C \le \Delta T \le 800°C \tag{6.6a}$$

$$\lambda_a = 27.3 \qquad 800°C \le \Delta T \le 1200°C \tag{6.6b}$$

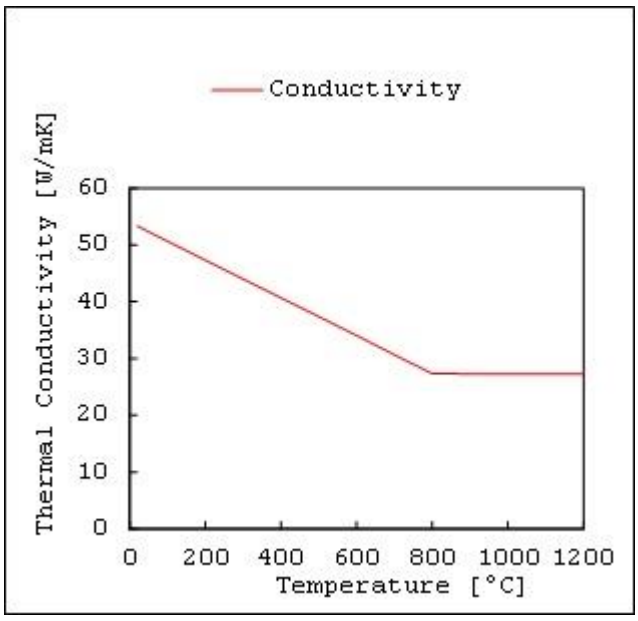

Figure 6.2 - Variation of the thermal conductivity of the carbon steel (adapted from (EN 1993-1-2, 2005))

In simple calculation models the thermal conductivity may be considered to be independent of the steel temperature with the following average value

$$\lambda_a = 45 \qquad \text{[W/mK]} \tag{6.7}$$

6.1.2. Mechanical properties

When designing steel elements without fire, an elastic-perfectly plastic constitutive law is generally assumed. This is a reasonable assumption, since the stress-strain diagram of mild steel at 20 °C shows a well-defined yielding point followed by a plateau. This means that the stiffness of the material suddenly drops to zero and plastic irreversible deformations occurs after that. If the hardening branch is neglected on the safe side, the plateau can be extended up to 20-25% strain, thanks to the high ductility of the steel (Giuliani, 2011).

When the steel is heated, not only are the mechanical properties deteriorating, but also the stress-strain diagram changes: after an initial elastic response, the stiffness decreases progressively with the deformation, so that a smooth curve precedes the plateau. A yielding point cannot be identified anymore and the curve becomes smoother and smoother as the temperature of the steel gets higher (Figure 6.3 right).

Different test regimes were used to obtain yield strength and elastic modulus of steel at elevated temperature. The variations in test parameters resulted in different test measurements, thereby leading to differences in the existing relationships.

Figure 6.3 shows the constitutive law proposed by Eurocode. Eurocode distinguishes between two strength limits: the proportionality limit, and the yield limit. The proportionality limit represents the end of the linear portion of the stress-strain curve, after which point the stress-strain relation remain elastic but becomes nonlinear. The yield limit is the point after which the relationship becomes both nonlinear and inelastic.

Steel Temperature T	$k_{E,T}=\frac{E_T}{E}$	$k_{P,T}=\frac{\sigma_{p,T}}{\sigma_p}$	$k_{y,T}=\frac{\sigma_{y,T}}{\sigma_y}$
20	1.0	1.0	1.0
100	1.0	1.0	1.0
200	0.9	0.807	1.0
300	0.8	0.613	1.0
400	0.7	0.420	1.0
500	0.6	0.360	0.78
600	0.31	0.180	0.47
700	0.13	0.075	0.23
800	0.09	0.050	0.11
900	0.0675	0.0375	0.06
1000	0.045	0.025	0.04
1100	0.0225	0.0125	0.20
1200	0	0	0

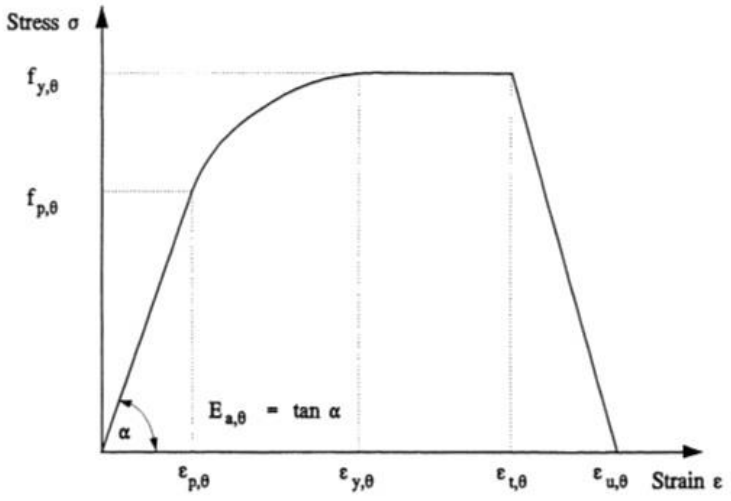

Figure 6.3 – Stress-strain relationship for structural steel adapted from (EN 1993-1-2, 2005)

It is important to note that the theory behind introducing proportionality limit in the Eurocode stress-strain curves is to capture viscoelastic behaviour that is partly due to creep effect. This simplification enables the stress-strain curves of the Eurocode to partly account for high temperature creep strain at elevated temperature (Kodur & Dwaikat, 2010).

Figure 6.4 shows the variation of yield strength and modulus of elasticity with temperature proposed by Eurocode 3, ASCE model, and the NIST model. The equations are detailed in the scheme in Table 6.1. It can be noted that there are considerable variations: Eurocode model provides a higher reduction in elastic modulus, while the NIST model propose a very small reduction of elastic modulus compared to the other two; Eurocode predicts less reduction in yield strength and assumes no reduction in steel yield strength up to 400 °C, while ASCE and NIST models assume a loss around of 30% at the same temperature.

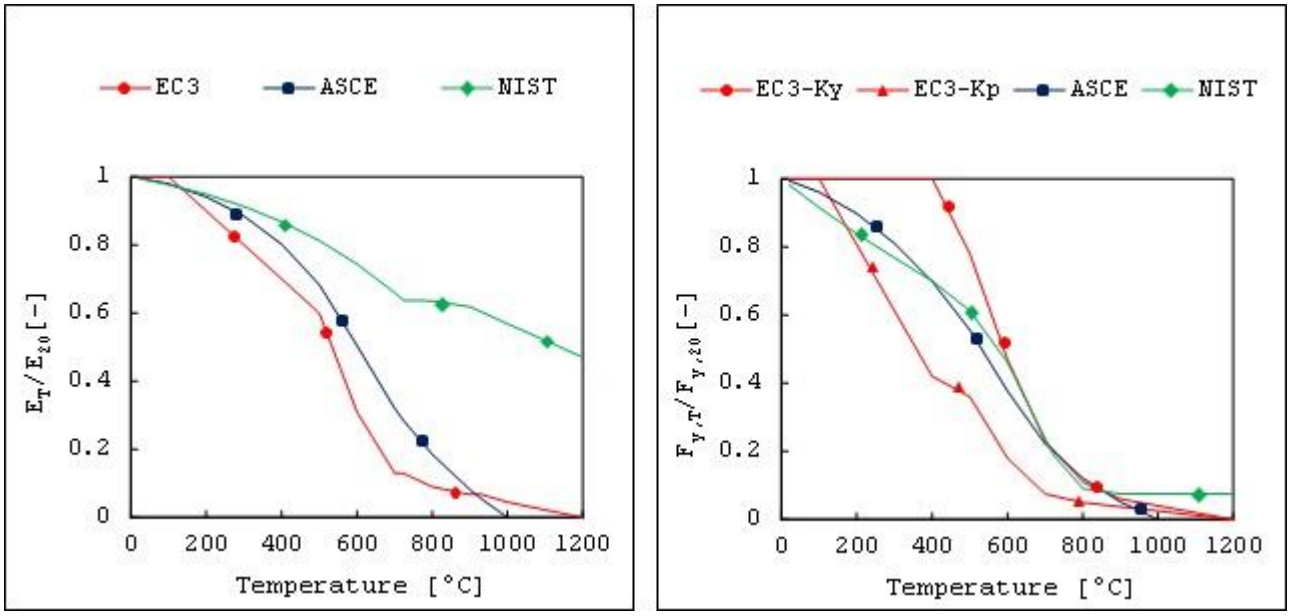

Figure 6.4 - Young's modulus and yield strength with temperature. Comparison of the values proposed by EC3, NIST and ASCE

6.1.3. Deformation properties

The deformation properties that influence the fire response of steel structures are thermal strain and high temperature creep. Thermal strain of steel increases with temperature up to nearly 750 °C at and minimal differences exist between the models proposed by Eurocode, NIST and ASCE. Creep is defined as the time-dependent plastic strain under constant stress and temperature. Creep strains occur due to movement of dislocations in the slip plane. Normally, steel composition contains a

variety of defects that act as obstacles to dislocation motion. At room temperature, the amount and distribution of these defects remain almost uniform; therefore, creep deformations occur at very slow time pace. However, at high temperature, vacancies in the crystal structure can diffuse and cause the dislocation to move faster to an adjacent slip plane; thus allowing for more deformation to occur. Therefore, creep deformations accelerate with increase in temperature. The temperature range in which creep deformation may occur differs in various materials. For steel, creep strain becomes evident at around 400 °C, that is around 30% of its melting point (1400 °C). Thermal expansion is the tendency of materials to change in volume in response to a change in temperature. The degree of expansion divided by the change in temperature is called the material's coefficient of thermal expansion and varies with temperature. The linear thermal expansion coefficient α of steel and the relative thermal elongation ε_{ther} can be determined from the following (Figure 6.5):

$$\alpha = \frac{\varepsilon_{ther}}{\Delta T} \tag{6.8}$$

$$\varepsilon_{ther} = 1.2\times10^{-5}\cdot\Delta T + 0.4\times10^{-8}\cdot\Delta T^2 - 2.416\times10^{-4} \qquad 20°C \le \Delta T < 750°C \tag{6.9a}$$

$$\varepsilon_{ther} = 1.1\times10^{-2} \qquad 750°C \le \Delta T \le 860°C \tag{6.9b}$$

$$\varepsilon_{ther} = 2\times10^{-5}\cdot\Delta T - 6.2\times10^{-3} \qquad 860°C < \Delta T \le 1200°C \tag{6.9c}$$

where:

ΔT [K] is the temperature increment of the material

ε_{ther} [-] is the relative elongation of the element $\Delta L/L$

ΔL [m] is the elongation of the element

L [m] is the initial length of the element

In sample calculation models the relationship between thermal elongation and steel temperature may be considered to be linear with the following

$$\varepsilon_{ther} = 14\times10^{-6}\cdot\Delta T \tag{6.10}$$

6.1.4. Influence of creep

Even if high temperature creep has a significant influence on the fire response of steel members, a review of literature clearly indicates that the effect of creep on the fire response of steel members did not receive much attention. Much of the reported creep studies were mainly focused at the material level (see for example (Dorn, 1955), (Harmathy, 1967), (Williams-Leir, 1983)), and very

little information is available on the effects of high temperature creep on the global structural response. An investigation on the influence of creep strain on fire response of steel beams was carried out by (Anderberg, 1988). However, the small scale simply supported beams used in his study (L=1.15 m) do not represent any realistic condition as encountered in practice. Even if Anderberg found that creep has significant influence on the fire response of steel beams, his results cannot be generalized.

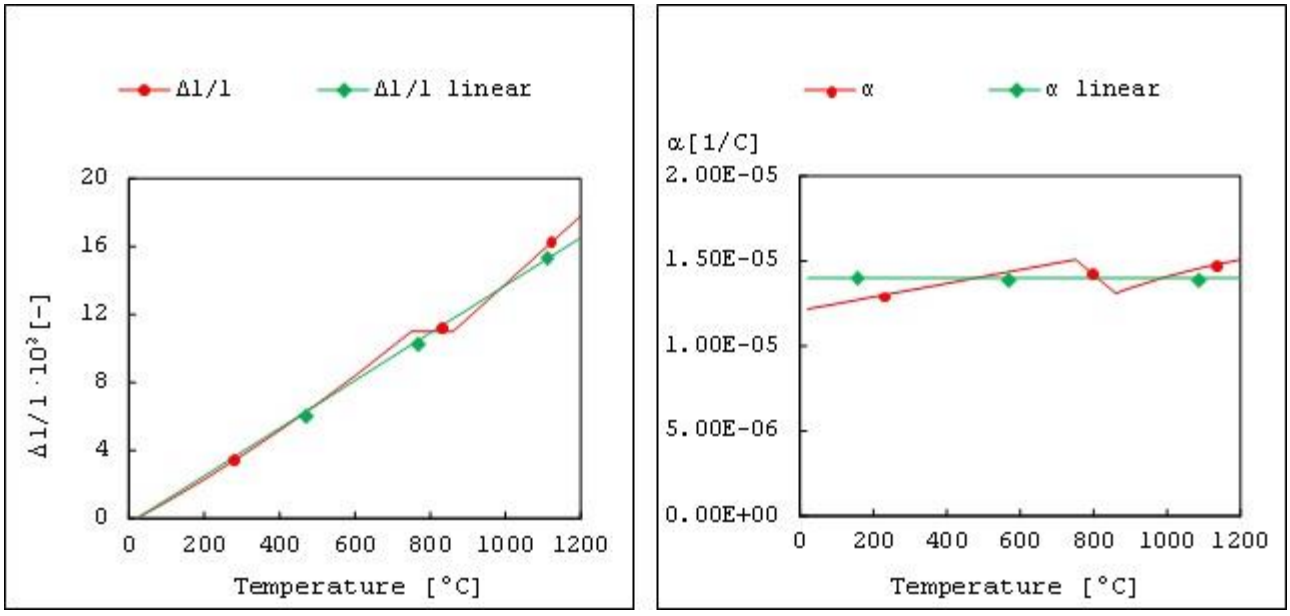

Figure 6.5 – Variation of the relative elongation of the carbon steel (adapted from EN19931-2-:2007)

The stress-strain relationships suggested in standards and codes consider the creep deformation in different ways. Eurocode 3 states that "the effects of transient thermal creep need not to be given explicit consideration" (clause 4.3.3(4) of EN 1993-1. This suggests that some consideration to creep has been given in the constitutive model. In fact, the case studies will show that the curves have been created in such a way that part of the viscoelastic deformation is caught. The ASCE model is not able to take into account creep deformation. For this reason the ASCE manual of practice states that high temperature creep should be accounted for in fire resistance analysis trough one of two options.

The first option is to use "effective" temperature stress-strain temperature curves derived from transient-state tests at relevant heating and strain rates (ASCE, 1992), (Buchanan, 2002). The second option is to use specific high-temperature creep models developed from structural steel. It is left to the user to choose which creep model to use.

Table 6.1 - Temperature stress-strain relationships for structural steel as for Eurocode 3, ASCE and NIST models

	Eurocode 3 (2005)	ASCE (1992)	NIST (2011)

Temperature σ-ε relationships

$$\sigma_s = \begin{cases} \varepsilon \le \frac{F_{p,T}}{E_{s,T}} \\ E_{s,T}\cdot\varepsilon \\ \frac{F_{p,T}}{E_{s,T}} < \varepsilon < c_1 \\ F_{p,T} - c + \frac{b}{a}\sqrt{a^2-(c_1-\varepsilon)^2} \\ c_1 < \varepsilon < c_3 \; and \; T < 400℃ \\ \frac{(F_{u,T}-F_{y,T})\varepsilon + c_3F_{y,T} - c_1F_{u,T}}{(c_3-c_1)} \\ c_3 < \varepsilon < c_4 \; and \; T < 400℃ \\ F_{u,T} \\ c_4 < \varepsilon < c_5 \; and \; T < 400℃ \\ F_{u,T}\frac{(c_5-\varepsilon)}{(c_5-c_4)} \\ c_2 < \varepsilon \le c_4 \; and \; T \ge 400℃ \\ F_{y,T} \\ c_4 < \varepsilon < c_5 \; and \; T \ge 400℃ \\ F_{y,T}\left[1-\frac{(\varepsilon-c_2)}{(c_3-c_2)}\right] \\ \varepsilon \ge c_5 \\ 0.0 \end{cases}$$

$$a^2 = \left(c_1 - {}^{F_{p,T}}\!/_{E_{s,T}}\right)\left(c_1 - {}^{F_{p,T}}\!/_{E_{s,T}} + {}^{c}\!/_{E_{s,T}}\right)$$

$$b^2 = c\left(c_1 - {}^{F_{p,T}}\!/_{E_{s,T}}\right)E_{s,T} + c^2$$

$$c = \frac{\left(F_{y,T}-F_{p,T}\right)^2}{\left(c_1 - {}^{F_{p,T}}\!/_{E_{s,T}}\right)E_{s,T} - 2\left(F_{y,T}-F_{p,T}\right)}$$

$$\sigma_s = \begin{cases} \varepsilon \le \varepsilon_p \\ E_{s,T}\cdot\varepsilon \\ \varepsilon > \varepsilon_p \\ (c_1\cdot\varepsilon + c_2)F_{y,T} - \frac{c_3\cdot F_{y,T}^2}{E_{s,T}} \end{cases}$$

$$\sigma = K(T)\left(\frac{\dot{\varepsilon}}{\dot{\varepsilon}_0}\right)^{m(T)}\varepsilon^{n(T)}$$

$$K(T) = k_0 exp\left(-\left(\frac{T}{k_2}\right)^{k_1}\right)$$

$$n(T) = n_0 exp\left(-\left(\frac{T}{n_2}\right)^{n_1}\right)$$

$$m(T) = m_0 + m_1 exp\left(\frac{T}{m_2}\right)$$

$k_0 = 799.9; k_1 = 4.566;\; k_2 = 561.35$
$n_0 = 0.228;\; n_1 = 4.1799; n_2 = 623.49;$
$m_0 = 0.007583;\; m_1 = 0.000389; m_2 = 121$

Elastic modulus

$$\frac{E_{s,T}}{E_s} = \begin{cases} 1 & T < 100℃ \\ c_6T + c_7 & 100\,℃ \le T < 500℃ \\ c_8T + c_9 & 600\,℃ \le T < 700℃ \\ c_{10}T + c_{11} & 700\,℃ \le T < 800℃ \\ c_{12}T + c_{13} & 800\,℃ \le T < 1200℃ \\ c_{14}T + c_{15} & 1200\,℃ \le T \\ 0.0 \end{cases}$$

$$\frac{E_{s,T}}{E_s} = \begin{cases} 1 + \frac{T}{c_9 ln\left(\frac{T}{c_{10}}\right)} & T \le 600℃ \\ \frac{c_{11} - c_{12}T}{T - c_{13}} & T > 600℃ \end{cases}$$

T<723 ℃
$E(T) = e_0 + e_1T + e_2T^2 + e_3T^3$
T>910 ℃
$E(T) = \gamma_1(1-(T-\gamma_2)\gamma_3)$
723 ≤T≤ 910 ℃
$E(T) = E(723) + \frac{E(910)-E(723)}{910-723}(T-723)$

Strength

$$\frac{F_{y,T}}{F_y} = \begin{cases} 1 \\ c_{28}T + c_{29} \\ c_{30}T + c_{31} \\ c_{32}T + c_{33} \\ c_{34}T + c_{35} \\ c_{36}T + c_{37} \\ c_{38}T + c_{39} \\ 0.0 \end{cases} \quad \frac{F_{p,T}}{F_y} = \begin{cases} 1 & T < 100℃ \\ c_{16}T + c_{17} & 100\,℃ \le T < 400℃ \\ c_{18}T + c_{19} & 400\,℃ \le T < 500℃ \\ c_{20}T + c_{21} & 500\,℃ \le T < 600℃ \\ c_{22}T + c_{23} & 600\,℃ \le T < 700℃ \\ c_{24}T + c_{25} & 700\,℃ \le T < 800℃ \\ c_{26}T + c_{27} & 800\,℃ \le T < 1200℃ \\ 0.0 & 1200\,℃ \le T \end{cases}$$

$$\frac{F_{y,T}}{F_y} = \begin{cases} 1 + \frac{T}{c_4 ln\left(\frac{T}{c_5}\right)} & T \le 600℃ \\ \frac{c_6 - c_7T}{T - c_8} & T > 600℃ \end{cases}$$

$c_1 = 0.02; c_2 = 0.02; c_3 = 0.04; c_4 = 0.15; c_5 = 0.20;$
$c_6 = 1x10^{-3}; c_7 = 1.1; c_8 = 2.9x10^{-3}; c_9 = 2.05; c_{10} = -1.8x10^{-3}; c_{11} = 1.39; c_{12} = 4x10^{-4}; c_{13} = 0.41;\; c_{14} = -2.25x10^{-4};\; c_{15} = 0.27; c_{16} = -1.933x10^{-3};\; c_{17} = 1.193$
$c_{18} = -0.6x10^{-3};\; c_{19} = 0.66;\; c_{20} = -1.8x10^{-3};\; c_{21} = 1.26;$
$c_{22} = -1.05x10^{-3}; c_{23} = 0.81;\; c_{24} = -2.5x10^{-4};\; c_{25} = 0.25;\; c_{26} = -1.25x10^{-4};\; c_{27} = 0.15;\; c_{28} = 2.2x10^{-3}; c_{29} = 1.88;\; c_{30} = -3.1x10^{-3}2.05;\; c_{31} = 2.33;\; c_{32} = -2.4x10^{-3};\; c_{33} = 1.91;\; c_{34} = -1.2x10^{-3};\; c_{35} = 1.07;\; c_{36} = -5x10^{-4}2.05;\; c_{37} = 0.51;\; c_{38} = -2x10^{-4};\; c_{39} = 0.24;\; c_{40} = 1.25;\; c_{41} = -2.5x10^{-3};\; c_{42} = 2$

$c_1 = 12.5; c_2 = 0.975; c_3 = 12.5; c_4 = 900; c_5 = 1750; c_6 = 340; c_7 = 0.34; c_8 = 240; c_9 = 2000; c_{10} = 1100; c_{11} = 690; c_{12} = 0.69; c_{13} = 53.5$

$e_0 = -0.04326$ GPa/°C; $e_1 = 3.502x10^{-5}$GPa/(°C)^2
$e_2 = -6.592 \times 10^{-8}\frac{\text{GPa}}{(℃)^3}$; $\gamma_1 = 216$ GPa; $\gamma_2 = 26.85℃; \gamma_3 = 4.7 \times 10^{-4}℃$

The model developed by (Luecke, et al., in press) of the National Institute of Standards and Technology (NIST model) considers the high temperature steel deformation behavior with a stress-strain relationship that explicitly depends on the strain rate $\dot{\varepsilon}$ and is able to capture together the work hardening and the strain rate sensitivity.

Figure 6.6 shows the temperature stress-strain curves from Eurocode 3, ASCE manual and NIST paper at room temperature and at 500 °C respectively. The y-axis represents normalized stress and the x-axis represents strain. As discussed, these relations account for specific features, such as the yield plateau and the effect of strain hardening. Moreover NIST relationship, depending on the strain rate, explicitly takes into account the creep deformation at elevated temperature. It can be noted that the creep effect at room temperature is almost negligible, and the two NIST curves are almost coincident, while it becomes significant at elevated temperature.

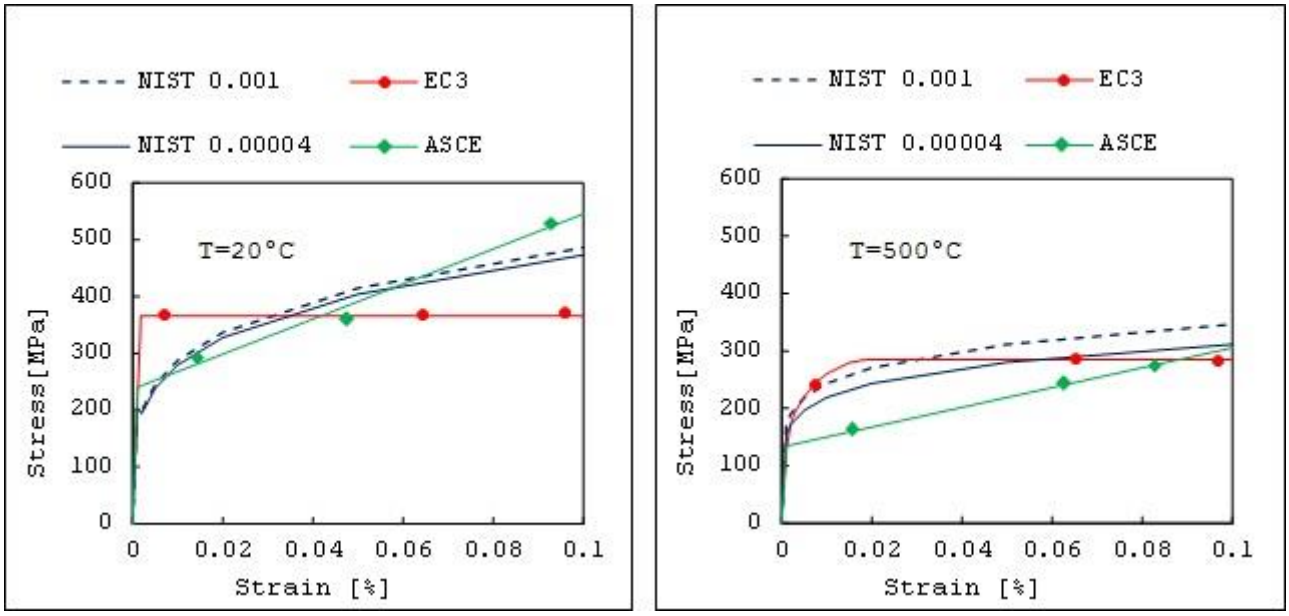

Figure 6.6 - Temperature stress-strain relationships at room temperature and for T=500 C as for Eurocode 3, ASCE and NIST models

6.2. CONCRETE BEHAVIOUR UNDER FIRE

Reinforced concrete structures are generally considered to perform well in case of fire due to the thermal properties of concrete and the protection offered to the reinforcement. This is only partially true, as witnessed by some examples of fire-induced collapse of concrete buildings (Meacham, et al., 2010), (NILIM, 2005), (Gann, 2008).

As a matter of fact, the temperature that should not be exceeded for a full recovery of an ordinary, not fire proof concrete is relatively low (ca. 300°C). At this temperature micro-cracks develop as a consequence of material dehydration and thermal expansion of the aggregates: at this point the strength loss is permanent, leading to high costs of repairing even in case the structure survives the fire without any collapse (Hertz, 2005), (Hertz, 2003).

For this reason, in addition to the evaluation of the response during a fire, the residual performances of concrete elements after a fire are also important criteria to be considered in view of an efficient and sustainable design of concrete structures (Shipp, 2007), (ISO 15392, 2008).

Even if the need of assessing and classify the damage level of a structure after a fire or a damaging event is recognized by most researchers and practitioners operating in the field (Portland Cement Association, 1994), (Concrete Society, 2008), (Wang, et al., 2010), (Sgambi, et al., 2012), no or very little indications on how to do that to be found in the European codes to date. Many different parameters are considered in literature as indicators of the severity of the fire damage (Gustaferro, 1983), (Anderberg, 2009), (Guo & Shi, 2011), (Annerel & Taerwe, 2011). They generally refer to the condition either of the concrete (cracking, spalling) or of the reinforcement (temperature, yielding). Further, there is the possibility of evaluating the fire damage just by means of a visual inspection (e.g. color or sound of the concrete, amount of concrete that has fallen down, deflection or permanent deformation of the element etc.) or by carrying out a deeper investigation on the structural element (depth of burnt concrete, reduction of the effective cross section, temperature field, etc.). Finally, the properties of the damaged element can be evaluated at a sectional level (moment capacity, curvature, residual effective area, etc.), but could also be referred to the whole element (load bearing capacity, stiffness. mid-span displacements) or in some cases to the whole structure (global load bearing capacity, stiffness matrix, displacement at the top of the building, etc.). A final aspect in the assessment of indicators capable of accounting for the damage caused by a fire on a structural element concerns the time at which the damage is evaluated, i.e. at the end of the fire or after the fire is extinguished. Usually different severity grades of the fire are considered, mostly in the form of increasing durations of a standard fire. In this way, a general regularity in the increment of the damage with the severity can be checked and a critical time of exposure for the element can be identified when an abrupt decrement of the considered indicator occurs. However, a time that exceeds the duration of the fire is hardly considered in literature studies and the performances of the concrete elements are usually evaluated in a situation when the steel is the hottest (hot condition) and the concrete core is cold. This situation does not represent the permanent damages after the fire is extinguished, nor always account for the highest reduction of the element

performances. The latter is the case, for example, for most tall concrete section, where: the strength reduction of the concrete core, which generally occurs when the bottom reinforcement has already cooled down (cold condition), may be more significant than the steel strength reduction in the hot condition (Hertz, 2005).

6.2.1. Thermal properties

- Specific heat

For both siliceous and calcareous aggregates, the specific heat c_p may be determined from the following:

$$c_p = 900 \qquad 20°C \le \Delta T < 100°C \qquad (6.11a)$$

$$c_p = 900 + (\Delta T - 100) \qquad 100°C \le \Delta T < 200°C \qquad (6.11b)$$

$$c_p = 1000 + \frac{(\Delta T - 200)}{2} \qquad 200°C \le \Delta T < 400°C \qquad (6.11c)$$

$$c_p = 1100 \qquad 400°C \le \Delta T < 1200°C \qquad (6.11d)$$

In order to consider the influence of moisture, it is necessary consider a $c_{p,peak}$ situated between 100°C and 115°C as Figure 6.7 shows.

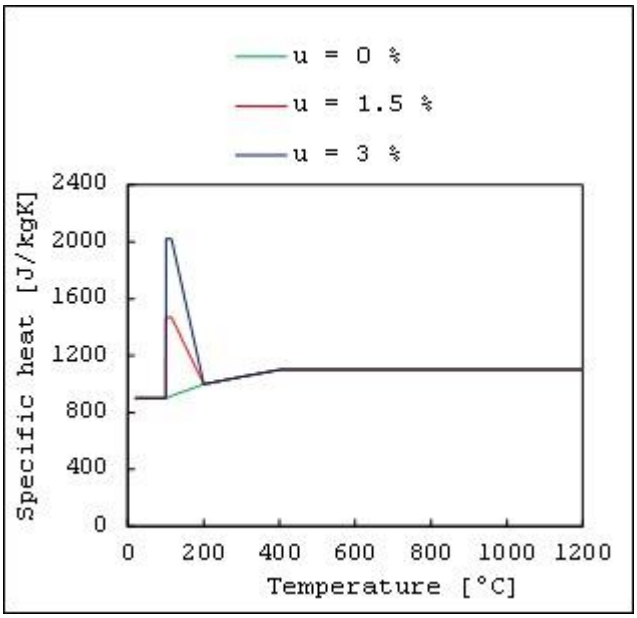

Figure 6.7 – Specific heat of concrete (adapted from (EN 1992-1-1, 2004)

- Thermal conductivity

Eurocode provides fields of acceptability with regard to the thermal conductivity λ_c. The upper limit may be determined from:

$$\lambda_c = 2 - 0.2451 \cdot \left(\frac{\Delta T}{100}\right) + 0.010754 \cdot \left(\frac{\Delta T}{100}\right)^2 \qquad 20°C \le \Delta T \le 1200°C \qquad (6.12)$$

The lower limit may be determined from:

$$\lambda_c = 1.36 - 0.136 \cdot \left(\frac{\Delta T}{100}\right) + 0.0057 \cdot \left(\frac{\Delta T}{100}\right)^2 \qquad 20°C \le \Delta T \le 1200°C \qquad (6.13)$$

6.2.2. Mechanical properties

Eurocode provides a relationship the temperature dependent stress-strain relationship for heating rates between 2 and 50 K/min. It assumes that the heating rates normally fall within the specified limits.

- Compressive behaviour

The stress-strain relationship given in Figure 6.9 (left) is defined by two parameters:

- the compressive strenght $f_{ct;}$
- the strain $\varepsilon_{cu,T}$ corresponding to f_{ct}.

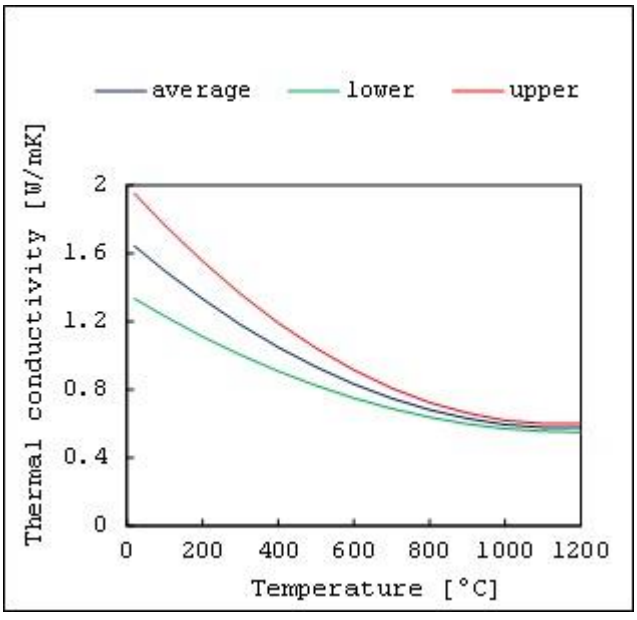

Figure 6.8 – Thermal conductivity of concrete (EN 1992-1-1, 2004)

The reduction factors in function of the temperature (Figure 6.9 right) allow finding stress-strain relationships.

Tensile behaviour

Conservatively the tensile strength of concrete may be assumed to be zero. If tensile strength is taken into account in verifications carried out with an advanced calculation model, it should not exceed the values proposed in Figure 6.10.

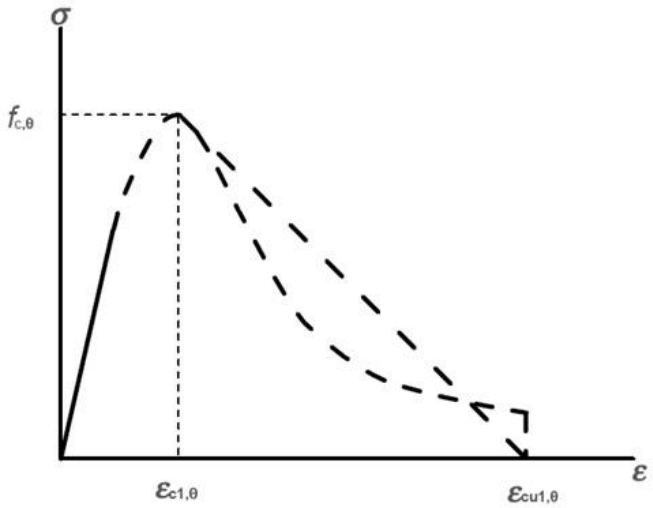

Concrete temp. θ	Siliceous aggregates			Calcareous aggregates		
	$f_{c,\theta}/f_{ck}$	$\varepsilon_{c1,\theta}$	$\varepsilon_{cu1,\theta}$	$f_{c,\theta}/f_{ck}$	$\varepsilon_{c1,\theta}$	$\varepsilon_{cu1,\theta}$
[°C]	[-]	[-]	[-]	[-]	[-]	[-]
1	2	3	4	5	6	7
20	1,00	0,0025	0,0200	1,00	0,0025	0,0200
100	1,00	0,0040	0,0225	1,00	0,0040	0,0225
200	0,95	0,0055	0,0250	0,97	0,0055	0,0250
300	0,85	0,0070	0,0275	0,91	0,0070	0,0275
400	0,75	0,0100	0,0300	0,85	0,0100	0,0300
500	0,60	0,0150	0,0325	0,74	0,0150	0,0325
600	0,45	0,0250	0,0350	0,60	0,0250	0,0350
700	0,30	0,0250	0,0375	0,43	0,0250	0,0375
800	0,15	0,0250	0,0400	0,27	0,0250	0,0400
900	0,08	0,0250	0,0425	0,15	0,0250	0,0425
1000	0,04	0,0250	0,0450	0,06	0,0250	0,0450
1100	0,01	0,0250	0,0475	0,02	0,0250	0,0475
1200	0,00	-	-	0,00	-	-

Figure 6.9 – Compressive strength of concrete in function of temperature (EN 1992-1-1, 2004)

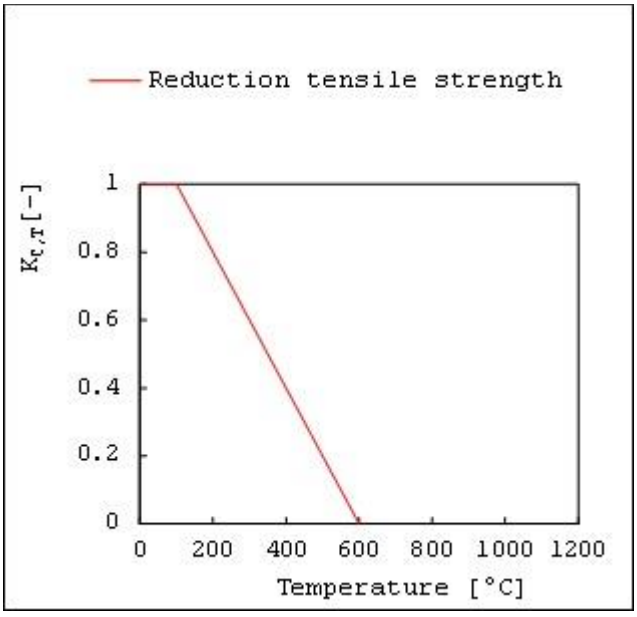

Figure 6.10 – Reduction of tensile strength as function of temperature (EN 1992-1-1, 2004)

6.2.3. Deformation properties

The thermal elongation $\frac{\Delta L}{L}$ of concrete may be determined from the following:

Siliceous aggregates:

$$\frac{\Delta L}{L} = -1.8\times10^{-4} + 9\times10^{-6}\cdot\Delta T + 2.3\times10^{-11}\cdot\Delta T^3 \qquad 20°C \le \Delta T < 700°C \qquad (6.14a)$$

$$\frac{\Delta L}{L} = 14\times10^{-3} \qquad 700°C \le \Delta T \le 1200°C \qquad (6.14b)$$

Calcareous aggregates:

$$\frac{\Delta L}{L} = -1.2\times10^{-4} + 6\times10^{-6}\cdot\Delta T + 1.4\times10^{-11}\cdot\Delta T^3 \qquad 20°C \le \Delta T < 805°C \qquad (6.15a)$$

$$\frac{\Delta L}{L} = 12\times10^{-3} \qquad 805°C \le \Delta T \le 1200°C \qquad (6.15b)$$

In simple calculation models the relationship between thermal elongation and concrete temperature may be considered to be linear:

$$\frac{\Delta L}{L} = -1.8\times10^{-6}\cdot\Delta T \qquad (6.16)$$

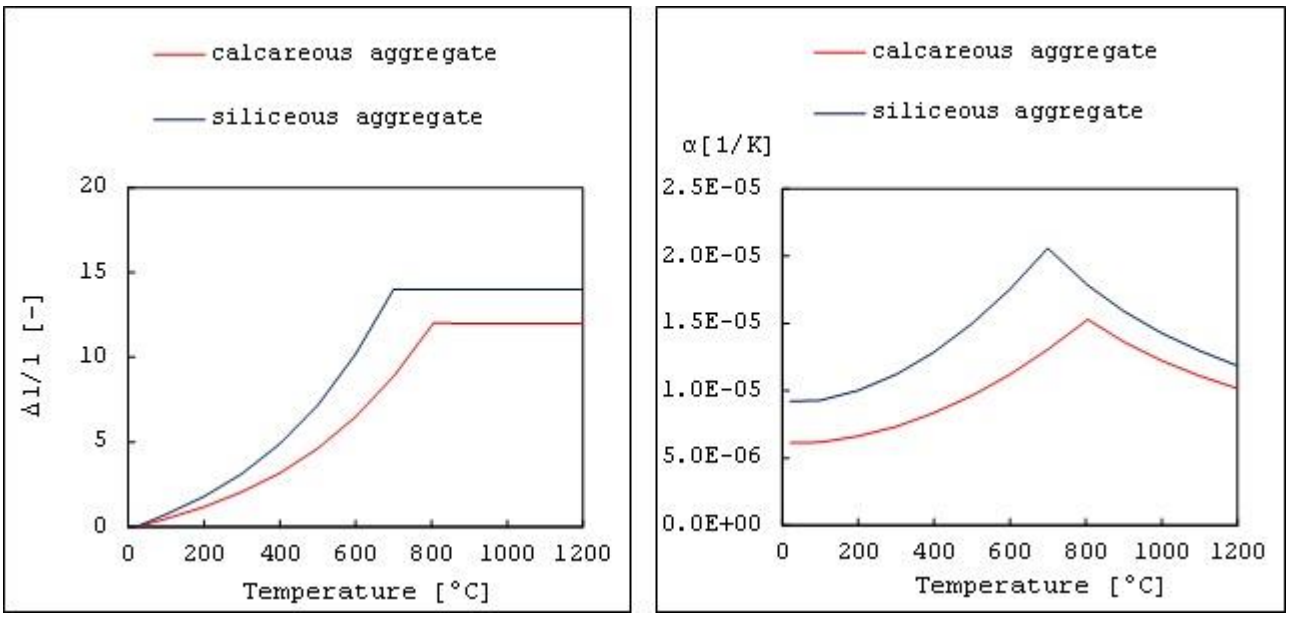

Figure 6.11 – Thermal elongation of concrete as function of the temperature (EN 1992-1-1, 2004)

Chapter 7

7. STRUCTURAL BEHAVIOUR

7.1. ISOLATED STEEL ELEMENTS

Behaviour of steel structure in fire is dominated by the effects of material degradation, eigenstresses induced by hindered thermal expansion and large deflections and runaway resulting from the action of imposed load on the weakened structure. If the consideration of material degradation is well established in all fire verifications, the effects of eigenstresses can be only partially accounted when fire verifications are limited to single elements. The effects of large deflections, due to the difficulties of being integrated in simple verification methods, are mostly completely disregarded in usual prescriptive-based fire design. It seems difficult to a-priori evaluate if and to which extend the lack of a punctual consideration of these aspects leads to an over-conservative design, e.g. for the triggering of a catenary action or may instead lead to unsafe collapse mechanisms, e.g. in case of a particularly unfortunate combination of actions, or after the required time of resistance, when fire design is performed using a nominal fire and a prescribed resistance class for the elements (Hertz, 2006). Aim of this paragraph is to highlight how some basic mechanisms can be triggered or modified by the presence of fire on part of a structural system, such as bowing effects and buckling.

7.1.1. Bowing effect

The study of the collapse of a simply supported steel beam under fire is presented below (Figure 7.1). The beam, of 4 m in length, is an IPE 500 and is loaded at mid-span with a vertical force of 450 kN, sufficient to determine the yield strength. A standard fire is applied on the beam and the results in term of displacement of the central node and of roller obtained with ABAQUS (ABAQUS, 2010) are presented. As expected and described in literature (Petterson, et al., 1976), the beam moveable support slides outwards as consequence of the beam thermal expansion in the beginning, then starts to move backwards when the vertical displacement becomes larger due to the material degradation and the effect of is prevailing on the thermal expansion. It is interesting to point out how neglecting the coupling between horizontal and vertical displacement due to large

displacements (Figure 7.2), would not just lead to an approximated evaluation of the displacement, but would result in a complete different collapse configuration.

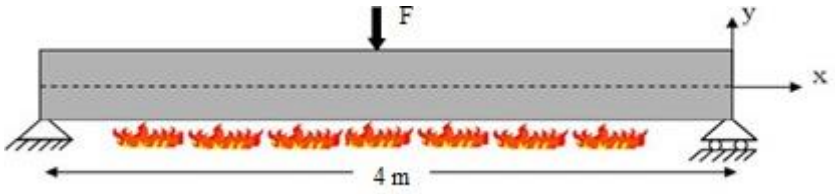

Figure 7.1– Single pinned beam studied

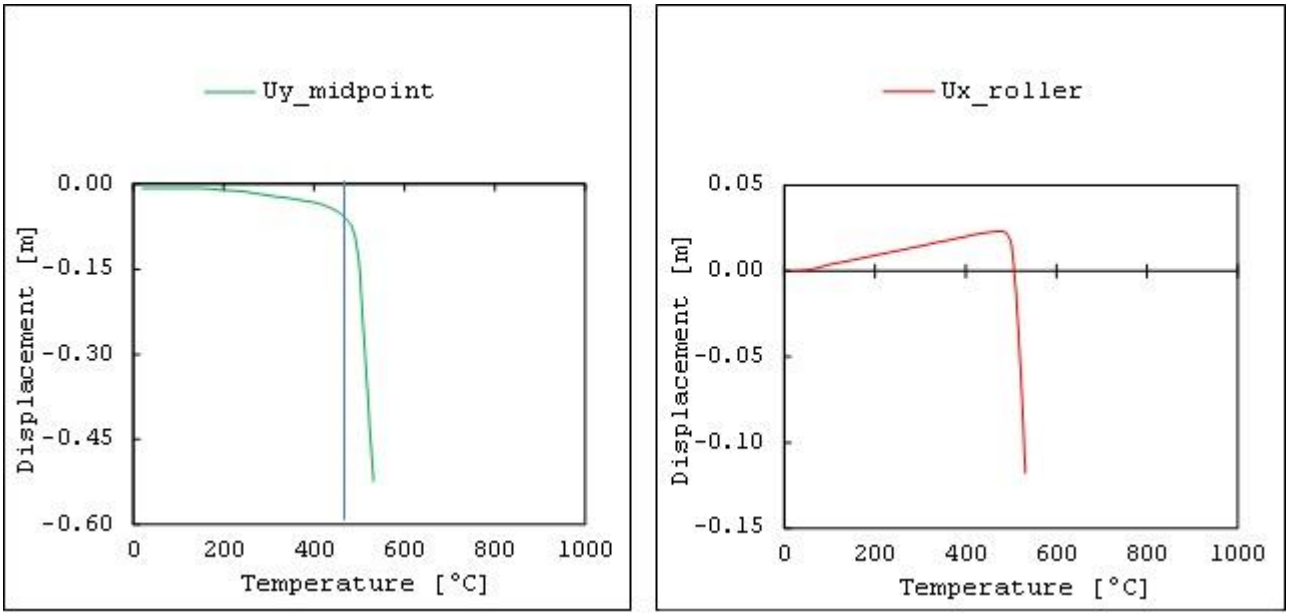

Figure 7.2 - Vertical (midspan) and horizontal (roller) displacements of a centrally loaded beam under fire obtained with Abaqus.

7.1.2. Thermal buckling

A four meter long beam has been considered as example (Figure 7.3). The beam has two pinned support at the ends, which provides fully horizontal restrain, and is exposed to a standard fire, which is considered to heat the elements uniformly. The material is modelled by considering an elastic plastic constitutive relation and material degradation at elevated temperature is considered for the stiffness, the effective yielding and the thermal expansion coefficient, in accordance to the Eurocode (EN 1993-1-2, 2005). Two sections are taken in consideration for the beam, an IPE 270 profile and HEM500 profile. In the first case, the beam is slender even at room temperature, while in the second case the beam is not. An out of plane buckling can be induced by the hindered thermal expansion when the beam is subjected to fire and is therefore investigated in the following. To this

aim an initial beam imperfection has to be considered in the model, which is simulated by means of a pointed force at the beam mid-span, acting perpendicularly to the element axis. The value of force is such as to cause a displacement equal to L/10000, where L is the beam length.

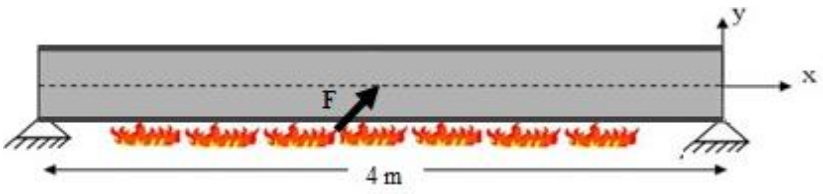

Figure 7.3 - Two pinned beam studied

The slender beam is expected to collapse out of buckling before the yielding of the material is reached according to Euler's elastic theory. The stocky beam instead should first become plastic and then buckle immediately after, due to the reduction of stiffness modulus in the plastic range, in accordance to Shanley's theory (Shanley, 1947), which uses the Euler formula substituting the elastic stiffness with the tangent modulus. The results of the investigation are reported in Figure 7.4, which shows the axial stress (indicated as "r_A") and the mid-span displacements ("Uz_midpoint") in function of the temperature. The plastic load ("P_{Yield}") and the critical loads in the elastic ("$P_{cr\text{-}Elastic}$") and inelastic ("$P_{E\text{-}P}$") range are also reported. The buckling can be identified at the point where the transversal displacement shows a sudden increment: for the slender beam, this happen at a very low temperature of 80°C, when the elastic buckling load (Euler) is reached and no material degradation has developed in the section; the stocky beams buckles instead at 115°C, when the plastic limit is reached and the buckling load drops suddenly as a consequence of the reduction of the stiffness in the inelastic range (Shanley). The results are summarized in Table 7.1.

Table 7.1 - Synthesis of results

	IPE 270	**HEM 500**
Area [mm^2]	4590	34430
I min [mm^4]	4200000	191500000
Type of collapse	Elastic Buckling (Euler)	Elastic-Plastic Buckling (Shanley)
Temperature [°C]	80	115

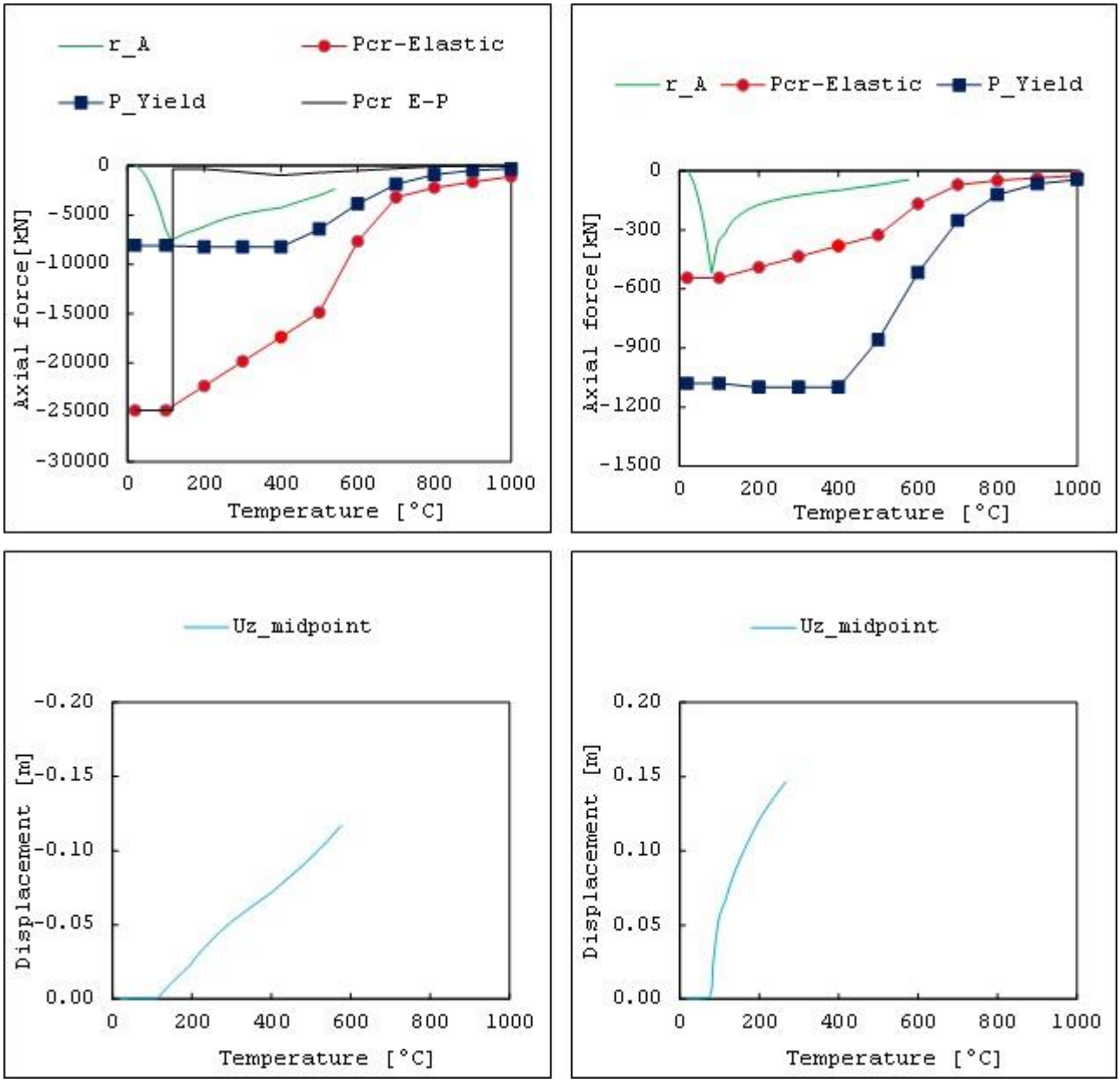

Figure 7.4 - Collapse for thermal buckling of an element IPE270 (left) and of an element HEM 500 (right) in terms of axial force (above) and midpoint displacement (below)

7.2. STEEL FRAMES

7.2.1. Sway and no-sway collapse

The positive effect of restraints mentioned in the previous paragraph is particularly evident when observing the behaviour of the two steel frames, presented in the following (Figure 7.5).

In the first case (A), a three short span frame is considered, where a fire is assumed to trigger and be contained in the central area. In the second case (B) a two-long-span frame is considered, where fire

is assumed to trigger and be contained in one of the two symmetric span areas. In both cases, the fire is modelled by means of a standard temperature-time curve, applied to the beam nodes of the considered frame span.

In the first structure (A) the beam suffers a runaway deflection when, after 10 min of standard fire, its temperature approaches 700 and plastic hinges are developed at the beam ends and at mid-span due to the significant degradation of the material. However, when geometrical nonlinearities are duly considered in the modelling, it's possible to see how at certain point the tension forces developed in the beam provide equilibrium for the three-hinge mechanism and the beam runaway is contained as long as the structure recovers some stiffness.

In the second structure instead this stiffness recovery is not present, due to the lower grade of horizontal restraint provided to the collapsing beam by the lack of another adjacent frame on the left, which was instead present in the first structure.

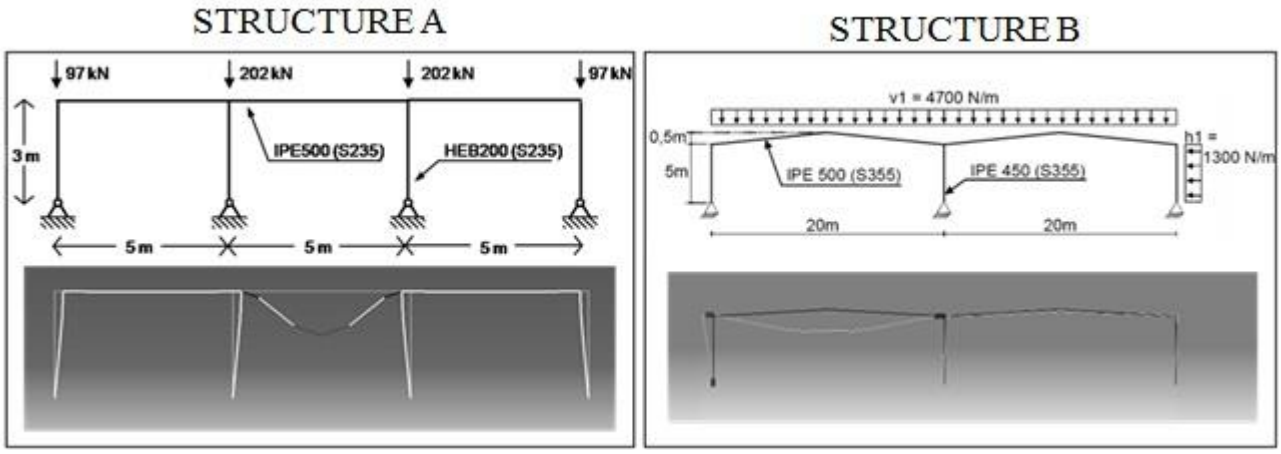

Figure 7.5 – Sway and no-sway collapse of Structure A (left) and Structure B (right) in terms of temperature (second row), displacement (third row) and force (last row).

Another important difference in the behaviour of the two presented structures under fire concerns the modality of collapse (Figure 7.5), which is an inwards collapse (no-sway) for the first structure (A) and an outwards collapse (sway) for the second one (B). It's easy to understand that frames that sway sideways during a fire may collapse outwards and lead to adjacent property being damaged or persons outside the building being endangered (Moss, et al., 2009). An inward collapse mechanism is in this respect less dangerous. On the other hand, it has to be considered that the impact of collapsing section on other part of the same building could result in a less confined final damage of the system.

7.2.2. Behaviour of single-storey portal frames in fire

In this paragraph some parameters that influence the collapse mode of single-storey frames in fire are investigated. Starting from an initial geometry and fire condition, different schemes have been defined. By means of the commercial non-linear finite element software ABAQUS®, a model of the frame is defined through beam elements. This study is aimed to understanding on how and why the collapse occurs, to assess the influence of local action and constructional details on the frame behaviour under fire action.

The analysis of the effects of internal fires in industrial buildings requires the definition of different scenarios. In a two dimensional analysis the number of possible scenarios is relatively low: in fact, the fire could affect only one of the columns, both columns or no one of them, but certainly the hot gases heat the rafter.

In an initial fire phase, the portal rafter begins to heat and expand (for the gathering of hot gasses un-der the ceiling), this causes an outward deflection of the eaves together with an upward deflection of the apex. As the fire continues to burn, the rafter temperature rise and the thermal expansion increase. If the columns have an adequate stiffness to retain the thermal expansion of the rafter, plastic hinges are realized on the rafter which loses its resistance and droop into a catenary causing the columns to lean inwards, defining a no-sway collapse. General condition for this kind of behaviour is a moment resistant base connection for the column and a ratio of the span to the height to eaves less than two (Newmann, 1990).

Starting from an initial configuration for the portal frame, some parametric analyses have been carried out to assess the structural behaviour under fire condition.

The initial configuration is shown in Figure 7.6. The IPE 500 standard profile is used for columns and beam, joined with moment and shear resisting connections. The restraints to the ground are assumed to be ideal, frictionless hinges. The constitutive law of steel (S355) used is the relationship de-fined in the ENV 1993-1-2: Section 3.2 for heating rates between 2 and 50 K/min. Vertical and horizontal loads are also considered as shown in Figure 7.6.

The considered fire scenario involves the left column and the rafter. This assumption is consistent with the case of a fire triggered in a corner of the structure, so that the most heated elements would be the column near the flame and the beam heated by the hot gasses, that gather under the roof.

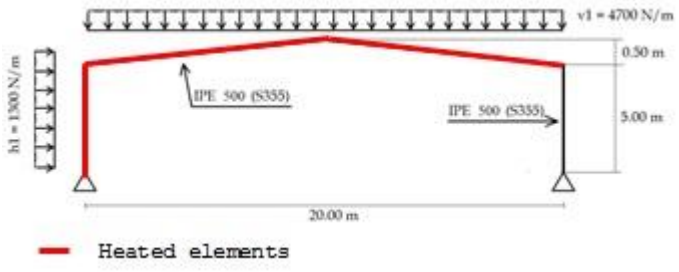

Figure 7.6 - Initial configuration of portal frame

The thermal action on the heated element is modelled with the nominal fire curve ISO 834 (European standard curve), shadow effect is not considered. The temperature in the heated elements is assumed uniform and equal to the temperature defined by the fire curve.

The structure is modelled by beam elements; no limits for the rotational capacity of the beam-column connections are considered; bi-dimensional, nonlinear transient analyses have been performed taking in-to account the effects of displacements on the overall behaviour.

With reference to general considerations of the collapse typology given in 7.2.1, in the paper, for an asymmetric fire scenario, the following definitions are taken into account:

- Inward (or no-sway) collapse is defined when a opposite direction shift of top of the columns is ob-served at the collapse.
- Outward (or sway) collapse is defined when a same direction shift of top of the columns is ob-served. Sway collapse could be left side or right side direction.

Collapse is defined by the runaway of appropriate parameters.

Three response parameters have been assumed as representative of the structural behaviour: the vertical displacement of the mid-point of the beam (dyP2) and the horizontal displacements at the top of the columns (dxP1, dxP3) as shown in Figure 7.7.

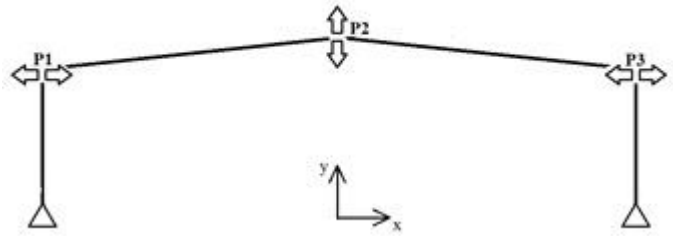

Figure 7.7- Monitored displacements.

The trend of these parameters versus the applied temperature for the initial configuration is shown in Figure 7.8. It is possible to define two different phases. In the first one, under 600 °C, the elastic expansion of the rafter causes an outward deflection of the eaves. Then the decreasing of the stiffness of the frame, caused by the plastic hinge formation, lead to a rapid increasing of the displacements. Looking at the direction of the top of the columns displacements is possible to identify a sway collapse to the left side. The critical temperature is 732°C.

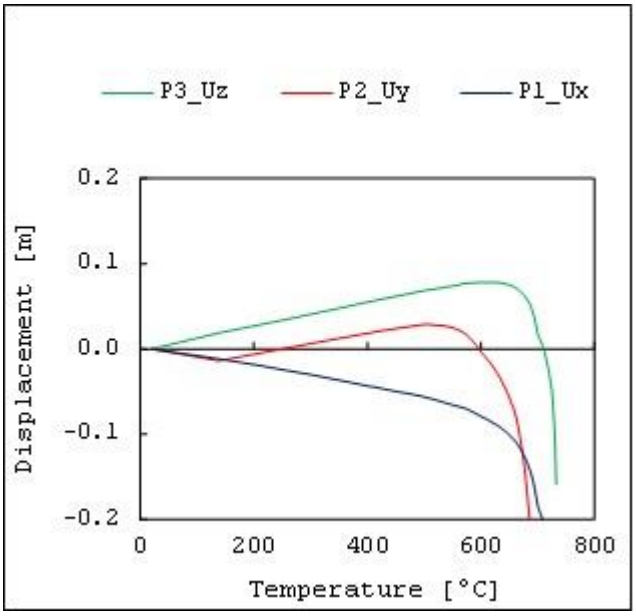

Figure 7.8 - Analysis results.

7.2.3. Parametric analysis

A parametric analysis has been carried out in order to understand the influence of the design parameters on the frame collapse modality. The basic assumptions for the different models are always the same (defined in 7.2.2), if different specifications are not provided.

The influence of the following parameters on the collapse modality has been investigated: support conditions, load conditions, frame height, column and beam sections. The comparison of the different models is made for eight different column sections.

The outputs monitored are the displacements (defined in 7.2.2), for the definition of the collapse mode, and the critical temperature (the temperature of col-lapse).

Pinned vs fixed support conditions

The first parameter analysed is the support conditions. A pinned frame (an ideal, perfect, frictionless pinned support) is compared against a fixed frame (rigid, full strength support). The

cross section (IPE 500) of the beam has been maintained, while the cross section of the column has been varied.

Table 7.2 - Results for pinned vs fixed support

Column section	**Pinned** Tcr [°C]	**Fixed** Tcr [°C]
IPE 400	681(l-sw)	735(no-sw)
IPE 450	699(l-sw)	740(no-sw)
IPE 500	732(l-sw)*	746(no-sw)
IPE 550	726(r-sw)	756(no-sw)
IPE 600	723(r-sw)	765(no-sw)
IPE O600	723(r-sw)	776(no-sw)
IPE 750x137	723(r-sw)	780(no-sw)
IPE 750x196	723(r-sw)	782(no-sw)

Where:

(l-sw) left sway collapse (r-sw) right sway collapse (no-sw) no sway collapse

* initial configuration

From the results of the analysis (shown in Table 7.2) is possible to understand that in case of a pinned support, large rotations are realized and the consequence is a sideways of the frame. In this condition the column's section parameter influences not only the temperature but also the direction of the sway collapse.

A fixed support is able to retain the thermal expansion of the rafter, and the column section variation influence only the temperature and not the mode of the collapse, which is always a no sway typology.

As a result of analysis performed three different collapse typologies have been founded: inward collapse, left side sway collapse and a right side sway collapse.

The only condition able to retain the expansion of the rafter and inducing an inward collapse is a moment resistant for the columns. This can be explained by looking at the evolution of the stress and plastic hinge formation on the structure. Referring to the schematic behaviour defined in Figure 7.9: in the first phase (Figure 7.9.a) due to the thermal expansion of the beam in elastic range, a moment reaction at the base of the columns is induced. That moment increases with the temperature inducing a plastic hinge formation at the base of the heated column (Figure 7.9.b). The resistance of the beam is reducing so the next plastic hinges are on the beam, due to the plastic expansion (Figure

7.9.c, Figure 7.9.d) and vertical load (Figure 7.9.e). The formation of a plastic hinge at the mid-length of the beam creates inward force at the top of the column (due to vertical load), together with an inversion of the moment at the bases of the columns, which rises until reaching the maximum column moment strength.

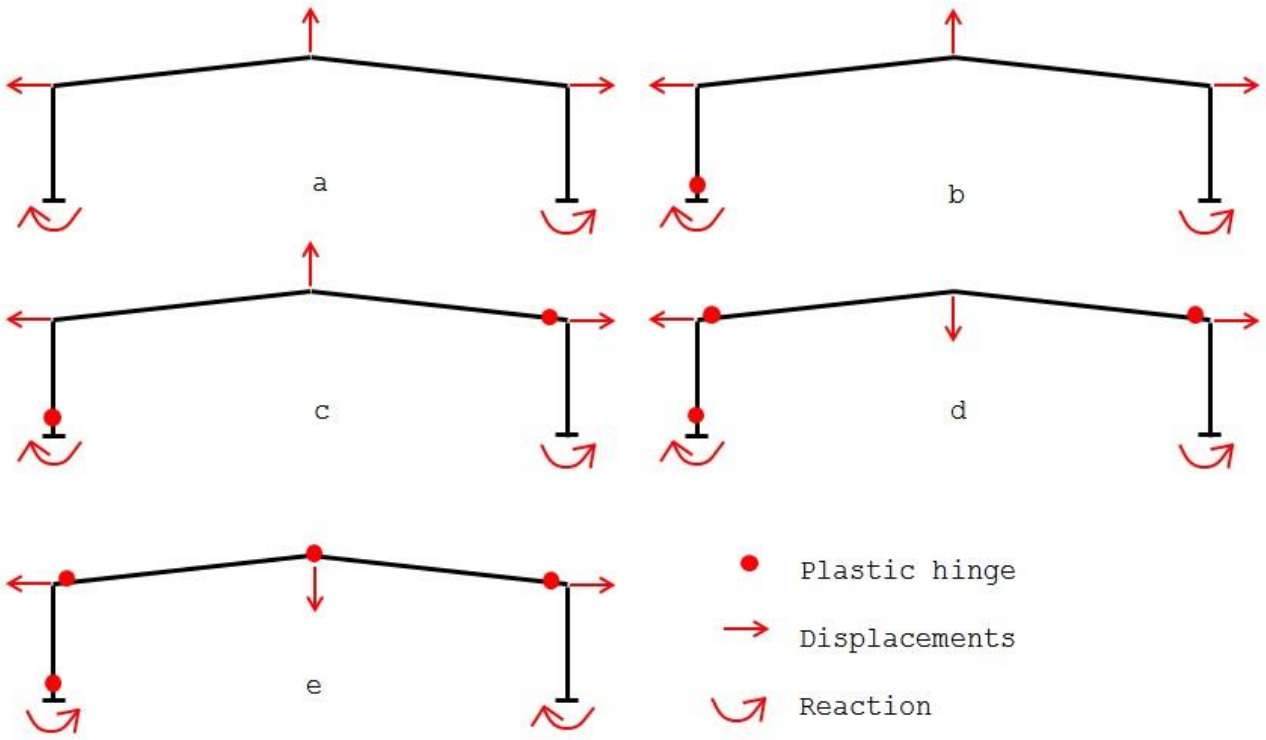

Figure 7.9 - Fixed support collapse scheme.

As expected, increasing the dimension of the columns' section leads to an increasing of the collapse temperature. Pinned columns' support is not able to retain the expansion of the rafter and inducing an outward col-lapse. In this case are noticeable two different direction of the sway collapse as defined in Figure 7.10. The parameter which influences the direction of the col-lapse is the resistance of beam to column stiffness ratio.

All the left sway collapses happen when the stiffness of the column is less than the beam's one (column's weaker section than the beam's one). As evidenced in Figure 7.10.1, in this case the first plastic hinge is formed on the top of heated column (Figure 7.10.1.b). From this stage both the horizontal load and the force induced from the thermal expansion of the beam cause significant deformation of the heated column.

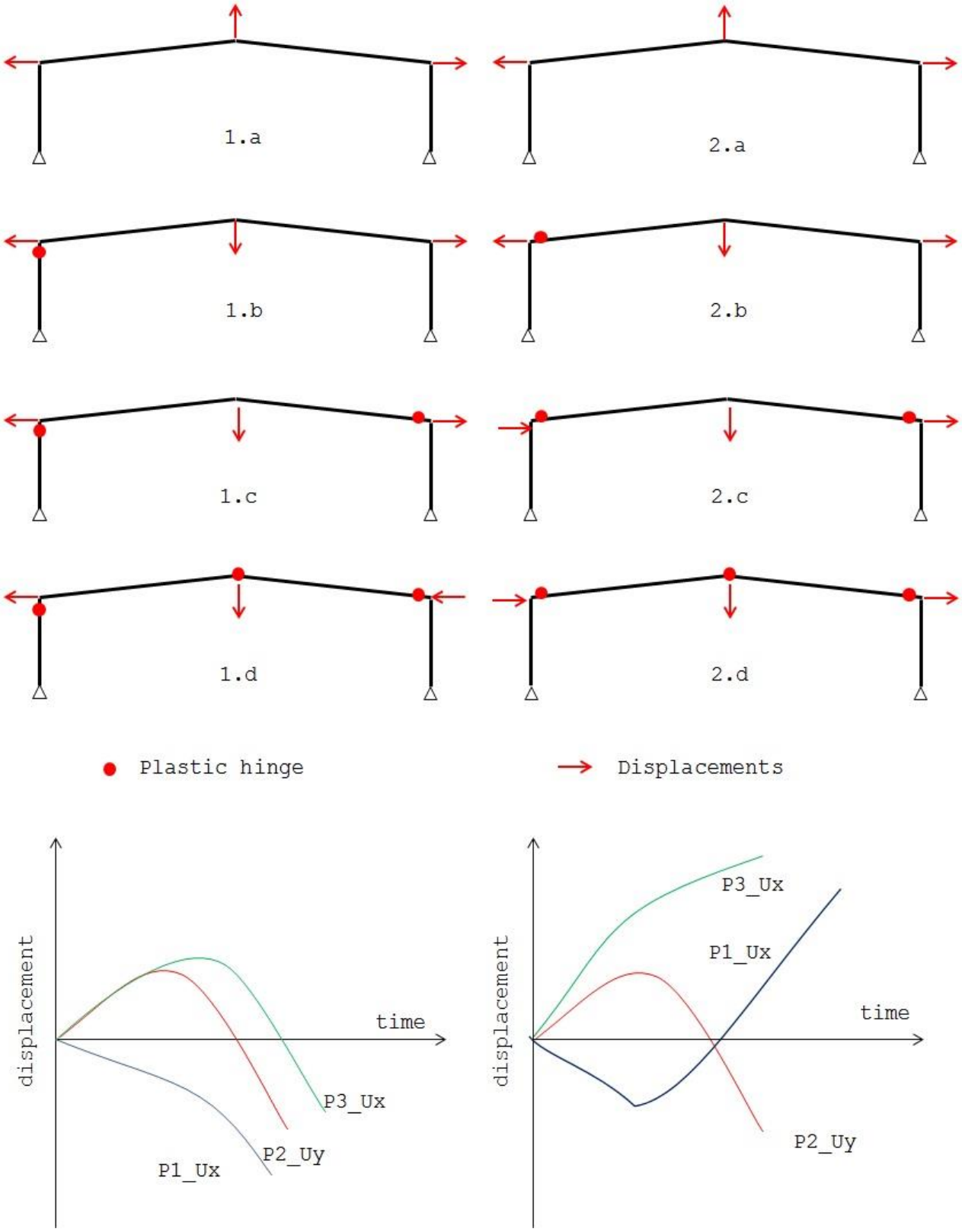

Figure 7.10 - Pinned support collapse scheme. Left sway collapse (left); right sway collapse (right).

The subsequent loss of stiffness of the structure with the formation of the plastic hinge on the beam, due to the thermal expansion (Figure 7.10.1.c) and vertical load (Figure 7.10.1.d), determines the

collapse towards the heated column, caused from the high plastic deformation on the column and the loss of vertical alignment of the structure.

All the right sway collapses happen when the stiffness of the column is greater than the beam's one. As evidenced in the Figure 7.10.2, this case the first plastic hinge is formed on the beam in proximity of the heated column (Figure 7.10.2.b). With the formation of the other plastic hinge on the beam, due to the thermal expansion (Figure 7.10.2.c) and vertical load (Figure 7.10.2.d) the beam lose its stiffness and the structure became instable for horizontal load, defining by its direction the side of the sway collapse.

It is worth to highlight that the value of the col-lapse temperature increases as the dimension of the columns' cross section grows. This behaviour occurs until the cross section of the column is weaker than the beam. While, when the section of the columns became stronger then the beams one (IPE 500) the critical temperature of the portal frame became steady (because the plastic hinge on the rafter hap-pen always at the same temperature).

Is of interest to remark some points:

- when the collapse is induced by the plastic deformation of the beam the temperature of collapse is always equal to the temperature of 723°C due to the collapse of the beam;

- a slight increasing of the temperature of collapse is obtained for frames having the column and the beam with approximately the same stiffness. In these cases the zone of plastic deformation is greater than the previous, the elements are allowed to experiment significant deformations and the stress in the connection between the heated column and the beam are reduced;

- due to the chosen load combination, horizontal load acts in the opposite direction of the thermal expansion induced by the fire, it is possible to point out how, in this condition, the strength of the column in relation to the beam strength is the parameter that influence the direction of the sway collapse.

In conclusion is remarkable that a fixed support frame have a greater resistance to this load combination than the pinned support frame (approximately 3-8% in terms of temperature), this is due to the inversion of the sign of the flexural moment at the base of heated column which delays the collapse.

Load conditions

The second parameter that has been analysed is the load combination. The section profile of the beam is still an IPE 500 and the columns have a pinned support. Three different load combinations

are investigated: LOAD 0 (only vertical load); LOAD 1 (vertical plus horizontal load on the left column pushing to the right side); LOAD 2 (vertical plus horizontal load on the right column pushing to the left side). Results are listed in Table 7.3.

Table 7.3 - Results for load conditions

Column section	**LOAD 0** Tcr [°C]	**LOAD 1** Tcr [°C]	**LOAD 2** Tcr [°C]
IPE 400	675(l-sw)	681(l-sw)	672(l-sw)
IPE 450	693(l-sw)	699(l-sw)	690(l-sw)
IPE 500	722(l-sw)	732(l-sw)*	713(l-sw)
IPE 550	732(l-sw)	726(r-sw)	720(l-sw)
IPE 600	732(l-sw)	723(r-sw)	722(l-sw)
IPE O600	734(l-sw)	723(r-sw)	722(l-sw)
IPE 750x137	734(l-sw)	723(r-sw)	722(l-sw)
IPE 750x196	734(l-sw)	723(r-sw)	722(l-sw)

The results confirm that pinned support is unable to adequately retain the thermal expansion of the rafter and the consequence is a sideways of the frame.

It is important to remark how the LOAD 1 combination is defined from a horizontal load which pushes the frame in an opposite direction from the one of the thermal expansion due to the fire. This is the optimal load condition for the structure and the temperature of the collapse reaches the maximum value. The worst load combination is LOAD 2.

Except for the LOAD 1 case, all the other load combinations cause always a left sway collapse. The collapse explanation is not different from the previous, but when the structure became unstable for horizontal load, the collapse occurs in the direction of the maximum deformation (LOAD 0) or in the direction of horizontal load (LOAD 2).

Columns height

The third investigated parameter has been the columns height. Three different heights are defined, 4, 5 and 6 meters, the span length is always the same, 20 meter. The section profile of the beam is always an IPE 500 and the columns have pinned supports. Results are listed in Table 7.4.

Table 7.4 - Results for column height variation

Column section	**H = 4 m** Tcr [°C]	**H = 5 m** Tcr [°C]	**H = 6 m** Tcr [°C]
IPE 400	681(l-sw)	681(l-sw)	681(l-sw)
IPE 450	699(l-sw)	699(l-sw)	699(l-sw)
IPE 500	732(l-sw)	732(l-sw)*	734(l-sw)
IPE 550	729(r-sw)	726(r-sw)	719(r-sw)
IPE 600	728(r-sw)	723(r-sw)	717(r-sw)
IPE O600	728(r-sw)	723(r-sw)	717(r-sw)
IPE 750x137	728(r-sw)	723(r-sw)	717(r-sw)
IPE 750x196	726(r-sw)	723(r-sw)	716(r-sw)

The load combination and the fire scenario considered is the one previously defined as LOAD 1. In this case is important to evidence as the variable parameter is the beam to column stiffness ratio.

The obtained results confirm the consideration given above. When the collapse is induced from the plastic hinge on the heated column, the maxi-mum temperature is not influenced from height and stiffness of the columns. When the collapse is induced by the plastic hinge on the beam the stiffness of the columns has a small influence on the maximum reached temperature (the deformations of slender and longer, column allow greater deformation of the beam).

Beam section

The fourth investigated parameter has been the beam section. Four different beam sections are considered: IPE 450, IPE 500, IPE 550 and IPE 600. The columns have a pinned support and the height of the column is 5 meters while the span of the beam is equal to 20 meters. The load combination and the fire scenario is the one previously defined as LOAD 1. The results are listed in Table 7.5.

The beam section is the most important parameter in the de-termination of the resistance of the frame in fire situation. Increasing the strength of the beam the maxi-mum temperature reached from the frame increase. On the other side, is also confirmed how the relationship between the strength of the column and the beam, for asymmetrical fire scenario and opposite horizontal load, is the main factor in the determination of the direction of the sway collapse.

Table 7.5 - Results for beam section variation

Column section	**IPE 450** Tcr [°C]	**IPE 500** Tcr [°C]	**IPE 550** Tcr [°C]	**IPE 600** Tcr [°C]
IPE 400	670(l-sw)	681(l-sw)	696(l-sw)	723(l-sw)
IPE 450	690(l-sw)	699(l-sw)	716(l-sw)	740(l-sw)
IPE 500	687(r-sw)	732(l-sw)*	765(l-sw)	759(l-sw)
IPE 550	684(r-sw)	726(r-sw)	756(no-sw)	798(l-sw)
IPE 600	684(r-sw)	723(r-sw)	764(r-sw)	794(l-sw)
IPE O600	684(r-sw)	723(r-sw)	762(r-sw)	792(r-sw)
IPE 750x137	684(r-sw)	723(r-sw)	762(r-sw)	792(r-sw)
IPE 750x196	684(r-sw)	723(r-sw)	761(r-sw)	791(r-sw)

7.3. EFFECT OF CREEP MODELLING

In order to show the differences between the structural responses using the three discussed constitutive models, two case studies have been analysed. The first case study regards a simple supported beam subject to fire. A parametric study has been carried out to evaluate the influence of the heating rate and the stress level. The second example deals with a frame structure exposed to the ISO fire curve. In both the examples the structural response has been evaluated considering the three different constitutive models and the results have been compared.

7.3.1. Simple supported beam

The simple supported beam considered in this example is shown in Figure 7.11. It is an IPE 500, 6 m length. The material is S235 steel. It is loaded by a punctual load applied in the middle span point. The beam is heated at a constant rate. The extent of creep deformation is strictly related to some parameters, as for example the stress level and the heating rate. In order to investigate the effect of these parameters on the overall structural response a parametric study has been carried out: first the stress level has been varied, keeping constant the heating rate, then, the heating rate is varied at fixed stress level.

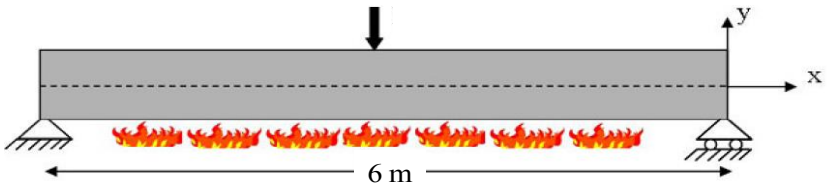

Figure 7.11 - Simple supported beam considered in the parametric study

Three different load levels have been considered: a concentrated force able to stress the middle span section at 1/3, 1/2, and 2/3 of the yielding stress respectively; the tested heating rate are: 100°C /h, 300 °C /h, 600 °C /h.

In Figure 7.12 the results obtained varying the heating rate are shown. The plots represent the horizontal displacement of the right restraints (on the left hand) and the vertical displacements of the middle span point (on the right hand), for a fixed stress level of 1/3 of the yield strength. The EC3 and ASCE models are not able to consider the time dependent deformation, so, in the three cases, they give the same results. On the other hand, the NIST curves are able to reproduce the small variation related to the different heating rate. If the application of temperature is slow, the beam collapses for lower values of the temperature. It is also possible to note that the ASCE model, if the creep is not accounted in some way, gives unsafe predictions.

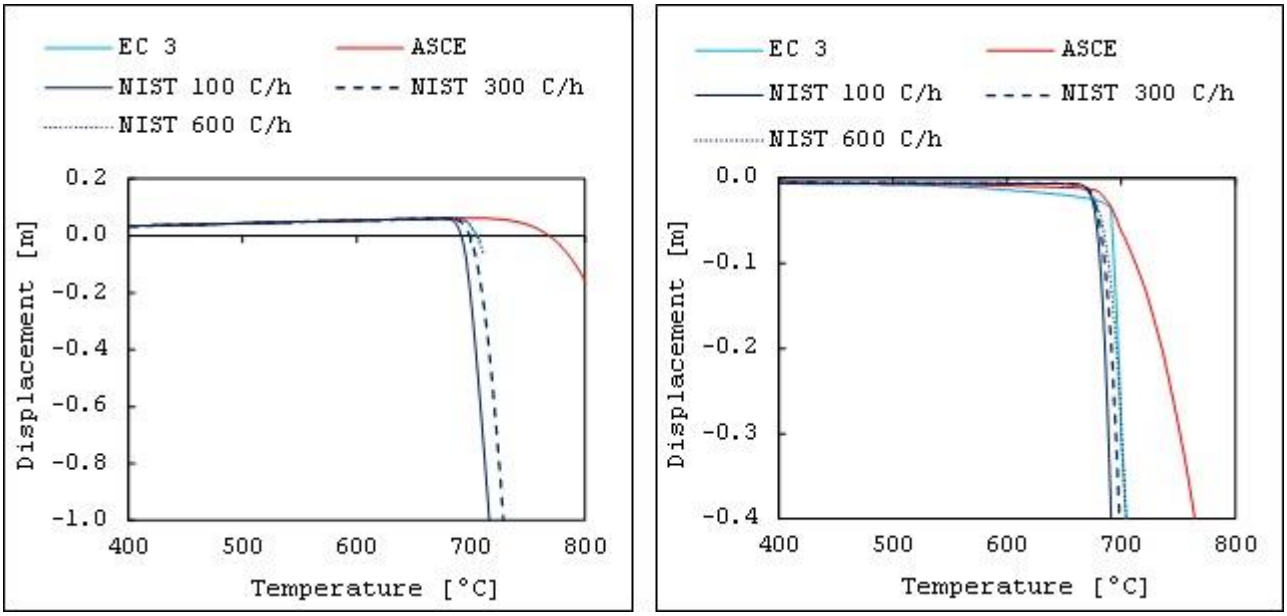

Figure 7.12 - Results of the parametric study: variation of the heating rate. Left hand: horizontal displacement of the right restraints; right hand: vertical displacements of the middle span point

In Figure 7.13 the results, for the same two points, obtained considering different stress level are shown. As expected by other investigations (Kodur & Dwaikat, 2010), the results indicate that the

influence of high temperature creep increase with the load level. For lower stress levels, Eurocode and NIST model give similar results, while for higher values of stress, the results diverge. The ASCE model, due to the shape of the hardening part of the stress-strain curve (Figure 6.6), overestimates the structural resistance in all the cases.

The results have shown that the variation of the heating rate can be caught only by the NIST model: if the application of temperature is slow the beam collapses for lower values of the temperature. Regarding the stress level, the results indicate that the influence of high temperature creep increase with the load level: for lower stress levels Eurocode and NIST model give similar results, while for higher values of stress, the results diverge. The ASCE model overestimated the structural resistance in all the cases.

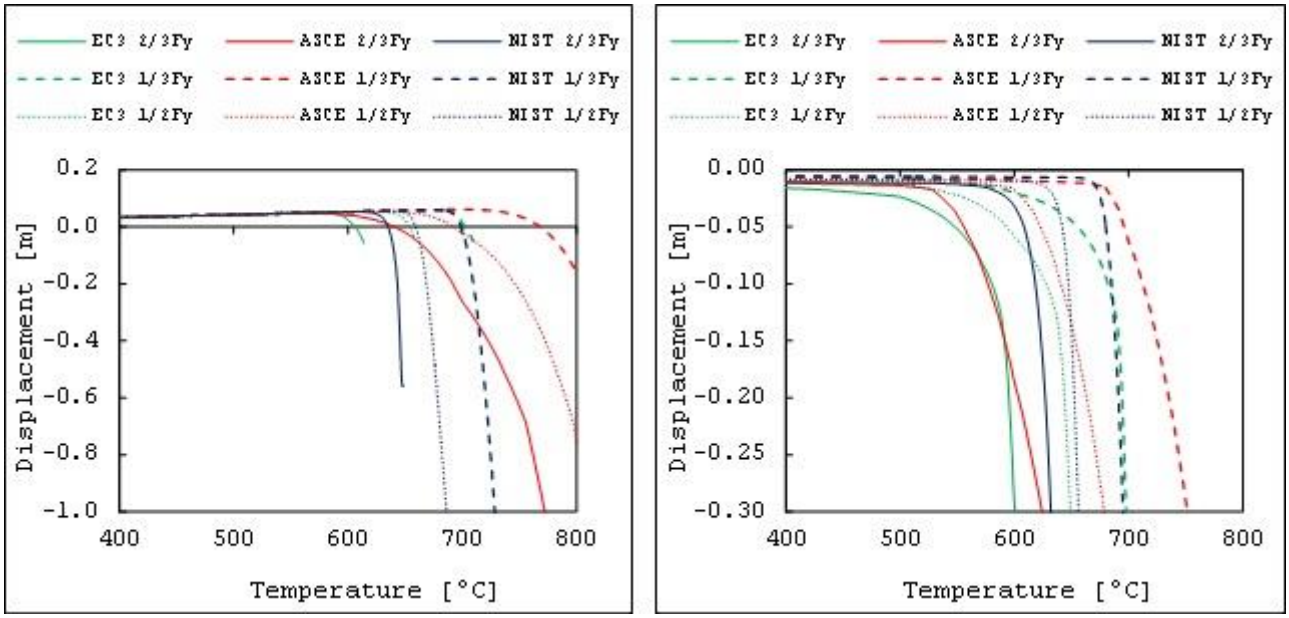

Figure 7.13 - Results of the parametric study: variation of the stress level. Left hand: horizontal displacement of the right restraints; right hand: vertical displacements of the middle span point

7.3.2. Frame structure

The second case study regards a frame structure subject to a standard design fire curve (Gentili, et al., 2011). The main dimensions of the structure and the applied loads are shown in Figure 7.14; marked elements are the heated ones.

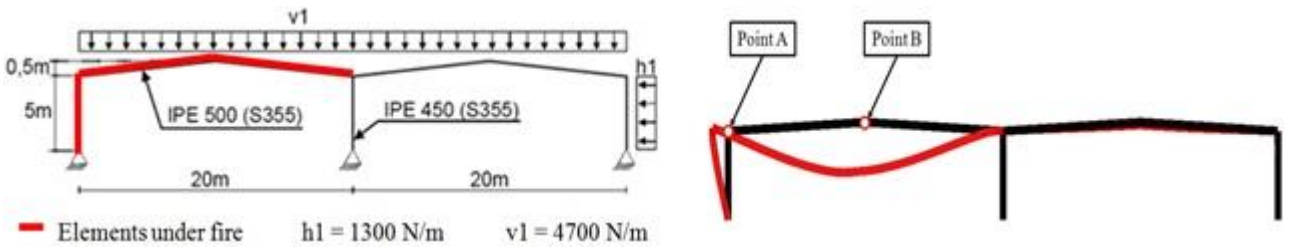

Figure 7.14 - Frame structure considered in the second case study and deformed shape

The standard ISO curve has been applied and the overall structural response has been evaluated. In Figure 7.15, the results in point A and B (Figure 7.14) obtained considering the three different constitutive relationships are shown. The plots represent the horizontal displacements of the point at the head of the left column (on the left hand) and the vertical displacement of the middle span point of the left frame. It is possible to note that the ASCE model also in this case lead to unsafe predictions. EC3 model leads to conservative results showing that the stress-strain curves account for visco-elastic deformation.

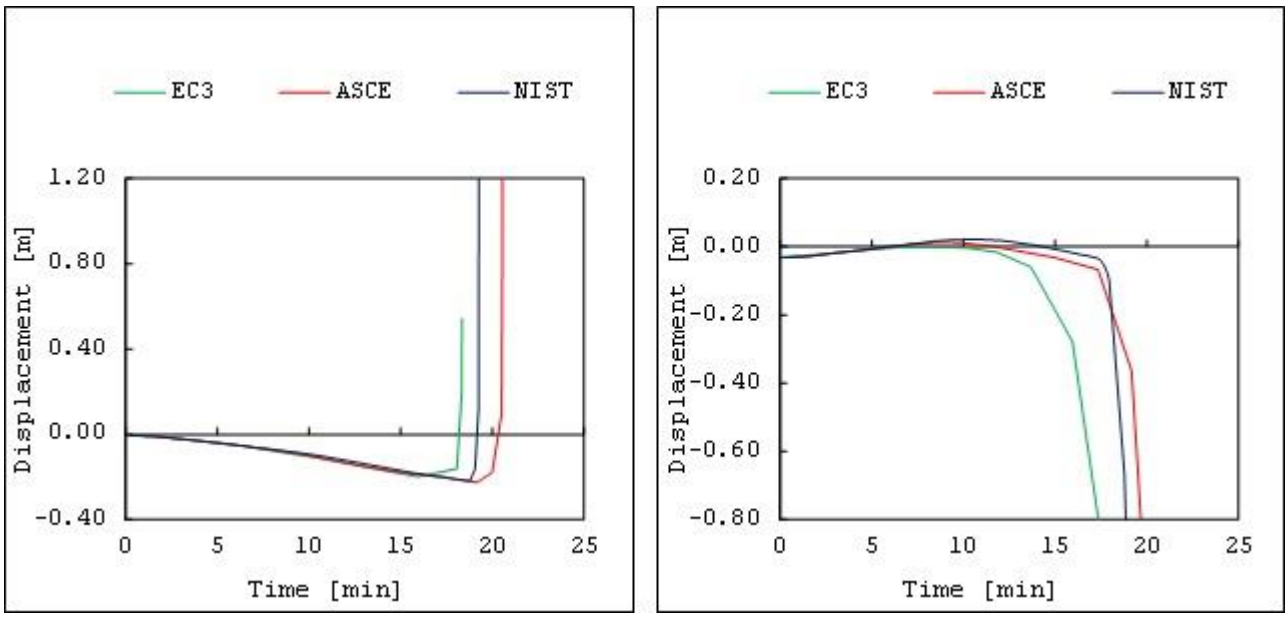

Figure 7.15 - Left hand: horizontal displacement of the head of the left column; right hand: vertical displacements of the middle span point of the left frame.

The second case study has shown that the EC3 model, even if not explicitly, account for viscoelastic deformation leading to conservative results. The results obtained in this work are related to the considered structures and quality of steel. In order to validate the obtained results, different case studies and different steels should be analyzed, comparing the results also with experimental tests.

7.4. CONCRETE SLABS

The above-mentioned collapses of concrete buildings highlight in particular the important role played by deck slabs in the response to fire of the whole building. As a matter of fact, the failure of a slab element during fire may be responsible of a vertical propagation of both the fire and the damages.

The propagation of the fire is a consequence of the loss of compartmentalization as a result of the slab failure. The vertical propagation of the damages may be triggered by the impact of a collapsing slab on the floor underneath or by a possible instability of the walls consequent to the loss of horizontal restrain (Usmani, et al., 2003), (Gentili, et al., in press). Usual fire design procedures does not account for either of the two events, whose occurrence can therefore be very critical for complex structures (Petrini, in press) and especially for high-rise buildings, as it may lead to a progressive or disproportionate collapse of the structure.

A proper representation of the slab response in case of fire is therefore of great importance in view of a safe and sustainable design of buildings. However, this task can be particularly difficult in case of slabs with cavities or light materials, due to the presence of materials with very different thermal and mechanical properties and their complex interaction. Being lighter than other deck solution, these type of floor-deck are frequently used in tall buildings especially and their employment is of great interest nowadays, in consideration of the savings they allow in term of material costs and CO2 production (Hertz & Bagger, 2011).

The aim of this paragraph is to compare the performances of two different light concrete floor slabs under fire, namely: i) a T-beam concrete deck with light-concrete blocks, referred to as T-deck; ii) a biaxial concrete deck with hollow polyurethane spherical void, referred to as V-deck. The first element has been studied by Josephine Voigt Carstensen, while I conducted the analysis on the second slab.

The slabs have the same length and have been designed to carry the same live loads in a permanent design situation, so that they are representative of two design solutions that could be alternatively used in a building.

The fire situation has been investigated with respect to 90 min of standard fire considering in particular three different conditions: i) the beginning of the fire, with this term referring to a condition where the mechanical loads and properties of the slabs for the fire design situation are considered, but the fire action has not started yet; ii) during the fire development, when the heat

penetrates the slab sections and the displacements of the slabs increases as a consequence of the material degradation; iii) the end of the fire, when the temperatures and the mechanical properties of the slabs are those achieved after 90 min of standard fire. The consideration of a fourth situation referred to the conditions of the slab after cooling has not been considered in this paper and is left for further studies on the subject.

For the comparison, the displacement has been assumed as representative indicator of the performance (Arangio, 2012) of the slabs during fire, while the load bearing capacity has been considered as representative of the structural integrity of the slabs. The slabs have been therefore compared in terms of: a) mid-span displacement during the fire development (condition ii); and b) decrement of load bearing capacity, calculated as a difference between the load bearing capacity at the end of the fire (condition iii) and the load bearing capacity at the beginning of the fire (condition i).

With respect to the choice of the fire action, the use of a nominal fire curve has been preferred over a more realistic parametric or natural fire, in order to prescind from the different fire compartments in which the slabs may be used and to refer solely to the intrinsic characteristic of the two structural elements.

7.4.1. Slab description

In the following, the mechanical and geometrical properties of the T-deck and V-deck slabs are described and the loading conditions at the beginning of the fire are reported, as they generally have a strong influence on the fire resistance.

In this respect, it is important to underline that the intention of the study was to compare two alternative design solutions for a floor slab of an office compartment. As such, the slabs have the same length (7 m), the same support conditions (simply supported), and a cross-section, whose dimensions have been chosen in a way so that the slabs are able to carry the same live loads (2.5 kN/m^2), according to the load combination for the ultimate limit state (ULS) shown in Equation 7.1.

$$p_{sd} = \gamma_G \cdot G_k + \gamma_Q \cdot Q_{k1} \tag{7.1}$$

As shown in Table 7.6 and Table 7.7, the load-to-resistance ratio (LRR) of the slabs at the ULS is therefore very similar for both slabs, even if not identical, due to the design constraints related to the discrete dimensions of steel bars available in the market. It has to be noted that the difference between the LRR of the two slabs may differ with respect to fire design consideration, due to a

possible different reduction of the solicitant load and resistance of the slabs. This is a consequence of the reduced partial safety coefficients for the loads (EN 1991-1-2, 2004) and the materials (EN 1992-1-2, 2004), (EN 1993-1-2, 2005) foreseen by the Eurocodes in the accidental design situation, which the fire refers to (EN 1990, 2002).

T-deck

T-beams of ordinary concrete casted on light-concrete blocks form the first slab considered. The blocks have a section of width equal to 40 cm and of height equal to 30 cm and are spaced 10 cm in the transversal direction. An ordinary concrete of class C30/37 is cast on the blocks, which acts as disposable formwork. A depth of 5 cm of ordinary concrete is left on the upper concrete part of the slab. Therefore the T-beams have a web width of 10 cm and a flange height of 5 cm, while the total height of the slab is 35 cm (Figure 7.16).

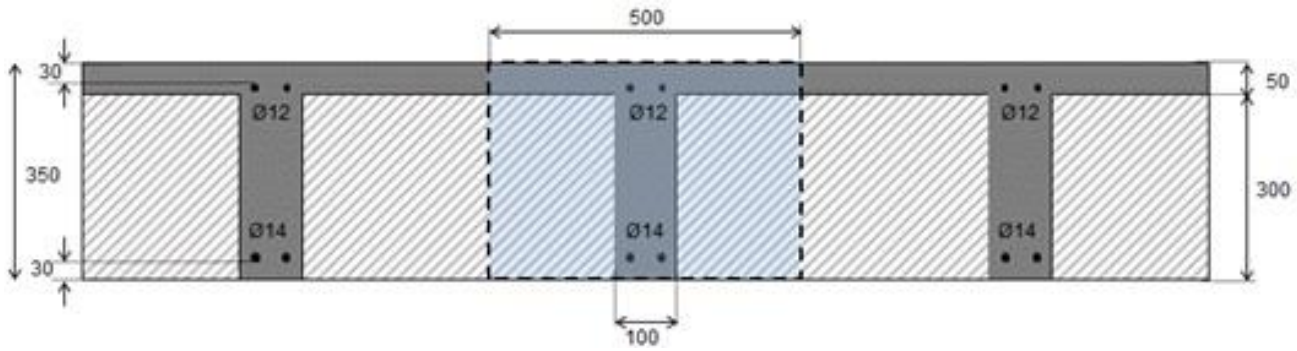

Figure 7.16 - Cross-section of the composite slab

The following properties have been assumed for the ordinary concrete at 20°C: a density ρ = 2300 kg/m^3 a thermal conductivity λ = 1.64 W/(m·K); a thermal expansion coefficient α = 6·10-6 K^{-1} and a specific heat capacity c_p = 900 J/(kg·K).

The concrete aggregate of the light-blocks has the following mechanical and thermal and properties at 20°C: characteristic strength f_{cu} = 2.3 MPa; density ρ = 600 kg/m^3; thermal conductivity λ = 0.3 W/(m·K); thermal expansion coefficient $\alpha = 8 \cdot 10^{-6}$ K^{-1}; specific heat capacity c_p = 900 J/(kg·K). In absence of experimental data on the light aggregate, the specific heat capacity has been taken equal to the ordinary concrete, as suggested by Pettersson and Ödeen (Petterson & Odeen, 1978).

The ordinary concrete has a characteristic strength significantly higher than the characteristic strength of the light concrete. As a consequence, the contribution of the blocks to the overall resistance of the slabs in a permanent design situation is quite limited. However, due to the higher porosity of the light aggregate, the blocks have a much lower density and thermal conductivity and

therefore an insulating effect on top slab, which significantly contribute to the fire resistance of the deck. Each T-beam is reinforced with 2 φ12 bars at the top and 2 φ14 at the bottom and has a rebar cover of 3 cm. The bars are made of steel B450c, with a stiffness E_s = 210 GPa and a steel strength f_y = 440 MPa. Simplified analytical calculations of the flexural resistance gives a load bearing capacity of p_u = 11.9 kN/m^2 at 20°C. This value is related to the ULS design values of the steel and concrete, which are obtained by dividing the characteristic values by the material safety coefficients $\gamma_{m,s}$ = 1.2 and $\gamma_{m,c}$ = 1.5, respectively and it has been obtained by means of simplified hand calculations. As usual for design purpose, the tensile resistance of the concrete is neglected in these preliminary calculations and a parabola-rectangles stress-strain diagram is assumed for the compressive behaviour of the concrete, so that the stress-block method could be used. More refined calculations have been also carried out with a computer program for the sectional analysis of R.C. elements (Pfeiffer, 2011), where a constitutive relation accounting for softening and tensile resistance was assigned to the concrete T-section. The resulting load bearing capacity does not differ from the simplified calculations, showing that the effect of tensile strength is not very significant for this slab.

Considering that the self-weight of the slab and the permanent weight of the superstructure gives a total dead load of 5.9 kN/m^2, a total imposed load of p_{sd} = 10.2 kN/m^2 can be obtained from Equation 1, when a live load equal to 2.5 kN/m^2 is assumed, as per design objective. The LRR at ULS therefore becomes equal to LLR_d = 86%, as reported in Table 7.6.

Table 7.6 - Design load, load bearing capacity and LRR of the T-deck at ULS

Design	γ_G	G_k	γ_Q	Q_k	p_{sd}	$\gamma_{m,s}$	$\gamma_{m,c}$	p_u	$p_u - p_{sd}$	LRR_d
T-deck	1.1	5.9	1.5	2.5	10.2	1.2	1.5	11.9	1.7	86%

V-deck

The second solution consists of a deck obtained by pouring an ordinary C30/37 concrete on hollow spheres made of high-density polyethylene and symmetrically distributed in the longitudinal and transversal direction. The deck is 40 cm high. The spheres have a diameter of 27 cm and are positioned at a distance of 4 cm from the bottom surface of the deck with a spacing of 30 cm. In correspondence of their maximum diameter of the spheres, i.e. at a depth of 17.5 cm in the slab, the thickness of the concrete between the sphere is at a minimum and specifically equal to 3 cm, as visible in Figure 7.17.

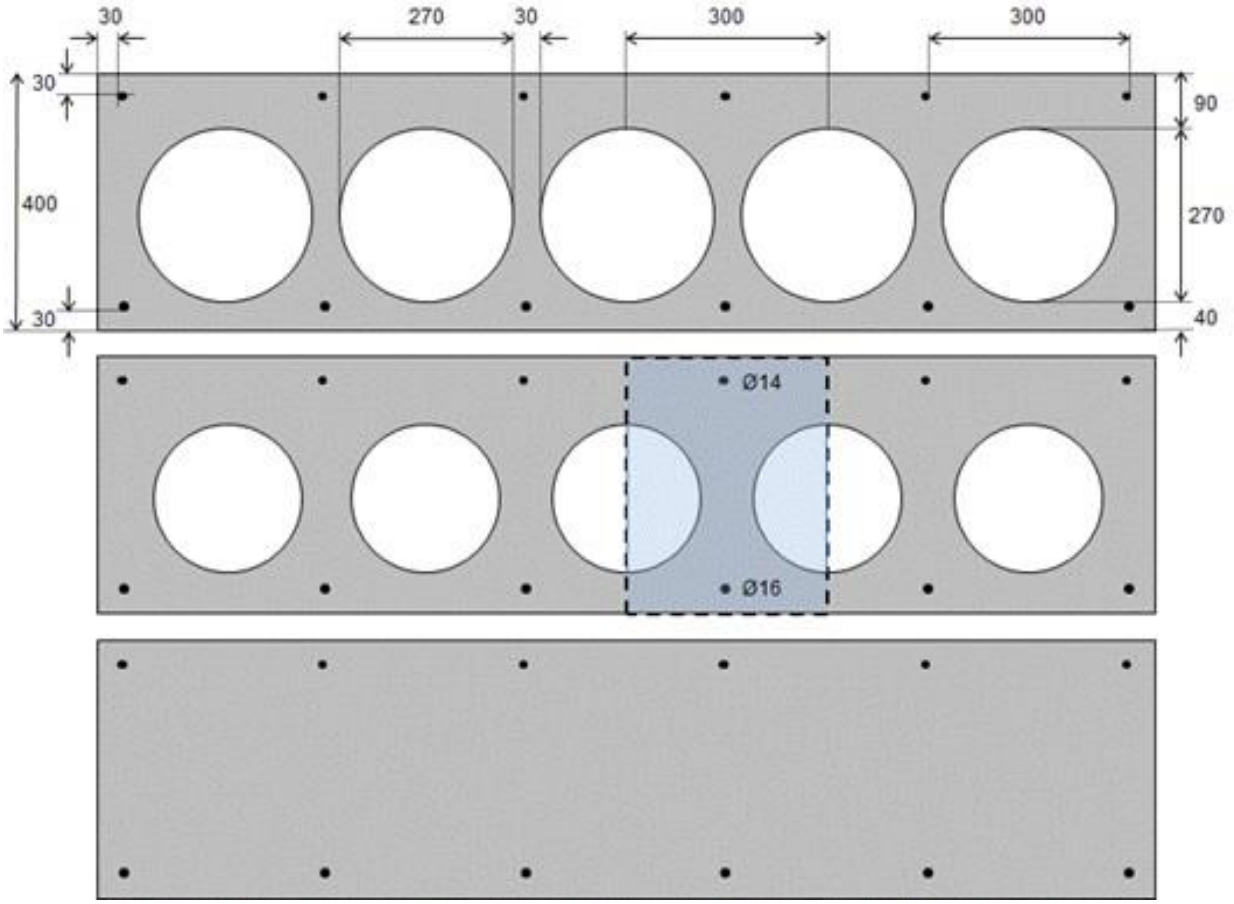

Figure 7.17 - Variable cross section of the V-deck. Top: section in correspondence with the maximum sphere diameter; bottom: section at the center line between two rows of spheres; center: section at an average distance between the two previous sections. The highlighted area corresponds to the reference section used in the investigations.

The reinforcement consists of φ=14 bars at the top and φ=16 bars at the bottom. The bars are made of B450c steel (Eurocode 10027-1, 2005), are spaced 30 cm along both the longitudinal and transversal direction, and have a cover of 3 cm. The steel and ordinary concrete are the same used in the T-beam slab, and hence the thermal and mechanical properties listed above also apply for this deck.

Simplified hand calculations of the flexural resistance, with the same assumptions mentioned for the T-deck, give a load bearing capacity of p_u = 14.9 kN/m^2 at 20°C, when the ULS material safety coefficients are used (see Table 7.7). More refined calculations carried out with a sectional program (Pfeiffer, 2011) accounting for softening and tensile resistance of concrete showed no significant difference in the load bearing capacity obtained with hand calculations.

Considering that the self-weight of the slab and the permanent weight of the superstructure gives a total dead load of 8.6 kN/m^2, a total imposed load of p_{sd} = 13.2 kN/m^2 is obtained by Equation 7.1, when a live load of 2.5 kN/m^2 is assumed, as per design objective. The resulting LRR at the ULS therefore equals LRR_d = 89%, as reported in Table 7.7.

Table 7.7 - Design load, load bearing capacity and LRR of the V-deck at ULS

Design	γ_G	G_k	γ_Q	Q_k	p_{sd}	$\gamma_{m,s}$	$\gamma_{m,c}$	p_u	$p_u - p_{sd}$	LRR_d
V-deck	1.1	8.6	1.5	2.5	13.2	1.2	1.5	14.9	1.7	89%

7.4.2. Analysis and assumptions

The investigations on the slabs availed a thermal and a structural model and considered the three conditions discussed in the following:

- Beginning of the fire

  At first, a separate structural analysis without fire has been carried out on each slab in order to assess its initial load bearing capacity. In this analysis two sequential nonlinear (for material and geometry) incremental static steps have been implemented. In the first step the slab has been considered loaded according to the accidental design and in the second step the uniform vertical load has been incremented until the collapse of the element. The load bearing capacity at the beginning of the fire is found as the sum of the vertical reaction of the last analysis step, when the end of the plateau is reached in the force-displacement curve.

- During fire

  In order to investigate the response of the slabs during fire, a thermal and a structural analysis have been performed in sequence, as explained in the following.

  - Thermal analysis: a two-dimensional model of the section of each slab has been implemented and the bottom part of each section has been considered exposed to fire. From the thermal analysis a thermal map of each section has been obtained at discrete times from the start to the end of the fire.
  - Structural analysis: two subsequent nonlinear analysis steps have been considered. In a first analysis step each slab has been subjected to the mechanical loads calculated for the accidental design situation. Then the temperature-time curves obtained by the thermal analysis at different depths of the sections have been used as input for the second step,

where the behaviour of the slabs during the fire is investigated by means of a transient analysis. The displacements of the mid-span of the two slabs have been monitored, providing a direct comparison of the performances of the two slabs during fire.

- End of the fire:

  A third subsequent nonlinear incremental static analysis step has been added at the end of the transient analysis. In this step, the temperatures are constant and equal to those reached at 90 min (the end of the second step), while the uniform vertical load has been progressively incremented on the slabs. For each deck, the load bearing capacity obtained from this investigation has been subtracted from the initial load bearing capacity at the beginning of the fire and the decrement has been then compared for the two slabs.

Structural models

The structural investigations have been performed with the avail of ABAQUS (ABAQUS, 2010), a commercial finite element software, capable of accounting for mechanical and geometrical nonlinearities and for temperature dependent mechanical and thermal properties of materials.

Different structural models with an increasing grade of refinement have been considered for the two slabs. In particular, the structural models are analyzed using both two-dimensional and three-dimensional finite elements, referred to as 2D FEM and 3D FEM, respectively.

All models refer to the behavior of a single strip of the slabs. This simplification seems appropriate for a mono-directional floor slab such as the T-beam deck, but it can lead to a slight underestimation of load bearing capacity of the V-deck. This underestimation however holds also in case of fire and does not seem essential to the purpose of comparing the decrement of the load bearing capacity. Furthermore, it allows for a feasible computational onus and permits a better highlight of the effects of the different lightening solutions of the section in the response to fire.

For the T-deck, a 50 cm wide strip has been considered, corresponding to a single T-beam and two half-blocks on the side of the beam web (Figure 7.16). The structural contribution of light-blocks was only considered in the 3D FEM. In the 2D FEM plane elements with two different thicknesses were used for representing the ordinary concrete of the flange and of the web.

For the V-deck a 30 cm wide strip of the slab has been considered (Figure 7.17). The section of the V-deck strip varies along the length due to the spherical shape of the voids. This variation has been duly represented in the 3D model, as visible in Figure 7.18. In the 2D FEM and in the thermal model, the intermediate section shown in the center of Figure 7.17 has been considered for sake of

simplicity. The assumption of a constant intermediate section seems reasonable from both a structural and a thermal point of view, since it represents an average value of the sectional resistance and it gives intermediate temperature values at each point of the section. In the 2D FEM seven different thicknesses have been assigned to the plane elements along the section height, to ensure that the smooth variation created by the spherical void had been sufficiently approximated.

In both the 2D and the 3D FEMs the reinforcement has been modelled as one-dimensional rods embedded in the concrete. An elastic-plastic constitutive relation and a degradation of the stiffness, elastic strength and ultimate strength have been considered for the steel, in compliance with what specified in the Eurocodes (EN 1993-1-2, 2005). A damage plasticity model has been adopted for the concrete, which requires the definition of a compressive hardening and a tension-stiffening model. As well-known (Feenstra & De Borst, 1995), the presence of softening in the constitutive relation causes a dependency of the results on the mesh size, due to possible localization of the strain (Bontempi & Malerba, 1997). The objectivity of the solution has been therefore ensured by preserving the fracture energy with a proper calibration of the material softening relation on the mesh, which respects the size limits for the consideration of the interaction contribution (Cervenka, et al., 1990) with the given reinforcement ratio. As noted in Carstensen (Carstensen, et al., in press), the validity of this calibration could be weakened during fire, as the fracture energy and the interaction contribution degrade with the temperature. However, in lack of experimental knowledge on the variation of the tensile fracture energy with temperature, the temperature dependency of the constitutive tensile relation has been modelled by assuming the same stiffness degradation as for compression and a degradation of the peak tensile strength as given in the Eurocodes (EN 1992-1-2, 2004).

The temperature dependency of the compressive stress-strain relation for ordinary concrete has been also taken from the same code. Since no indication on the degradation of the structural properties of the light concrete can be found in the code or in the literature, the degradation of stiffness and strength with temperature of the light-block has been assumed equal to that of normal concrete in the 3D FEM of the T-deck. Due to the presence of geometric nonlinearities, the thermal expansion is expected to affect, even if in a limited way, the vertical displacement of the slabs and therefore their performance during fire. In addition to the degradation of the mechanical properties of the materials, a temperature dependent expansion coefficient has therefore been considered in the structural models both for the steel and the concrete, according to the specifications of the Eurocodes (EN 1993-1-2, 2005), (EN 1992-1-1, 2004).

Thermal models

Since a constant section has been assumed for both the T-deck and the V-deck, it was possible to perform all thermal analyses on a 2D-model representing only the section of the slab strips. The bottom part of the two sections has been considered exposed to fire, while the other sides have been considered adiabatic. In each slab model, a temperature history of 0 to 90 min of the ISO834 standard fire curve has been assigned to the nodes of the exposed surface. The adiabatic conditions of the other surfaces are justified by the symmetry conditions on the sides of the strip and by the insulation provided by paving and possible sound insulation on the upper surface of the slabs.

In the T-deck both the concrete T-beam and the light concrete blocks have been modelled, so that the insulating effect of the blocks is duly represented in the structural investigation, even for the 2D FEM, where the mechanical contribution of the light blocks is neglected.

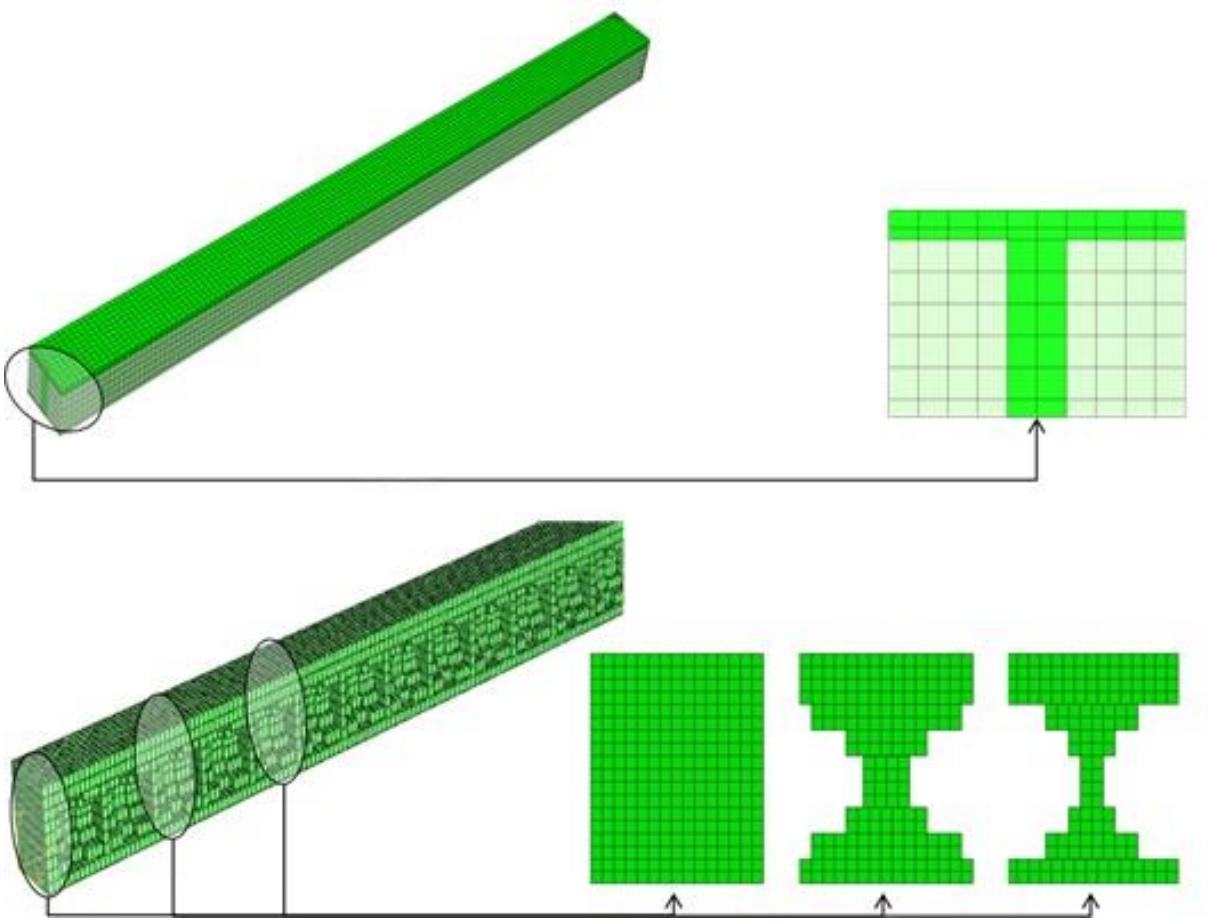

Figure 7.18 - Structural (left) and thermal (right) model of the T-deck (top) and of the V-deck (bottom)

In the V-deck the air in the void has not been modelled and therefore the surface of the spheres is regarded as an insulating surface during the whole duration of the fire. This assumption is valid in a first phase of the fire, when the air in the void is hindering the transport of heat to the upper part of

the section and the temperatures in the bottom flange gets higher than those of a full slab without voids. At a later stage however, this assumption could lead to a slight overestimation of the temperatures of the bottom concrete and underestimation of the temperatures of the upper concrete, since the heat radiation through the holes is not simulated in this model and the consequent heat transported from the bottom part of the slab to the upper part is neglected. Furthermore, the steel in the sections has not been modelled, as the difference in the temperature field would be negligible, and the steel temperatures have been assumed equal to the concrete temperatures pertinent to the node where the reinforcement is placed. The thermal properties assigned to the materials refer therefore only to the thermal properties of the ordinary and light concrete previously specified.

The degradation of the thermal properties of the ordinary concrete follows the indications given in the Eurocodes (EN 1992-1-1, 2004), while the thermal properties of the light concrete have been considered constant at the initial 20°C value specified in the previous section. In particular, Pettersson and Ödeen (Petterson & Odeen, 1978) showed that the conductivity of light aggregate concrete does not vary much with temperature and a constant value can be assumed as simple approximation.

7.4.3. Outcomes

In this section the results of the investigation are reported and discussed with reference to the three fire design situations presented above.

Beginning of the fire:

The load bearing capacity of the decks are reported in the following with respect to a uniformly distributed load and a 1 m deck width. Due to the fire design situation, the characteristic strength of both steel and concrete has been considered for the assessment of the load bearing capacity.

The results of the pushover analyses are given in Figure 7.19: a load bearing capacity of 14.9 kN/m^2 is observed for the T-deck, whereas a capacity of 19.3 kN/m^2 is found for the V-deck. In Table 7.8 these values are reported in the column indicates as $p_u{}^{fi}{}_0$ and they are found to be in good agreement with the results obtained by simplified calculations that were performed to validate the models. Specifically, the simplified hand calculations yielded load bearing capacities of 14.3 kN/m^2 for the T-deck and 17.8 kN/m^2 for the V-deck, while more refined calculations carried out with the avail of a sectional analysis program are resulted in load bearing capacities of 14.5 kN/m^2 and of 18.2 kN/m^2 for the T-deck and V-deck, respectively. For a direct comparison with the results of the pushover analyses, the latter values are indicated as dotted lines in Figure 7.19.

The resistance of the slabs at the beginning of the fire is compared with the imposed loads in accidental design situations, calculated according Equation 7.2. These loads are reported in Table 7.8 in the column indicated as p_s^{fi}. The difference (p_u^{fi}-p_s^{fi}) and the ratio (LRR^{fi}_0) between these two values are also reported in the last two columns of Table 7.8.

As mentioned in the previous section, even though the slabs have been designed to carry the same variable loads, the reduction of the material and load coefficients prescribed by the Eurocodes for the fire design situation (EN 1992-1-1, 2004) causes the slabs to have different LRRs at the beginning of the fire. In particular, the V-deck has a higher self-weight than the T-deck and therefore experiences a lower reduction of the soliciting load, as visible by observing the ratio p_s^{fi}/p_{sd} reported for both decks in Table 7.9.

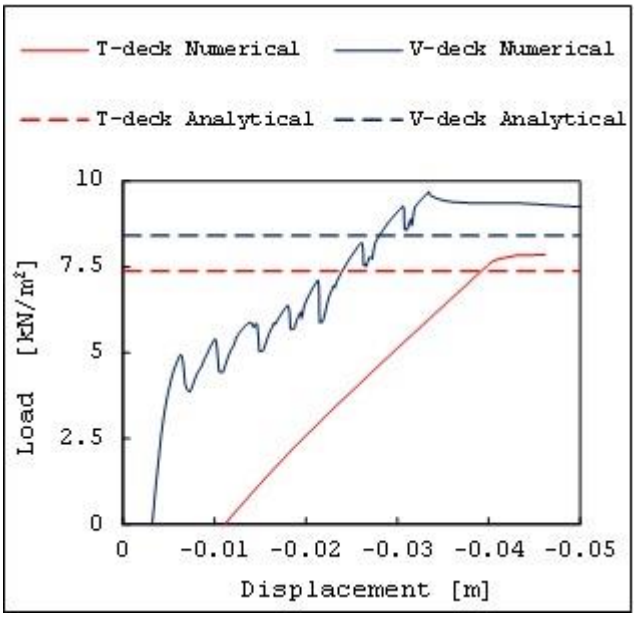

Figure 7.19 - Pushover curves of the T-deck (red) and of the V-deck (blue) and respective ultimate capacities calculated analytically (dotted lines)

However, the V-deck also experiences a higher increment of the resistance than the T-deck, as visible by observing the ratio $p_u^{fi}{}_0/p_u$ reported for both decks in Table 7.9. Therefore, even if the load decrement and the resistance increment are different for the two slabs, they counterbalance in the LRR. As a consequence, the decrement of the LRR is very similar for the two slabs, as visible in the column LRR^{fi}_0/LRR_d of Table 7.9. This small dissimilarity is therefore not expected to lead to significant differences in the structural response to fire.

$$p_s{}^{fi} = \gamma_G{}^{fi} \cdot G_k + \psi_{1,1} \cdot Q_{k1} \tag{7.2}$$

Table 7.8 - Imposed load, load bearing capacity and LRR at the beginning of the fire

Beginning of the fire	γ_G^{fi}	G_k	$\psi_{1.1}$	Q_k	p_s^{fi}	$\gamma_{m,s}$	$\gamma_{m,c}$	$p_{u\ 0}^{fi}$	$p_{u\ 0}^{fi}-p_s^{fi}$	LRR^{fi}_0
T-deck	1.0	5.9	0.4	2.5	6.9	1.0	1.0	14.9	8.0	46%
V-deck	1.0	8.6	0.4	2.5	9.6	1.0	1.0	19.3	9.7	50%

Table 7.9 - Variation of solicitant load, resistance and resulting LRR in the accidental design situation for the two slabs

	T-deck			V-deck		
	p_s	p_u	LRR	p_s	p_u	LRR
Design	10.2	11.9	86%	13.2	14.9	89%
Beginning of the fire	6.9	14.9	46%	9.6	19.3	50%

	p_s^{fi}/p_{sd}	$p_{u\ 0}^{fi}/p_u$	LRR^{fi}_0/LRR_d	p_s^{fi}/p_{sd}	$p_{u\ 0}^{fi}/p_u$	LRR^{fi}_0/LRR_d
Ratio	68%	125%	54%	72%	129%	56%

<u>During the fire:</u>

The results of the thermal analysis of the decks are reported in Figure 7.20. In the upper parts of the figure, the variation of the temperatures in the centre of the section along the height of the two slabs is reported for 30, 60, and 90 min of fire.

As can be seen by comparing the graphs of the T-deck and of the V-deck on the left and right of the figure respectively, the temperatures in the two slabs are very similar. In the bottom part of the figure, the thermal maps of the two decks at 90 min are shown. The convexity of the isotherms in the thermal map of the V-deck reflects the insulating effect of the voids. As mentioned in the previous section, at the same depth into the slab, the temperatures of the concrete are higher just beneath the spheres and are higher in-between, where the heats can be absorbed by the concrete web. The bottom part of a slab with voids will therefore have higher temperatures in correspondence of the voids and lower temperature in correspondence of the concrete web than a

slab without voids. This situation will revert when temperatures at the bottom of the holes become very high and heat is radiated through the holes to the upper part of the section (Schiermacher & Poulsen, 1987). At this point, the assumption of adiabatic surfaces for the void and the consequent convex isotherms will lead to an overestimation of the temperatures beneath the holes and an underestimation of the temperatures beneath the concrete web. However, this effect is not expected to be crucial for the considered time of fire exposure and a more refined consideration of the thermal model has been disregarded study.

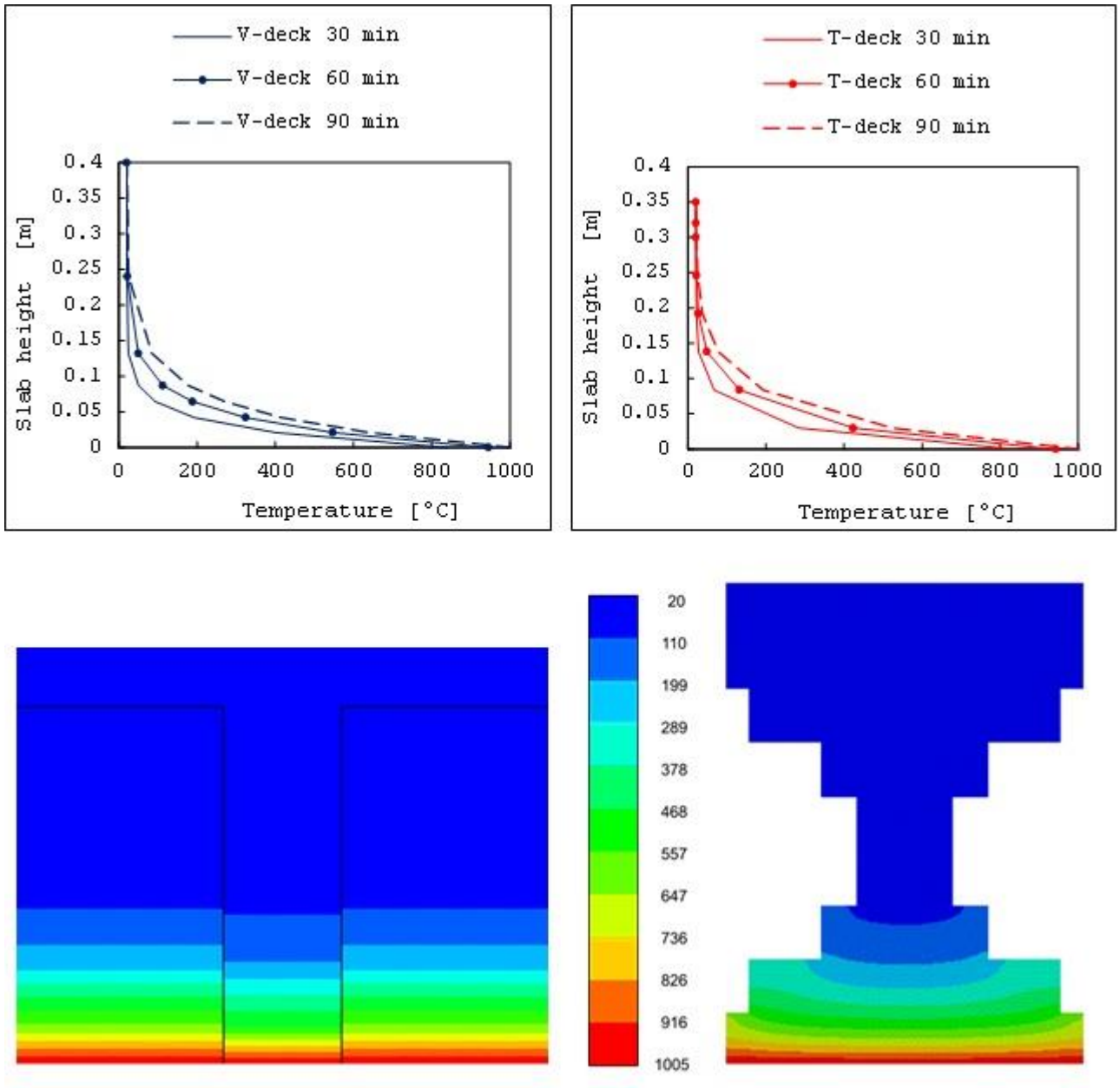

Figure 7.20 - Thermal analysis of T-deck (left) and V-deck (right). Top: variation of the temperatures at the center of the section along the slab height at 30-60 and 90 min; bottom: thermal maps at 90 min of exposure.

The results of the structural investigations during fire on the 2D FEMs of the slabs are reported in Figure 7.21 in terms of mid-span displacement over time. It is seen that the mid-span displacement of the T-deck, which was equal to 9 mm at the beginning of the fire, increases to 178 mm after 90 min of fire. The increment is significant however not critical, as the moment capacity still is sufficient to sustain the load and no runaway of the mid-span displacement is triggered. A similar behaviour is seen for the V-deck, which also resist 90 min of fire without failing. The displacements of the V-deck are however slightly different to those of the T-deck. This applies in particular to the beginning and at the end of the fire, when the mid-span displacements of the V-deck are equal to 3 mm and 193 mm, respectively.

Before fire, the V-deck is stiffer than the T-deck, as a result of the contribution of the bottom concrete flange to the bending. However, due to a higher sensitivity of the V-deck to fire, this advantage is rapidly lost as the temperature increases. As seen in Figure 7.21, it is found that over time of exposure the displacements of the V-deck become similar to those of the T-deck and ultimately even slightly higher.

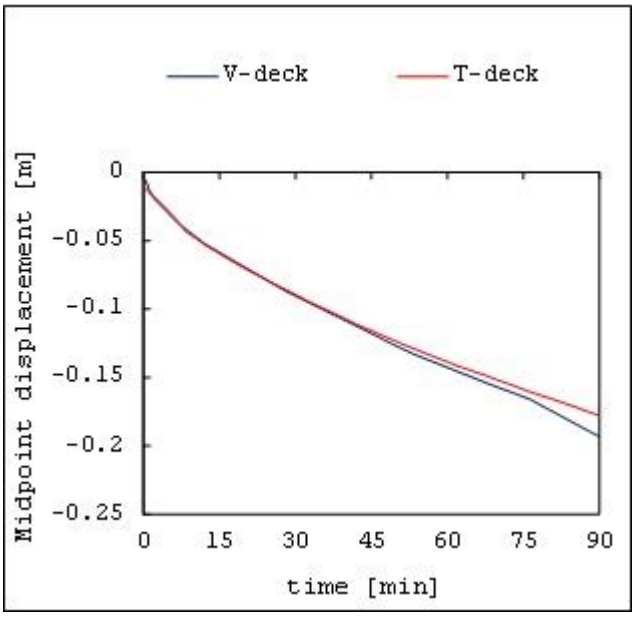

Figure 7.21 - comparison of the mid-span displacement over time of the 2D model of the T-deck (red line) and V-deck (blue line).

End of the fire:

The load bearing capacities of the two slabs at the end of the fire have been investigated with respect to a width of 1 m and to a uniformly distribute load.

The outcomes of the pushover analyses are visible in Figure 7.19 and summarized in Table 7.10, where the load bearing capacities of the slabs $p_u^{fi}{}_{90}$ and the imposed load for the fire condition p_s^{fi}, calculated by Equation 7.2, are reported. The difference ($p_u^{fi}{}_{90}$-p_s^{fi}) and the ratio ($LRR^{fi}{}_{90}$) between these two values are also given in the last two columns of Table 7.10.

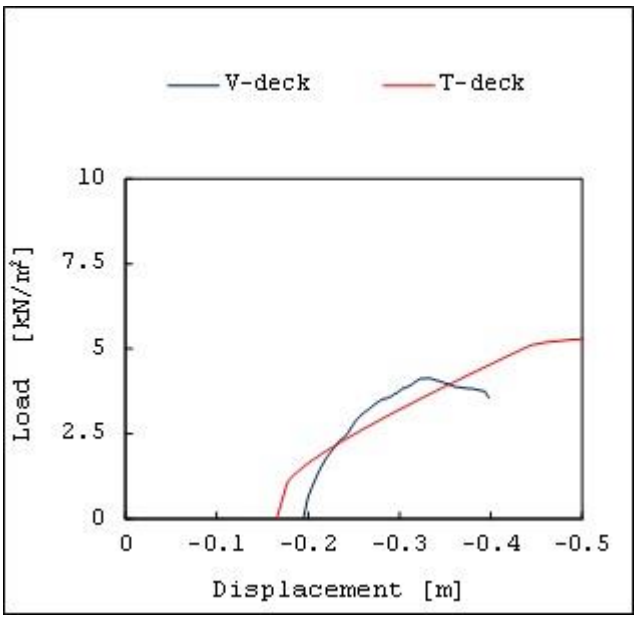

Figure 7.22 - Pushover curves of the T-deck (red) and of the V-deck (blue) at 90 min of fire

It can be observed that the V-deck, which initially had a higher load bearing capacity than the T-deck (Table 7.8), has significantly decreased its perquisite after 90 min of fire. At this point, the load bearing capacities of the T-deck and of the V-deck are quite similar and equal to 12.3 kN/m^2 and 13.7 kN/m^2, respectively (see Table 7.10). The difference between the load bearing capacity and the imposed loads on the slabs ($p_u^{fi}{}_{90}$-p_{sd}^{fi}), that can be interpreted as the additional load the slabs can carry before failure also illustrates this effect. At the beginning of the fire the V-deck has a higher capacity for additional load than the T-deck, specifically 9.7 kN/m^2 vs. 8.0 kN/m^2. After 90 min of fire this situation is reverted, as the additional load that V-deck can carry is assed as 4.1 kN/m^2 vs. 5.4 KN/m^2 of the T-deck. As a result, the LRR_{90}^{fi} is significantly higher for the V-deck than for the T-deck, and specifically equal to 70% and 56%, respectively.

Table 7.10 - Imposed load, load bearing capacity and LRR at the end of the fire

End of the fire	γ_G	G_k	$\psi_{1.1}$	Q_k	p_s^{fi}	$\gamma_{m,s}$	$\gamma_{m,c}$	$p_u^{fi}{}_{90}$	p_u^{fi}-$p_s^{fi}{}_{90}$	LRR_{90}^{fi}
T-deck	1.0	5.9	0.4	2.5	6.9	1.0	1.0	12.3	5.4	56%
V-deck	1.0	8.6	0.4	2.5	9.6	1.0	1.0	13.7	4.1	70%

7.4.4. Validation of the thermal and structural models

The thermal models have been validated against simplified analytical methods for calculating the temperatures through a concrete slab exposed to fire from the bottom. These are based on the unidirectional transmission of heat through the slab depth. Specifically, the empirical formula introduced by Wickström (Wickstrom, 1986) and reported in Equation 7.3, and the analytical formula proposed by Hertz (Hertz, 1981), adopted in the past Danish building code for concrete (DS411, 1999), and reported in Equation 4, have been considered.

Wickström: $$T_c(z, t_h) = \left[0.18 \cdot \ln\left(\frac{\alpha}{\alpha_c}\frac{t_h}{z^2}\right) - 0.81\right] \cdot \left(1 - 0.0616 \cdot t_h^{-0.88}\right) \cdot T_g(t_h) \quad (7.3)$$

where:

t_h is the time of exposure to a standard fire expressed in hours;

T_g is the temperature of the fire at the time th;

z is distance from the exposed surface of the slab to the point of interest;

T_c is the concrete temperature at a depth z into the slab and at a time th;

α_c is the reference diffusivity, equal to 1.5•10-3 m2/h

α is the slab diffusivity, calculated as $\alpha = \sqrt{\tilde{\lambda}_c / \tilde{\rho}_c \cdot \tilde{c}_{p,c}}$ = $5.68 \cdot 10^{-7}$ m^2/s from the average values of specific heat, density and thermal conductivity of concrete in the estimated temperature interval, which are respectively: ρ_c = 2200 kg/m3; $c_{p,c}$ = 1000 J/(kg·K); λ_c = 1.25 W/(m·K).

Hertz: $$T_c(z, t) = \frac{312}{345} \cdot (T_g - 20) \cdot e^{-1.9 \cdot k(t) \cdot z} \cdot \sin\left(\frac{\pi}{2} - k(t) \cdot z\right) \quad \text{with:} \quad k(t) = \alpha \Big/ \sqrt{\frac{\pi}{750 \cdot t}} \quad (7.4)$$

where:

t is the time of exposure to a standard fire expressed in minutes;

T_g, z, T_c, and α have the same meaning as above.

In Figure 7.23, the temperatures of the slabs obtained by the thermal analyses are compared with the outcomes from Equation 7.3 and 7.4. On the left side of the figure, the temperatures along the slab depth after 90 min of fire are reported. On the right side of the figure, the temperatures calculated at a depth of 3 cm along the central vertical axis are illustrated for the whole duration of the fire. This point corresponds to the position of the reinforcement in both slabs and the temperature can be therefore interpreted as the temperature of the steel bars in the slabs.

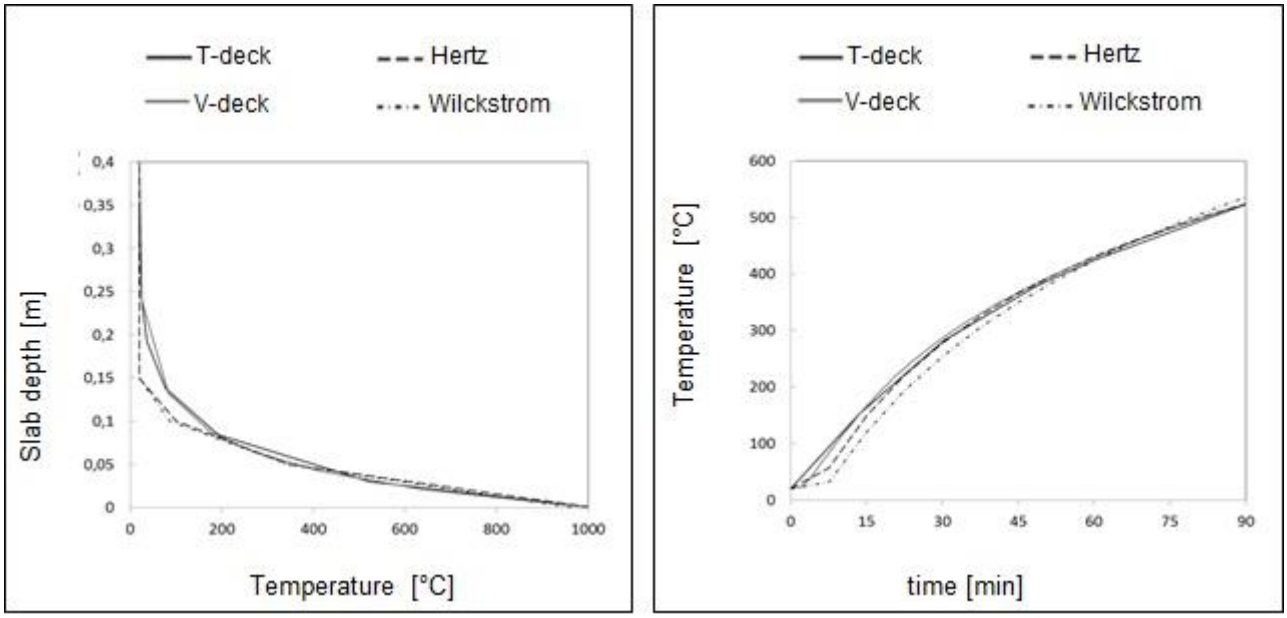

Figure 7.23 - Validation of the thermal models of the T-deck and of the V-deck. Comparison of the temperatures along the central vertical axis of the two slabs at 90 min (left) and of the temperatures of the bottom steel bars over time (bottom)

The temperatures obtained for the steel by the analytical calculations are equal to 524°C and 536°C for Hertz's and Wickström's method, respectively. Despite the complex configuration of the slabs, which the above formulas cannot take into account, the simplified calculation are in good agreement with the results of the thermal analysis, which give 523°C for the T-deck and 524°C for the V-deck.

With respect to the structural analysis, a comparison of the results obtained by the 2D and 3D FEM is provided in terms of displacements under fire for the T-deck and pushover analysis before fire for the V-deck (Figure 7.24). For both slabs, the differences in the outcomes obtained with the two FEMs are not significant and justify the use of the 2D model for further investigations.

For the T-deck, the difference in the displacements found for the 2D- and 3D-FEM on the left of Figure 7.24 is very small, indicating that the contribution of the light aggregate concrete blocks is negligible and that the difference in thermal expansion between the two materials does not have a significant effect on the overall response to fire.

The 2D- and 3D-FEM of the V-deck instead reveals a small difference in the stiffness of the slab at the beginning of the pushover analysis. This can be ascribed to the approximation made in the 2D-FEM, where a constant section has been considered along the slab length. However, both 2D and 3D-FEM give the same ultimate resistance and show a very similar global behaviour of the slab.

Therefore, in consideration of the significantly higher computational onus, the 2D-model has been used for the investigations presented.

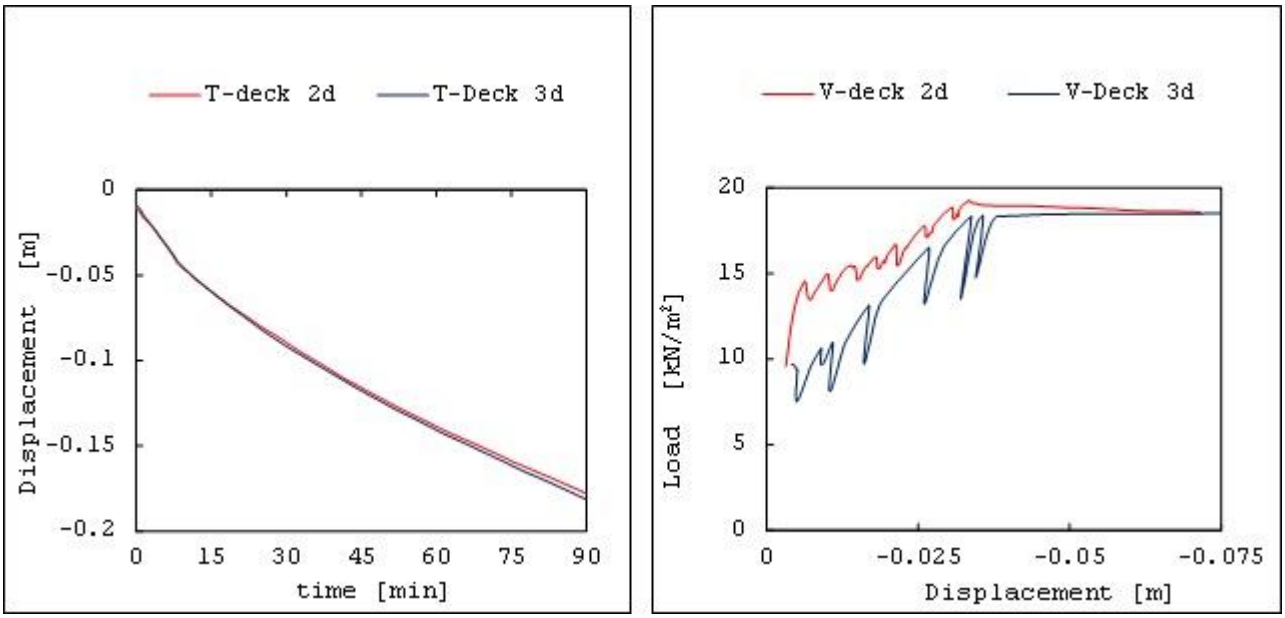

Figure 7.24 - mid-span displacement of the T-deck during fire (left) and pushover on the V-deck before fire (right), obtained with 2D-FEM (continuous line) and 3D-FEM (dotted line)

7.4.5. Summary of the outcomes

In Table 7.11, an overview of the main outcomes is provided. It can be seen that the slabs have been designed to carry the same load. At the beginning of the fire however the V-deck can carry a higher additional load than the T-deck, as a consequence of a different increment of the resistance and a different reduction of the loads in the accidental design situation for the two slabs. At the end of the fire this situation is reverted and the T-deck has a slightly higher additional load carrying capacity than the V-deck, resulting from a significantly higher decrement of the load bearing capacity of the V-deck after the exposure to the fire.

Table 7.11 - Summary of the outcomes for the T-deck (left side) and V-deck (right side)

	T-deck				V-deck			
	p_s	p_u	p_u-p_s	LRR	p_s	p_u	p_u-p_s	LRR
Design	10.2	11.9	1.7	86%	13.2	14.9	1.7	89%
Beginning of the fire	6.9	14.9	8.0	46%	9.6	19.3	9.7	50%
End of the fire	6.9	12.3	5.4	56%	9.6	13.7	4.1	70%

Considering that the LRR of the two slabs at the beginning of the fire is slightly different but still comparable and that the temperature increment the slabs experience during fire is very similar, the higher decrement of load bearing capacity of the V-deck is mainly ascribable to its different structural configuration, which lead to a higher sensitivity to the temperatures, i.e. a higher vulnerability to fire. This is clearly visible in Figure 7.25, where the differences in the pushover analyses of the slabs before fire are compared with the pushover analyses at the end of the fire. The values reported on the vertical axis of the two graphs represent the load imposed during the pushover analysis, depurated from the soliciting loads of the accidental design situation. The drop of the ultimate values represents therefore the decrement of the additional loads that can be carried by each slab after 90 min of standard fire.

It can be concluded that the V-deck, which is more resistant than the T-deck in the nominal situation, is more vulnerable to fire, as it experience a bigger decrement of the load bearing capacity after the same fire exposure.

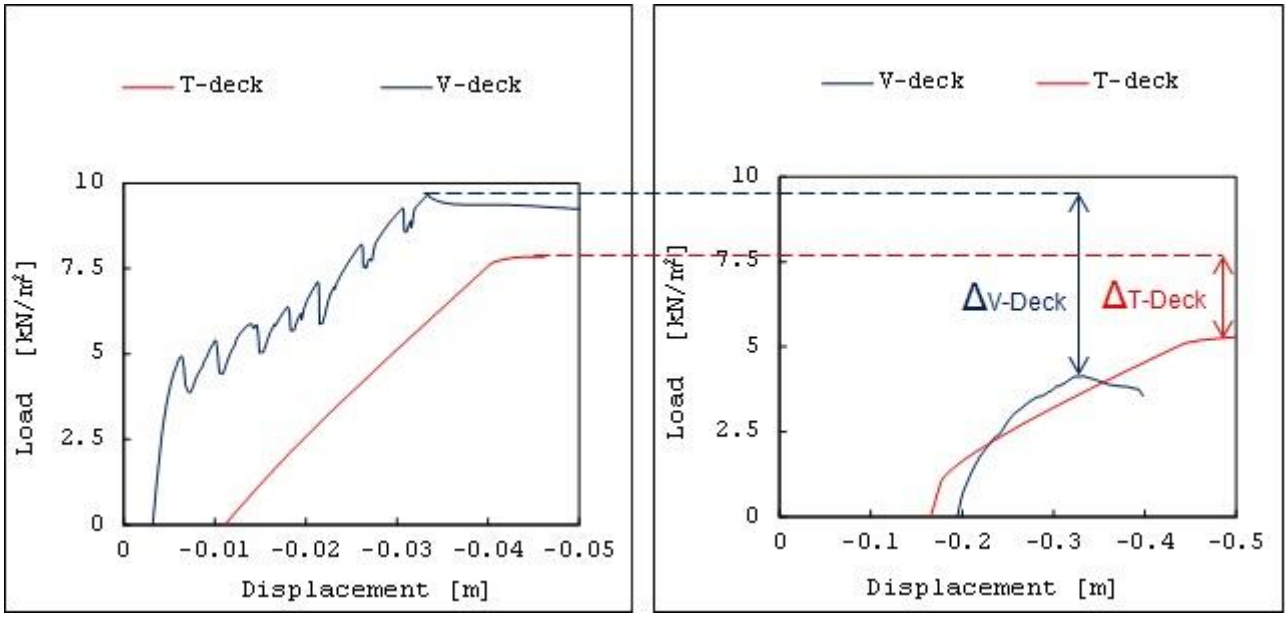

Figure 7.25 - Comparison of the resistance decrement for the two slabs

7.4.6. Structural vulnerability to fire

In order to extend this procedure to other slabs, which may differ one another for having different loading conditions and different initial resistance, it seems sensible to compare the decrement of the load bearing capacity to the nominal load bearing capacity. The same relative decrement expressed in percentage can be found in literature for the assessment of the fire performance of R.C. beams

and is referred to as the Damage Factor (Jayasree, et al., 2011). In Equation 7.5, the relative decrement of the load bearing capacities in percentage of the two slabs is calculated as:

T-deck: V-deck:

$$\frac{\Delta p_u^{90}}{p_u^{0}} = \frac{(14.9\text{-}12.3)\,kN/m^2}{14.9\,kN/m^2} = 17\% \qquad \frac{\Delta p_u^{90}}{p_u^{0}} = \frac{(19.3\text{-}13.7)\,kN/m^2}{19.3\,kN/m^2} = 29\% \tag{7.5}$$

This index represents a simple way of assessing and comparing the vulnerability of structural elements to a given fire: the higher the index, the higher the vulnerability of the element. However, it should be noted that this simple procedure only allows a comparison of elements exposed to the same fire. Since the load bearing capacity does not typically show a regular decrement with the temperature, it is not possible to express the vulnerability to fire as a general property with a single index, such as the ratio between the decrement of the load bearing capacity and the level of fire exposure. However, the decrement of the load bearing capacity can be monitored for increasing levels of fire exposure (e.g. 30, 60, 90 min of standard fire) and a curve can be obtained, whose derivative can be interpreted as the structural vulnerability of the element to fire.

Reference can be made to Giuliani (Giuliani, 2012) where the decrement of load bearing capacity of a structure was monitored with respect to an increasing number of failed elements, referred to as damage level in the study. A similar definition of the damage level is used in Brando et al. (Brando, et al., 2012), where the variation of the stiffness matrix eigenvalues of a structure is monitored for increasing level of damage. In both cases, the diagram of the monitored quality over increasing damage levels provide information on the robustness of the structures, intended as sensitivity of the system to local failures (Starrosek, 2009).

Similarly to what suggested with respect to the robustness curves of a structure in Giuliani (Giuliani, 2008), important information on the susceptibility of elements to fire can be obtained from the above mentioned vulnerability curve. This includes the maximum resistance time (e.g. the exposure time corresponding to a null residual load bearing capacity) and the convexity of the curve, which can reveal an early or late abrupt increment of the damage factor.

SECTION 3:

APPLICATIONS

Chapter 8

8. ADVANCED NUMERICAL ANALYSES FOR THE ASSESSMENT OF STEEL STRUCTURES UNDER FIRE

8.1. KEY FACTORS OF FIRE STRUCTURAL ANALYSIS

Several factors can affect the analysis of the response to fire of single storey steel structures. The chapter wants to highlight some of them Figure 8.1:

- Sometimes a reliable evaluation of collapse mechanisms can be made only by investigating the full three-dimensional structure. In this chapter this aspect is addressed by comparing the collapse mechanisms obtained by three different structural models (see section 8.3): a plane model of a two-span frame, a spatial model of the same frame and the full 3D model of the whole structure.
- Since the deformed configuration of the structure under fire must be investigated, an efficient numerical algorithm is needed for solving the finite element problem. Section 8.4.1 is focused on the comparison of two different numerical algorithms available in FE codes (static, dynamic implicit and dynamic explicit) for the resolution of the structural analysis.
- The interaction of the heated elements with the rest of the structure can trigger different mechanisms of collapse as a function of mutual position of the elements. The decision about which elements are engaged by the fire determines the collapse mechanisms and the collapse time. In section 8.4.2 this issue is addressed by investigating the structural response obtained by changing the location of the fire. In the first case, the (ISO, 1975) curve simulates the development of fire and provides for each time a value of gas temperature. The assumption of uniform and homogeneous heating of elements allows evaluating their surface temperature.
- The section 8.5 of this chapter focuses on natural fire approach that represents the most conducive solution in order to evaluate realistic fire scenarios. In relation to fire model, some analyses have been performed by means the free CFD software, Fire Dynamics Simulator ((NIST, 2009). In this case, the CFD model studies the fire development and the

adiabatic surface temperature (AST), (Duthinh, et al., 2008), solves the heat transfer model and provides the input for the subsequent performance investigations carried out by FE codes.

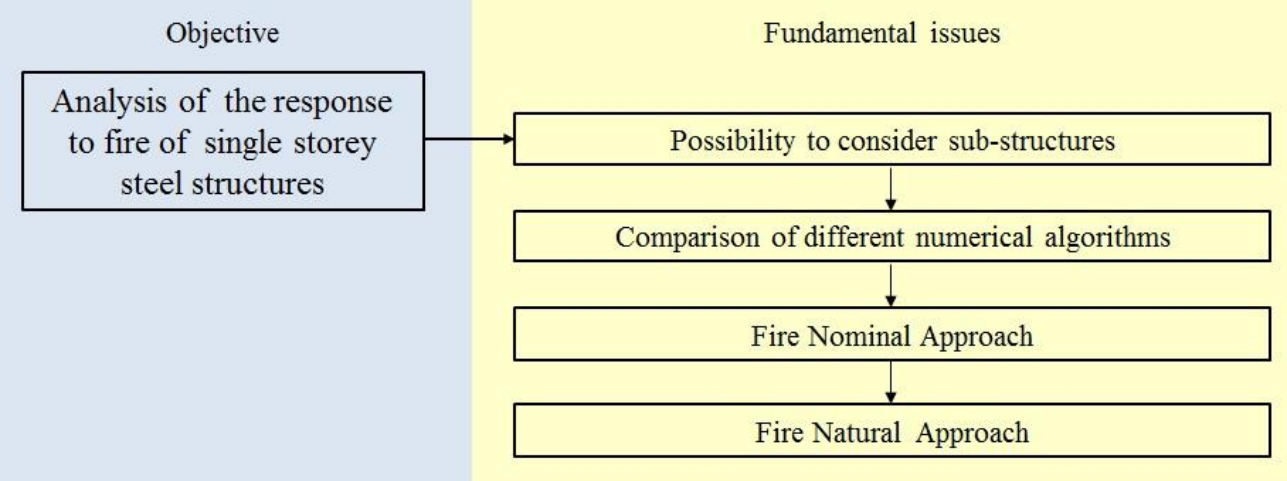

Figure 8.1 - Key factors of fire structural analysis.

8.2. CASE OF STUDY

The industrial hall considered as a case study is shown in Figure 8.2. This structure has been previously investigated by (Vassart, et al., 2004). The system is composed by 5 pitched portals, jointed by means of purlins. The length of the main rafter is 20 m, and the height of the 15 columns is 5 m.

Due to the presence of doors, which are located on the longest building facade with an area of 30 m^2, and of the windows, located on the shortest sides with an area of 28 m^2, the opening factor is taken equal to 0.0265 $m^{½}$ ((Petterson, et al., 1976). The premises are assumed to be used as sawmill and the fire load is represented by 18 wood stacks of dimension 1.2m x 1.2m x 3m, which results in a fire load density of 65 MJ/m^2 floor. The fire load has been calculated on the basis of a HRR of the single stack of 6.81 MW/m^2 floor as reported by (La Malfa & La Malfa, 2009) and calorific value of wood assumed equal to 14.5 MJ/kg. The thermal inertia was considered to be b = 1070 J/($m^2s^{1/2}$K).

Reference is made to the Eurocodes (EN 1993-1-2, 2005) for the modelling of material degradation under fire. For what concerns mechanical properties, strain hardening is not considered while a linear decay of strength has been taken into account between 15% and 25% strain.

The use of two different structural codes in each analysis has allowed a mutual validation of the models (ABAQUS, 2010), (DIANA, 2008).

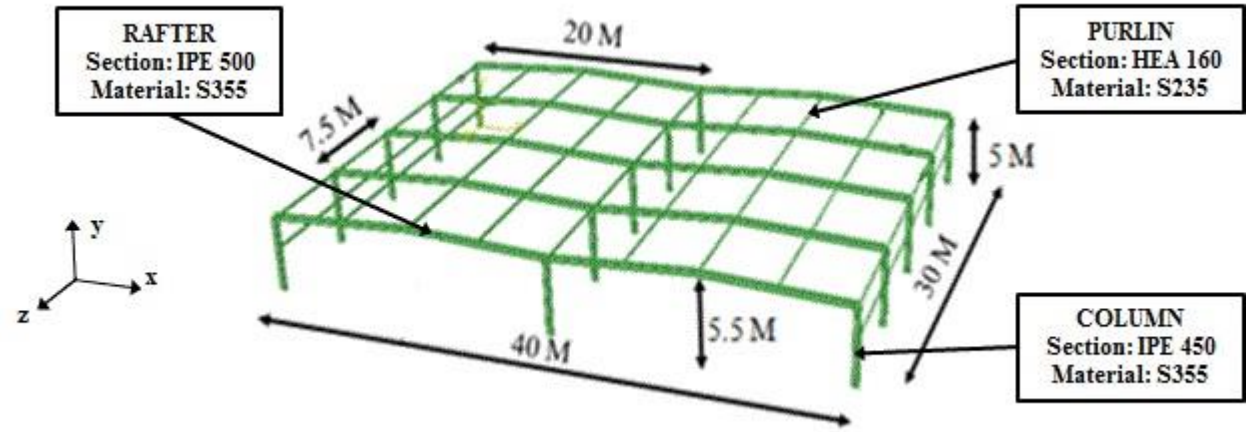

Figure 8.2 - Structure considered as case-study.

8.3. EFFECTS OF STRUCTURAL MODELLING

The analysis of single structural elements allows understanding some fundamental mechanisms of collapse (Usmani, et al., 2003). Sometimes however this is not sufficient for assessing the real behaviour of a complex structure, because redundant systems can find different load paths to carry the external actions when individual members fail. Sometimes the collapse of individual elements can be acceptable for economic reasons and for the exceptional nature of the action. In these cases, the objective of the analysis is to identify the global behaviour of the structural system, after the achievement of local collapse condition. Furthermore, the analysis of individual elements does not allow evaluating global mechanisms (e.g. instability) and effects of heated elements on the rest of structure. Members within a structure can expand when heated, which in some cases will have negative effects, for example by pushing columns out of alignment, but the thermal expansion may also have positive effects, for example by initiating compressive membrane action in a concrete slab.

Several deformation modes of such building under fire are possible: frames can collapse into the building (inwards collapse) or, when sway sideways, frames may collapse outwards due P-delta effects and may lead to adjacent property being damaged or persons outside the building being endangered (Moss, et al., 2009). The first analysis highlights the differences between the structural responses obtained by a two span frame in two dimensions (model 1), a two-span frame in three

dimensions, which has been restrained in the third direction in order to take in account the interaction with the rest of the structure (model 2), and the same frame when the whole structure is modelled (model 3). The fire at this stage has been modelled by the time-temperature ISO 834 curve (ISO, 1975), while indications of Eurocodes for unprotected elements (EN 1991-1-2, 2004) has been followed concerning the thermal transfer model: here the convective coefficient α has been assumed equal to 25 W/m^2K, the resultant emissivity ε has been chosen equal to 0.5 (no shadow effect is considered). Table 8.1 summarizes the analysed models, while the time development of the temperatures of the gas and of the elements is reported in Figure 8.3.

Table 8.1 - Considered models

ID MODEL	FIRE MODEL	HEAT TRANSFER MODEL	STRUCTURAL MODEL
1	Nominal Curve ISO 834	From EN 1993-1-2:2005	A double frame in 2 dimensions
2	Nominal Curve ISO 834	From EN 1993-1-2:2005	A double frame in 3 dimensions
3	Nominal Curve ISO 834	From EN 1993-1-2:2005	A full study in 3 dimensions

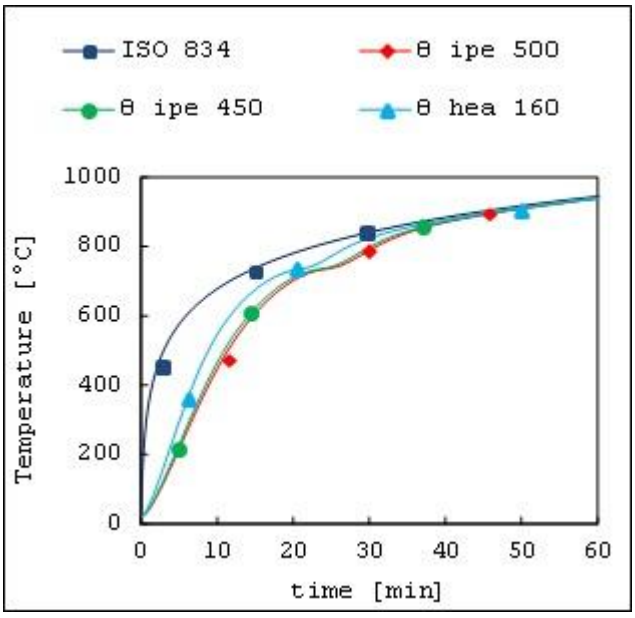

Figure 8.3 - Temperatures of gas and elements.

8.3.1. Two–span pitched portal in two dimensions (model 1)

According to many studies on the behaviour of a frame with a span in fire conditions (Bong, 2005), (Song, et al., 2009), (Wong, et al., 2000), (O'Meagher, et al., 1992), the collapse of single-span frames occurs in two ways. The collapse is caused by the outward movement of the columns due to the change of geometry and to thermal expansion of the rafter. This determines rotations at the base that can induce an initial mechanism. This initial mechanism may lead to collapse of the whole frame, or the columns may be pulled back towards the upright position due to the collapse of the rafters (Song, et al., 2007). (Newman, 1990) describes the behaviour of multi-bay frames and suggests that the frames will deform in very similar ways to that of single-bay frames (Bong, 2005).

The main features of model 1 are shown in Figure 8.4, where the heated elements are represented with bold lines. Figure 8.5 shows instead the last configuration obtained in the static analysis (here intended as a transient computation carried out by neglecting the inertial effects): an initial expansion due to fire causes a lateral displacement of the left column and a little upwards movement of the left rafter beam, then the drop of beam prevails.

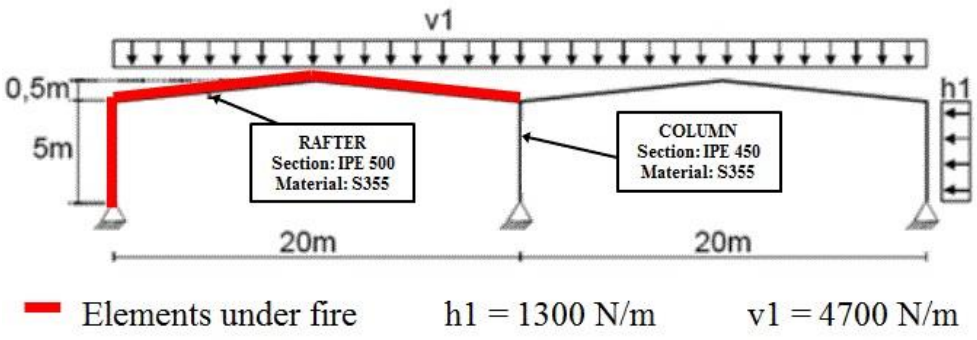

Figure 8.4 - Structural scheme of 1 model.

Figure 8.6 shows the lateral displacement of point A (top left), the vertical displacement of point B (top right), the normal force with respect to the time at the connection between the central column and the beam under (bottom left) and the shear of base of the left column with respect to the displacement of head of the same column (bottom right). The static analysis aborts after about 25 minutes. This analysis is not sufficient to understand the real collapse mechanism. The right frame, which is not under fire, remains in its initial position and it is not affected by the left frame collapse.

It is expected that the left frame collapses inwards, but the static finite element analysis aborts before node A (top of the heated column) starts moving inwards. At this stage, the failure of the column has not yet occurred, and in order to overcome the aborting, the structure has been analysed by making use of the code's dynamic solver.

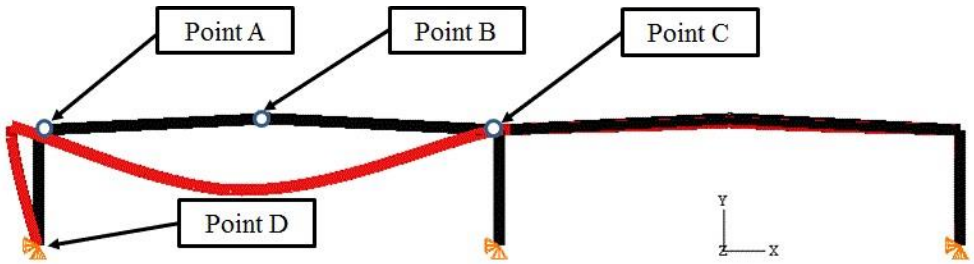

Figure 8.5 - Deformed shape (scale factor 5) of the 2D frame (model 1) at the end of static analysis.

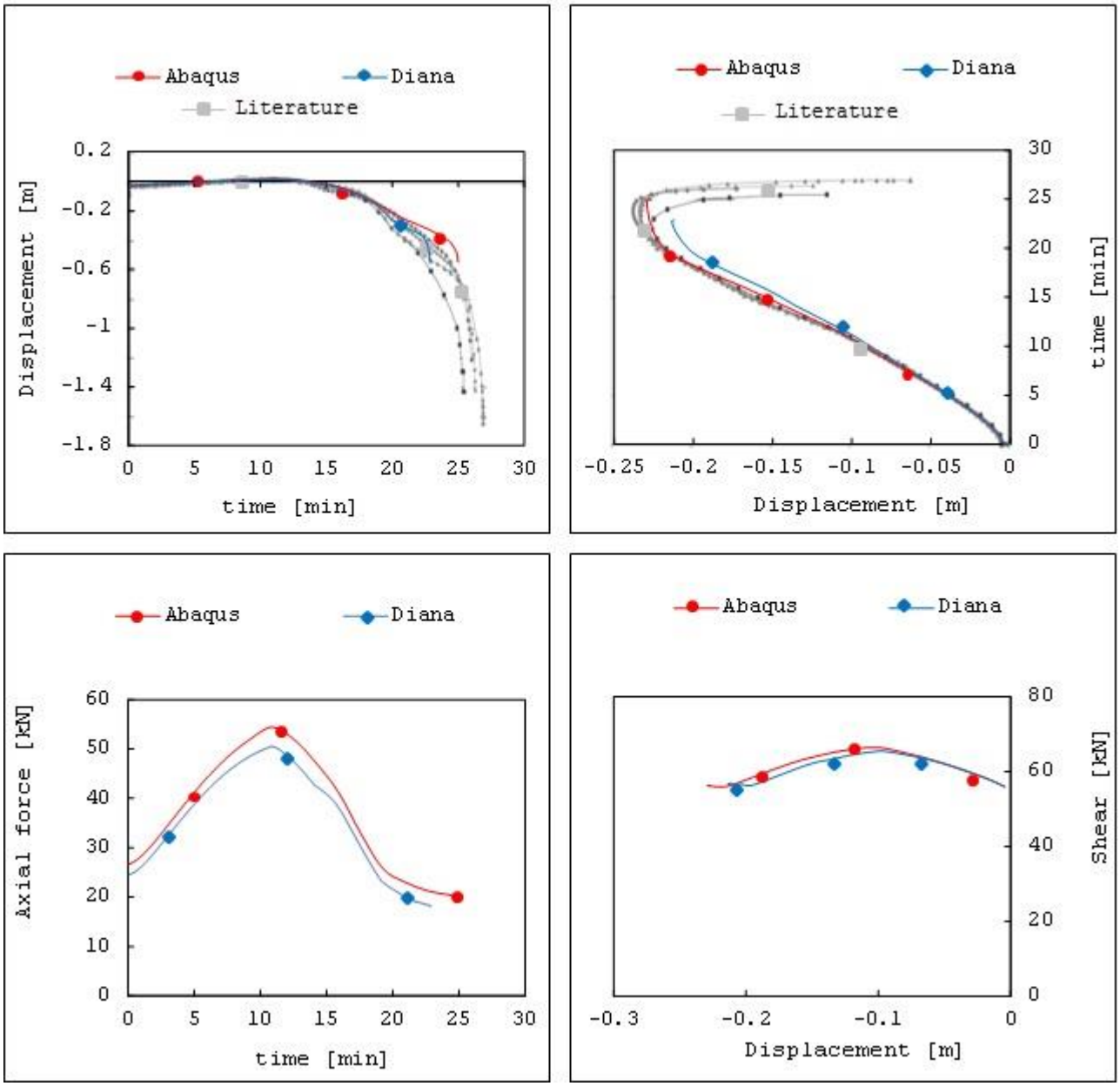

Figure 8.6 - Static analysis of the 2D pitched portal: lateral displacement of point A (top left); vertical displacement of Point B (top right); normal force in point C (bottom left); shear force of point D with respect to lateral displacement of point A (bottom right).

This allows seeing the snap-through instability of the rafters (Figure 8.6 left) and the inwards displacement of the column (Figure 8.6 right). It seems that only one of the adopted structural codes was able to compute this kind of structural response.

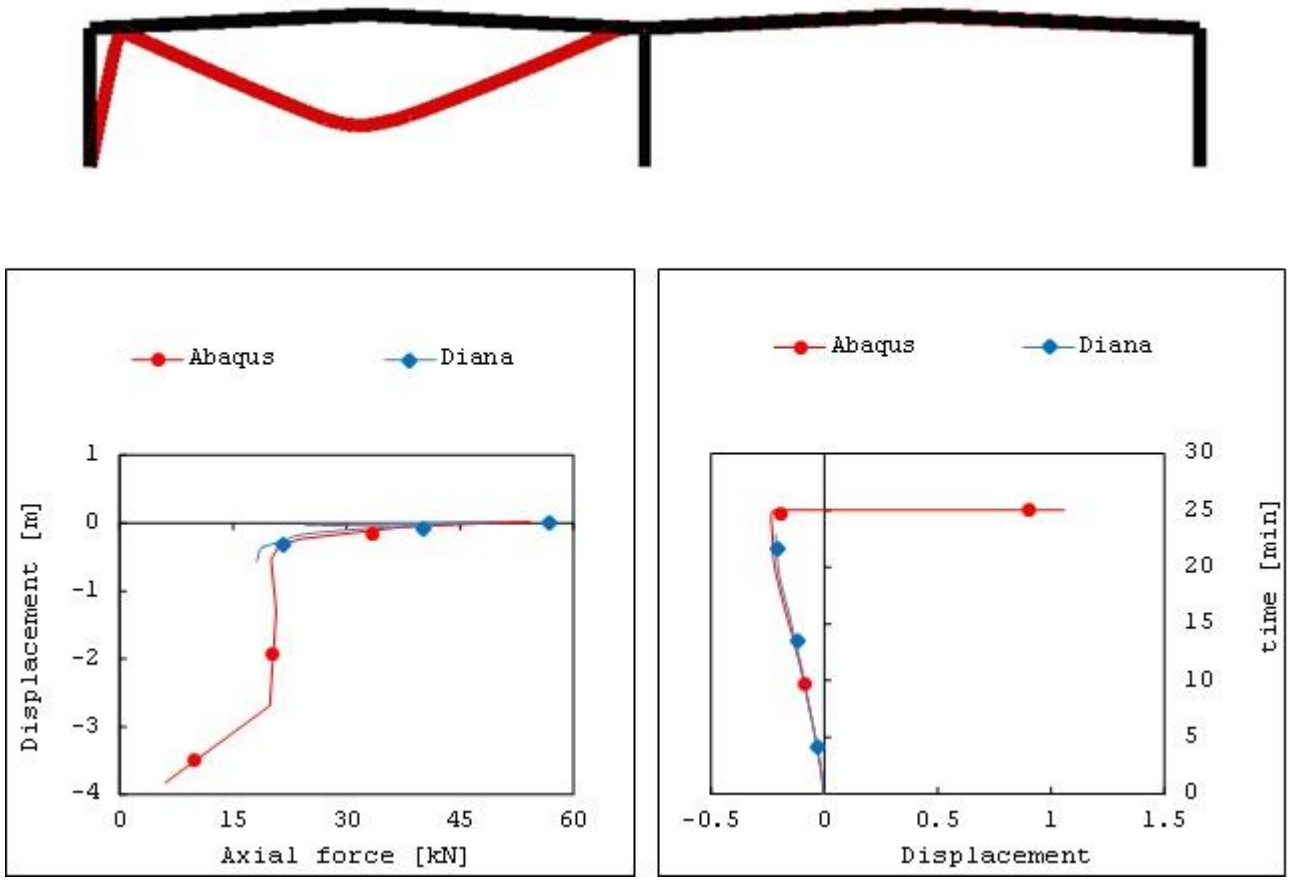

Figure 8.7 - Dynamic analysis of the 2D pitched portal: deformed shape (scale factor 1) (top); vertical displacement of point B with respect the normal force (left); lateral displacement of point A (right).

8.3.2. A two – span pitched portal in three dimensions (model 2)

In order to conduct a three–dimensional analysis without modelling the rest of the structure, the out-of-plane degrees of freedom needs to be activated and the structure must be restrained against out of plane displacements in several points. These constraints reproduce the interaction between the frame and the rest of the structure. The middle of the beams and the middle of the columns are fixed in the third dimension Z. An initial deformation having a sinusoidal shape is contained in the XZ plane.

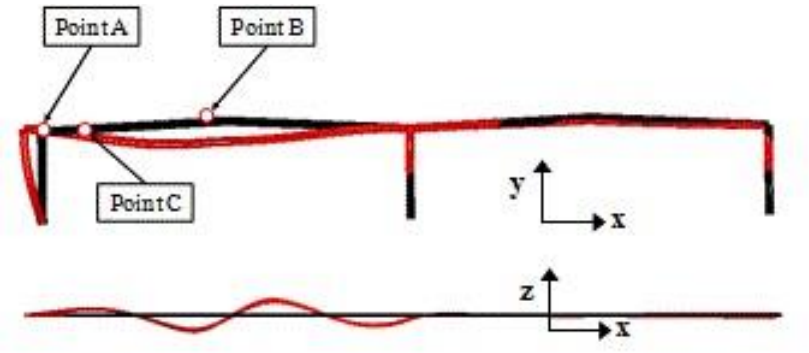

Figure 8.8 - Deformed shape of the 3D frame (model 2); top: plane XY (scale factor 5); bottom: plane ZX (scale factor 10) (bottom).

The 3D frame has initially the same behaviour than the previous 2D frame (Figure 8.8 top), but here a strong influence of spatial effects can be noticed (Figure 8.8 bottom), which determines an out of plane displacement of point C (Figure 8.9).

The collapse of the 3D frame occurs few minutes before what obtained with the 2D model due to the lateral buckling of the beam under fire. For this substructure, the dynamic analyses do not clearly exhibit the snap-through of the rafter (Figure8.9 right).

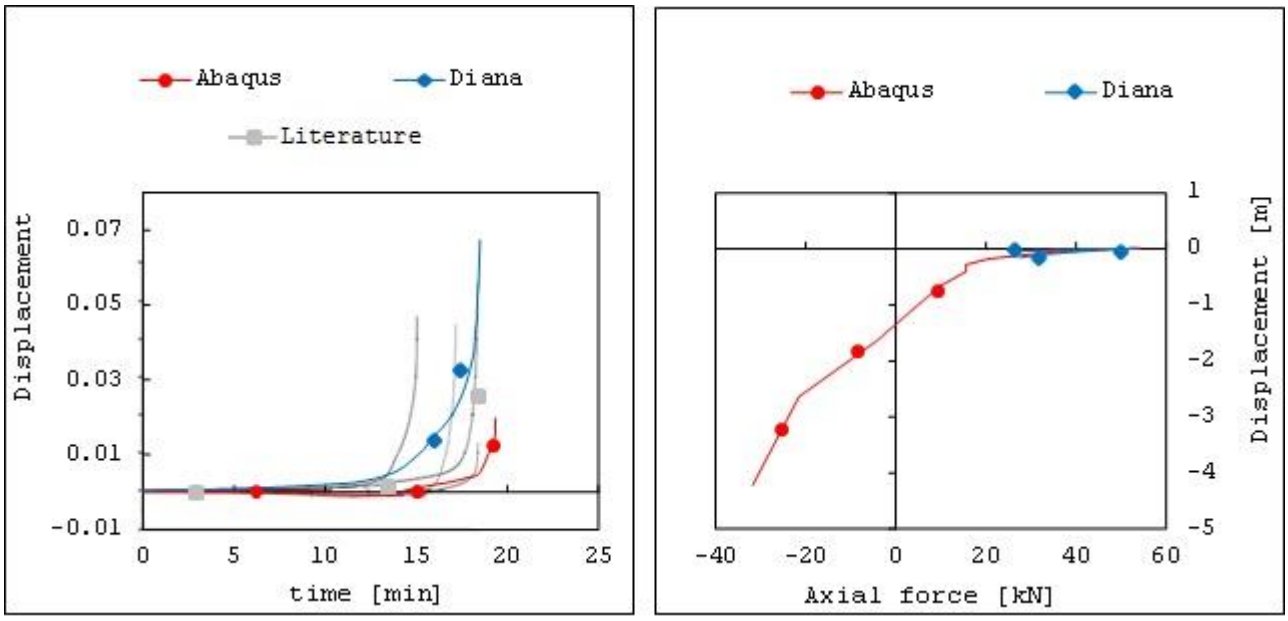

Figure 8.9 - Out plane displacement of point C (left) and axial force in the rafter (right).

8.3.3. Whole 3D structure (model 3)

The two-span frame is included in a full 3D structure with other parallel frames connected together by purlins (Figure 8.10 left). In Figure 8.10 (right) the deformed shape is shown at the end of the simulation.

An initial lateral expansion of frame is followed by a drop of the rafter. Figure 8.11 presents the evolution of some parameters during simulation: the vertical displacement of the mid-span of the rafter (top left); the horizontal displacement of point A, which is the node at the top of the column (top right); the normal force in the rafter (point C) with respect to the vertical displacement of point B (bottom left); the shear of base of the left column (point D) with respect to the lateral displacement of point A (bottom right).

From Figure 8.11 it can be observed that the collapse of the structure is not really visible. Through the purlins the loads are progressively transferred from the central frame to the neighbouring frames, which sustain the central frame and withstand the collapse. The greater time resistance of the 3D whole model with respect to the 3D frame can be ascribed to this mechanism. Considering the strong non-linearity of the structural response and the high level of system redundancy, it can be said that the results are in substantial agreement with literature (Vassart, et al., 2004).

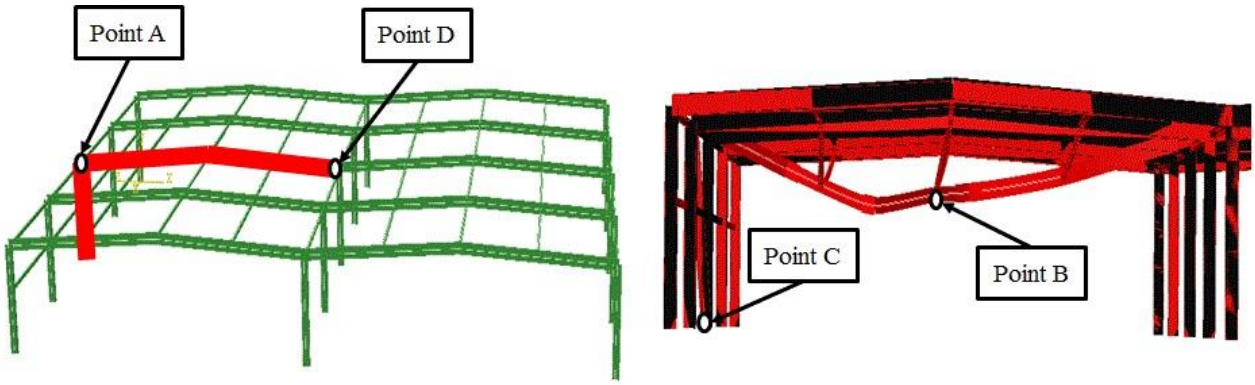

Figure 8.10 - 3D structure (model 3): heated elements (left) and partial view of deformed shape (right)

8.3.4. Comparison of the outcomes

The 2D model (model 1) shows a snap through of the heated beam. This mechanism means that (and is expected when) the restrain of the examined frame given by the rest of the structure is not adequate.

The 3D model (model 2) takes into account partially of spatiality of the problem. The out of plane displacement of the structure is qualitatively reproduced by the model, but the contribution of the

rest of the structure to the frame stiffness is not rigorously considered in the 3D model and the use of horizontal and vertical springs of appropriate stiffness would be necessary for obtaining more realistic results.

The full 3D structure (model 3) can catch with more detail the behaviour: it does exhibit neither the collapse of the structure nor the snap through of the beam, indicating the ability of structure of redistributing the external actions to non-collapsed elements.

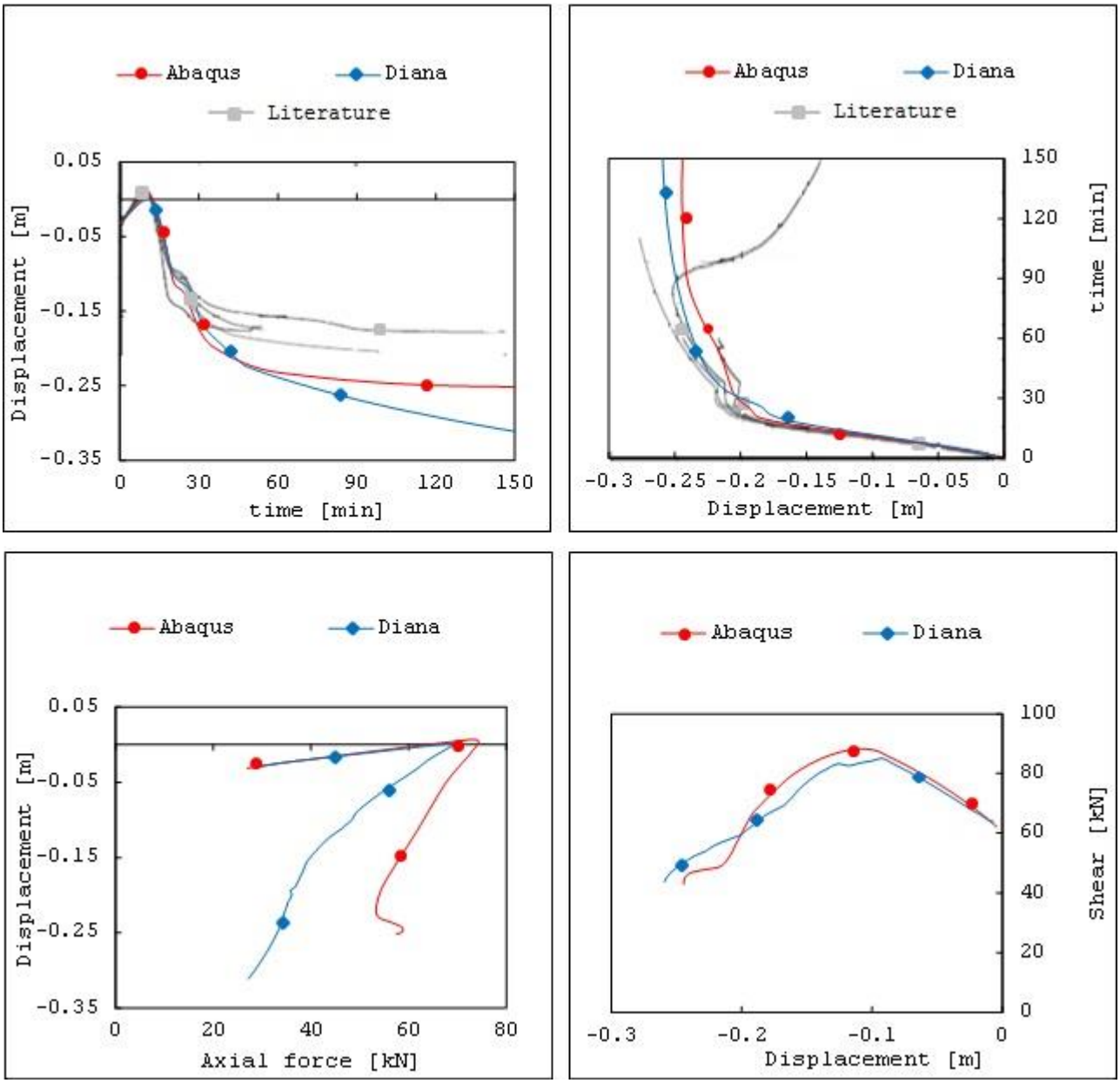

Figure 8.11 - 3D structure (model 3): vertical displacement of mid-span of the rafter (top left); horizontal displacement at the top of the column (point A) (top right); normal force in the rafter (point C) with respect to the vertical displacement of point B (bottom left); shear at the base of the left column (point D) with respect to the lateral displacement of point A (bottom right).

8.4. ANALYSIS ISSUES IN PERFORMANCE–BASED APPROACHES FOR DESIGN

It is of interest to investigate the failure mechanisms of a structure under fire and to highlight a possible disproportionate influence of a local failure triggered by fire on the response of the whole structure.

In the view of a Performance-Based approach for Fire Design (PBFD), a limitation on the main beam deformation is chosen as performance criterion. Specifically, the maximum vertical displacement has been chosen as the main parameter for performance evaluation. The load-bearing capacity of a steel girder can be considered exhausted when its rate of deformation is infinitely large (Petterson, et al., 1976). The results of experimental and theoretical investigations indicate that the following failure criterion (Eq.8.1) is suitable for use in conjunction with steel girders under fire exposure conditions (Robertson & Ryan, 1959):

$$y_{cr} = \frac{L^2}{800 \cdot h} \tag{8.1}$$

where y_{cr} is the critical mid-span deflection [m], L is the span of the girder [cm] and h is the depth of the girder [cm].

For load bearing elements in the UK, (British Standards Institution, 1987) defines three criteria for insulation, as well as the integrity and stability that must be passed in order to achieve a fire resistance rating. For stability of load bearing horizontal structural elements (e.g. beams and floor slabs), failure is defined at a deflection of:

$$y_{\max} = \frac{L}{20} \tag{8.2}$$

where y_{max} is the critical mid-span deflection [m] and L is the beam length.

Another possibility is to consider the runaway of the beam, with this term meaning the accelerating and irreversible downward displacement (Usmani, et al., 2003) of the beam mid-span node.

In Table 8.2 the main assumptions and chosen performance threshold for the displacement are reported. Since the length of both primary and secondary beams is high, local instabilities in secondary elements are likely to occur before the displacement threshold is exceeded by the main beams. In order to follow the propagation of failures up to the beam displacement threshold, which conventionally defines the global collapse, the analyses should therefore be able to overcome local instabilities and convergence problems.

The collapse of a purlin (vertical displacement at mid-span equal to 37.5cm) represents only a local phenomenon; on the other hand, the collapse of a beam (vertical displacement at mid-span equal to 1m) reveals a global collapse. Figure 8.12 shows 4 remarkable scenarios: in the first scenario a lateral column, a beam and parts of 10 purlins are heated; in the second scenario part of 2 beam and 3 purlins are heated; in the third scenario the central column, part of 2 beams and of 6 purlins are heated; in the fourth scenario the heated elements are the same of the second scenario, but a natural fire is considered instead of the standard curve, so a realistic fire can be investigated. Each scenario involves about 150 m^2 (12.5% of total compartment area).

Table 8.2 - Goal, performance, criteria and limits

Goal	Avoid collapse and mechanism
Performance criterion	Limitation of the main beams deformability
Structural response parameters performance evaluation	Maximum vertical displacement of main beams
Performance threshold (conventional collapse)	$\frac{\text{Beam length (L)}}{20}$

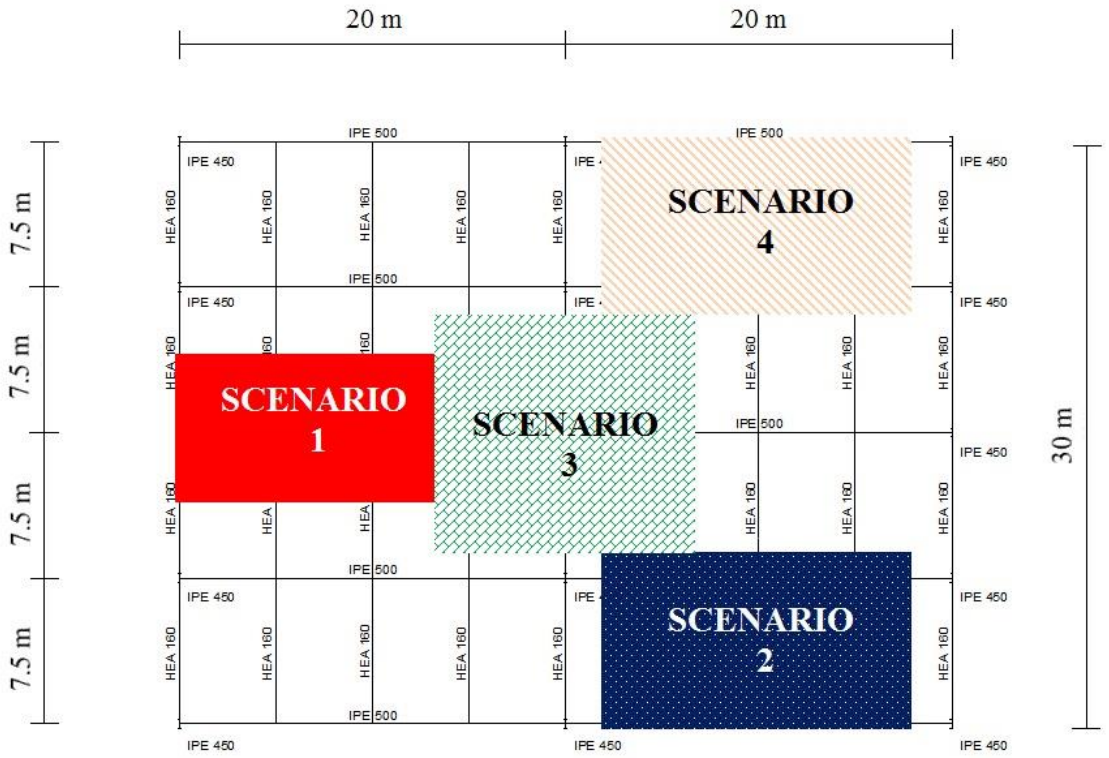

Figure 8.12 - Fire scenarios.

8.5. NOMINAL FIRE APPROACH

8.5.1. Scenario 1

Figure 8.13 shows the elements heated in the first scenario and some reference points. The first local instability occurs in purlin #15 (point A in Figure 8.13) after about 18 minutes (Table 8.3), when the steel temperature (HEA 160) is 717 °C and the room temperature, according to the ISO curve, is 765 °C.

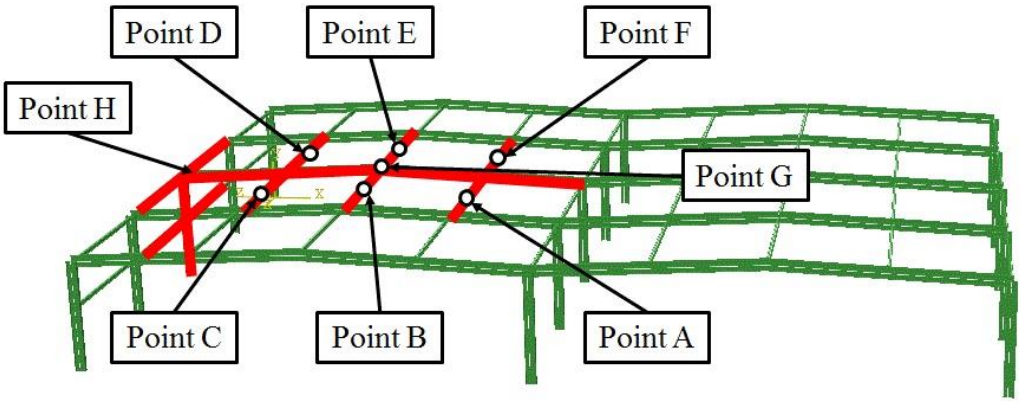

Figure 8.13 - Heated elements in fire scenario 1.

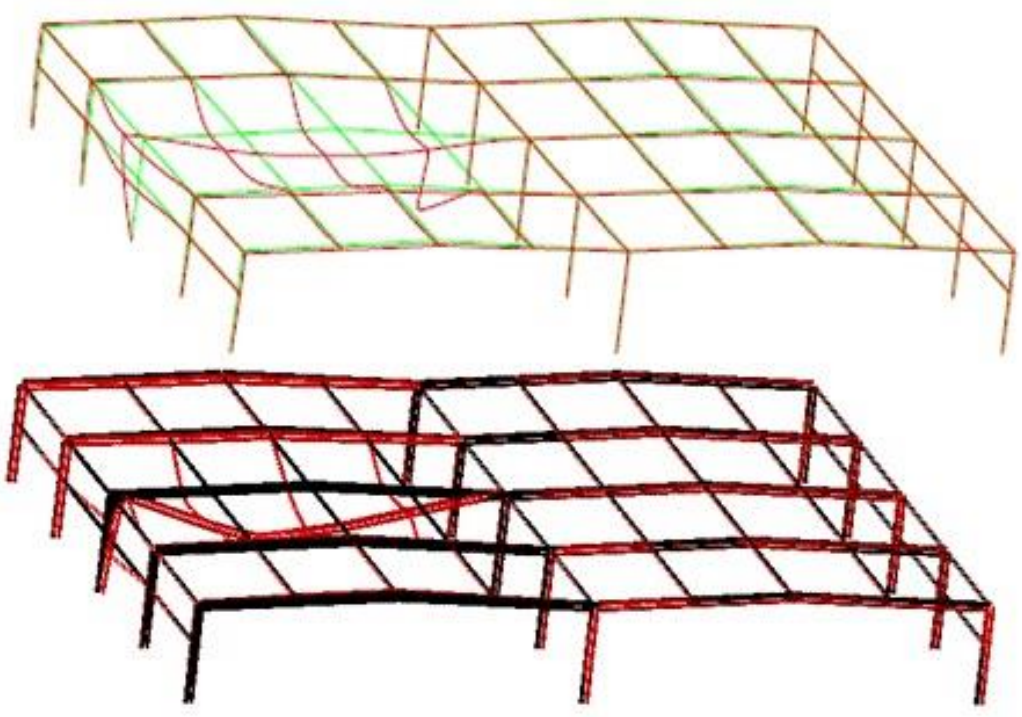

Figure 8.14 - First local instability in Diana® (top) and global collapse in Abaqus® (bottom).

The analyses follow the behaviour of the structure after the first local collapse (Figure 8.14 top):

just after the first purlin, other 5 ones loose stiffness and resistance and a global collapse occurs at this point.

The vertical displacement of the heated beam (IPE 500) exceed the established limit (1 m) after about 27 minutes according to the outcomes obtained with Diana® and after 22 minutes according to the outcomes obtained with Abaqus® (Figure 8.14 bottom). The element temperatures are 753°C and 723°C respectively. Table 8.3 shows the sequence of failures. While the two codes lead to similar results concerning the sequence of collapses, some differences can be noticed in the post-peak behaviour. Diana® estimates a progressive loss of stiffness at both local (Figure 8.15 left) and global (Figure 8.15 right) level. In Abaqus® the stiffness drop is more abrupt. This is why the time of collapse is greater in Diana®, despite the collapse mechanism is the same.

Table 8.3 - Time of resistance of scenario 1

Element	**Collapse**	**Time [min]**			
		Implicit (S.C. 1)	**Explicit (S.C. 1)**	**Static (S.C. 2)**	**Implicit (S.C. 2)**
P15 – Point A	Local	17	18	18	18
P11 – Point B	Local	20	20	21	21
P14 – Point C	Local	21	22	23	23
P5 – Point D	Local	21	22	23	23
P6 – Point E	Local	21	22	23	23
P10 – Point F	Local	21	22	23	23
B5 – Point G	Global	21	22	27	27

8.5.1. Analysis of the other scenarios

The analysis of other fire scenarios highlights the possibility of different structural crises. Scenarios 2 and 4 represent the most restrictive conditions for rafters.

Figure 8.16 shows the heated elements (top left) and deformed shape (top right) in scenario 2. The local collapse of a purlin occurs after about 15 min (bottom left) and the global collapse of the rafter occurs after about 18 min (bottom right).

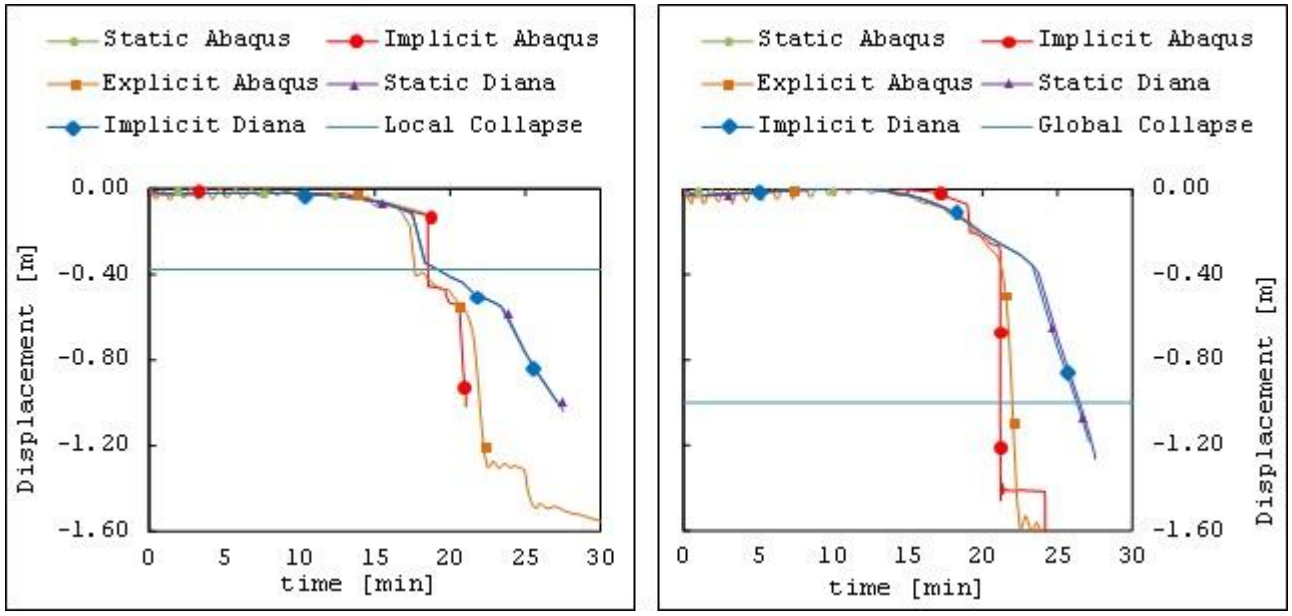

Figure 8.15 - Local and global collapse.

Scenario 3 shows the crisis of the structural system in the area around the central column, which occurs after more than 35 minutes. Figure 8.17 shows heated elements (top left), deformed shape (top right) local collapse of a purlin (bottom left), and global collapse of a rafter (bottom right).

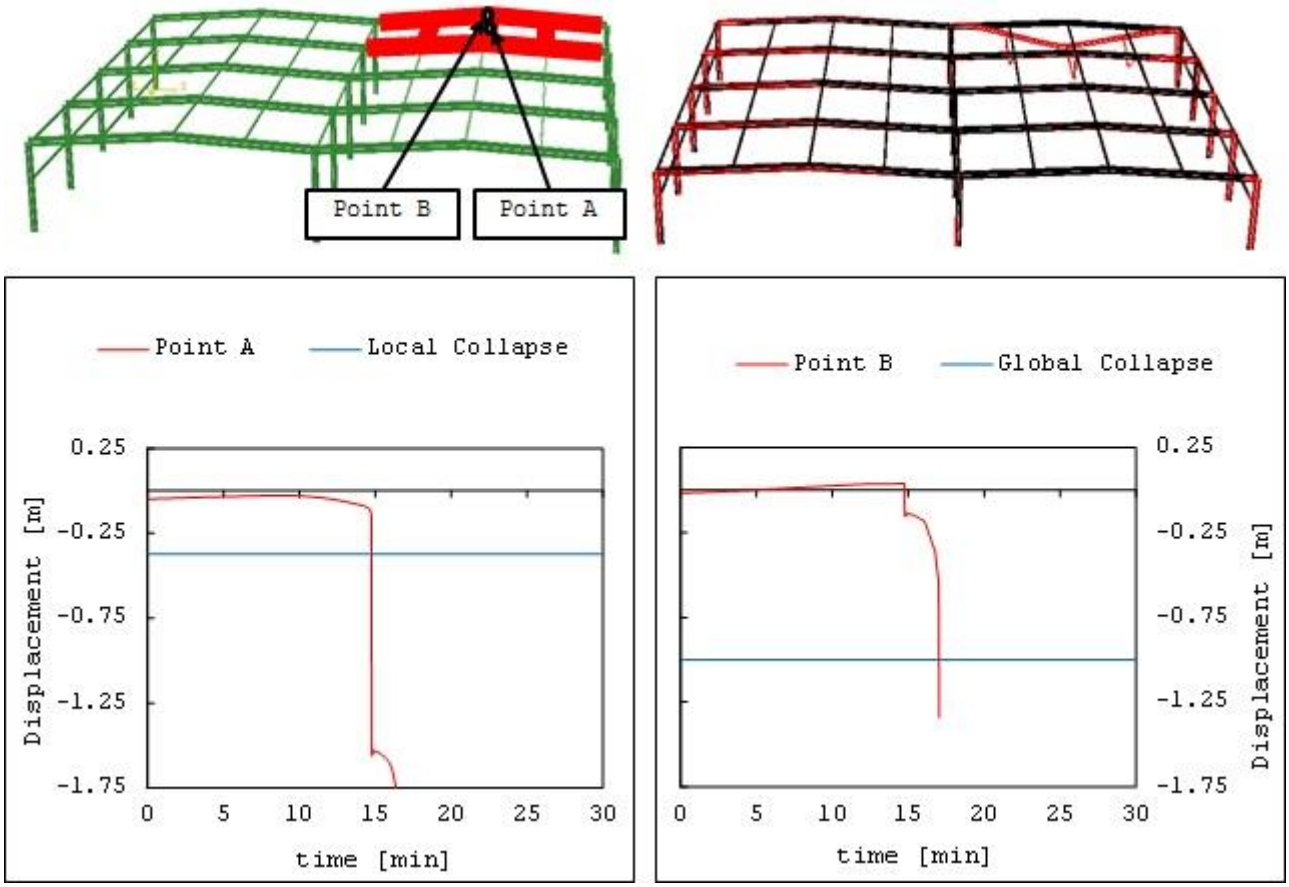

Figure 8.16 - Scenario 2

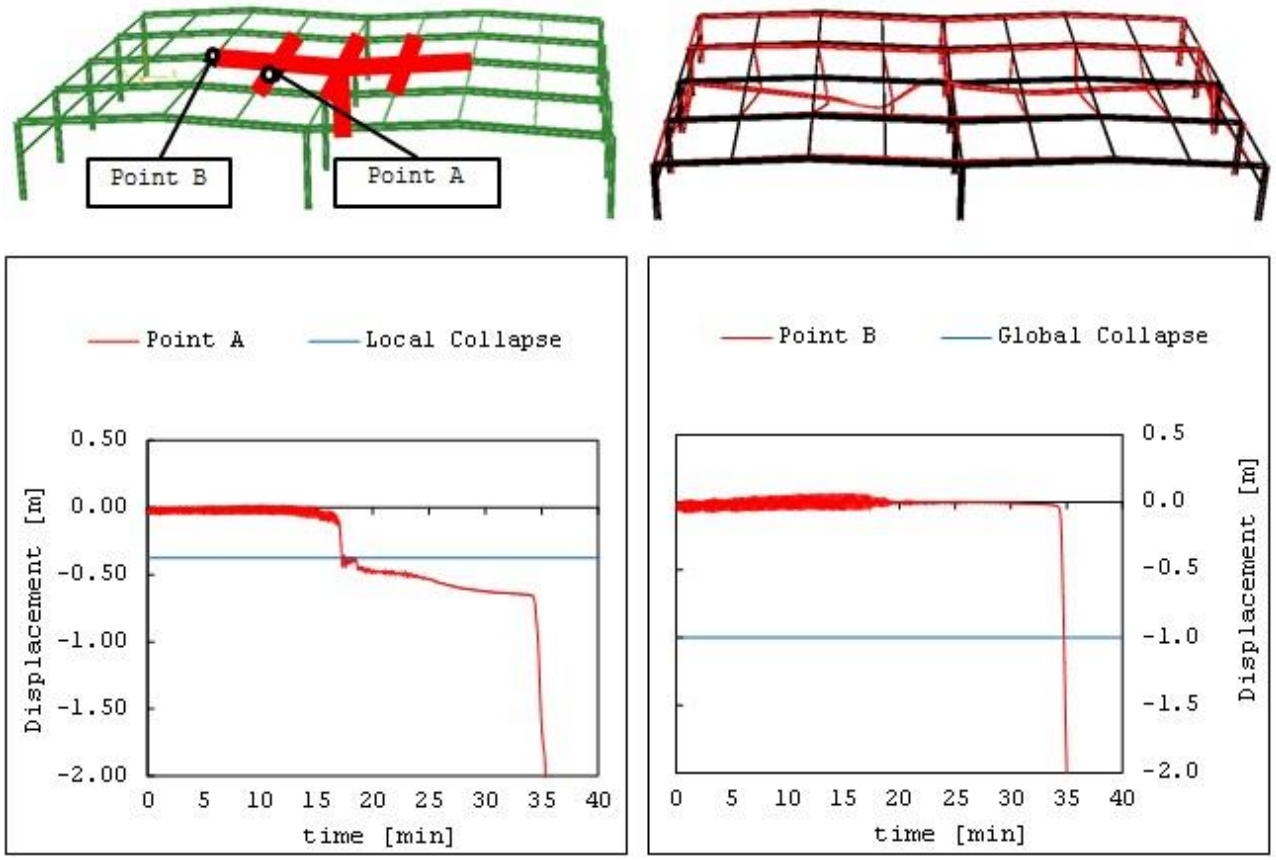

Figure 8.17 - Scenario 3: heated elements (top left); deformed shape (top right); local collapse of a purlin (bottom left); global collapse of a rafter (bottom right).

The Table 8.3 summarizes the results of the analyses carried out. Temperatures relate to the structural elements.

Table 8.3 - Investigation results.

Scenario	Local Collapse			Global Collapse		
	Time [min]	Temperature [°C]		Time [min]	Temperature [°C]	
		Gas	Element		Gas	Element
1	18	765	717	22	765	723
2	15	738	676	18	788	671
3	17	757	705	34	860	832
4	15	738	676	18	788	671

8.6. NATURAL FIRE APPROACH

Computational Fluid Dynamics (CFD) simulations play an important role in fire research (Yeoh & Yuen, 2009), allowing evaluating the fire development and providing a new, efficient, reliable and economic tool for fire investigations. With the wide adoption of performance-based fire safety design, CFD simulations are becoming a routine practice for obtaining the necessary fire design information. With new developments in modelling techniques and fast increase of computing power it is expected that CFD simulations will keep gaining popularity in the fire research community. A CFD model permits a quite realistic representation of fire scenarios, because it takes into account the distribution of fuel, the geometry and the occupancy of individual compartments in a structure. This approach allows the application of more realistic temperature-time curve also in structural elements outside the tributary area of scenario. The simulations shown in this chapter were carried out by Fire Dynamic Simulator (FDS).

8.6.1. Identification of the fuel properties

The identification of the appropriate fire scenarios is essential to the design of a building that fulfils the fire safety performance objectives (ISO/TR 13387-1, 1999). Fire scenarios define the ignition and fire growth process, the fully developed stage and the decay stage. In this case the fire triggered by the ignition of wood pallets has been considered (Babrauskas, 2002).

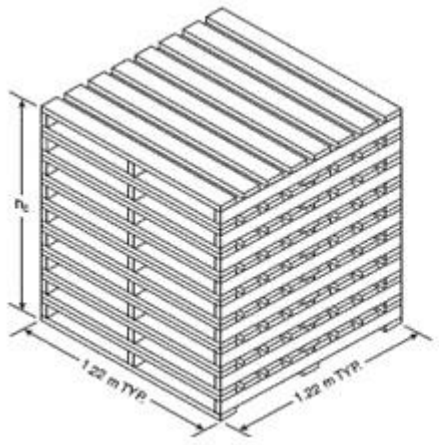

Height	3.05m
Size	1.2m x 1..2m
Weight of one pallet	15 kg
Weight of one stack of pallets	300 kg
Weight of all stacks	5400 kg
$HRR_{s\,max}$	6.81 MW/m^2
t_g	80 s
Where $HRR_{s,max}$ is the maximum of heat release-rate per unit area and t_g is the characteristic time of fire	

Figure 8.18 - Fuel description. Left: geometry of wood pallet (after (Babrauskas, 2002); right: characteristics of considered pallets.

Conceptually, a wood pallet is a similar arrangement to a wood crib (Drysdale, 1999). The geometry, however, is different. Instead of being composed of identical rows of square-section sticks, pallets are made up of rectangular elements, whose typical setup is shown in Figure 8.18. A

typical experimental Heat-Release-Rate (HRR) curve shows that a constant plateau can be seen if the stack is reasonably high (Krasner, 1968). The burning of 18 stacks of pallets has been considered as a fire scenario.

8.6.2. Optimization and validation of the model

The reliability of the CFD predictions is influenced by the size of the grid adopted for computation. In FDS the mesh is chosen in function of a parameter called characteristic fire diameter D*, whose value is given in Eq. (8.3), (McGrattan, et al., 2009):

$$D^* = \left(\frac{\dot{Q}}{\rho_\infty \cdot c_p \cdot T_\infty \cdot \sqrt{g}} \right)^{2/5} \tag{8.3}$$

where: $\dot{Q}$ is the heat release rate, ρ_∞ is the ambient density, T_∞ is the ambient temperature, c_p is the specific heat, and g is the acceleration of gravity. This parameter affects the combustion model, playing a role in the calculation of the fraction mixture, and determines the stoichiometric reaction that takes place. FDS employs a numerical technique known as Large Eddy Simulation (LES) to model the "sub-grid" motion of the hot gases. The effectiveness of the technique is largely a function of the ratio between the fire characteristic fire diameter D*, the size of a grid cell δx (mesh): the greater the ratio D*/δx, the more the simulation is accurate. A ratio of 4 to 16 usually produces favourable results at a moderate computational cost (McGrattan, et al., 2009). According to other studies on the LES (Baum & McCaffrey, 1989), a good representation is obtained by using values of δx within 0.1•D* and 0.3•D*.

	time [min]	HRR [MW]
t_0	0	0
t_F	10	54
t_A	11	176
t_B	14	176
t_C	18	0

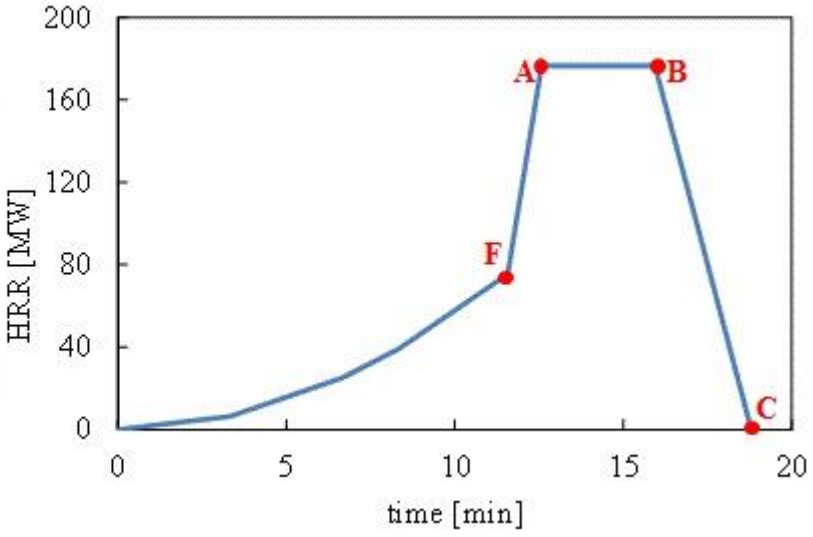

Figure 8.19 - HRR curve considered in case of simultaneous involvement of all pallets

In Figure 8.20 (top left) the values are shown, which are assumed by the above described parameters in the numerical investigations. In order to get a simpler feedback on the model validation and to choose the correct mesh, a simplified even if unrealistic assumption of a simultaneous involvement of all pallets has been initially considered in the first model. Following this assumption and according to the directions given in (ISO/TR 13387-1, 1999), the heat release rate curve shown in Figure 8.19 has been calculated. A size of 50 and 60 cm does not allow for an adequate simulation of the phenomenon in terms of: i) heat release rate (Figure 8.19 top right); ii) maximum temperature (Figure 8.20 bottom left); iii) and height of the smoke (Figure 8.20 bottom right). Discretization of 40 cm provides a quite appropriate overall description, but if a strong temperature gradient occurs, the resulting accuracy is still not satisfactory (Figure 8.20 bottom). For these reasons, a model with the mesh size of 30cm has been used in the investigations presented in the following.

dx	%D*	Dx/ D*	Number of cells
0.3	0.039	25.31	298080
0.4	0.052	18.98	126360
0.5	0.065	15.18	64512
0.6	0.075	12.65	38880

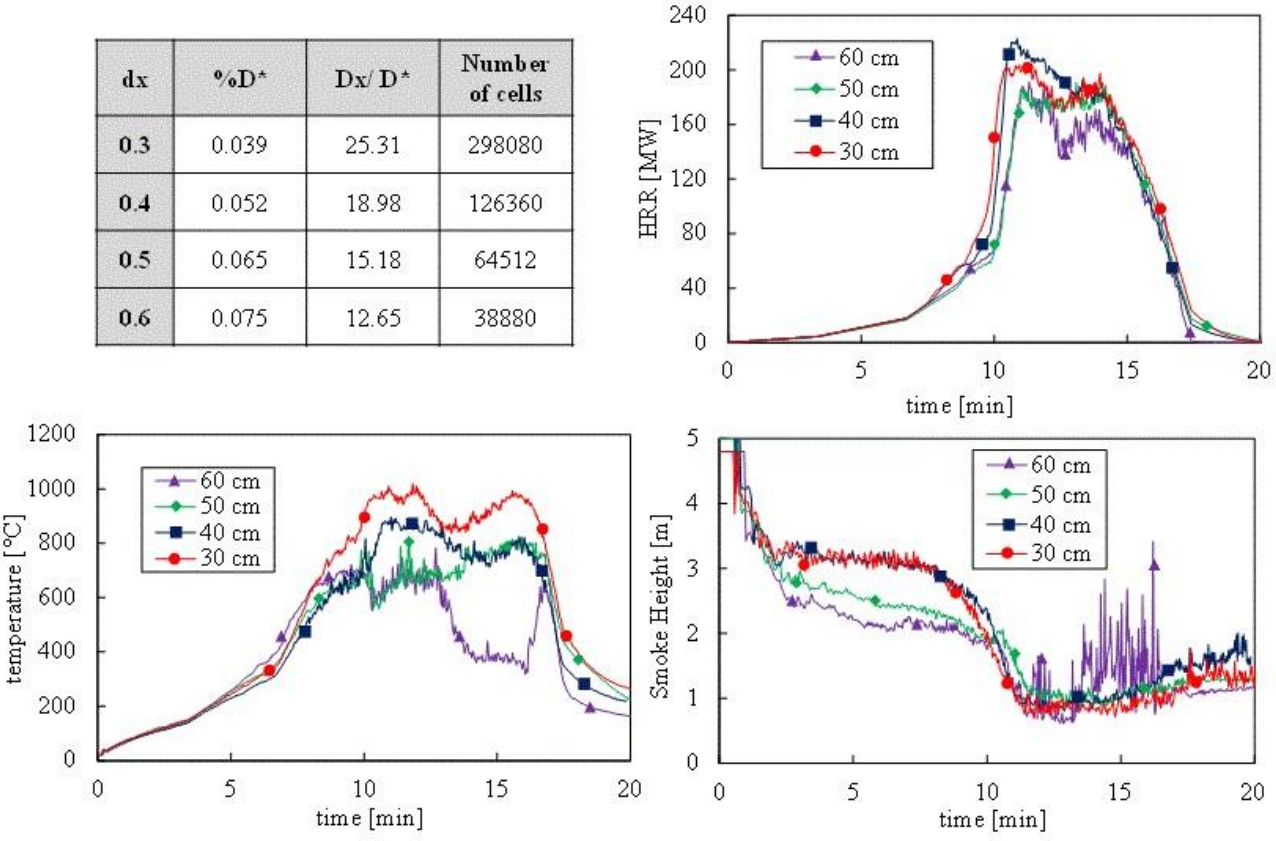

Figure 8.20 - FDS models: effect of different mesh sizes (top left); heat release rate (top right); maximum temperature (bottom left); smoke height (bottom right).

The modelling of the exact dimension of each pallet would require a very fine grid size (0.01m) in FDS, which will lead in turn to impractical computational efforts for the simulation. To overcome

this limitation, the whole group of pallets was modelled as a layer object of size 1.2m x 1.2m x 3.0m. A surface burning area factor was introduced to ensure that the fuel area modelled in the simulation was equivalent to the fuel area calculated.

8.6.3. Fire and heat transfer models

The fire development is greatly influenced by the position of the fuel in relation to the geometry of the compartment. In particular, the proximity of the combustible material to the compartment openings can play a significant role. The first scenario consists of 18 pallets on fire, which are located in the proximity of a corner near one of the windows; in the third scenario instead the pallets are in the middle of the compartment; in the second and fourth scenario the pallets are positioned along one long wall: the difference between the last two cases is that in the second scenario the fuel is near to a door, while in the fourth, the pallets are very far from the openings (Figure 8.21).

(NFPA, 2009) indicates an expression for estimating the minimum value of thermal power HHRmin, which can lead only to radiant heat ignition of combustible materials. This calculation determines whether the ignition of a combustible material is able to spread the fire on the adjacent one:

$$HRR_{\min} = 30 \cdot \frac{(d + 0.05)}{0.019} \tag{8.4}$$

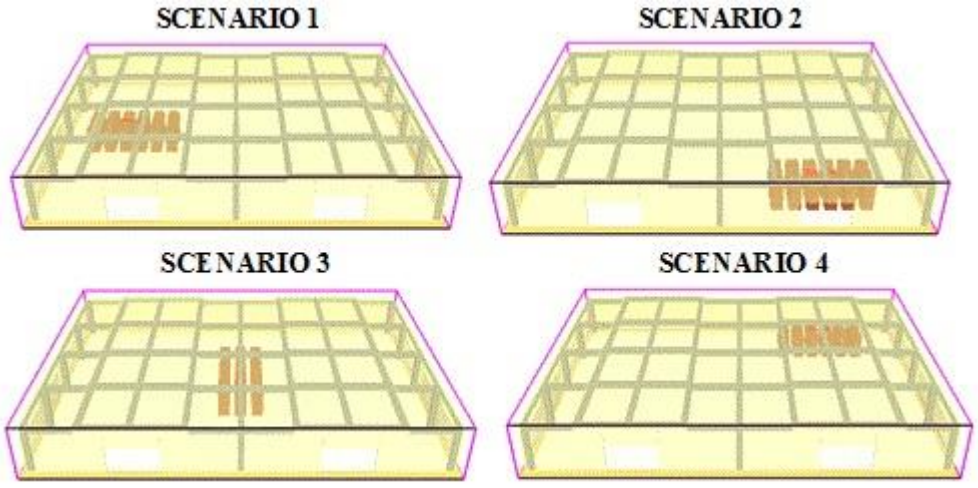

Figure 8.21 - Variation of the fuel position in the considered fire scenarios.

where HRRmin is the minimum heat release rate necessary for the ignition and d is the distance between combustible materials. In Figure 8.22 (left) a possible subsequent involvement of group of pallets is shown with respect to the third fire scenario. The right side of the figure shows the comparison between the calculated HRR curve and the HRR curve obtained in FDS.

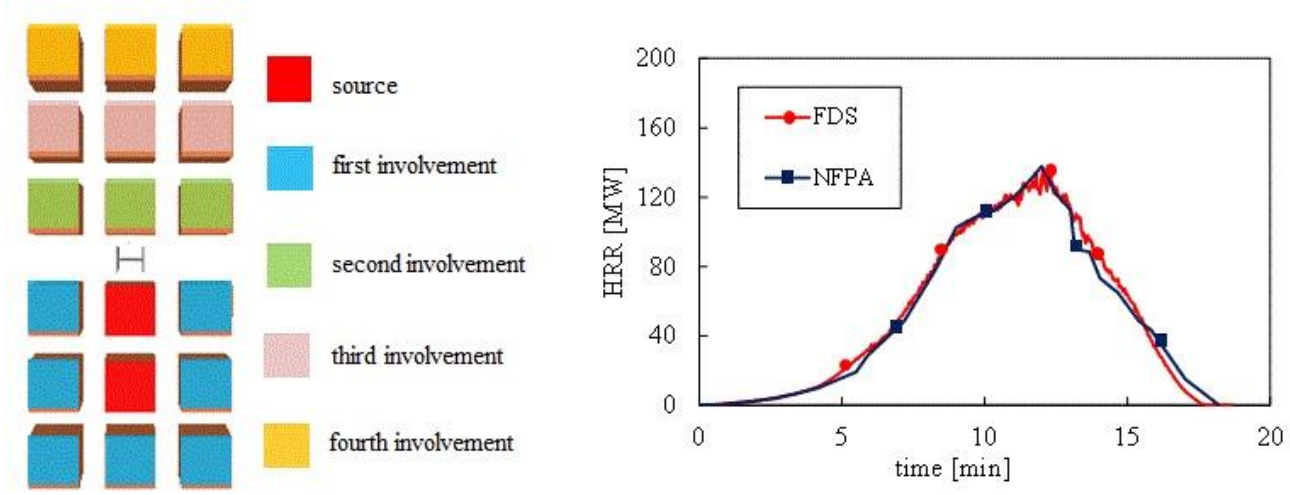

Figure 8.22 - Possible involvement of pallets in scenario 3 (left); comparison between HRR assumed and found in FDS (right).

The considered fire is a very intense phenomenon of short duration and in each scenario temperatures higher than those prescribed by the ISO curve are recorded in the fire area. Figure 8.23 shows the evolution of fire in relation to scenario 2, while Figure 8.24 shows the temperature recorded in some points for scenario 1.

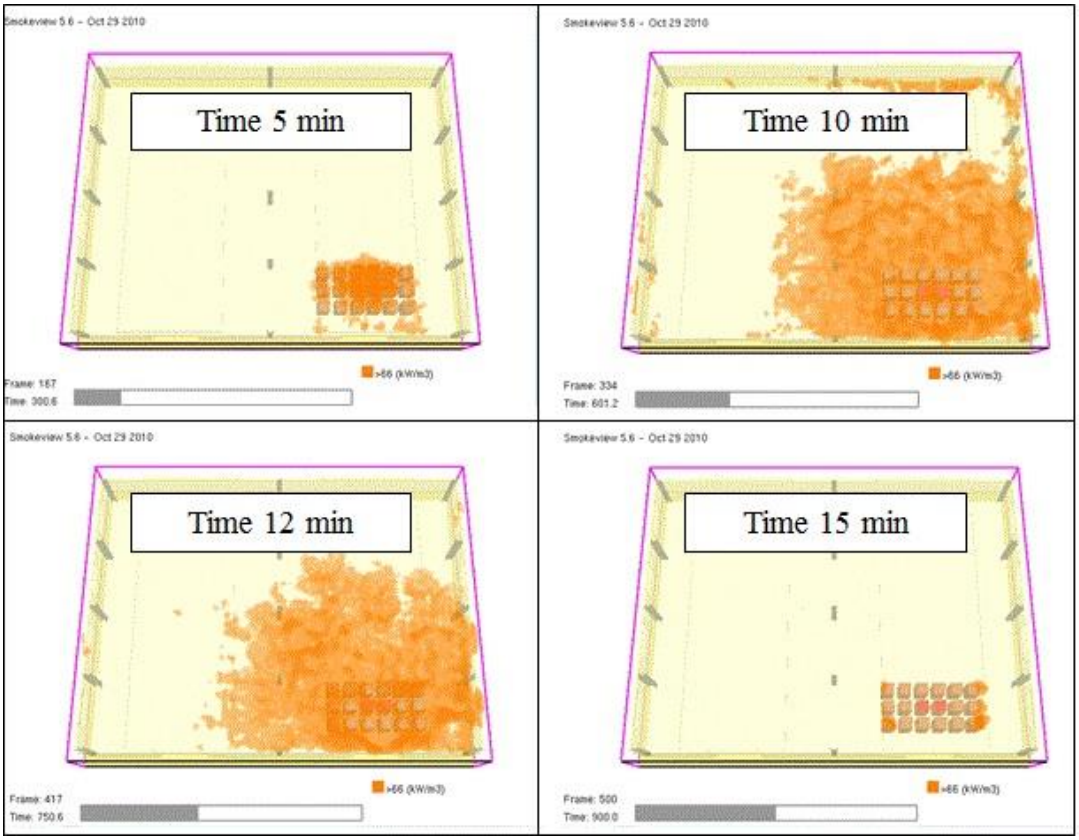

Figure 8.23 - Evolution of fire in scenario 2.

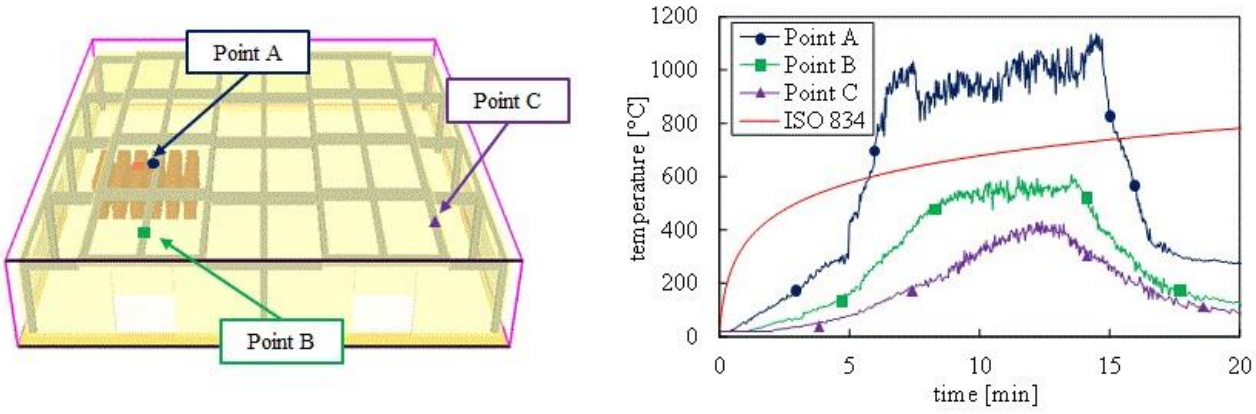

Figure 8.24 - Temperatures obtained for scenario 1.

8.6.4. Structural model

Table 8.5 shows the time of collapse for the different fire scenarios, while Figure 8.25 summarizes the main results of the simulations. The application of the natural fire curve determines a behaviour that is qualitatively similar to that found after application of the ISO curve. Moreover, in this case the structure presents a considerable reduction of resistance times with respect to the one subjected to the ISO curve. In particular in scenario 1, a local buckling of a purlin occurs immediately (Point B of Figure 8.25a), followed by the collapse of the rafter (Point A in Figure 8.25a). The same behaviour is observed in scenario 2 (Figure 8.25b) and in scenario 4 (Figure 8.25d). In scenario 3 the crisis of the column is clearly visible (point E of Figure 8.25c).

Table 8.5 - Time of collapse for fire scenarios

Scenario	**Local Collapse**	**Global Collapse**
	Time [min]	**Time [min]**
1	7	8
2	4	8
3	5	11
4	4	8

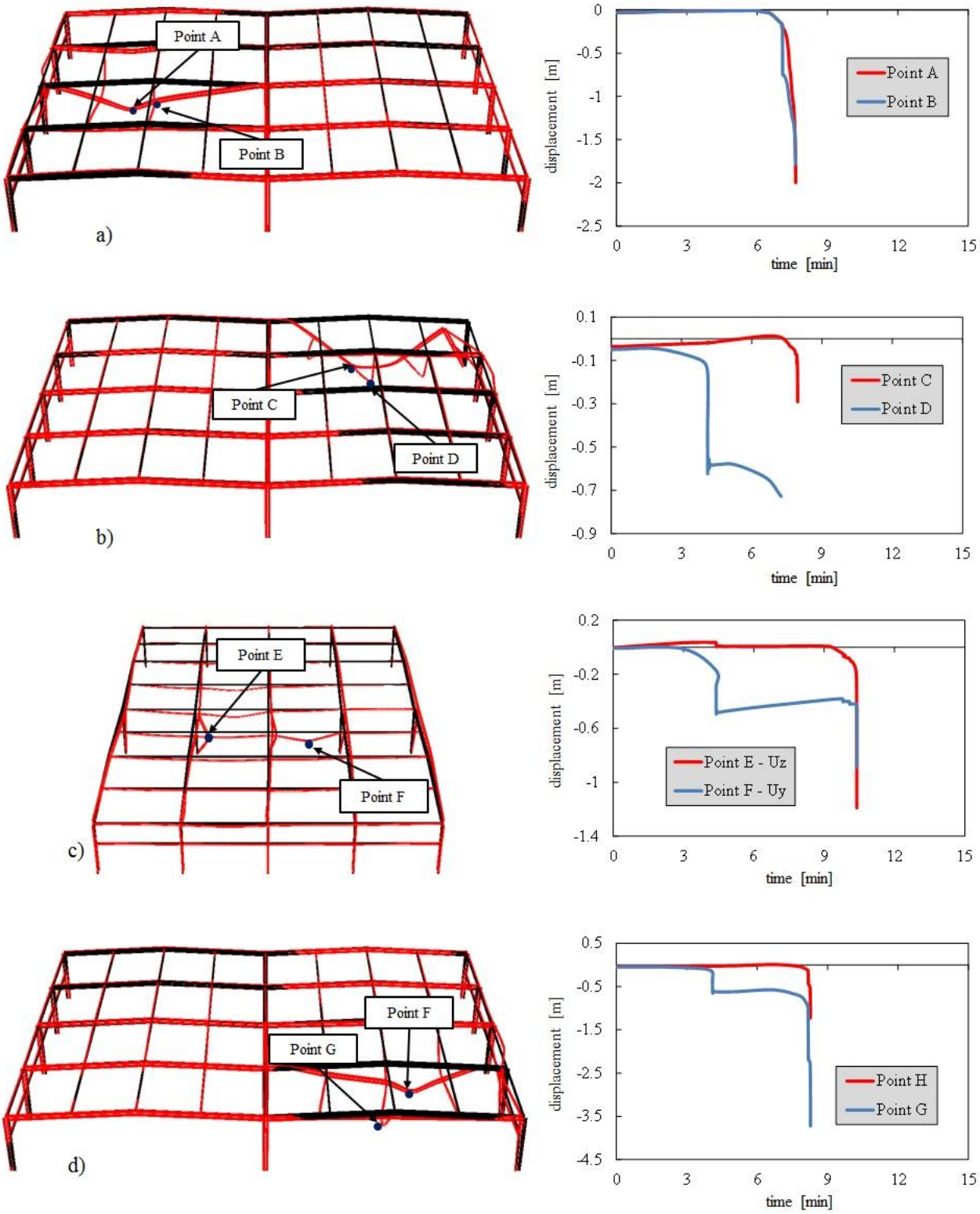

Figure 8.25 - Results of structural investigations carried out in Abaqus®: a) scenario 1; b) scenario 2; c) scenario 3; d) scenario 4.

8.7. CONCLUSIONS

In this chapter some significant issues related to structural analysis in case of fire have been presented. A key aspect of fire safety investigation is the multi-physics nature of problem, which requires a multi-disciplinary approach. Knowledge in fire dynamics, risk assessment, and numerical computational aspects are necessary. The chapter has analysed the influence of some factor in the assessment of safety in case of fire. Both structural non-linear and CFD numerical analyses have been carried out in order to assess the fire resistance of a steel industrial hall already evaluated in other studies. The structural analyses aim to evaluate the global collapse of the structure as triggered by a local failure, while CFD analyses aim to assess the fire development and its effect on the structural response.

It has been shown that simplified models do not always allow understanding the real behaviour of the structure in case local for global failures are triggered in the structure. In the first two cases analysed (model 1 and model 2), when a local failure triggers the structure can no longer sustain any further loading and collapse occurs. However, a redundant structure allow for different load paths and different load carrying mechanisms to support additional load when local resistance is reached at a single location. In order to highlight the role played by redundancy in the considered case, the modelling of the overall 3D structure (model 3) is necessary.

In facing the problem of investigating a complex structural behaviour like the one of structures in fires, aspects such as non-linear geometry and thermo-plastic material are of particular importance. In these cases advanced structural analyses (dynamic implicit or explicit) should be carried out in order to assess the overall resources of the structure.

The choice of the fire scenario is also another key aspect of fire safety assessment. Under the same fire severity, a collapse can occur at different times depending on the position of the fuel. The analysis of four different fuel positions shows the need of considering several fire scenarios, since it's not always possible to a priori identify the worst case.

In this study, some aspects concerning the role of CFD analyses have been inquired and an application has been presented, where the response to fire of a steel structure is quantitatively assessed. The chapter underlines how a more refined representation of the fire can be obtained with the avail of CFD code and modelling aspects concerning the position and development of the fire have been presented and discusses. The outcomes show that the use of a simplified thermal model, such the consideration of a standard fire heating only the elements belonging to the area of the fire

scenario, does not always lead to conservative results. In those cases, the consideration of a natural fire model may be necessary for a more realistic evaluation of the fire effects.

Chapter 9

9. FIRE ACTION IN A LARGE COMPARTMENT

9.1. INTRODUCTION

This chapter focuses on the modelling of fire in case of different distributions of combustible materials in a large compartment.

This aspects are discussed with reference to an industrial steel building is taken as case study. Fires triggered by the burning of wooden pallets stored in the premises are investigated with respect to different stacking configurations of the pallets with the avail of a Computational Fluid Dynamics (CFD) code. Advanced fire models obtained with the avail of CFD investigations becomes particularly important if greater design flexibility is desired or untraditional architectural or structural solutions are employed.

In particular, even if large halls are typically neither heavily cluttered nor densely furnished, the distribution of goods or furniture may be strongly inhomogeneous, leading to possible concentration of the fuel load, whose effects need to be carefully investigated.

Problematic issues of the CFD modelling concerning the presence of uncertainties, the objectivity of the solution, and the reduction of computational onus are presented and discussed. The advantage of more realistic simulations that take into account the effects of fire propagation and the distribution of the combustible are also stressed out.

The results in term of temperatures of the hot gasses and of the steel elements composing the structural system are compared with simplified analytical model of localized and post-flashover fires, with the aim of highlighting limitation and potentiality of different modelling approaches. In particular, it is shown that a high variability of temperatures characterizes some type of large compartment fires. In those cases, the consideration of post-flashover fires, which assume a uniform distribution of the temperature along the compartment, can be not very representative of the real phenomenon and possibly lead to an underestimation of element temperatures.

9.2. CASE STUDY

9.2.1. Description of the structure

A steel industrial hall has been considered as case study. The structural system considered has been taken from the report (Hadjisophocleous & McCartney, 2005), where FEM investigations of the structural response are presented with respect to a standard fire.

This chapter focuses instead mainly on aspects related to the modelling of the fire for structural design. The configuration of the structural system and the properties assumed for the compartment and the combustible are described below and summarized in Table 9.1, Table 9.2 and Table 9.3 with respect to the property of the compartment, of the combustible and of the structural elements respectfully.

9.2.2. Geometry of the compartment

The premises, whose geometry is shown in Figure 9.1, consists in a large hall, 40 m long and 30 m wide and covering a floor area of 1200 m^2. The hall has a double pitched roof, which rises from 5.0 m to 5.5 m, so that the average height of the hall is 5.25 m. The total enclosure area results therefore to be equal to 3135 m^2.

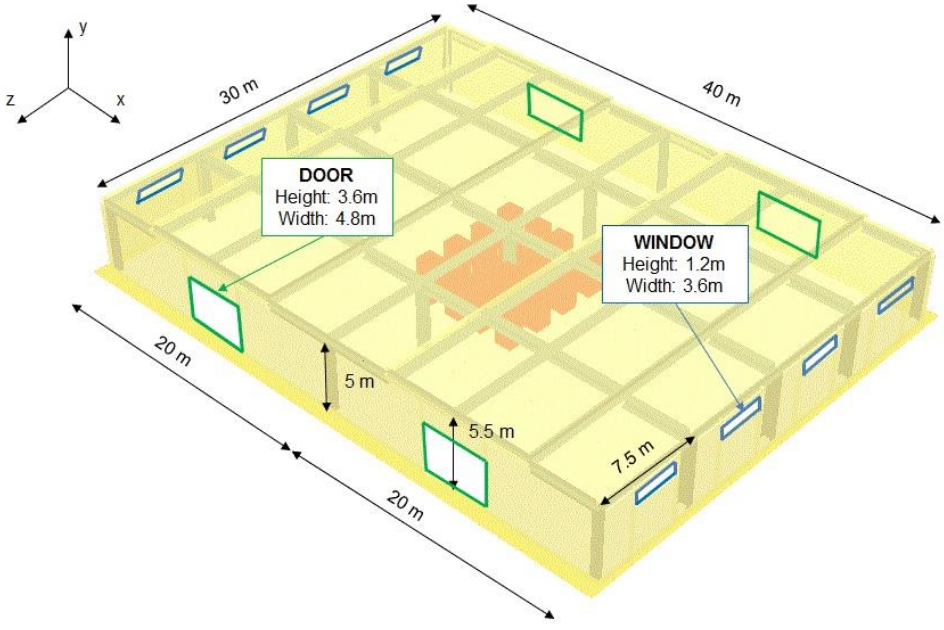

Figure 9.1 - Industrial hall considered as case study

9.2.1. Amount and properties of the combustible

The premises are devoted to storage of goods and are assumed to be empty at the time of fire. Only the presence of 320 wooden pallets Figure 9.2 used to support and transport goods is considered in the premises and the effects of different disposition and stacking of the pallets are investigated.

Each pallet has dimensions 1.2 m x 1.2 m x 0.15 m and a weight of 15 kg. The pallets are assumed to be made of wood with a calorific value of 17.5 MJ/kg, so that the total amount of fuel load in the premises results to be equal to 84000 MJ, as reported inTable 9.2.

Wooden pallets are typically stored in stacks of different height, so that each pallet stack can be considered similar to a firewood crib (Bystrom, 2012) and a constant plateau of the heat release rate (HRR) can be seen if the stack is higher than 0.5 m (SFPE).

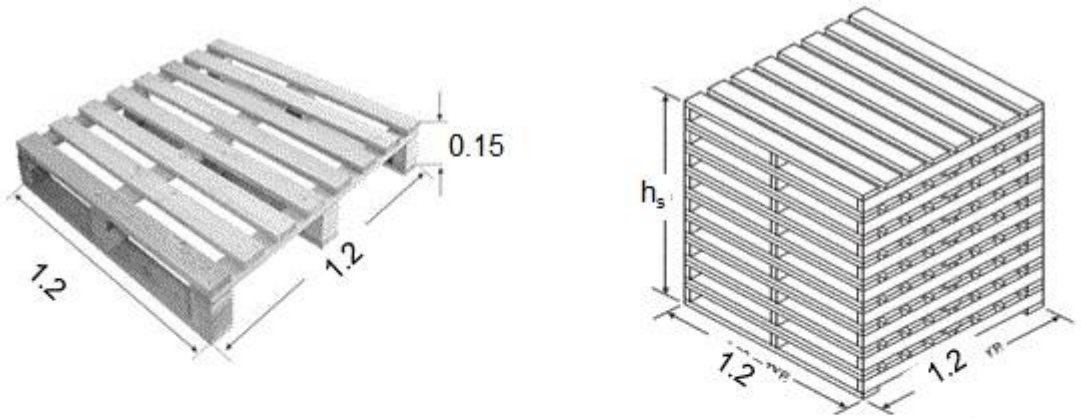

pallet height	0.15	m
pallet area	1.44	m^2
pallet weight	15	kg
no. pallets in the hall	320	---
moisture content	4	%

stack height	3.0	1.5	1.2	0.6	m
no. of pallets in a stack	20	10	8	4	---
HRR_{max} of a stack	6.81	3.86	3.28	2.10	MW
no. stacks in the hall	16	32	40	80	---
$HRR_{max, tot}$	157	178	189	242	MW

Figure 9.2 - Geometry (top) and property (bottom) of a single pallet (left) and of a pallet stack (right)

The maximum heat release rate (HRR_{max}) of a pallet stack can be therefore calculated with the expression proposed by (Krasner, 1968) and reported in Eq. (9.1), where the HRR of a pallet stack is given per unit area of the floor occupied by the stack (indicated as $HRR_{s,max}$). The HRR_{max} calculated for different stack height are visible on the right of Figure 9.2: for a stack of 3 m, the HRR_{max} results to be equal to 9.81 MW, which is consistent with the value reported by (La Malfa & La Malfa, 2009), where a value of 6.81 MW/m^2 of floor area occupied by a 3m pallet stack is

suggested; the calculated value is also quite close to the value of 7 MW reported for a 3m high palled by Karlsson&Quintiere (Karlsson & Quintiere, 2009).

$$HRR_{s,\max} = 9190 \cdot (1 + 2.14 \cdot h_p) \cdot (1 - 0.03 \cdot M) \quad (9.1)$$

where:

h_p indicates the height of a stack of pallets

M represents the moisture content of the wood

9.2.2. Ventilation of the compartment

Four doors and eight windows have been assumed to be placed with a symmetrical disposition on the external perimeter of the hall: in particular, a 4.8 m wide and 3.6 m high door has been placed in the centre of each external pitched bay, while a 3.6 m wide and 1.2 m high window has been placed at 3.6 m from the ground in the centre of each bay of the secondary frames in the transversal direction.

In case all doors and windows are assumed to be open during the fire, the opening factor of the premises results to be O = 0.055 $m^{½}$ and the limit heat release rate due to maximum oxygen income (HRR_{lim}) is equal to 306.3 MW, which ensure a well-ventilated condition for the development of the fire.

9.2.3. Materials of the enclosure and of the structural system

The structural system is composed by 5 main frames, connected by 9 transversal purlins sustaining a steel-concrete deck. The main frames consist of 2 bays, spanning 20 m between 5 m height columns. The beams have a pitched configuration, so that a maximum height of 5.5 m is reached in correspondence of the mid-span of each bay.

The steel elements have the profiles shown in Figure 9.3 and are realized with hot rolled S235 and S355 steel for purlins and main frames respectively. The main beams and the purlins are considered to be exposed to fire on three sides and insulated on the top flange by the presence of the roof deck.

The walls are assumed to be made of gypsum while the floor and the ceiling are considered to be made of concrete for the purpose of thermal inertia calculations, as shown inTable 9.1.

Table 9.1 - Properties of the compartment

ENCLOSURE PROPERTIES	SIZE	Width	B	30	M
		Length	L	40	M
		Height (average)	H	5.25	M
		Floor area	A_f	1200	m^2
		Enclosure area	A_t	3135	m^2
	OPENINGS	Average opening height	$h_{w,av}$	2.8	M
		Total opening area	Aw	103.7	m^2
		Air Flow Factor	AF	173.49	$m^{5/2}$
		Opening factor	O	0.055	$m^{0.5}$
	THERMAL INERTIA	Gypsum surface	A_1	1426	$W \cdot s^{0.5}/(K \cdot m^2)$
		Gypsum thermal inertia	b_1	762	m^2
		Concrete surface	A_2	1’920	m^2
		Concrete thermal inertia	b_2	1200	$W \cdot s^{0.5}/(K \cdot m^2)$
		Thermal Inertia	B	1017	$W \cdot s^{0.5}/(K \cdot m^2)$

Table 9.2 - Properties of the combustible

COMBUSTIBLE	FUEL PROPER.	Fire growing rate	α	0.156	kJ/s^3
		Calorific value of combustible	H	17.5	MJ/kg
		Weight of combustible	G	4800	Kg
	FUEL LOAD	Total fuel load	Q	84000	MJ
		Fuel load density (floor)	q_f	70	MJ/m^2
		Fuel load density (enclosure)	Q	27	MJ/m^2

Table 9.3 - Properties of the structural system

STRUCTURAL PROPERTIES	STEEL	Density	p_s	7850	kg/m^3
		Specific heat	c_{ps}	450	J/(kg·K)
		Resultant emissivity	e_r	0.5	---
	PROFILES	Purlin section factor	A_p/V_p	192	m^{-1}
		Rafter section factor	A_b/V_b	134	m^{-1}
		Central column section factor	A_c/V_c	162	m^{-1}

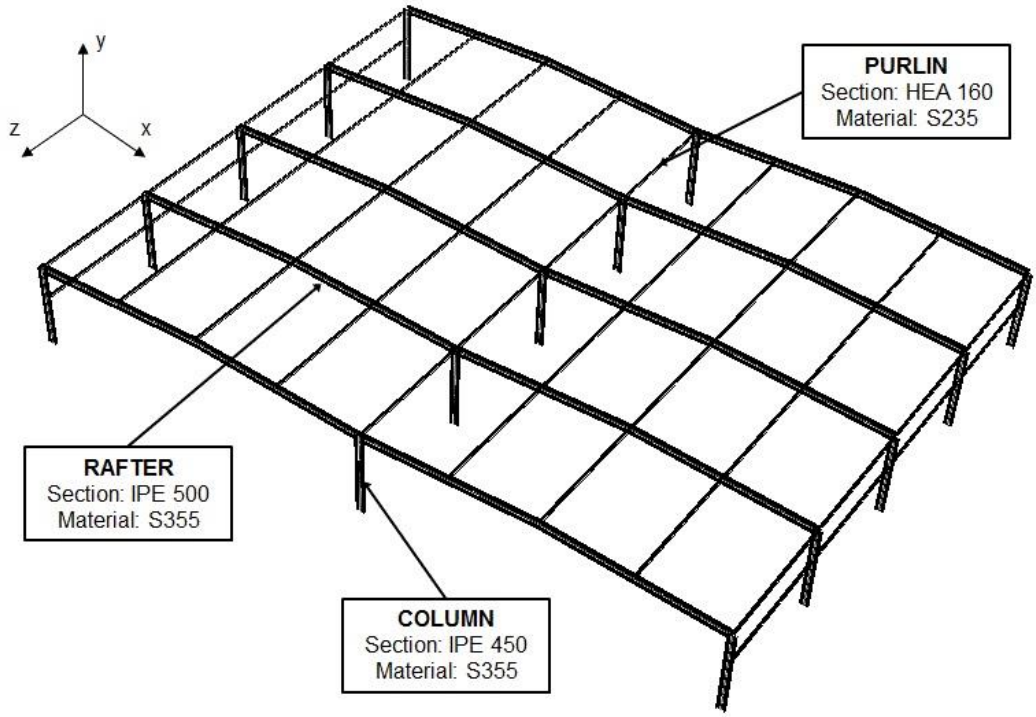

Figure 9.3 - Structural system and steel element profiles

9.3. SIMPLIFIED MODELS

Analytical models for describing the temperature evolution of the hot gasses and of the elements in a compartment can be roughly distinguished in pre- and post-flashover models.

Pre-flashover models can be used for describing localized fires both in case of a low flame (Heskestad, 1995) and of a flame impinging the ceiling (Hasemi & Tokunuga, 1984). For the purpose of structural fire safety design however, generally only post-flashover conditions are assumed. Simplified models describing post-flashover fires refer to either nominal fires, such as the standard ISO834 curve, or to parametric fire curves, characterized by a heating phase, a peak and a cooling phase.

Parametric fire curves were first introduced by (Petterson, et al., 1976) for describing post-flashover fires triggered in a compartment with standard thermal inertia and an air inflow capable of limiting the burning rate of the combustible. The method led to a graphical formulation of temperature-time curves of the hot gasses and of the steel elements for different opening factors of the compartment and fuel load densities of the combustible material. Further refinement of the model also allowed considering different values of the thermal inertia and following studies (Wickstrom, 1985), (Hertz, 2001) based on the same approach led to parametric curves described by analytical expressions. In

particular, the Danish regulation (Danish National Annex to Eurocode 1, 2008) a unique expression Eq. (9.2) indicates a natural fire curve described by a unique expression, which:

$$T_g(t) = \frac{20 \cdot \left[345 \cdot \log 10\left(8 \cdot \Gamma \cdot t + 1\right)\right]}{\left[1 - 0.04 \cdot \left(t / t_{\max}\right)^{3.5}\right]} \text{ with: } \Gamma = \frac{\left(O/0.04\right)^2}{\left(b/1160\right)} \text{ and } t_{\max} = 7.8 \cdot 10^{-3} \frac{q}{O} \tag{9.2}$$

where:

T_g is the temperature of the hot gasses in °C

t is the time in min

b is the thermal inertia of the compartment in $\left(W \cdot s^{05}\right)/\left(K \cdot m^2\right)$

O is the opening factor of the compartment in $m^{0.5}$

q is the fuel load density in MJ/m^2 of enclosure surface of the compartment

The parametric curve indicated by the Eurocodes (EN 1991-1-2, 2004) instead presents two different expressions describing the heating phase, represented by a monotonically increasing temperature, and the cooling phase, represented by a linear decrement of temperatures, whose a gradient depends on the duration of the heating phase.

In this parametric model, the assumption of ventilation controlled fire is removed and in case of well-ventilated fire a different expression of the fire curves can be used. A punctual comparison of design resulting by the choice of the two parametric curves is presented in (Petrini, in press). To the purpose of this chapter however, it seems relevant to point out that the use of the EN parametric fire with linear cooling may lead to a strong reduction of the fire severity: this can be observed on the left of Figure 9.4, where the parametric fires calculated for the considered case study are compared with the standard fire; on the right side of Figure 9.4 the temperature curve of the rafters related to the Danish parametric fire is instead reported, which results to be heated up to 400°C during the fire.

It has to be pointed out however that the use of the EN parametric fire is recommended for fuel load density calculated with respect to the enclosure are not trespassing the lower limit of 50 MJ/m^2 and for compartment not exceeding 500 m^2 of floor area and 4 m of height. The same prescriptions on the compartment size also apply to other parametric fire such as the Danish fire curve, limiting their applicability to small compartments. This is due to the fact that parametric fire curves assume a flashover-like fire with uniform temperature in the compartment, condition which hardly will occur in large hall and atria. These limitations however are often disregarded in the practice, both because no additional information can be found in the code for a simple modelling of fire in large compartments and because other codes and literature references (Hertz K., 2006), (PD 6688-1-2-2007, 2007) indicate that these limitations can be safely ignored at the expenses of a less economic

but conservative design. In particular, thanks to the symmetry of the structure considered as case study, exact results can be obtained by referring to ¼ of the compartment, as indicated by Hertz (Hertz, 2001), in case a flashover is assumed in the compartment. In this way, the floor area of the reduced compartment is compliant with the prescriptive limits, being equal to Af' = 300 m^2. Always according to the same document, conservative results are obtained for compartment higher than 4 m, provided that all the openings above 4 m will be ignored. If calculated in this way, the resulting opening factor of the reduced symmetric compartment will be 0.045. The parametric curves and the corresponding element temperatures shown in Figure 9.4 have therefore been calculated with reference to ¼ of the compartment and this reduced opening factor as according to what suggested in Hertz (Hertz, 2001).

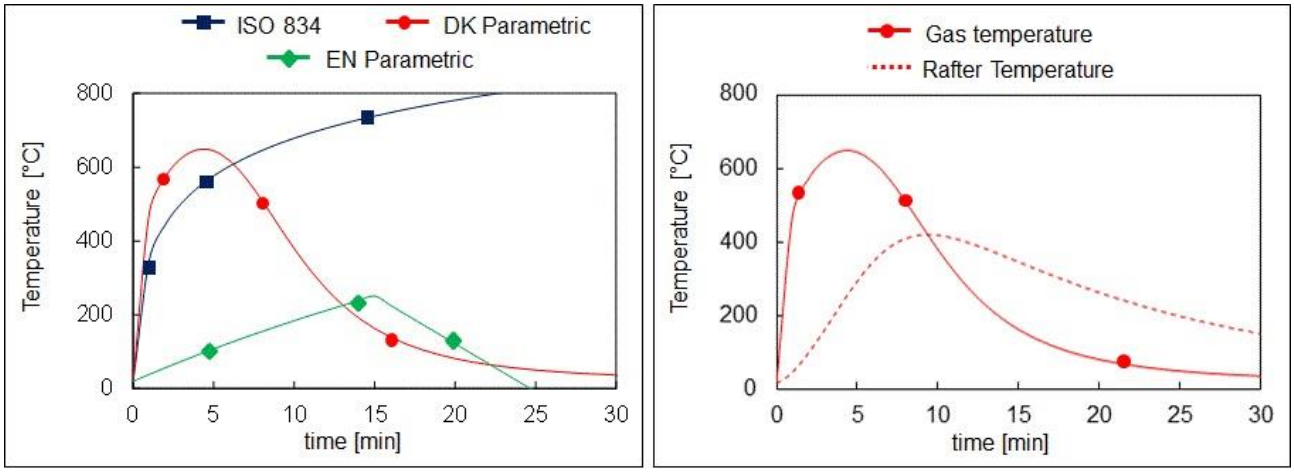

Figure 9.4 - Comparison between nominal (ISO834) and parametric (DK and EN) gas temperature (left) and temperature of the main beams according to the DK parametric fire curve.

9.4. ADVANCED MODELS

The limitations of parametric fire curves can be overcome in case more advanced fire models are used. In particular, the temperature evolution of hot gasses and elements can be obtained by CFD investigations as a variable of time and space and possible non uniform distributions of the temperatures in large compartments can be highlighted.

Non uniform distribution of temperatures can stem either from non uniform distribution in space of or from non uniform burning in time of the combustible:

i. in the first case, concentration of the fuel load in a relatively small area of the compartment could lead to an underestimation of the flame height and of the temperatures above:

ii. in the second case, a slow propagation of the fire would determine a longer fire duration than in case of a flashover-like burning of the combustible is assumed.

Both situations are likely to occur in large compartments (typically atria, auditoria, warehouses, industrial halls, etc.), where the need of free stream of people or goods require a low density of furniture and encumbering materials, which can be either piled up, leading to fuel load concentration (i) or placed far one from the other, leading to slow propagation of the fire (ii). Either way, the assumption of a uniform temperature in the compartment may result in an underestimation of the elements temperatures and possible structural failures.

Those aspects are better highlighted in the following, where the results of CFD investigations are presented, which refer to fires triggered by different distribution of the combustible materials. The investigations presented have been carried out with Fire Dynamic Simulator (FDS), which is a field CFD code released by NIST (McGrattan, et al., 2009).

9.4.1. Fire scenarios

An overview of the fire scenarios considered for the investigations is reported in Figure 9.5 with respect to ¼ of the model of the structure, which is symmetric about the horizontal and transversal centreline.

In every scenario, the pallets are considered to have been staked in the centre of the hall. The number of wooden pallets piled up in each stack varies from a maximum of 20 in scenario C to a minimum of 4 in scenario D, so that the number and height of the stacks in the hall varies accordingly (Figure 9.2): in particular, a maximum height of 3 m is reached by the stacks considered for scenario C and a minimum height of 0.6 m is reached by the stacks considered in scenario D.

This dispositions lead to different extension of the floor area involved in the fire, but also to different value of the HRRmax during the fire, which varies with the stack height, as explained above and summarized in Figure 9.2.

Furthermore, the different values of HRR_{max} determine a different speed of the fire propagation, given that the fire has been always assumed to trigger in the 4 central stacks and that the mutual distances between stacks on the floor have been held constant in all scenarios.

In the following sections, the outcomes of the investigations in term of temperatures of the fire and of temperature on the elements are presented, with respect to different locations within the compartment.

In particular, the temperatures of the hot gasses are referred to 8 thermocouples TC-1 to TC-8 placed at 4.5 m from the ground, while the temperatures of the elements have been measured with the adiabatic surface temperature method on the points AST-1 to AST-6. The position of the measurement device is visible in Figure 9.6 (right) and the coordinates of the points as reported as table in the same figure (left).

The outcomes of all considered scenarios are compared and three out of four scenarios are discussed in detail in the following, as representative of the most significant fire phenomena.

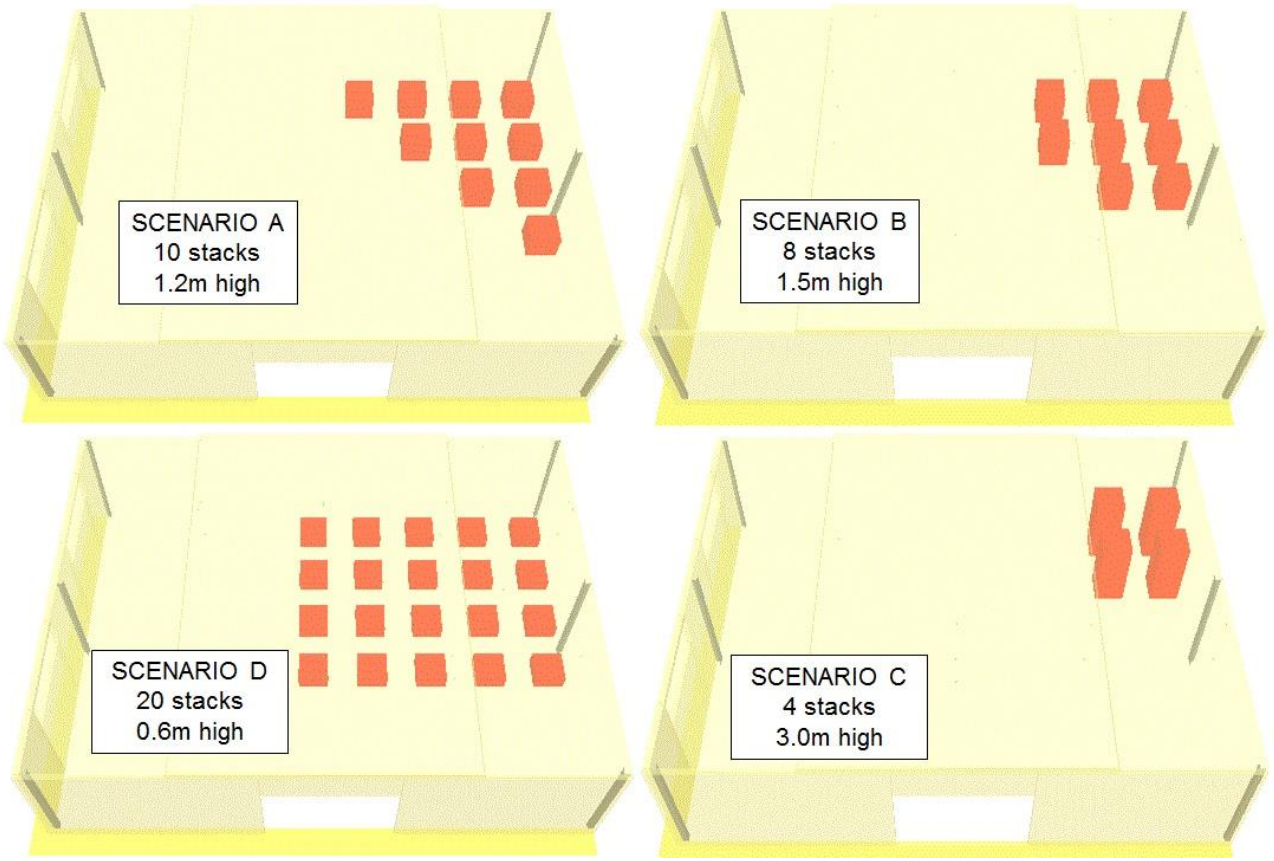

Figure 9.5 - Fire scenarios represented on ¼ of the model.

Scenario A: uniform distribution of temperatures

This scenario considers that the 320 wooden pallets have been piled up in group of 8, forming 40 stacks of height 1.2 m. The pallet stacks are placed at a mutual distance of 1.2 m in a regular pattern (Figure 9.5, top left), which covers a squared area of 162 m2 in the centre of the hall.

The outcomes of the investigation are reported in Figure 9.7 in term of temperatures of the gas (left column) and temperatures of the rafters (right column). The upper row refers to measures taken above the combustible, while the bottom row refers measures taken far from the flame.

THERMOCOUPLE							
ID	X	Y	Z	ID	X	Y	Z
TC – 1	5.0	6.0	4.5	TC – 2	5.0	12.0	4.5
TC – 3	10.0	6.0	4.5	TC – 4	10.0	12.0	4.5
TC – 5	15.0	6.0	4.5	TC – 6	15.0	12.0	4.5
TC – 7	20.0	6.0	4.5	TC – 8	20.0	12.0	4.5
ADIABATIC SURFACE TEMPERATURE							
ID	X	Y	Z	ID	X	Y	Z
AST – 1	6.6	0.0	4.8	AST – 2	16.8	0.0	4.6
AST – 3	6.6	7.5	4.8	AST – 4	16.8	7.5	4.6
AST – 5	6.6	15.0	4.8	AST – 6	16.8	15.0	4.6

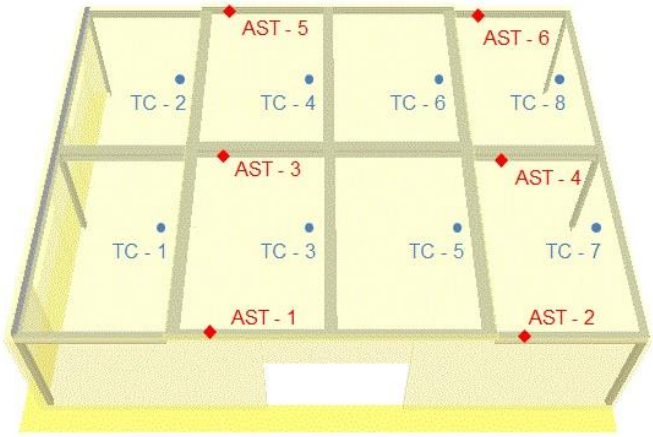

Figure 9.6 - Coordinates of thermocouples (TC) and devices for element temperatures (AST) (left) and their graphical representation on ¼ of the model (right)

With respect to the latter, the temperatures of the gas in two different locations of the hall are compared with the Danish parametric fire curve (Figure 9.7, bottom left). Either the temperature registered by the thermocouple most distant from the combustible area (TC-1) and a thermocouple closer to it (TC-5) show a good accordance with the temperatures provided by the parametric fire. The comparison between the two fire models has to be intended just as confrontation of the shape and temperatures of the fire, while a check on the starting time and initial growing rate of the two fires is hardly possible. The reason is that the parametric fire is a post-flashover model, which assumes the simultaneous burning of all combustible material present in the compartment. The fire scenario investigated instead refers to a fire, which triggers more realistically in few stacks and then propagates to the adjacent ones. Therefore also the initial phase of the fire is represented in the outcomes of the investigation.

The same accordance in term of shape and maximum temperatures stemming from simplified models is observable with respect to the elements outside the combustible area (Figure 9.7, bottom right), where the temperatures of two rafters are compared with the steel heating calculated from the Danish parametric fire for the rafter profile. Even if the position of the two rafter with respect to the fire is different (farer for AST-1 and closer for AST-3), the temperatures of the two elements are very similar and close to the steel heating curve.

The same uniformity of temperatures can be observed on all structural elements having the same profiles, except those just above the area occupied by the combustible (AST-6) or spanning from that area (AST-5). For those elements (Figure 9.7, top right).and for the thermocouples above the combustible area (TC6 and TC8 in Figure 9.7, top left) the temperatures are much higher, since the flame of the fire is impinging the ceiling. This is due to the relatively high pile of pallets, which

gives a HRR_{max} of 4.72 MW per stack and leads to a potential height of the flame equal to 5.53 m from the floor, according to the model of (Heskestad, 1995). It seems therefore more reasonable to refer to a localized fire model for a comparison of the temperature of those elements. The Eurocodes model for a localised high flame fire (EN 1991-1-2, 2004), which is based on the above referenced model of Hasemi (Hasemi & Tokunuga, 1984), would however lead to an overestimation of about 25% of the element temperatures in this case, as visible in the figure.

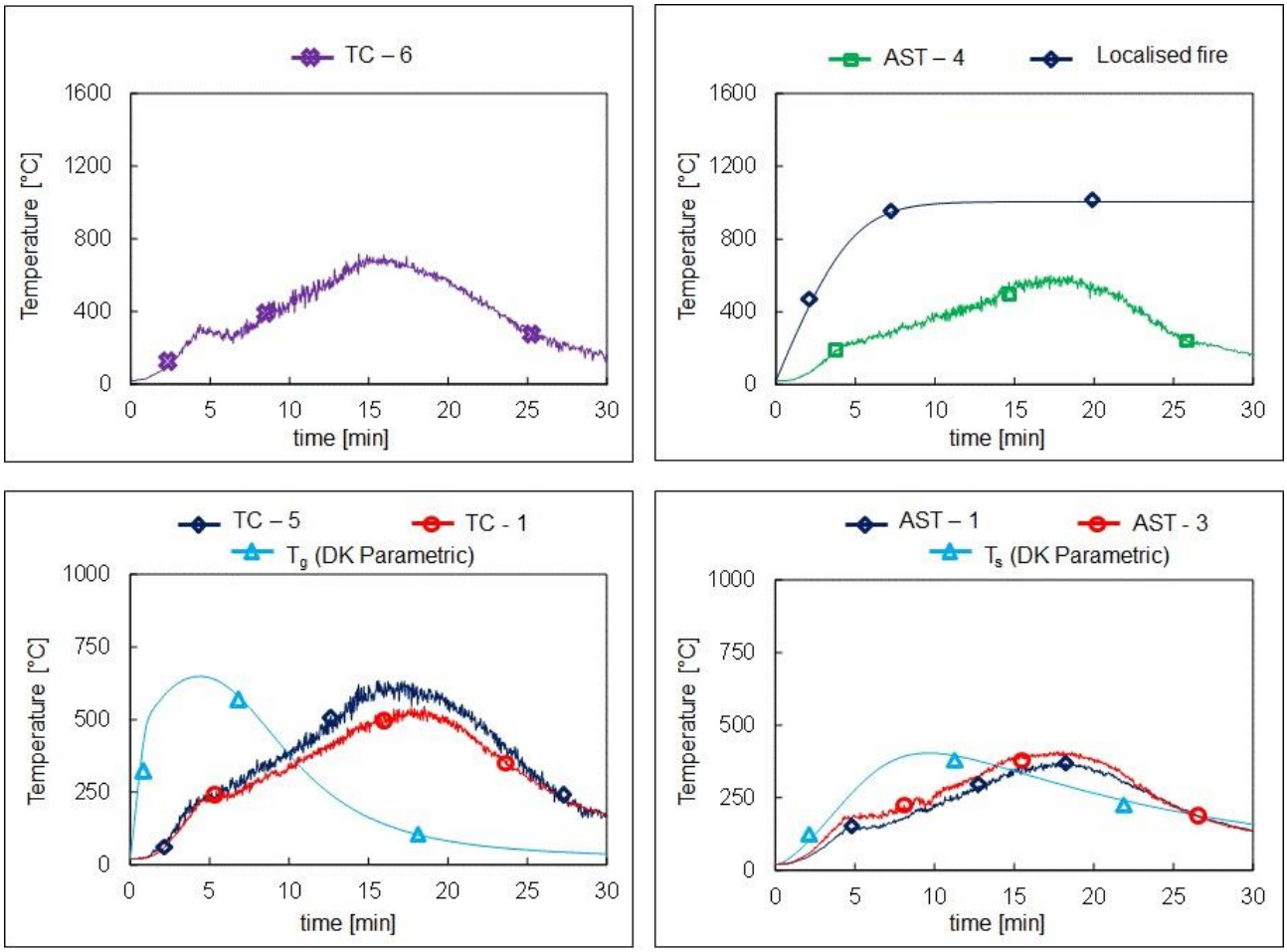

Figure 9.7 - Outcomes from scenario A in term of temperatures registered by the thermocouples (left) and on the element surfaces (right) inside (top) and outside (bottom) the area occupied by the combustible.

Scenario C: non uniform distribution of combustible in space

In this scenario, a higher stacking grade of the combustible is considered and the pallets are assumed to be piled up in group of 20, forming 16 stacks of height 3 m. The pallet stacks are placed at a mutual distance of 1.2 m in a regular pattern (Figure 9.5, bottom left), which a covers a squared area 72 m^2 in the centre of the hall.

Contrarily to the previous case, differences in the distribution of the gas and element temperatures along the compartment can be observed in this case also outside the area occupied by the combustible.

In particular, two temperatures of the gas outside the combustible are reported and compared with the Danish parametric fire (Figure 9.8 bottom left). Even if the temperature evolution of the parametric curve is much faster than the observed temperatures, due to what explained above, a consistency between the temperatures of the parametric fire and of the hot gasses can be observed only with reference to a point very far from the flame (TC-1). The temperature increases by moving towards the centre of the hall and even when the distance from the flame is still consistent (TC-5) a significant difference (around 40%) is shown with respect to the other curve (TC-1). The same difference reflects on the temperature of the elements measured at two different distances (AST-1 on the most external rafter and AST-3 on the adjacent one) from the combustible (Figure 9.8 bottom right).

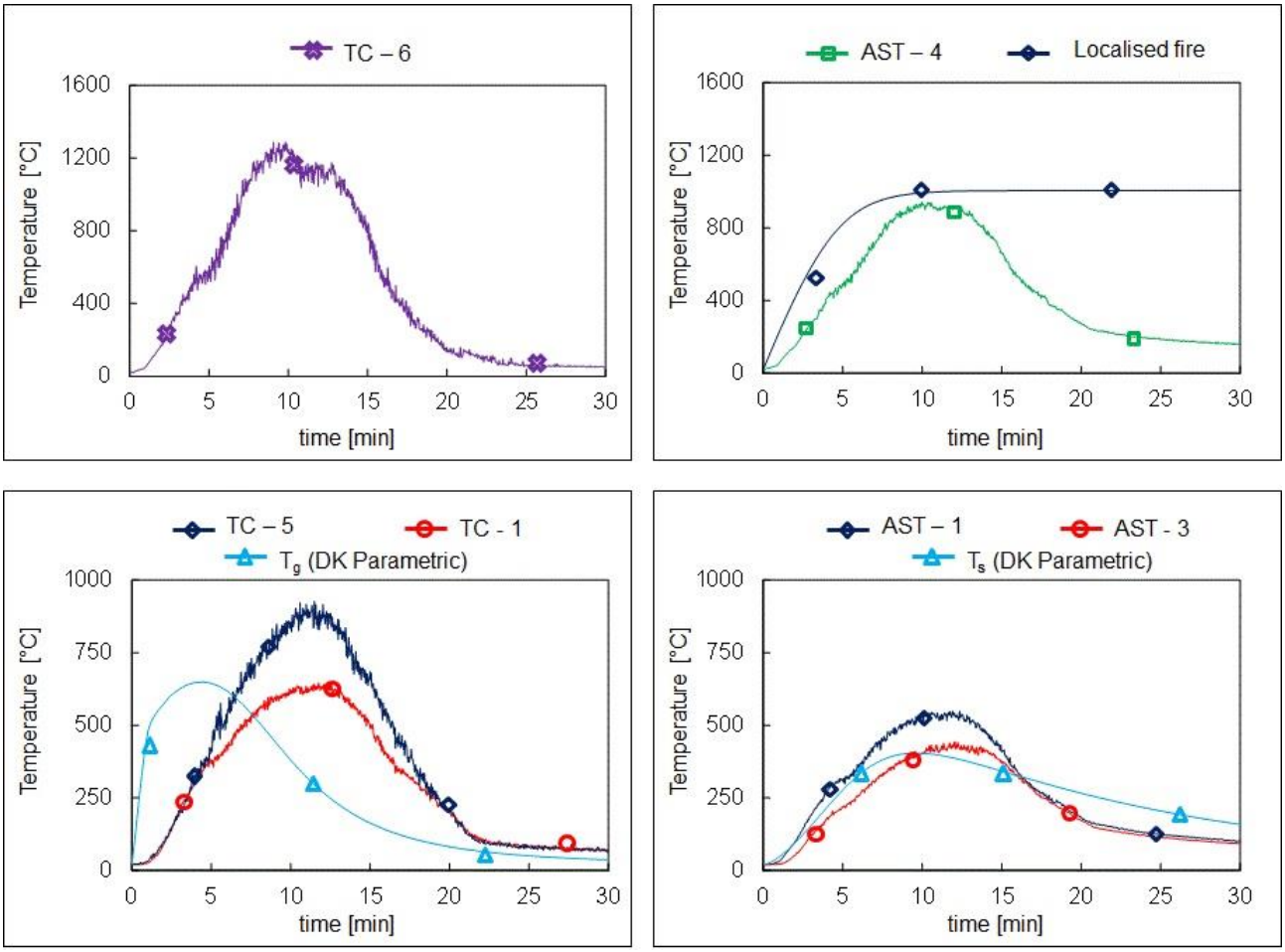

Figure 9.8 - Outcomes from scenario C in term of temperatures registered by the thermocouples (left) and on the element surfaces (right) inside (top) and outside (bottom) the area occupied by the combustible.

The temperatures shown in Figure 9.8 refer to the same measurement points as the previous case; however, since the stacking grade of the combustible is much higher, the area coved by the combustible is just 70.6 m^2 and the devices distance from the fire are higher, so that a lower difference on element temperatures could at first be expected. However, the HRR developed by the fire in this scenario (Figure 9.11) is higher, since the stacking grade of the combustible also affects the fire propagation, as better explained in the following section.

The higher stacks also determine a higher flame length. Therefore, also in this scenario the flame is impinging the ceiling and the temperatures above the combustible area registered either by the thermocouples TC-6 and TC-8 (Figure 9.8 top left) and by to the element devices AST-5 and AST-6 (Figure 9.8 top right) are higher than the in previous scenario.

Scenario D: non uniform burning of combustible in time

This scenario considers a lower stacking grade of the combustible and 80 stacks of 4 pallets with height of 0.6 m are assumed to be placed at a mutual distance of 1.2 m, covering a squared area of 229 m^2 in the centre of the hall.

The development of the fire and the consequent temperatures in the compartment and on the elements are very different in this scenario than in the previous ones. Due to the significantly lower grade of staking, the fire propagation is very slow and one stack gets on fire when the fire on the adjacent one is about to extinguish, as visible in Figure 9.9. The fire therefore moves from one stack to another, maintaining a low HRR and lasting much longer than a normal fire. This phenomenon has been evidenced and investigated in recent studies (Stern-Gottfied, et al., 2010), where it is referred to as travelling fire.

Results in term of temperatures of the gas and of the elements are reported in Figure 9.10 with respect to the first 30 min of fire. The duration of the fire however is very long in this case and the temperatures temperature of gas and elements significantly lower than in the previous cases. Furthermore, the gas temperatures are uniform in the area of the compartment not occupied by the fire and show almost a constant trend, as the temperature registered by the thermocouple TC-1, which is reported in the left part of Figure 9.10. The same constant trend is shown by the temperature of the elements outside the combustible area, as visible in the right part of Figure 9.10 with respect to the temperature registered for the device AST-1.

The temperatures of the thermocouples above the area occupied by the combustible show instead peaks of temperatures of short duration and then settle down to temperatures not very dissimilar, even if slightly higher, to the temperatures outside the combustible area. Due to the significantly

lower HRR_{max} of a stack, the flame height in this scenario is lower than the ceiling and is not impinging the elements, which never get very hot as in the previous scenarios. The same peaks characterize the temperatures of the elements inside the combustible area, at different time, depending on their distance from fire. The first peak is the one registered by the device AST-6 placed on the rafter just above the center of the fire, which is heated by the four central pallet stacks which are assumed to get on fire simultaneously and then propagate the fire.

The above mentioned studies on travelling fire show that, despite the low HRR, this type of fire can be detrimental for the structure, which is heated for a significantly longer time than in case of a flashover-like fire, especially in case of concrete structural system (Law, et al., 2011).

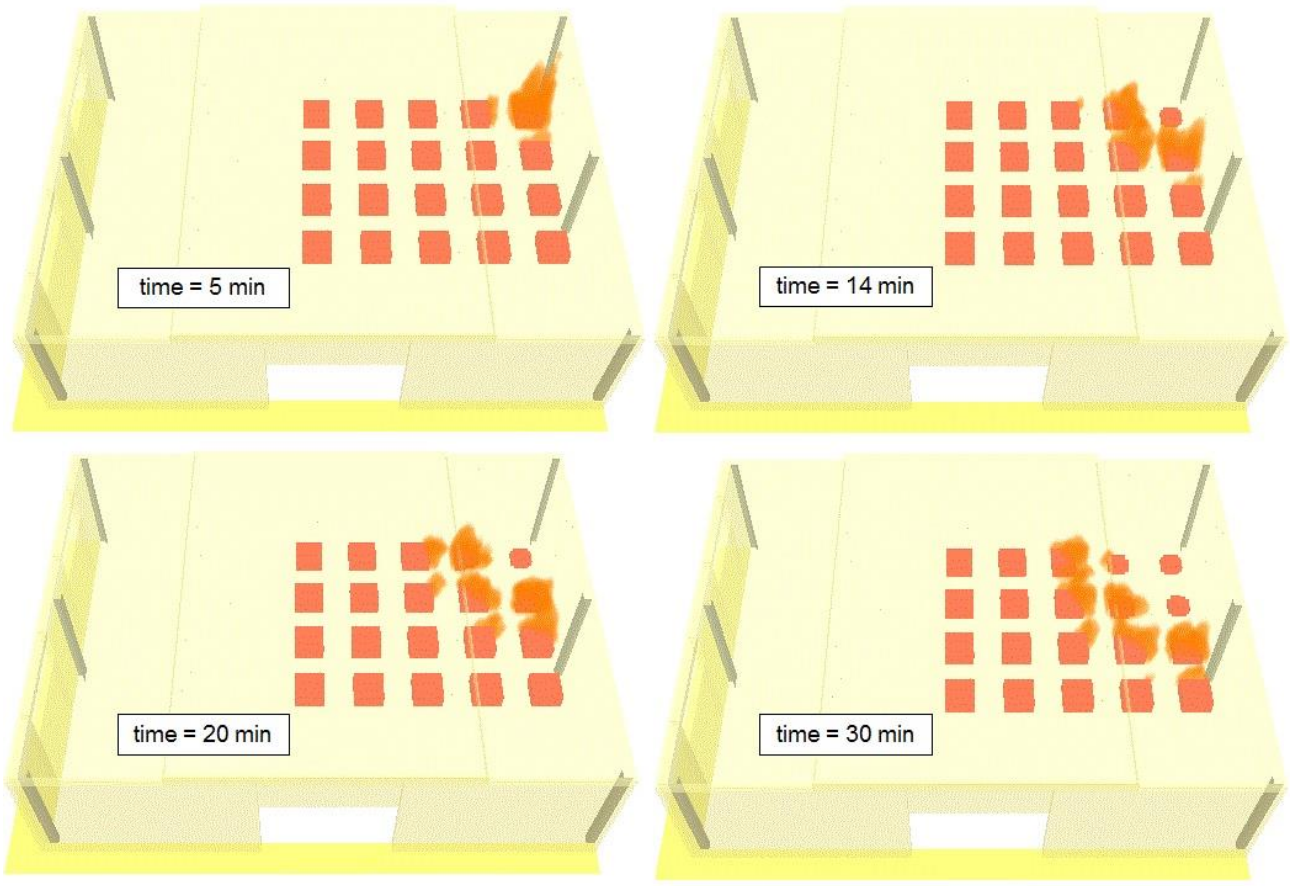

Figure 9.9 - Graphical representation of the HRR at different time for the fire scenario D.

This doesn't seem the case in this particular fire scenario, where, even if the temperature of the elements slowly increase with time, won't get to very high values. This can be explained considering that, in order to consider different stacking level of the combustible, in this study, a low fuel load has been assumed in the hall. When the combustible is concentrated in a small area, the local fuel load density is high, which may lead to fire that are locally much more severe than what

expected from a compartment fire. However, when the combustible is relatively spread along the compartment as in this case, the fuel load density is more uniform along the compartment and has a low value.

Despite specific considerations on the temperature values however, it seems important to point out that non uniform distribution in time and space of the temperatures, such as those generated by a travelling fire, may have negative effect on the structural behaviour, e.g. in case of cold elements hindering the thermal expansion of hot ones (Usmani, et al., 2003).

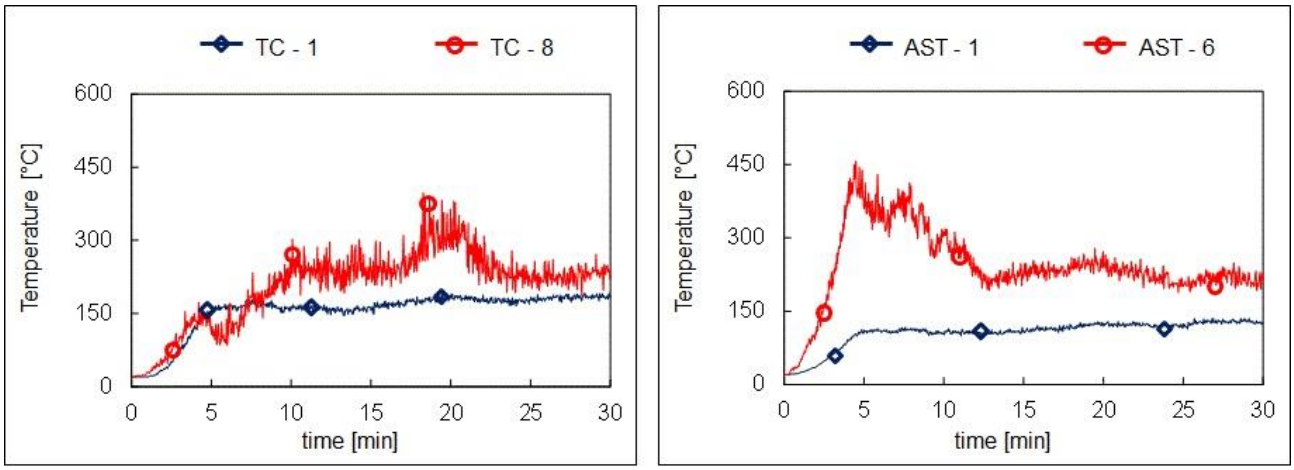

Figure 9.10 - Outcomes from scenario D in term of temperatures registered by the thermocouples (left) and on the element surfaces (right) inside and outside the area occupied by the combustible.

9.4.2. Comparison

The results obtained for all four fire scenarios considered (Figure 9.5) are summarized in Figure 9.11, with respect to the HRR (top left), the temperature of the hot gases far measured by the thermocouple TC-1 from the combustible area (top right), and by the thermocouple TC-8 above the combustible measured (bottom right), as well as the temperature of the central rafter measured by the device AST-6 above the combustible (bottom left).

By observation of Figure 9.11 it can be stated the primary effect of the grade of combustible stacking is the propagation rate of the fire. The fire propagation is strictly related with the maximum HRR which can be achieved by the fire and therefore with the fire duration. By moving from a high to lower grade of combustible stacking, the peak of the HRR decreases and fire becomes lower and longer, as visible in the top row of Figure 9.11. If the HRR becomes sufficiently low for a given distance of the combustible materials, a peak in the HRR curve cannot be evidenced anymore, as a

different fire phenomenon develops, where the fire moves throughout the compartment, as the combustible material of one area burns out.

Among the three scenarios A, B, and C, the most severe fire in term of element temperatures seems to be the one referring to the fire scenario C, which corresponds to a high staking grade of the combustible. This result is reported in the figure for the temperatures of the elements above the flame, but can be also evidenced in the temperatures of the elements outside the combustible area.

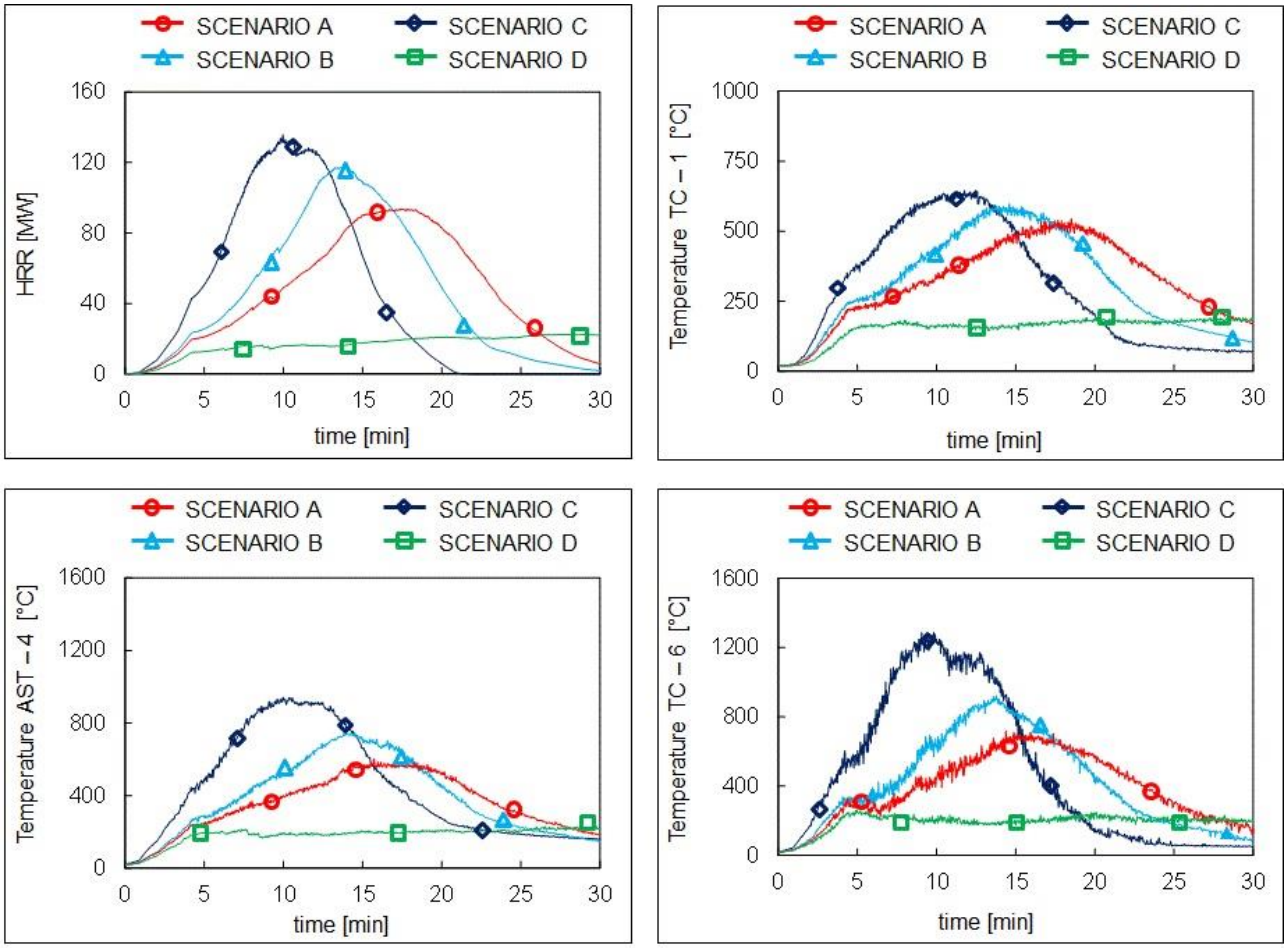

Figure 9.11 - Comparison of the outcomes for the different scenarios

9.5. PROBLEMATIC ASPECTS OF CFD MODELS

The results presented above show that simplified models are not capable of providing with a sufficient grade of accuracy the element temperatures in case of fire developing in large compartments. A more realistic modelling of the phenomenon can be obtained by means of CFD investigations, which can account for different distribution of the combustible and velocity of fire

propagation and are capable of describing possible inhomogeneous distribution of the temperatures within a compartment.

9.4.3. Reduction of computational onus

As discussed in the previous sections, the above mentioned aspects are particularly relevant for the design of large compartments. In case of large compartments however, CFD models requires generally a particularly high computational onus. This is partly due to the greater extension in space and time of the investigations: this problem can be however overcome in case some symmetry lines are present in the compartment. In the case study presented here for example, the compartment was symmetric about the horizontal and transversal central lines and a reduction of the computational onus has been obtained by carrying out the investigations in ¼ of the model (Figure 9.12), where appropriate boundary conditions have been considered for simulating the two symmetry planes. The validation of the reduced model against the full model is shown in Figure 9.13, where a complete accordance in terms of fire and element temperatures can be observed.

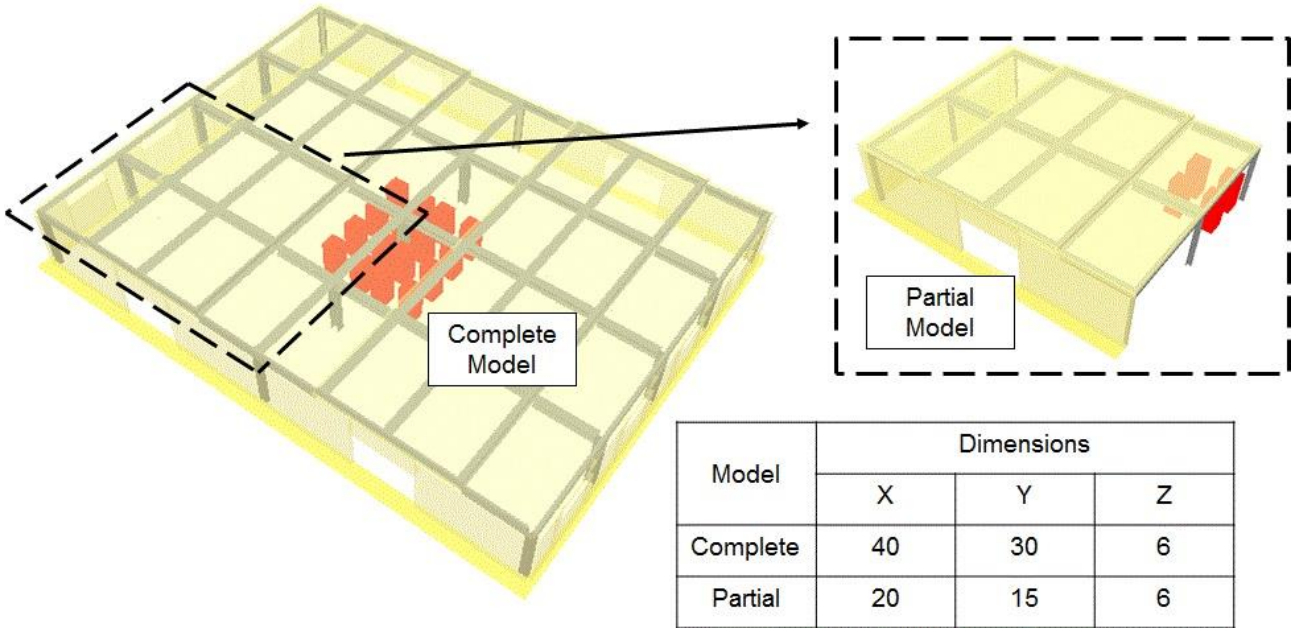

Model	Dimensions		
	X	Y	Z
Complete	40	30	6
Partial	20	15	6

Figure 9.12 - Full model and reduction to ¼ of the model

Apart from the greater physical dimensions of the problem and possible longer durations of the fire, more significant increment of the computational onus can be ascribed to the convergence problems, which may arise in case of highly concentrated or highly spread combustible materials, both representing situations likely to occur in large compartments: in the first case, difficulties stem from

a very high growing rate of the fire, while in the second case the slow propagation of the fire from one object to another can be an issue. As a consequence, the grid size required for this kind of investigations is generally smaller than for investigations of more conventional structures, as better explained in the following.

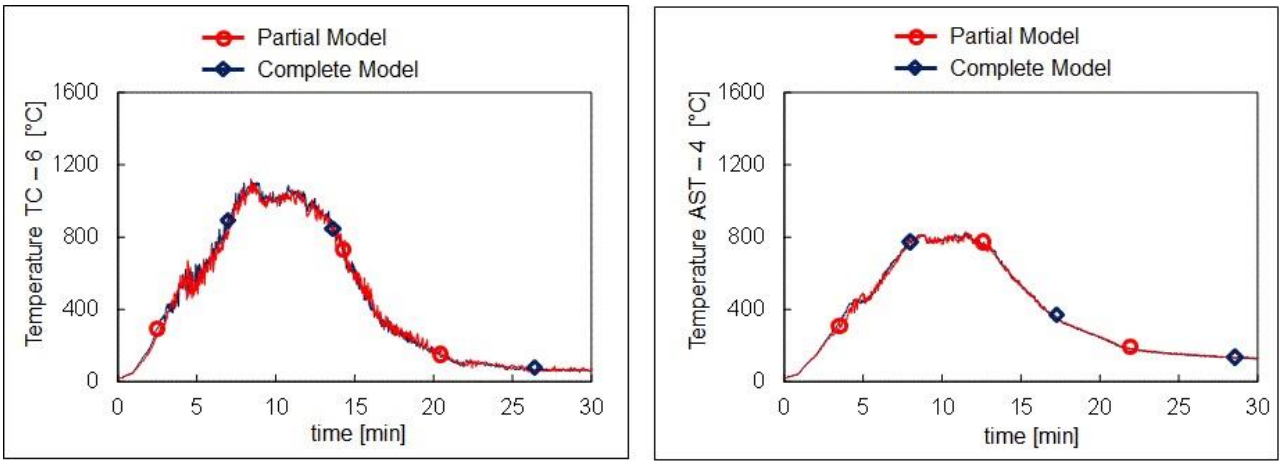

Figure 9.13 - Validation of the reduced model which refer to ¼ of the compartment, in case of scenario C

9.4.4. Mesh optimization

Even if FDS is one of the most acknowledged codes for fire modelling, the use of the program requires a certain attention in case the HRR has to be predicted rather than specified, such as in case the modelling of fire growth and spread is of interest. In these cases, the limits on the grid size are more severe than the value recommended in (NUREG 1824, 2007), (Ascenzi, 2010), (Best Practice Gruppen, 2009) and for an optimal representation of buoyant plume dynamic and a careful mesh sensitivity study becomes fundamental. With respect to the case study here investigated, despite the property of the compartment did not vary, different physical phenomena stemmed from the variation of the distribution of the combustible and different values of the optimal grid size had to be identified for each case. In the following, the study of the mesh sensitivity is reported for the case of scenario C. For the HRR of this scenario, the most severe limitation from the Danish CFD guide (Best Practice Group, 2009) recommends a mesh size around 0.7 m. A starting size of 60 cm has been therefore used for the sensitivity study and then the mesh size has been decreased until convergence in the temperature curves s is obtained. In Figure 9.14 the results of the sensitivity study are reported in term of HRR (top left), smoke height (top right), temperature of the gas registered by the TC-6 thermocouples (bottom right) and temperature of the rafter registered by the device AST-4.

It can be seen that the mesh of 60 cm leads to inconsistent results for both the HRR curve and the smoke height as well as the gas and element temperatures. A mesh of 30 cm would be sufficient for the representation of the smoke movements. However, the description of the HRR curve is not sufficiently accurate in this case and would lead to an underestimation of the gas and element temperatures which are of interest in this study. Finer mesh sizes of 20 cm and of 15 cm are therefore used. The sensitivity study shows that this temperature values don't change when a mesh finer that 20, which is therefore chosen for the investigation of this scenario.

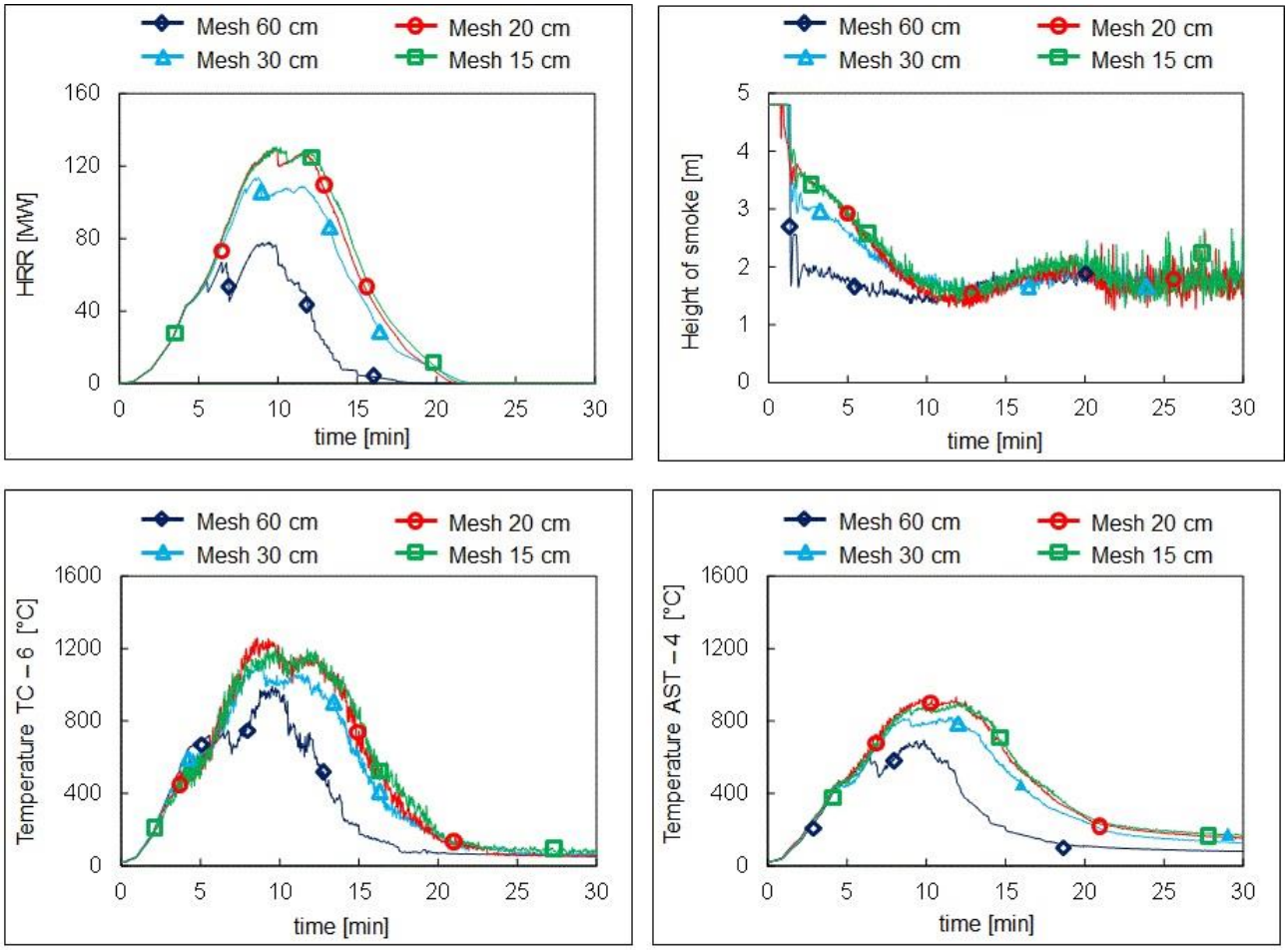

Figure 9.14 - Mesh sensitivity study for fire scenario C

9.6. CONCLUSIONS

Current design methods for structural fire safety refer to post-flashover conditions, where a uniform distribution of the temperatures can be assumed within the compartment. These methods have been

extensively tested and safely used in small compartment, which are typically dense furnished and present a reasonably uniform distribution of the combustibles along the floor area.

Large compartments may be instead less densely furnished and present therefore lower fuel load per square meter of floor area, as shown by several statistic investigations conducted in the ‘70ies in Sweden (Nilsson, 1970), (Forsberg & Thor, 1971) and more recently in Denmark (Danish National Annex to Eurocode 1, 2008). Nevertheless, the assumption of a uniform distribution of the combustible materials is generally unrealistic and, especially in case of industrial halls, furniture and other combustibles can occupy just a part of the premises or stored materials can be piled up with different grade of stacking.

Since the flashover is unlikely to occur in large compartments, the Eurocodes (EN 1991-1-2, 2004) indicates a relatively low limit on the compartment size for the applicability of parametric fire. If this don’t represent a problem for traditional residential buildings, it hider the use of simplified fire models for a growing number of structures, given that nowadays longer span width and innovative solutions for open spaces are made available by the constant advance in structural design. The need of a better comprehension and modelling of the fire which develops in large compartment seems therefore a critical aspect of the fire safety design.

In this chapter a well-ventilated fire in a large compartment devoted to storage of wood pallets has been investigated with respect to structural fire safety consideration. Different modelling of the fire development and few staking grade of the combustible have been considered and results in term of gas and element temperatures have been compared with a parametric fire modelling, which assumes a ventilation controlled fire and a uniform distribution of the fuel load.

The outcomes of the investigations show that simplified analytical models may not represent with sufficient accuracy the element temperatures, either in case of a highly concentrated fuel load and in case the combustible is spread along the compartment.

With respect to the first case, low fuel load density deriving from spreading the combustible over a large floor area, may result in very long fires, especially in case of a travelling fire, where the propagation of the fire to the adjacent combustible materials occurs only after the burnout of the first object. This phenomenon has been recognised to possibly have been responsible of major structural failures both in steel (Gann, et al., 2005) and concrete buildings (Fletcher & et al., 2007) . Even if in the case presented high element temperatures were not evidenced when a spread distribution of the combustible was considered, the occurrence of a travelling fire has been highlighted in this case.

With respect to the second case, a high staking grade of the combustible can result in a non uniform distribution of the temperatures of both fire and elements, also outside the area occupied by the combustible. Furthermore, due to the high local fuel load density, the temperatures of the elements above the flame may be heated up to temperatures much higher than those predicted by a flashover fire. This result may appear in contrast with recommendations for the structural fire design of large compartments (Hertz, 2001), which show that conservative results are expected if the limits on the compartment size for applicability of parametric fire are exceeded. It has to be stressed out however, that a value of 200 MJ/m^2 of enclosing surface is recommended for domestic buildings, offices, hospitals, schools and hotels, disrespectfully from the effective fuel load present. In the view of the results presented above, in case a uniform distribution of the combustible is assumed in large compartments, it seems essential to use a nominal high value of the fuel load, even when the amount of combustible is known to be lower, in order to take into account the effect of a possible stacking of the material.

Chapter 10

10. PROGRESSIVE COLLAPSE SUSCEPTIBILITY OF A HIGH-RISE BUILDING

10.1. INTRODUCTION

Due to the significant vertical elevation and complexity of the structural system, high rise buildings may suffer from the effects of fire more than other structures.

For this reason, in addition to evacuation strategies and active fire protection, a careful consideration of structural response to fire is also very important.

In this context, it is of interest to investigate the characteristics of the structural system that could possibly reduce local damages or mitigate the progression of failures in case of fire.

In this chapter, a steel high rise building is taken as case study and the response of the building is investigated up to the crisis of the structure with respect to a standard fire in a lower and in a higher storey: the comparison of the fire induced failures at the different height allows highlighting the role played in the resulting collapse mechanisms by the beam-column stiffness ratio and by the loading condition and a possible propagation of the initial failures to zones of the structure not directly involved in the fire. To this purpose, simplified fire design and verification methods on isolated elements are not sufficient and the response of the structural system as a whole (Usmani, et al., 2000) has to be investigated. This is a quite difficult task, which in case of complex structures such as a high rise building (Research Fund for Coal and Steel of the European Community, 2008) , necessarily requires some simplifying assumptions in the modelling of the action and of the structure.

It has to be pointed out that, as better explained in the following, the interest of this study is focused on the behaviour of the steel components. If this situation can be partly representative of a construction stage on one side, it is of greater interest in order to highlight some basic mechanisms of failure in steel framed structures.

The investigations take into account a full nonlinear response of the structure, influenced by material degradation at high temperatures, possibility of buckling, large displacements and

deformations and exploitation of plastic reserve of the elements. Investigations are carried out on substructures, particularly two 3D floor models (FM), which refer to the 5th and 35th storey, and a 3D sectional model (SM) of a vertical frame of the building, where all the stories are represented and a possible vertical propagation of the damages can be evidenced.

In the presentation of the performed investigations and in the discussion of the outcomes, a focus is done on methodological aspects concerning the definition of fire scenarios and collapse criteria, the modelling of the substructures and the identification of failure modalities.

10.2. CASE STUDY

The building considered as case study is a steel high-rise building, whose premises are devoted to offices and residential use. The building has been designed on the basis of the geometry of a building recently built up in Latina, Italy (Figure 10.1). The building is composed of 40 storeys and has a framed structural system. A vertical bracing system provides stiffness against horizontal actions, while no horizontal bracing system is present within the floor planes, since a bidirectional concrete floor slabs should provide the necessary in-plane stiffness.

The inclusion of hollow spheres in the concrete floor slab, together with the biaxial symmetry of the slabs, allowed for the presence of beams with relatively small profiles spanning long distances

On the contrary, the sections of the columns are quite big, as the resistance against horizontal loads is totally entrusted to the columns. As a result, the difference in the section dimensions of the horizontal and vertical elements is quite high in this type of structural system and becomes particularly significant in the bottom floors, where the column sections are the biggest. This characteristic may influence the structural response in case of fire, as better highlighted in the following.

10.2.1. Methodology

When attention is devoted at identifying collapse mechanisms that can possibly be triggered by fire in complex structures, prescriptive rules and simplified design procedures, mostly aimed at preventing the failures on isolated elements, cannot be used. In order to follow the progression of the failures, a more advanced investigation needs to be carried out on the structure, which generally requires the avail of Finite Element Method (FEM) programs and some design experience for modelling both the fire action and the structural response.

The flowchart of Figure 10.2 represents the general procedure to be followed in those cases. In the following sections, each step of the flowchart will be described and applied to the case study considered. The most relevant assumptions and modelling aspects will be presented and discussed, with the intention of exemplifying a general methodology for the advanced fire design of complex structures such as a high rise building.

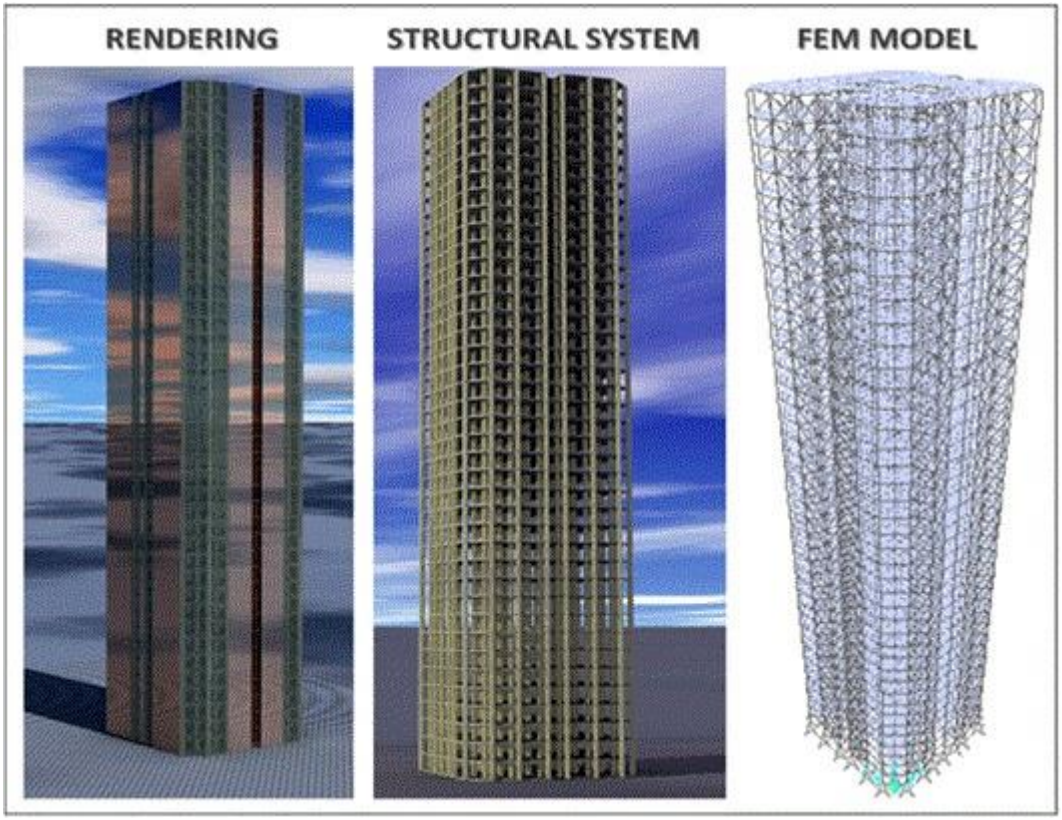

Figure 10.1- Rendering and FEM of the investigated high-rise building

10.2.2. Fire scenarios

The identification of relevant fire scenarios plays a key role for evaluating the response and a possible progressive collapse susceptibility of the structure in case of fire. In literature, the identification of design scenarios is often obtained by means of a risk analysis (Faber & Stewart, 2003), (Nii, et al., 2010), which is however a relatively onerous procedure. Furthermore, in case of Low Probability - High Consequence (LP-HC) events the risk assessment is complicated by the fact that most probable scenarios are not necessarily the most severe ones in term of consequences and costs.

Therefore, in practice, a number of fire scenarios is often identified on the building (Gkoumas, et al., 2008) on the basis of engineering experience and qualitative considerations or preliminary simplified investigations.

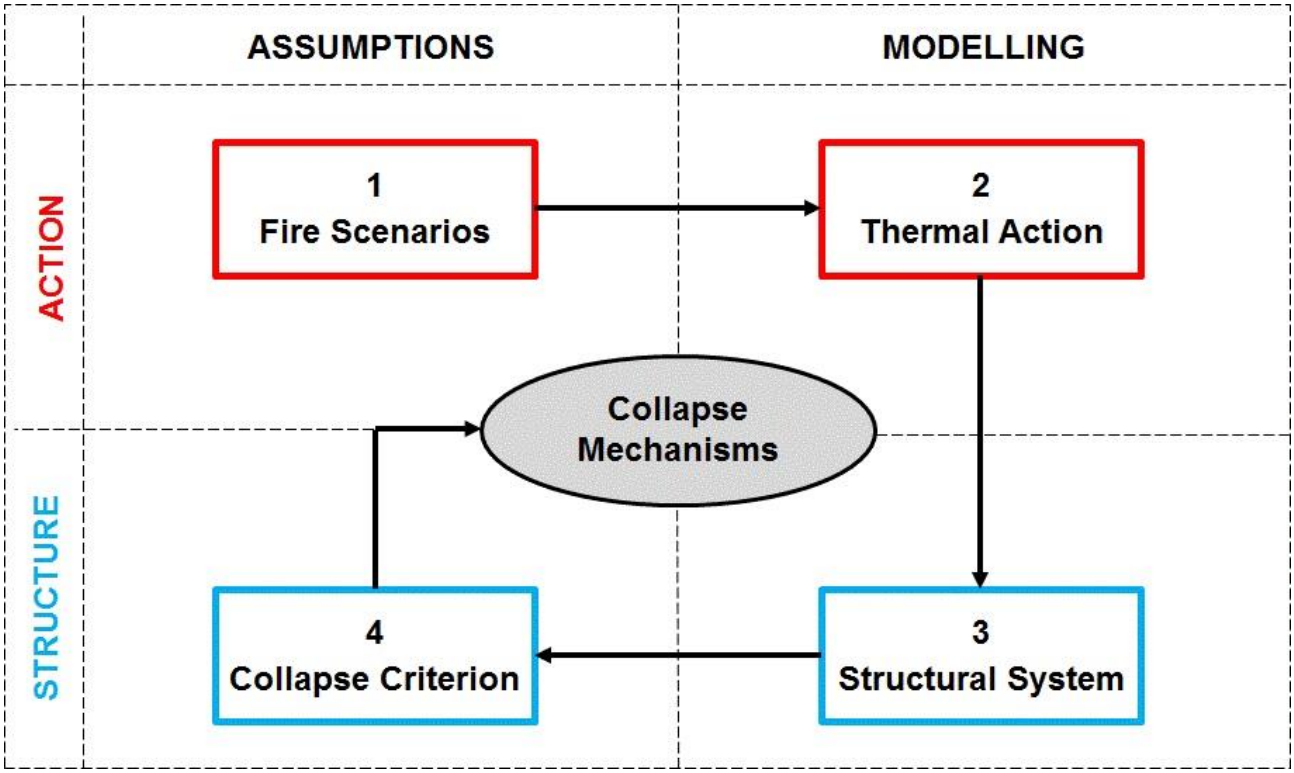

Figure 10.2 - Procedure for advanced investigation of the response of a complex structure to fire

In this study, fire is considered in two different areas of a floor. Furthermore, two reference storeys, specifically the 5th and 35th storey, have been considered for the triggering of the fire. As a result, a set of four different fire scenarios has been investigated on the floor models (Figure 10.3). With respect to the sectional model, the fire has been considered to affect either the beams only or both the beams and the columns. In addition to that, a possible loss of vertical compartmentalization has been considered and the fire has been assumed both to be localized within a single storey and to have spread along two subsequent storeys. These assumptions led to the investigations of six additional fire scenarios on the sectional model. All considered fire scenarios highlighted in Figure 10.5.

The choice of considering the triggering of the fire at two distinct heights is motivated by the different column profiles present at the bottom and top of the building, which can lead to a different structural response of the steel substructures. The comparison of the outcomes provides an insight

of the structural characteristics that play a role in the time and type of failures in a steel framed building and may suggest target modifications for improving the structural performances.

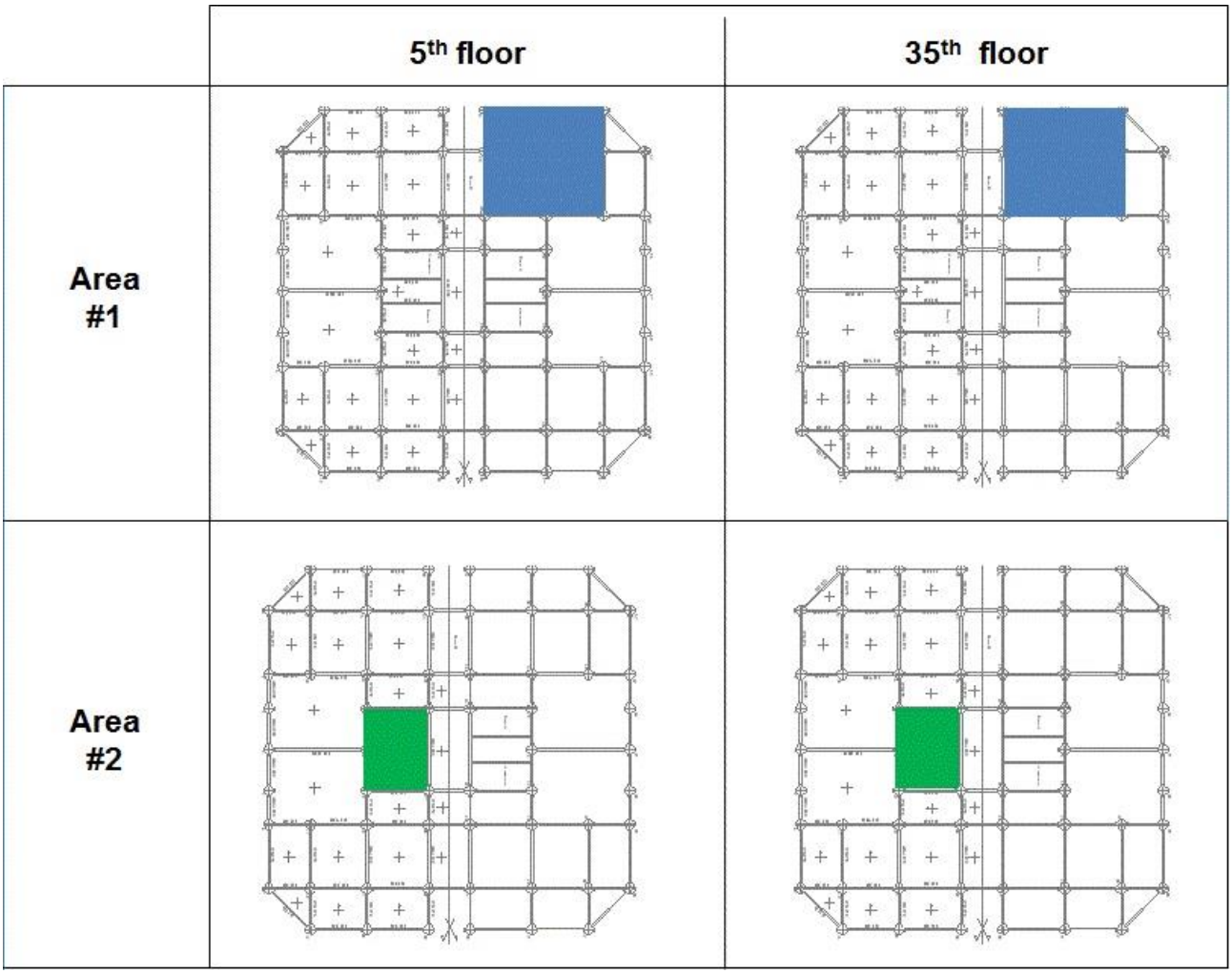

Figure 10.3 - Fire scenarios considered in the building.

Since the identification of collapse mechanisms is the main interest of this study, the consideration of compartment fires did not seem to be the most appropriate choice, as realistic compartment properties would not be available and damage conditions lower than those assumed would have been required in a realistic design. For this reason the use of a nominal monotonic fire has been preferred to a natural fire model, in order to be able to trace the progression of failures up to the crisis of the building. The use of a conventional fire however could also be preferred for the consideration in the design of unexpected circumstances, which could lead to fires more severe than what expected. Examples of that can be arsons or fires triggered by malevolent explosions or by the impact of a plane. Also less critical events may determine higher element temperatures, such as a refurbishment of the building, which leads to a lower the thermal inertia of the walls or a decrement

of the ventilation surfaces, as well as a change of occupancy of the premises, which determines a fuel load increment.

10.2.3. Thermal action

Once the fire scenarios have been identified, the fire action and the heat transfer to the elements have to be modelled. In the flowchart of Figure 10.2 both aspects of fire model and heat transfer model (Buchanan, 2002) are considered in the 2nd step named "Thermal action". With reference to the fire model, more or less realistic temperature-time curves can be considered for the fire, namely natural or nominal fire curves.

As mentioned above, in the study presented here a nominal fire has been assumed for the sake of simplicity in the form of the standard ISO 834 curve.

The heating curves of steel members have been calculated under the assumption of uniform temperature along the sections, according to the Eurocode formula for the heating of uninsulated steel profiles steel (EN 1993-1-2, 2005) and using a convective coefficient $\alpha = 25$ W/(m^{2}K) and a total emissivity $\varepsilon = 0.5$ (the shadow effect of the profiles is neglected on the safe side). The resulting temperatures have been applied as thermal load to all nodes of the elements in the tributary area of the fire scenario considered in each investigation.

10.2.4. Structural system

Modelling in detail such a big and complex structure can be quite onerous in term of analysis time, but also in term of difficulties in the interpretation of results, which is the main goal of each investigation: in order to understand properly the structural behaviour and also be able to check the validity of the outcomes, it's important to simplify the models as much as possible, provided that aspects that are of interest in the structural response will be duly represented.

In this respect, a central point of fire-induced investigations concerns the identification of a possible spread of the local damages from the heated members to elements not directly involved in the fire. In a 3D building, the collapse propagation can occur both within the floor plan where the fire has triggered and along the building elevation. Two different type of substructures have therefore been considered (Figure 10.4): i) a floor model, where the direct effect of fire on heated beams can be evaluated (vulnerability to fire) and then the consequence of a possible failure of the heated beams on the rest of the floor system can be investigated (structural robustness of the system); and ii) a sectional model, where a possible overloading and collapse of the columns consequent to beam

failure can be identified and a vertical propagation of the collapse can be identified. Here the term vulnerability is intended as sensibility to accidental actions (Giuliani, 2012) and the term robustness is referred to the sensibility to local failures (Starrosek, 2009). Concerning the floor substructure, it is important to point out that the floor slabs have not been modelled, since, as mentioned before, this study is mostly aimed at highlighting the role of the steel components in the failure mechanisms of framed tall structural systems. Concerning the sectional substructure, a spatial model has been implemented, capable of highlighting possible out of plane displacements of the elements,. In order to simulate the presence of beams perpendicular to the frame, transversal restraints have been applied to the sectional model in the 3rd dimension.

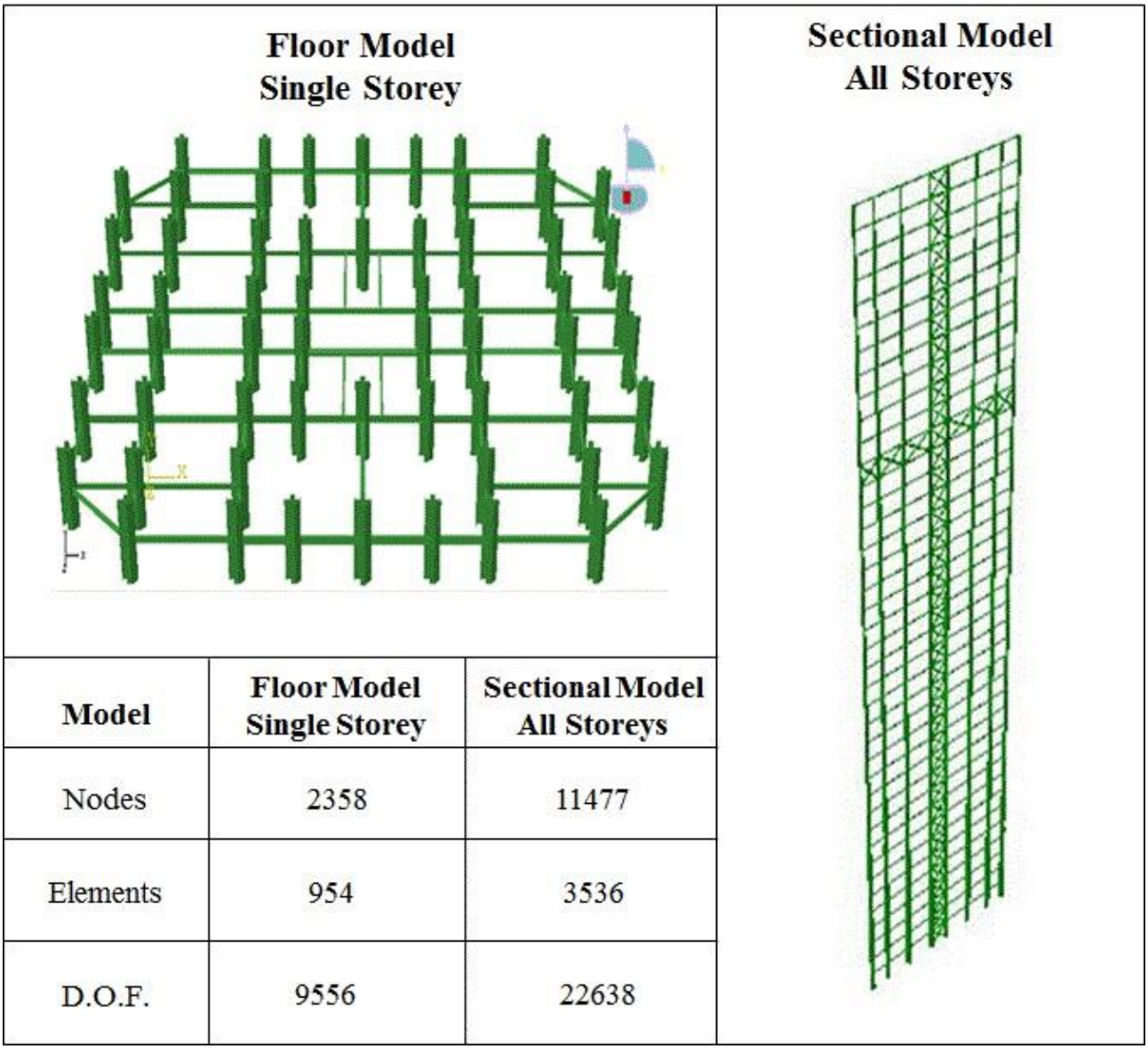

Model	Floor Model Single Storey	Sectional Model All Storeys
Nodes	2358	11477
Elements	954	3536
D.O.F.	9556	22638

Figure 10.4 - Different models considered for the investigations

A commercial finite element code has been used for the investigations (ABAQUS, 2010), which takes into account thermo-plastic material and geometric nonlinearities. Either the sectional and the floor models have been implemented by using beam elements, which has been properly meshed in order to have sufficient accuracy in: i) the application of thermal loads; ii) the calculation of displacements and forces; iii) the representation of the deformed shape and other output variables. With respect to the application of the thermal loads in particular, a sensitivity analysis of the displacement to the mesh size has been performed, which has led to the choice of an optimal discretization of the elements. Dead and live loads have been applied as line loads along the axis of the beams and considered together with the self-weight in a first load step. In a second load step the heating curves calculated for the steel profiles have been applied to the nodes of the elements pertinent to the area of the fire scenario considered, while other elements have been assumed to remain cold throughout the investigation. An explicit dynamic solver has been used in order to overcome convergence problems due to the formation of local mechanisms, thus enabling to trace down the propagation of failures.

10.2.5. Collapse condition

The last step of the investigation procedure concerns the interpretation of the results and the identification of collapse modes and collapse conditions for each fire scenario. For this purpose, a collapse criterion has to be chosen on the basis of the safety objectives defined for the structures. As explained in the first paragraph, the investigations presented here have two main different goals: it is of interest either i) to identify the time and type of failures, and ii) to outline a possible propagation of the collapse.

To the first aim, a limit on the displacement of significant points of the structure can be used and calibrated on the basis of the performance required to the structure. If the functionality of the structure should be maintained, a collapse condition, which is representative of the failure of one element, is the runaway of a significant point of the structure, with this term meaning the accelerating and irreversible downward displacement of the considered point (Usmani, et al., 2003). Conventional limit values for the maximum displacement of members are also found in literature and regulations with respect to steel elements in bending (Petterson, et al., 1976), (British Standard, 2004). In the discussion of the results, the displacement limit indicated in Eq.1b will be considered and compared with the runaway criterion, as identifiable from the qualitative observation of the monitored displacements.

To the second aim, the collapse condition is represented by a well-identifiable circumstance, namely the failure of elements not directly involved in the fire, which are assumed to remain cold in the investigations performed.

10.2.6. Main results

The most relevant results of the analyses are presented and discussed in the following. These results refer to both the floor (behaviour of beams) and the sectional model (behaviour of beams and columns). An overview of the investigations performed is given in Figure 10.5.

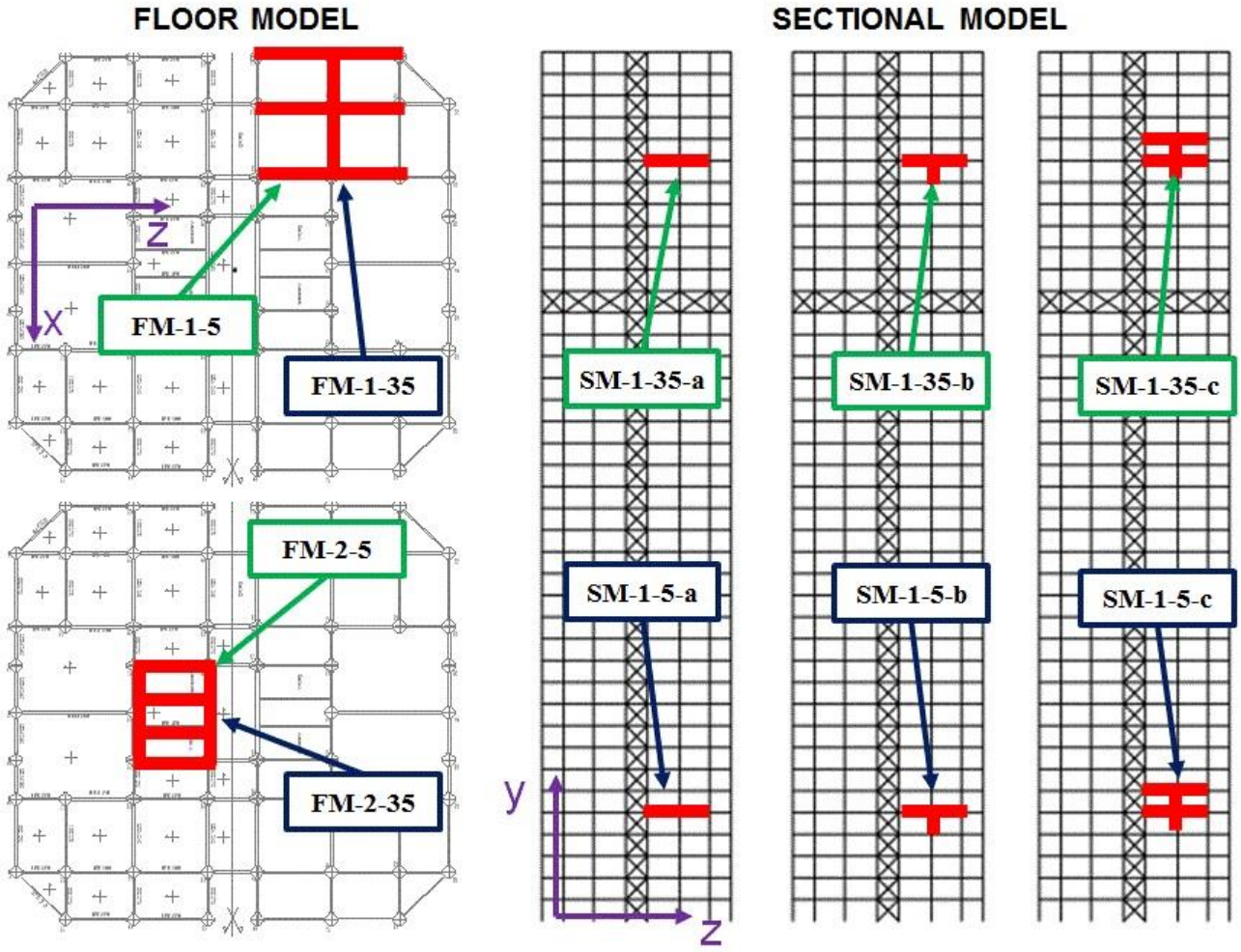

Figure 10.5 - Overview of models and scenarios considered and summary of the investigation performed

The abbreviations used for identifying the different investigations are formed by a set of two letters followed by two numbers separated by a dash, and have the following meaning:

- the first two letters of the abbreviation refer to the model studied (FM and SM stays for sectional model and floor model respectively);

- the first number refers to the area of the floor where the fire is assumed (scenario 1 or scenario 2)
- the second number refer to the story number (5th or 35th storey);
- in the investigation on the sectional model, a last letter is specified too, which refers to the extension of the fire; specifically the letter:

a indicates that the fire has been considered in a single floor and only on beam elements;

b indicates that fire is limited to a single floor but affects the beams and the related column;

c indicates that the fire is assumed to have spread upwards and the beams and columns of two consecutive floors have been considered to be affected by the fire.

10.3. FLOOR MODEL

10.3.1. Scenario 1 – Fire on beams of only one floor (FM-1-5 & FM-1-35)

The results of the analysis on the first scenario for the 5th floor highlight the following sequence of failures in the area involved in the fire (Figure 10.6):

1. After 2 min of fire, an out of plane buckling mechanism triggers, involving three beams that converge in the middle external column (i.e. the two external transversal beams, beam 18 and beam 32, and the longitudinal beam between them, beam 25). Almost contemporarily, the most internal beam on the left (beam 34) buckles out of plane too. The early failure of those beams is only due to the eigenstresses induced by the hindered thermal expansion of the beams, consequent to the strong column - slender beam frame type: specifically, all four beams have an IPE270 profile, while the columns adjacent to them have HEM1000* profiles. As a consequence, the beam failures trigger when the temperatures are still very low (around 100°C) and the degradation of the mechanical properties, which typically plays a determinant role in fire-induced collapses, has not occurred yet.

2. Shortly after the first four beams, the two transversal beams in the middle (beam 33 and beam 19), buckle out of plane too. The slightly higher resistance of these beams in comparison to the previous one can be imputed to the bigger sections of these beams, which have an IPE300 profile.

3. At about 10 and 15 minutes of fire respectively, also the last two beams directly involved in the fire (beam 34 and beam 26) buckle out of plane. The higher resistance of those beams is due to the different profile of the sections, which is a HEA240.

4. At this point the temperatures are quite high (ca. 600°C) and the internal beams, which carry higher load than the external ones, experience a vertical runaway and exceed the maximum acceptable displacement considered as nominal collapse criterion (Eq.1b). The material degradation is responsible for the runaway and determines the overcoming of the collapse condition.

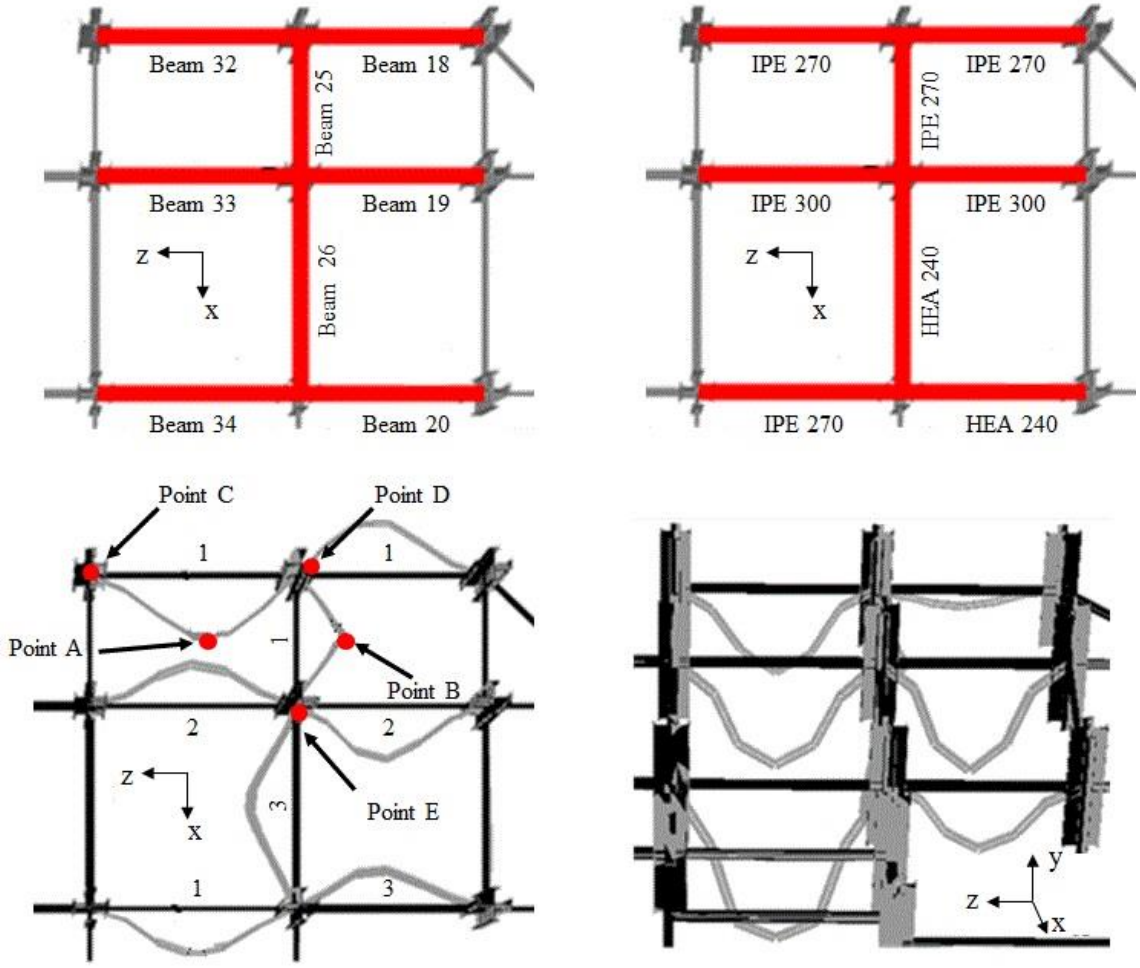

Figure 10.6 - Fire scenario 1 for the 5th floor: section of heated elements (top left), progression of collapse (top right), deformed configuration after 14 min (bottom left) and after 20 min (bottom right).

The results of the investigations carried out at the 5th floor are represented in Fig. 6 in term of deformed configurations and in Figure 10.7 in term of displacements vs. temperature and of axial force vs. temperature curves. In the first row of Figure 10.6 the name (left) and the sections (right) of heated elements are reported. The second row of Figure 10.6 shows on the left the deformed configurations at 14 min. Here the progression of beam failures is indicated by numbers from 1 to 4, which correspond to the steps illustrated above; on the right instead the deformed configuration at 20 min of fire is reported, where the in-plane buckling of beams is visible and significant vertical displacements of beams can be observed.

It seems relevant to highlight the fact that the same design characteristic that is responsible for the early failure of the beams, i.e. the strong column – slender beam system, ensures on the other side a compartmentalization of the collapsing sections of the structure and avoid the propagation of the collapse to the vertical elements, which are only slightly overloaded by the stress redistribution consequent to the beam failures and therefore could hardly be involved in the collapse mechanism.

The results of the investigation carried out at the 35th floor are reported in Figure 10.7in term of displacement vs. temperature (first row) and axial force vs. temperature (second row). From the observation of the displacements, it can be seen that the collapse mechanism at the 35th floor is similar to that one at the 5th floor, but it is slightly delayed.

This delay can be entirely ascribed to the different column profiles present at the 35th floor (HEM400), which offer less resistance to the thermal expansion beams: this is confirmed by the fact that the columns at the 35th floor are slightly displaced by the thrust of the beam, contrarily to what happen to the column at the 5th floor (third row of Figure 10.7).

10.3.2. Scenario 2 - Fire in one storey on beams (FM-2-5 & FM-2-35)

The outcomes for fire scenario 2 are shown with respect to a fire at the 5th floor and a fire at the 35th floor in term of deformed configurations (Figure 10.8) and of trend of displacement and axial force of members (Figure 10.9). At both the 5th and 35th floor a buckling mechanism occurs, which involves three of the heated beams and specifically beam 65 (whose mid-span is referred to as point F in Figure 10.8), beam 68 and beam 58. As occurred for fire scenario 1, the mechanism at the 35th floor is delayed with respect to the mechanism at the 5th floor. However in fire scenario 2, the buckling mechanism is different for the two floors: the beams at the 5th floor buckle out of the plane, while the same beams at the 35th floor have time for developing a significant vertical displacement before failing and the buckle occurs therefore along the vertical direction. Furthermore, a propagation of the failures of two beams not directly involved in the fire and specifically of beam 57 and beam 59 (whose mid-span is reported as point G in Figure 10.8) can be evidenced at 35th floor. This mechanism is observable in the right bottom part of Figure 10.8.

The higher buckling resistance at the 35th floor is again a consequence of the lower horizontal restrain provided by the tapering of the column profiles along the building height. However in this scenario this characteristic of the system leads to the occurrence of a different and less local buckling mechanism, which involves all heated beams and 2 beams that fall outside the fire scenario as well.

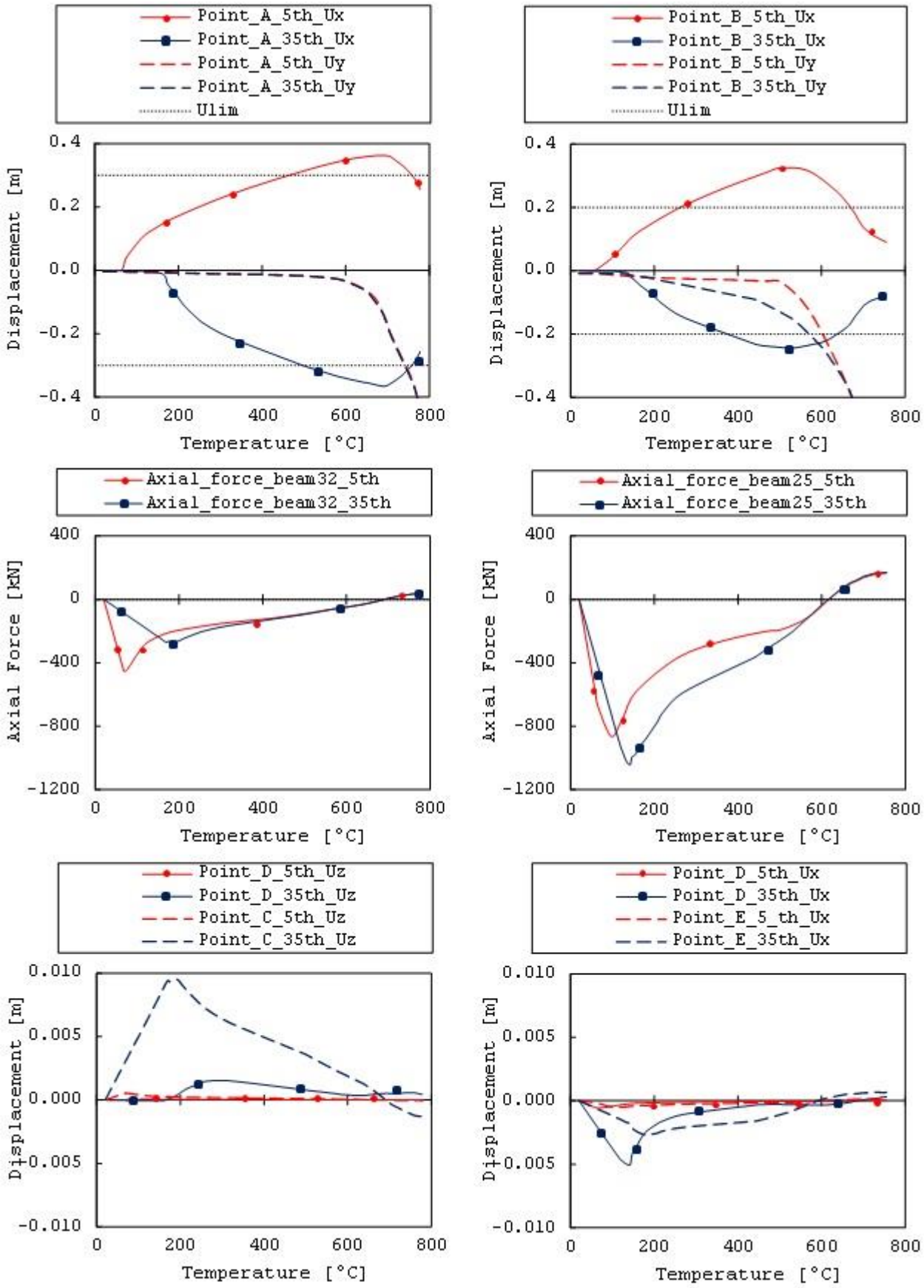

Figure 10.7 - Results of fire scenario 1, in term displacement of beams mid-span (first row), forces of the beam (second row) and displacement of the columns adjacent to the monitored beam (third row).

It has been previously said that a high vulnerability of the system could be ascribed to the very stiff columns (as at the 5th floor), which led to an early buckling mechanism due to the highly constrained thermal expansion of the beams; the presence of slender columns (as at the 35th floor) may lead instead to a delayed buckling and have therefore a positive effect on the overall resistance. Nevertheless, this example highlight that this delayed failure can also be detrimental, as the higher resistance of the beams to a local buckling determines the triggering of a larger buckling mechanism, which involves also elements not directly affected by the fire.

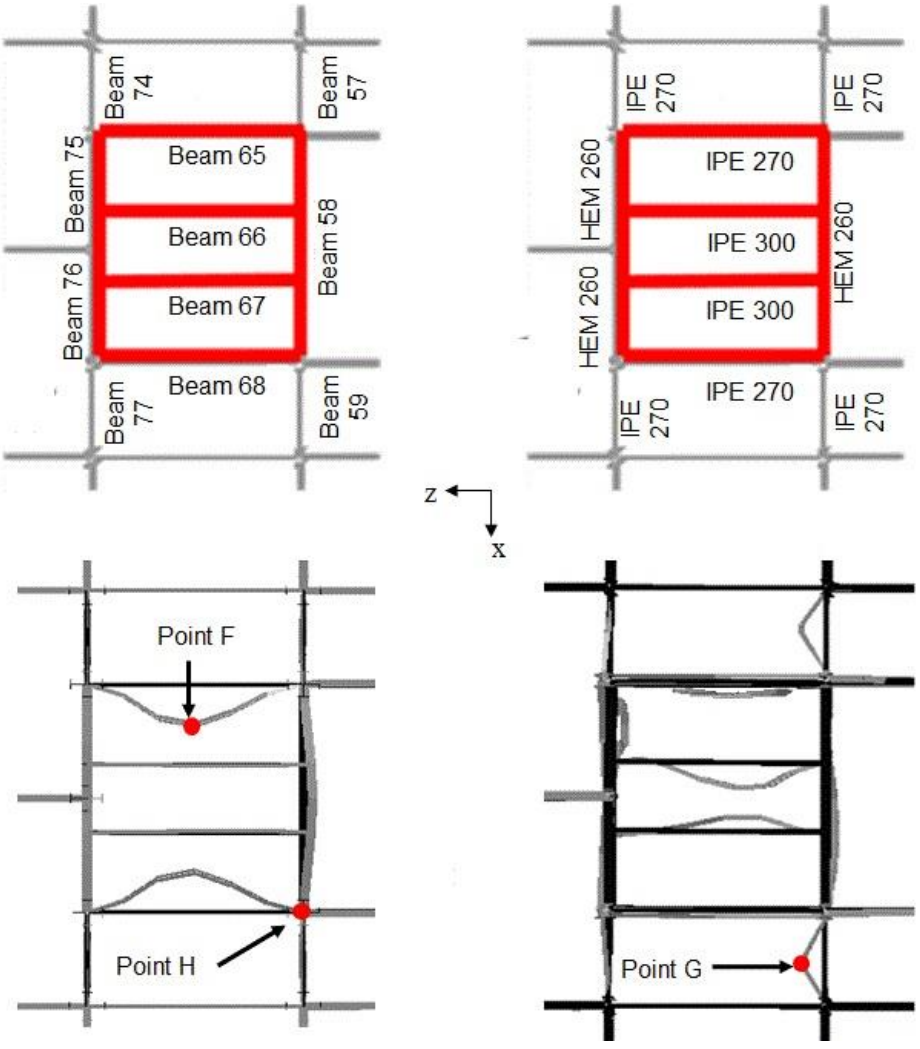

Figure 10.8 - Deformed shape of the 5th floor (left column) and of the 35th floor (right column) in case of fire scenario 2

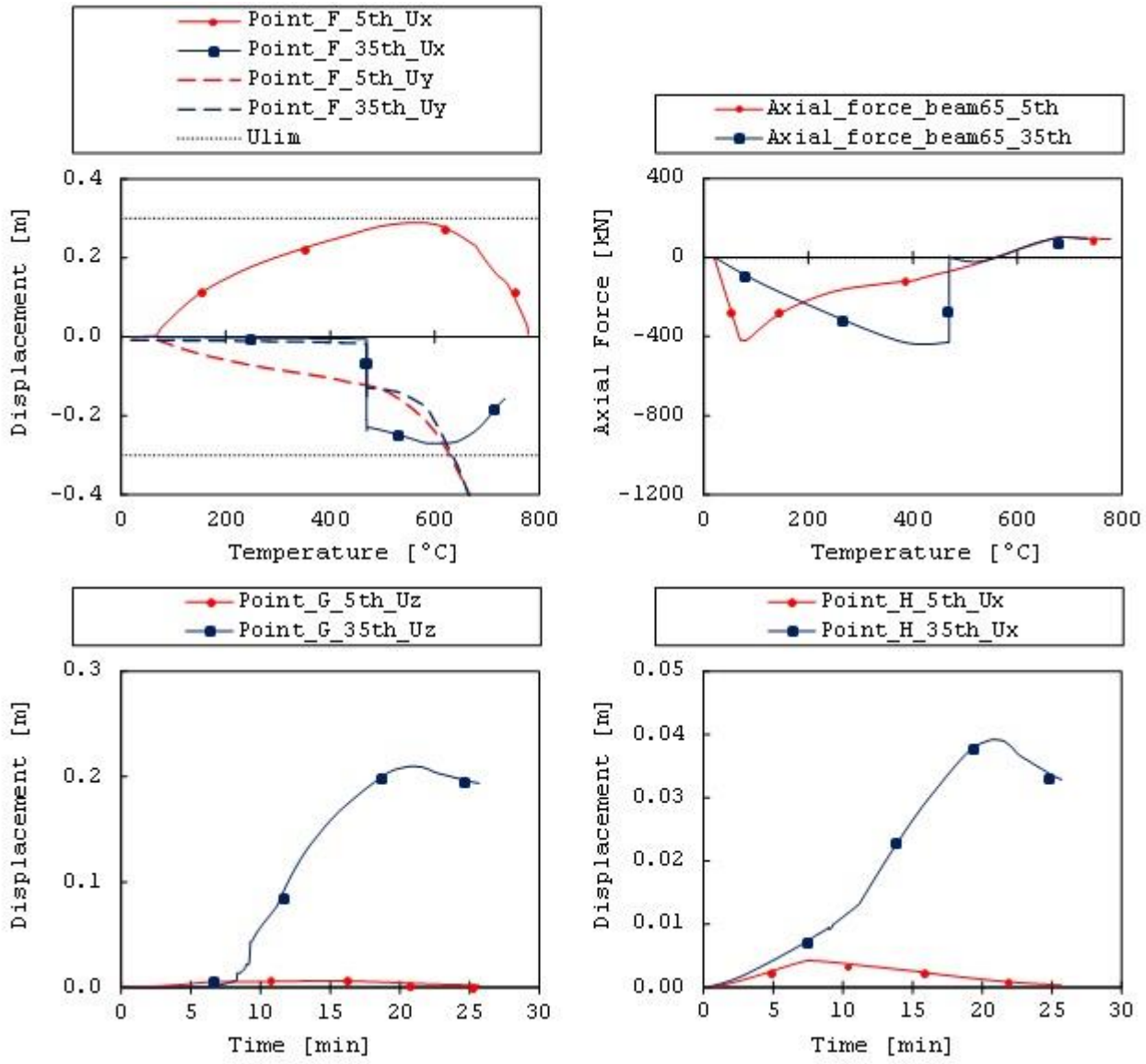

Figure 10.9 - Results of scenario 2: displacements of point F, representing the mid-span of beam 65 (top left) and in term of axial force of beam 65 (top right); outwards displacements of point G, representing the mid-span of the cold beam (bottom left) and of point H, which gives indication on the restrain provided to the beam by the adjacent column

10.4. SECTIONAL MODEL

10.4.1. Scenario 1 - One storey fire on beams (SM-1-5-a & SM-1-35-a)

In this investigation the sectional model of the building is considered and the fire is assumed to heat only the beams pertinent to the area considered for the fire scenario 1. The results of the sectional model are consistent with those obtained by the investigation of scenario 1 in the floor model (FM-

1-5) and are characterized by an early failure of the heated beams, which buckle out of plane just after few minutes of fire.

At the 5th floor, as evidenced also in the floor model, the failure of the heated beams occurs at relatively low temperatures and is almost exclusively due to hindered thermal expansion, since the material degradation has not become significant at those temperatures.

It seems relevant to highlight the fact that the very early beam failure prevents the redistribution of high stresses on the columns; therefore, the high vulnerability to fire of horizontal elements is accompanied by a robust behaviour of the vertical load carrying system. When the horizontal restrain provided by the beam is lost, the buckling length suddenly increases, possibly leading to the column failure (Usmani, et al., 2003). In this specific case however, a possible buckling of the vertical elements doesn't seem a concern, due to the low loading condition and the very high stiffness of the column at the 5th floor.

In Figure 10.10 the differences between the displacements at the 5th and 35th floor of the mid-span of a heated beam are reported and a delay in the out-of-plane buckling of the beam at the 35th floor with respect to the beam at the 5th floor is observable. This type of crisis remains however a local phenomenon, as it involves exclusively the heated elements and is limited to an area of about 100 m2, which represent around the 8% of the whole floor area. It may be interesting to compare this value with the limit of 15% (corresponding to 180 m^2 in this case) indicated by the old US guidelines (UFC, 2005) for defining a local collapse in case of accidental failure of a column.

10.4.2. Scenario 1 - One storey fire on beams and columns (SM-1-5-b & SM-1-35-b)

In this section the outcomes of the investigation performed on the sectional model are presented with respect to a fire affecting both horizontal and vertical elements pertinent to the area of scenario 1. The fire is considered to be localized within one storey, first at the 5th floor and then at the 35th floor. The consideration of the fire on the columns allows highlighting some differences in the evolution of collapse with respect to the previous case, where only beams were considered to be heated by the fire.

The results of the investigations are reported in Figure 10.11: the deformed configurations of the structure at 90 min of fire are represented for both the case of a fire at the 5th floor (left column) and at the 35th floor (right column), while in Figure 10.12 the displacements of some significant points are shown in the two cases.

At the 35th floor the column experiences a crisis when the critical temperature (around 800°C) is reached after 45 min of fire. In correspondence of these values, the displacement of mid-point of column (indicated with point L in Figure 10.11) increases greatly. The crisis occurs because the plastic limit is achieved, as observable in the top left graph of Figure 10.12.

The collapse occurs at very high temperatures, due to the combination of a low initial value and a low increment of axial forces.

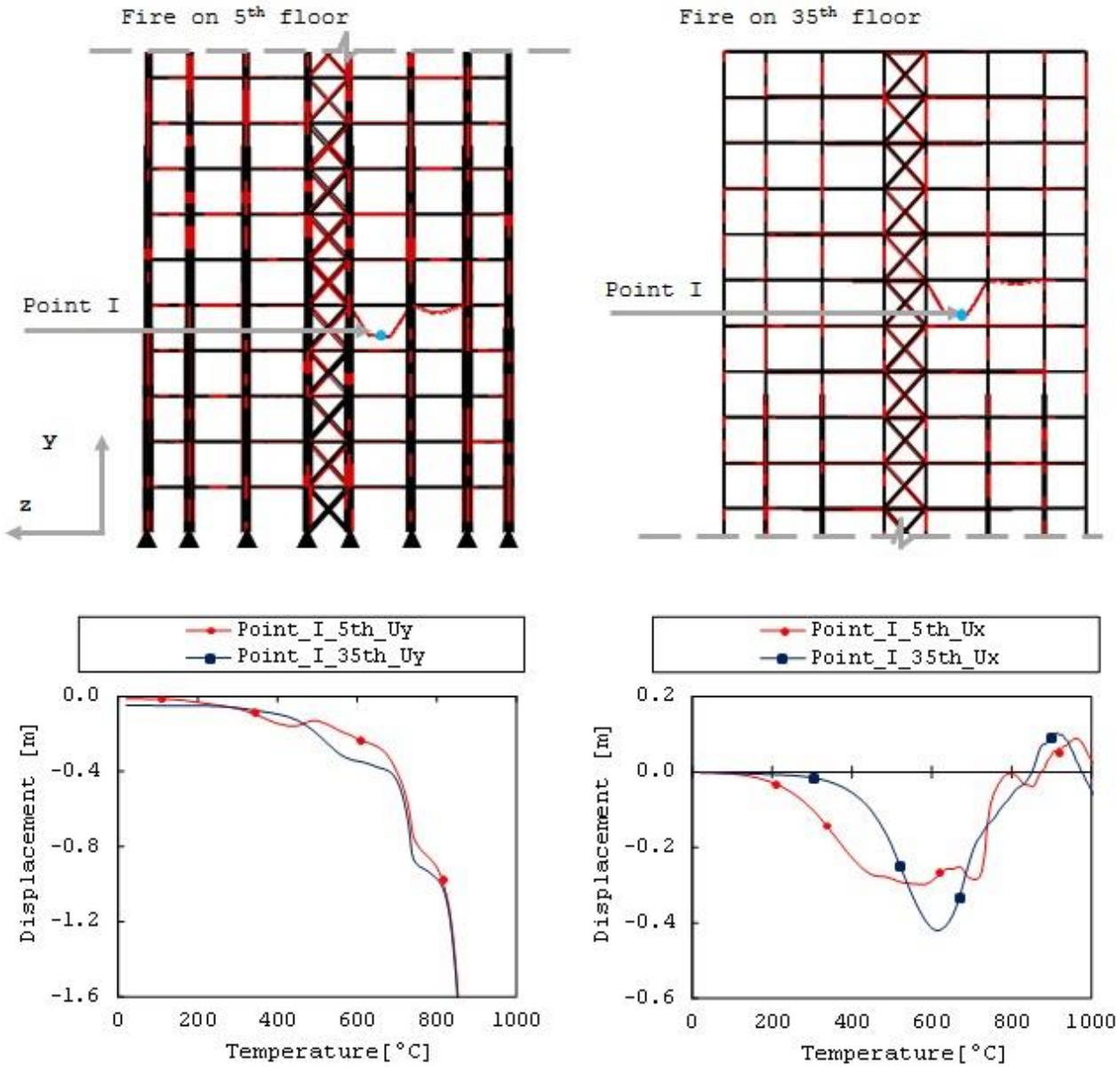

Figure 10.10 - Results of SM-1-5-a and SM-1-35-a: vertical (bottom left) and out of plane (bottom right) displacement of the mid-span of a heated beam (point I) at the 5th (top left) and 35th floor (top right).

With respect to the first aspect, the low load to resistance ratio of the column can be only partly ascribed to the fact that the column segment considered is just below the tapering of the profile. A more significant consideration concerns the low loading conditions that are assumed in case of fire. In this respect, it has to be highlighted that the building has been designed in compliance with the load combination (Eq. 10.2a) for the Ultimate Limit States (ULS), where wind, seism, snow and service loads have been considered as variable actions. The coefficients for permanent and live loads are compliant to those indicated in the Italian regulations: in particular, the most severe combination for the dimensioning of the columns is the one where wind is considered as leading variable action and in this case a safety factor $\gamma_{Q1} = 1.5$ is foreseen by the code (NTC 2008, 2008).

A different combination (Eq. 10.2b) has to be considered instead in case of fire, where loads are strongly reduced (Giuliani & Budny, 2012) and in particular almost permanent values of variable actions are assumed. This results in neglecting the presence of wind for fire design, since the coefficient ψ_{2i} associated to the wind action is 0 in the above mentioned code.

a) ULS: $\gamma_{G1} \cdot G_1 + \gamma_{G2} \cdot G_2 + \gamma_P \cdot P + \gamma_{Q1} \cdot Q_{k1} + \Sigma_{i=2,..n} (\gamma_{Qi} \cdot \psi_{0i} \cdot Q_{ki})$ (10.1)

b) ALS: $G_1 + G_2 + P + A_d + \Sigma_{i=1,..n} (\psi_{2i} \cdot Q_{ki})$

where symbols have the following meaning:

G_1 : permanent loads of all structural elements

G_2 : permanent load of all non-structural elements

P : prestressing loads

Q_{k1}: characteristic value of the leading variable action

Q_{ki}: characteristic value of the accompanying variable action

γ_{G1}: partial safety factor for structural permanent loads

γ_{G2}: partial safety factor for non-structural permanent loads

γ_{Qi}: partial safety factor for live loads

ψ_{0i}: combination factor for the rare value of actions

A_d : exceptional action

ψ_{2i}: combination factor for the almost permanent value of actions

As a result, the columns have a quite low load-resistance ratio, which is consistent with the high distance between the starting points of the curves representing the axial force and the yielding condition, which are shown in Figure 10.12.

With respect to the second aspect, a very low inclination of the curve representing the axial force is visible in Figure 10.12, which can be ascribed to the very low constraint provided by the slender

beam to the thermal expansion of the column. This is the main reason why the resistance of the column to fire is much greater that the resistance of the beam system.

The resistance of the column is of course a central aspect in the structural response of a high-rise building to fire, since a crisis of the columns could lead to a disproportionate collapse involving the upper floors. The displacements of the top of the building, specifically the horizontal displacement at the top of the last external column (point N) and the vertical displacement at the top of the last column directly above the heated one (point M) are reported at the bottom of Figure 10.12. These displacements can be takes as indices of the crisis of the whole structure, consequent to the buckling of the heated column, which is instead visible by observing the horizontal displacement of the mid-span of the column (point L) reported in Figure 10.12.

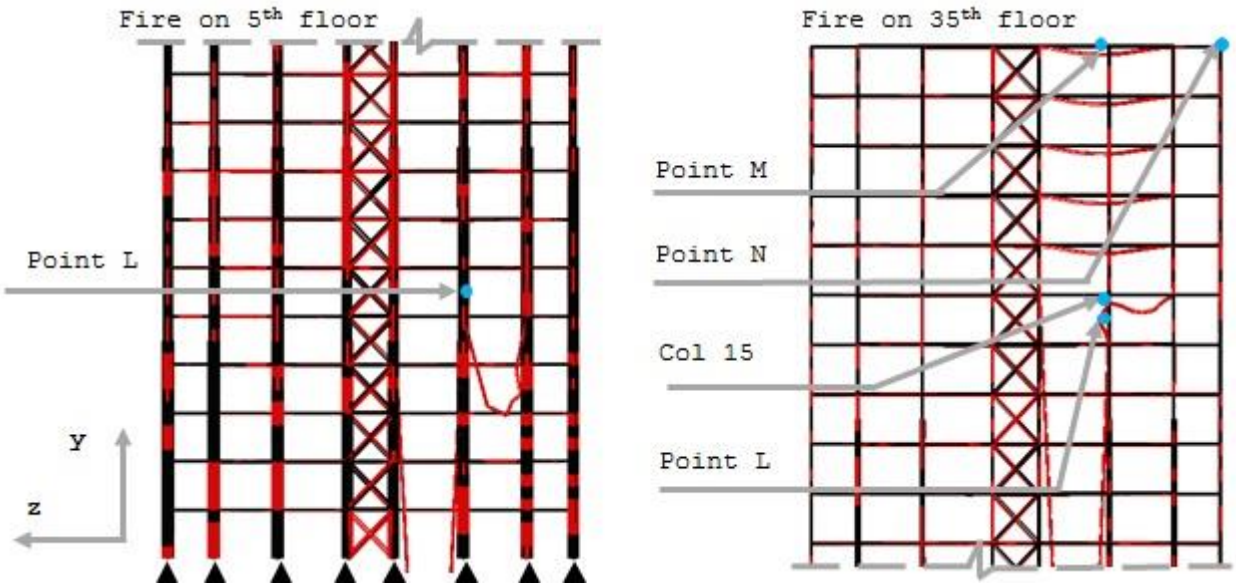

Figure 10.11 - Results of SM-1-5-b and SM-1-35-b: deformed configurations after 90 min of fire at the 5th (t left) and 35th floor (right)

The results discussed above refer to the case of a fire at the 35th floor. In case the fire is assumed at the 5th floor, the considerations concerning the low increment of the axial force in the column are still valid. However a crisis of the column at the 5th floor cannot be evidenced, since the bigger profiles of the columns ensure a greater buckling resistance with respect to the 35th floor. Therefore, while a fire at 35th floor causes the runaway of the head of the external column (point N - 35th) after about 90 minutes, this is not the case if the fire triggers at the 5th floor (point N - 5th).

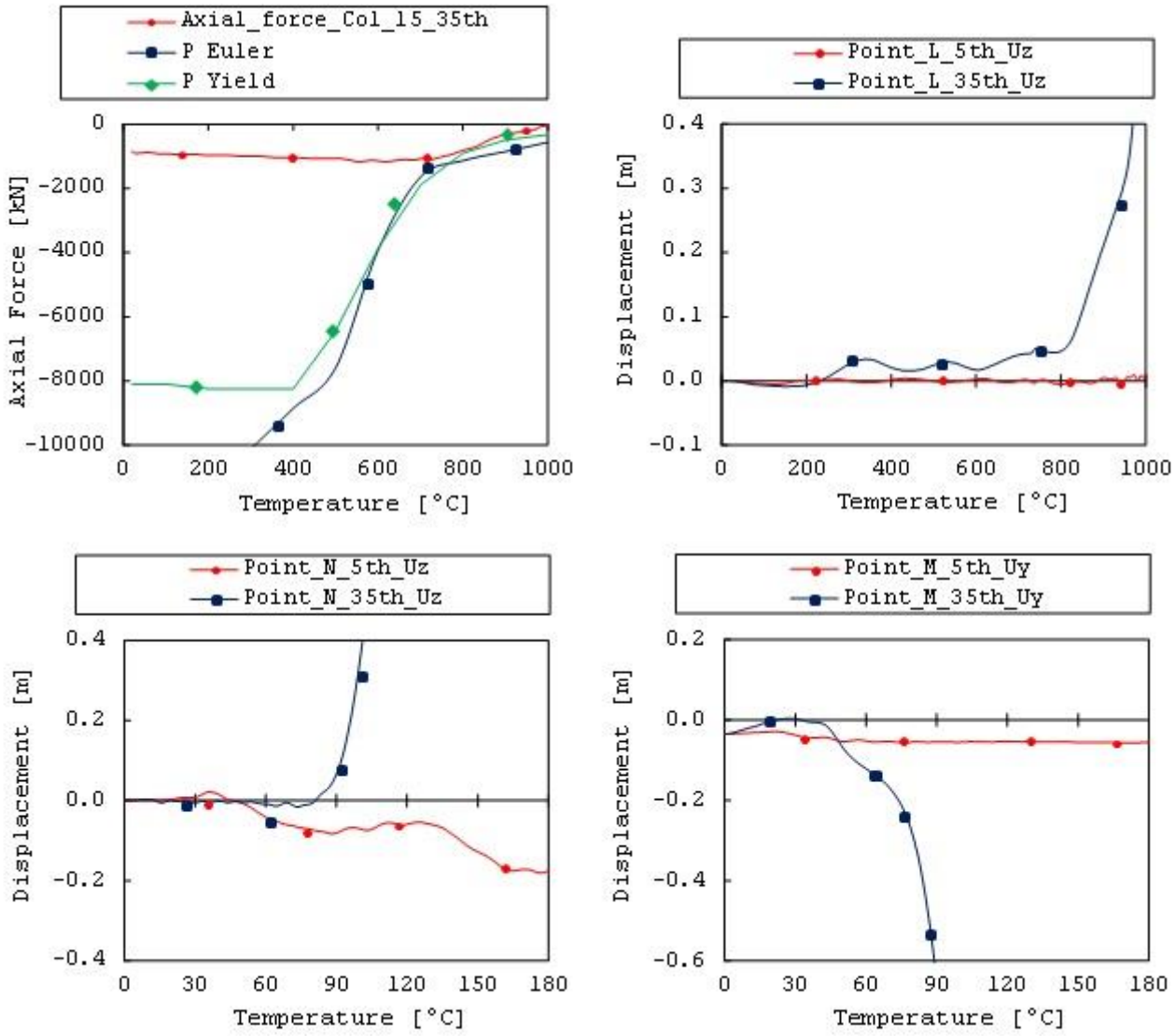

Figure 10.12 - Results of SM-1-5-b and SM-1-35-b: evolution of the axial force in the heated column (column 15) and yield crisis (top left); displacements of the mid-span of the heated column (point L) at the 5th and 35th floor (top right); horizontal displacement (bottom left) of the top of the external column (point N) and vertical displacement (bottom right) of the top node of the heated column (point M)

10.4.3. Scenario 1, Two storeys fire on beams and columns (SM-1-5-c & SM-1-35-c)

As mentioned above, a particular dangerous situation for high-rise building is represented by the fire spread on a number of adjacent storeys, as a consequence of external fire propagation throughout windows or ducts or of the loss of vertical compartmentalization in the building.

This situation has been contemplated by assuming that the fire heats both horizontal and vertical elements pertinent to the area of fire scenario 1on two adjacent floors and at two different heights in

the buildings, namely the 5th and 6th floor, as well as the 35th and 36th floor. Both in case a lower or higher height is assumed for the triggering of the fire, the first failures are represented by the crisis of the beams, which fail out of buckling in both cases. As a consequence, the heated column adjacent to the failed beams loose horizontal restrains in two points, with a considerable increment of the column buckling length.

In case of a fire at the 35th and 36th floor, a change in the failure mode of the column occurs and the column becomes slender as a consequence of the increased buckling length: the column is designed to have a plastic failure and, when the designed buckling length is preserved, the yielding resistance stays always under the Euler buckling load, as visible in the top left graph of in , which refers to the same column profile; when two horizontal restrained are lost however, the limit of the Euler buckling drops under the yielding limit, as observable in the graph on the left of Figure 10.13.

For what above said, the axial force in the column does not increase significantly; therefore this abrupt drop in the resistance doesn't determine an immediate buckling failure of the column, which resists up to about 650°C before failing and triggering the collapse of the upper part of the building. As expected, the behaviour of the structure in case of a fire in two adjacent storeys is worse either in term of critical temperature and in term of resistance time than in case the fire is limited to one floor only (SM-1-35-b).

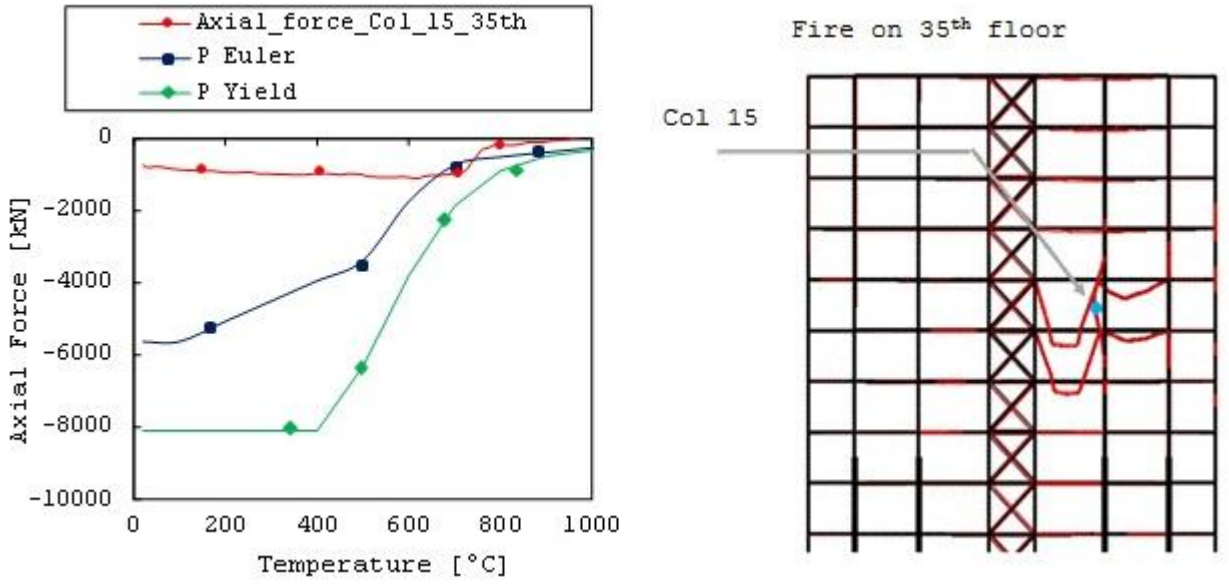

Figure 10.13 - Results of SM-1-35-c: deformed configurations after 50 min of fire at the 35th floor (right); evolution of the axial force in the heated column (column 15) and buckling crisis (left);

10.5. PROGRESSIVE COLLAPSE SUSCEPTIBILITY

According to Starrosek (Starrosek, 2009), a *progressive collapse* refers to a phenomenon where the collapse commences with the failure of one or a few structural components and then progresses over successive other components. While *robustness* is defined as insensitivity to local failure, as has been said previously (par. 2.3), *collapse resistance* can be defined as insensitivity to accidental circumstances, that is, to unforeseeable and low-probability – high-consequence (LPHC) events.

In this sense, the investigation about the extension and length of a fire can be of interest: in this way it is possible to highlight possible deficiencies and weaknesses of the structural system in order to improve and optimize it. In order to evaluate the progressive collapse susceptibility of the structure four fires with increasing extension were taken into account.

The top part of Figure 10.14 shows in red heated elements in fire scenarios: in all cases the thermal action involves the beams on the right side of the 5^{th} floor; in the first case (Case A), the fire is considered to directly affect only column no. 9 at the 5^{th} floor; in the second one (Case B), the fire is on columns no. 15 and 9; in the third one (Case C), fire is on columns no. 15, 9 and 24; in the last case (Case D) fire on columns 15, 9, 24 and 1. In the bottom part of Figure 10.14 the deformed shape of the frame is shown for the four cases.

Heated beams have been removed from the deformed shape of the frames, because they reached enormous displacement that led to their failure.

The colours in the figure show which elements are in the elastic range (blue) and which in plastic field (red).

In case A, after the beam failures, column no. 15 (green curve of Figure 10.15) reaches the plastic limit for 655°C after 27 minutes. The crisis of the column is absorbed by the structure through several load paths. The redistribution of the stresses caused to the plasticity of a beam in the outrigger. Despite the exposure to 180 min of fire no other damage occurred in the frame.

In case B, where fire involves also column no. 9, column no. 15 (red curve of Figure 10.15) is the first element that fails. The plastic limit is reached at a critical temperature of 675°C after 29 minutes of fire. About 1 minute after column 9 also goes into plastic range at a critical temperature of 695°C. The exposure to fire in this case leads to a greater spread of plasticity than in case A in the beams around the outrigger system.

In case C, although an additional central column is affected by fire, the behaviour of the frame is similar to the previous cases, except for a slight increase in the number of elements in the plastic range. The same three columns mentioned for case B fail after 29/30 minutes.

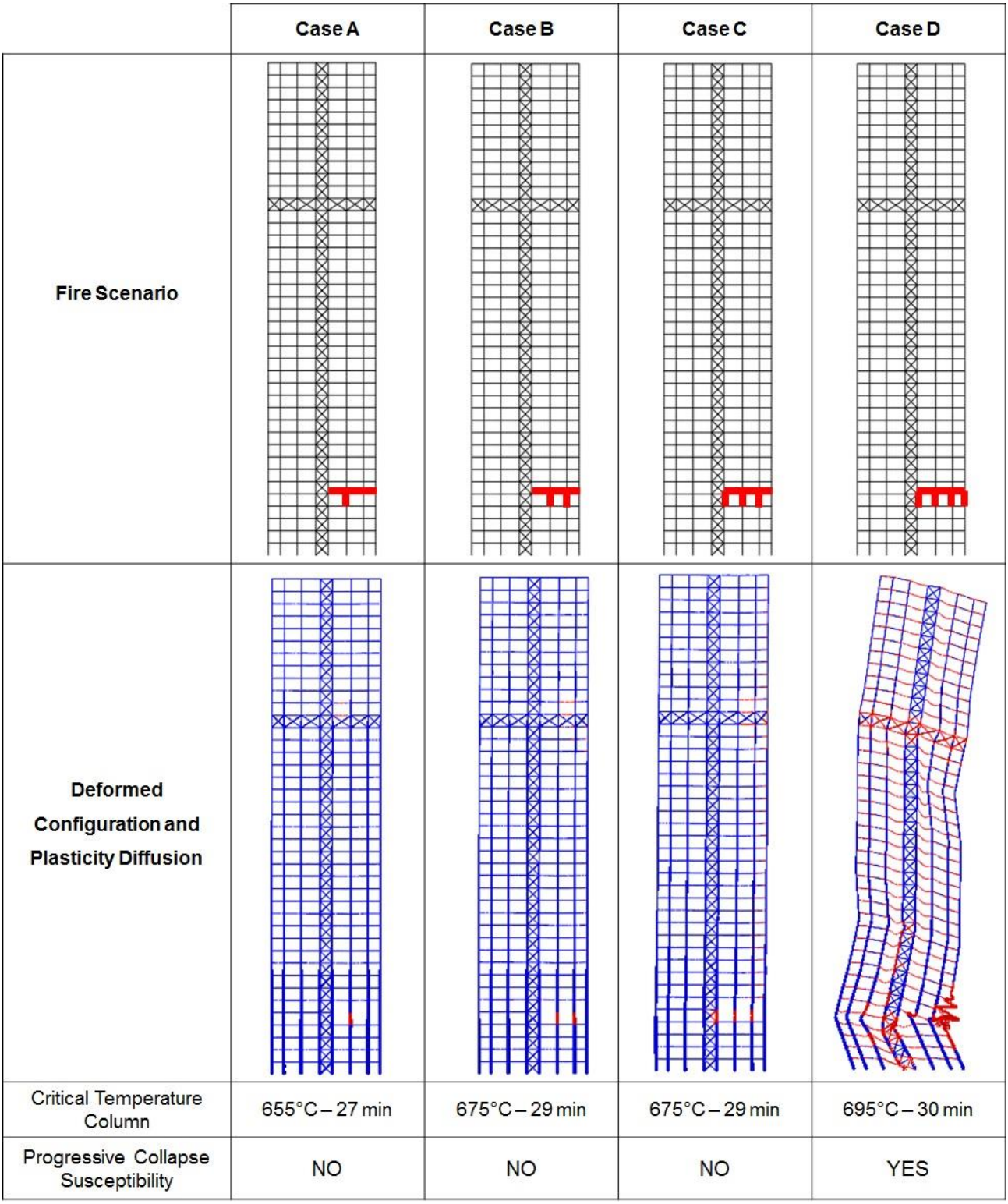

Figure 10.14 – Fire Scenarios and deformed shape of the frame.

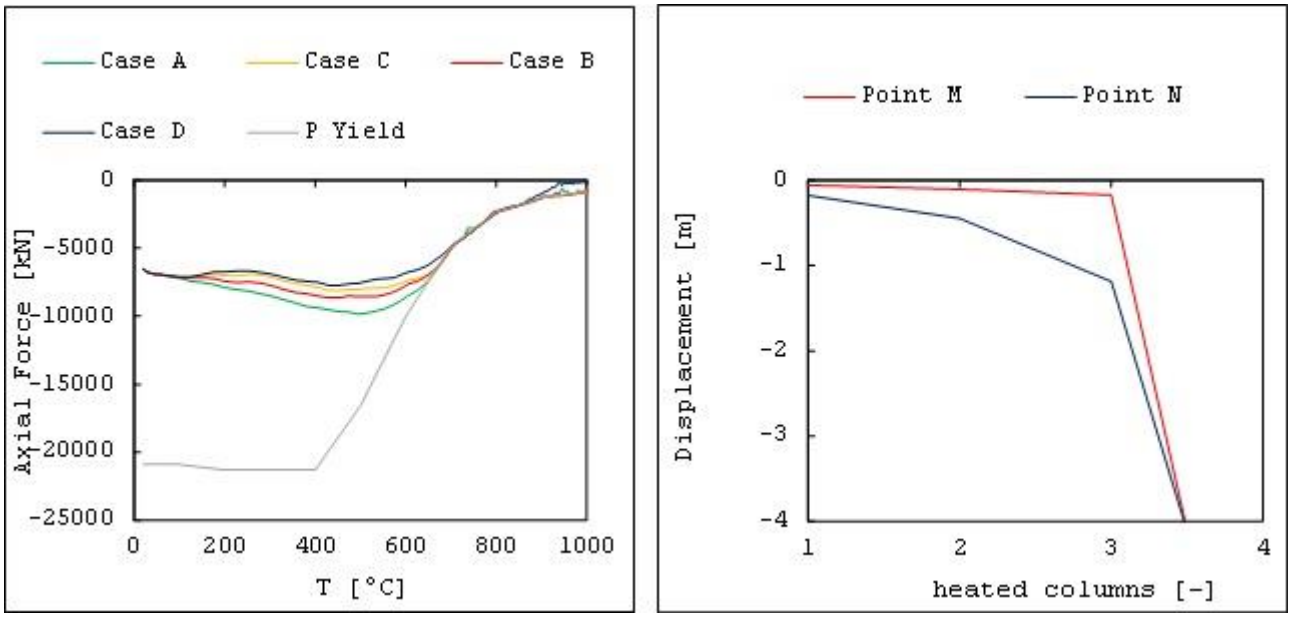

Figure 10.15 – Local and Global Collapse: on the left axial force of column 15; on the right vertical displacement of Point M and lateral displacement of Point N.

In case D, the crisis of the interior columns no. 15 and 24 is almost simultaneous and occurs after about 30 min at a critical temperature of ca. 700°C; the external columns no. 1 and 9 become plastic after about 35 minutes at a temperature of 740 ° C.

The comparison of the response to fire of the outrigger system in each case is shown in Figure 10.16. In case A an alternative load path without negative consequences is developed; in case B minimal damage spread diffusion occurs; the increasing spread of plastic areas in the case C does not cause the loss of effectiveness of the system; in the last case D, the extension of the plastic area is so wide that the outrigger no longer contributes to the strength of the structure and it is no longer effective in redistributing the stresses. In this case a progression of the failures occurs, which ultimately cause the collapse of the frame.

The crisis of column 15 represents in each case a critical local event. It is caused by the achievement of the yielding limit, which in each case occurs at slightly different temperature. This is a consequence of the different stress level reached by the heated elements, which have the same dimensions in the different cases, but different boundary conditions. The restrain provided by the beam to the thermal expansion of the column decreases as the number of columns involved in the fire increases. Therefore case D is the case where the thermal expansion of the columns is least hindered and the increment of axial stress in the columns is less significant than in the other cases.

Consequently, in these cases the axial force increases less significantly. Therefore, as visible in Figure 10.15, the collapse occurs later.

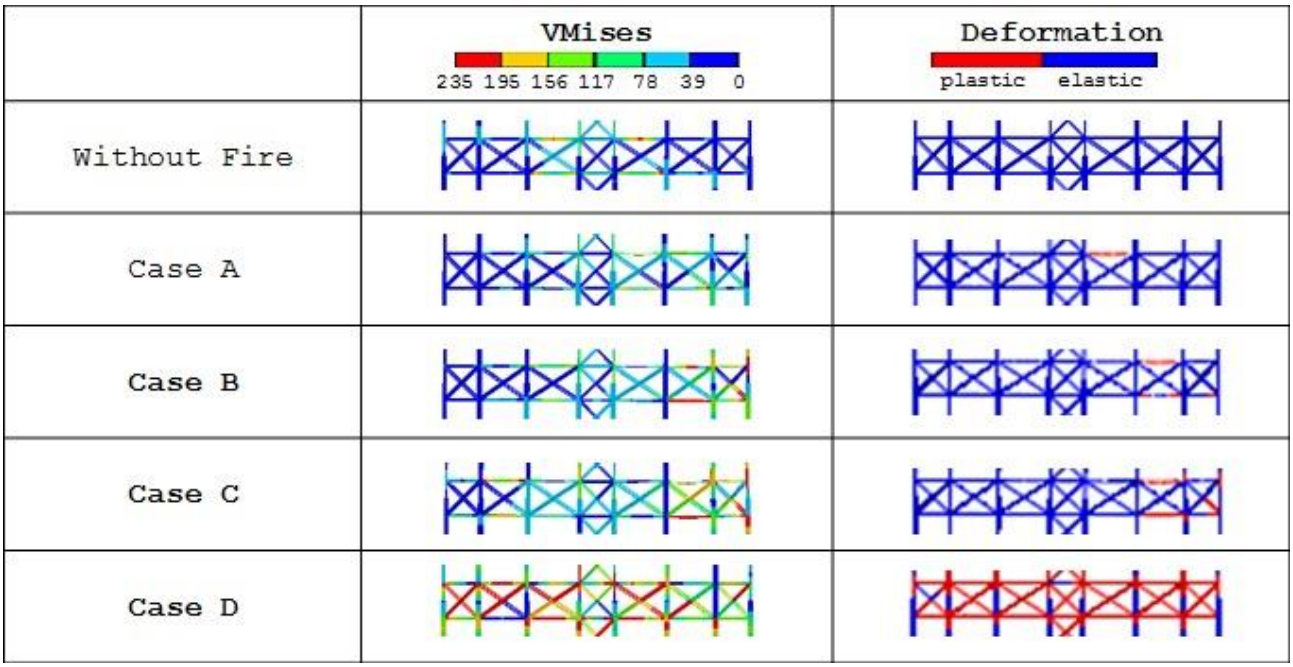

Figure 10.16 – Focus on the outrigger behaviour

10.6. EFFECTIVENESS OF BRACING SYSTEMS

In high-rise buildings, bracing elements play an important role in counteracting the horizontal forces. They allow limiting the lateral displacements by ensuring greater stiffness to the structure. Sometimes, the presence of outrigger systems can delay failures and possibly also collapses induced by fire, as happened in WTC according to the report of FEMA [REF].

In order to understand effective role of outrigger and in general of bracing systems, different structural configurations have been taken into consideration.

The scenario of fire was kept the same in each simulation: the fire involves the column no. 15 and the beams no. 19 and 33 of the 35th and 36th floors, as in the scenario called SM-1-35-c described in paragraph 10.4.

In a first phase of the study, the results obtained in Section 10.4 for the original configuration have been compared with those found in the investigation of the following configurations: (Figure 10.17 top):

- frame without outrigger (Configuration A);

- frame with outrigger at 36th floor (Configuration B);
- frame with outrigger at 40th floor (Configuration C).

In the central part of the figure the deformed shape of each configuration is reported: the outrigger at 29th floor (first configuration from left in Figure 10.17) does not influence the development of collapse as seen from the analysis in which the outrigger is not present (second configuration in Figure 10.17). The two structural configurations lead to the same results. The part of the structure situated above the plane of trigger collapses totally, but diffusion of the phenomenon in the floors below doesn't occur. It should be noted that in these analyses the impact of the failed floors on the lower floors were not taken into account: this prevents making remarks about the effectiveness of the outrigger as a stopper to collapse.

Place an outrigger on one of the floors where the fire spreads (third configuration in Figure 10.17) avoids the progressive collapse. In the studied case, there is the instability of the heated beams. The braces, which are connected to the columns with moment transmission, reach the crisis for plasticity. The instability of the column 15 of the floor 35 occurs for a temperature of 687°C after 29 minutes (Figure 10.18). In this case the presence of the brace allows assuming as a buckling length of that of a single floor. The column to the upper floor supports lower levels of stress during exposure to fire because the braces help redistribute the loads on the rest of the structure.

The outrigger on top of the frame (last configuration from left in Figure 10.17) has a better behaviour at the global level as seen by the lateral movement of the point N (Figure 10.19).

At the local level, the presence of the outrigger causes a greater restrain of the thermal expansion of the columns beneath. As a consequence, the axial force on column no. 15 increases rapidly and the column fails after 15 min of fire at a critical temperature of about 400°C (Figure 10.18).

Despite the local crisis of the column in this configuration occurs earlier than in all other cases presented above, the global behaviour of the building is the best one, as the collapse remains localized to the elements directly involved in the fire and has the lowest horizontal displacement. This is a direct consequence of the redistribution of stresses allowed by the outrigger and of its position: when placed above the fire, the outrigger acts like a big transfer girder, which the elements that have been left unsupported by the failed ones hang to. This is the case of the two floors above the fire, i.e. the 37th and 38th. After the failure of column no.15, the weight of the part of the floor left unsupported is sustained by the outrigger, which redistributed it on all other vertical elements of the building.

	Original Solution	Configuration A	Configuration B	Configuration C
Structural Configuration	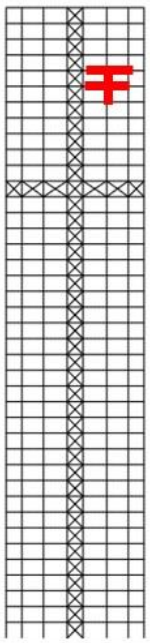	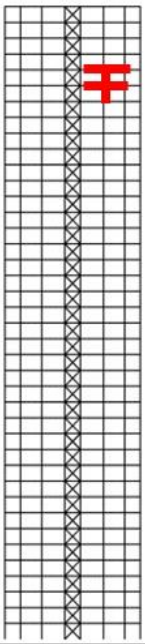	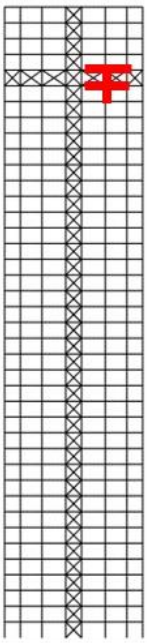	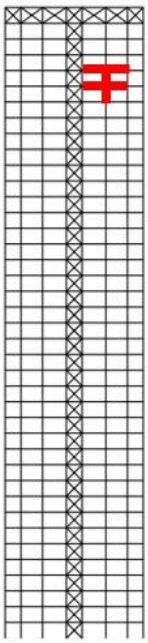
Deformed Configuration	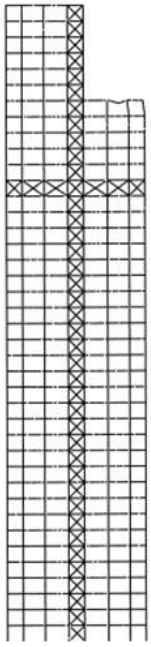	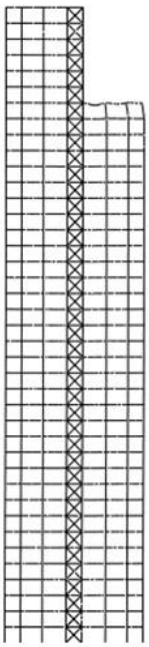	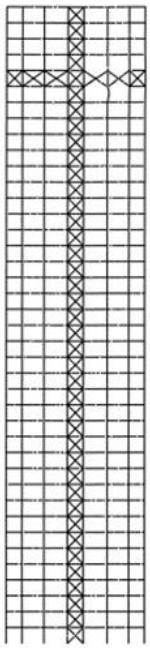	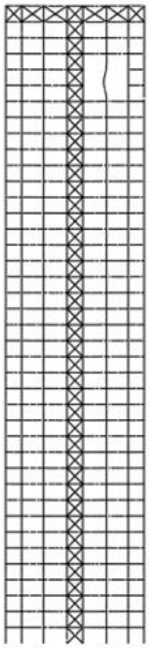
Critical Temperature Column	700°C – 30 min	700°C – 30 min	687°C – 29 min	400°C – 15 min
Vertical Displacements (Point M)	-16.275	-17.752	-0.037	-0.038
Lateral Displacements (Point N)	-10.699	-11.410	0.191	-0.048
Progressive Collapse Susceptibility	YES	YES	NO	NO

Figure 10.17 – Effectiveness of outrigger systems

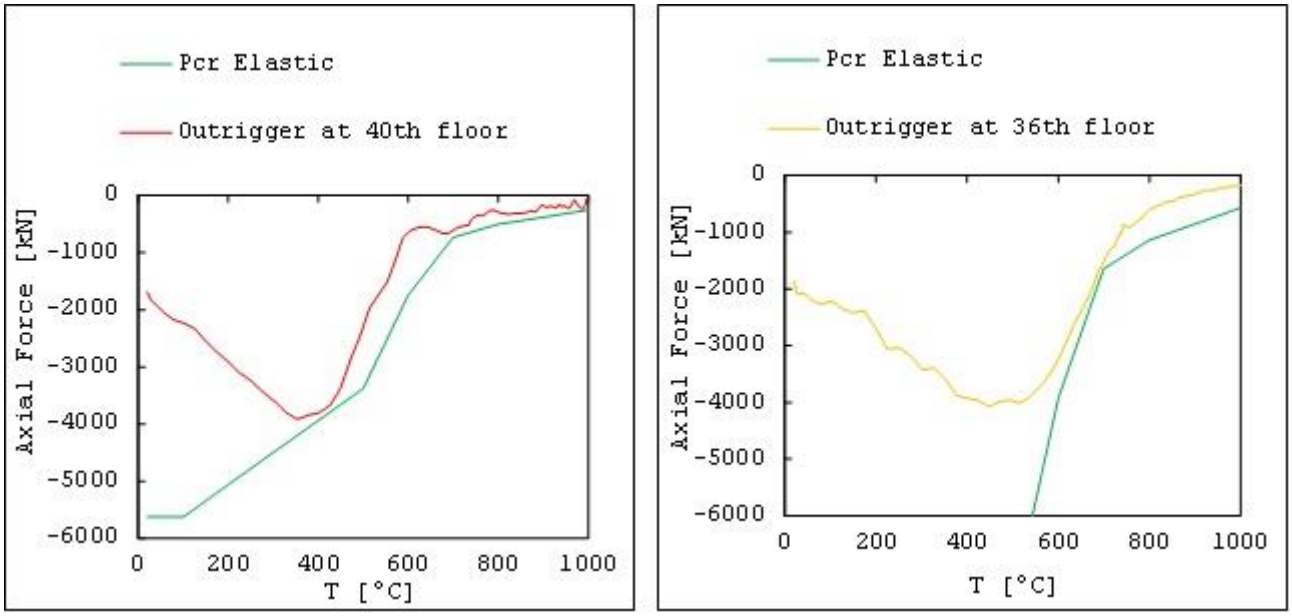

Figure 10.18 – Axial force of column 15 in function of outrigger systems

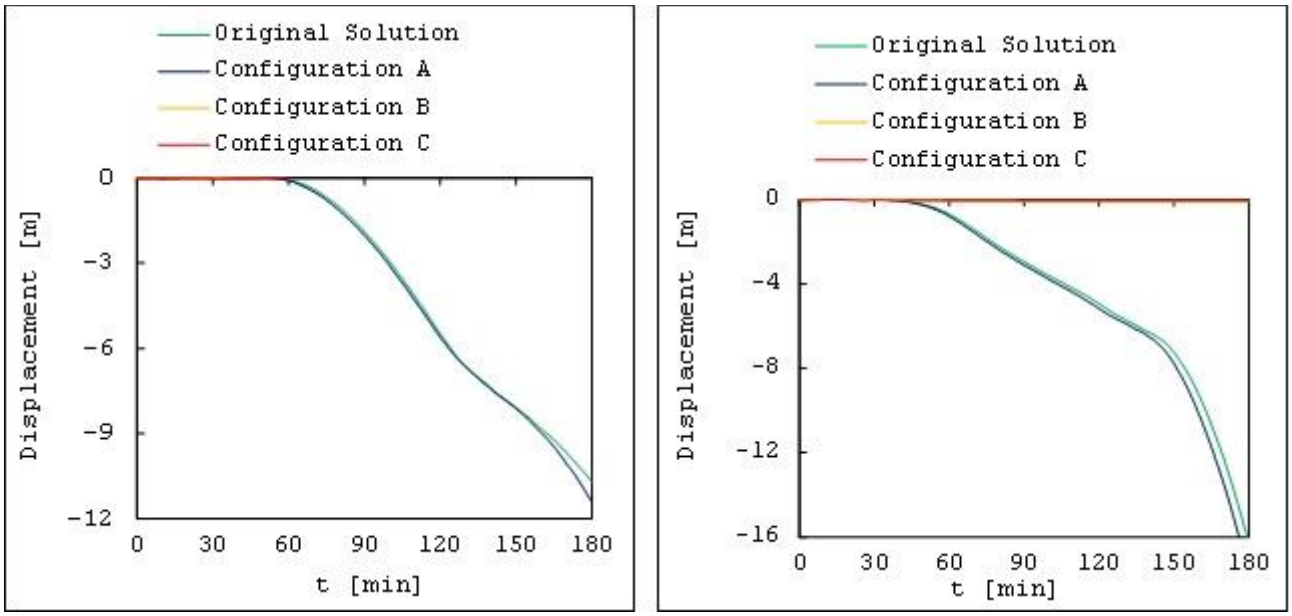

Figure 10.19 – Lateral displacement of Point N (left) and vertical displacement of Point M (right).

In a second part of the study, the effectiveness of the walls of bracing has been investigated. To this purpose, the results of the original structural configuration, presented in paragraph 10.4, were compared with the results of the following models (Figure 10.20):

- frame without vertical braced systems (Configuration D);
- frame with three vertical braced systems (Configuration E);
- frame with two vertical braced systems (Configuration F).

	Original Solution	Configuration D	Configuration E	Configuration F
Structural Configuration	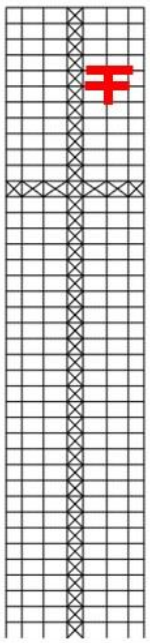	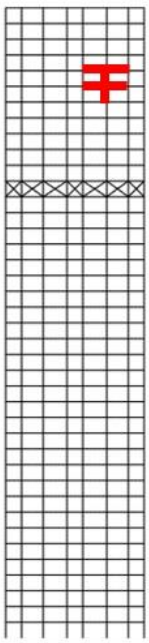	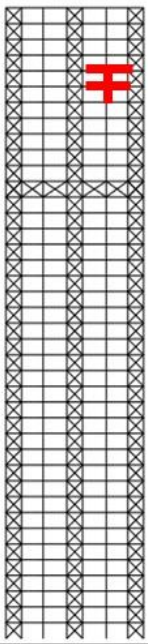	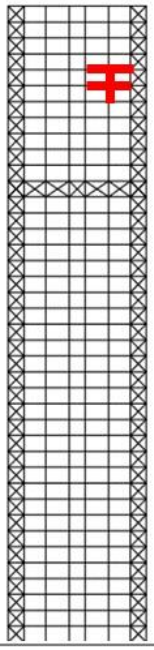
Deformed Configuration	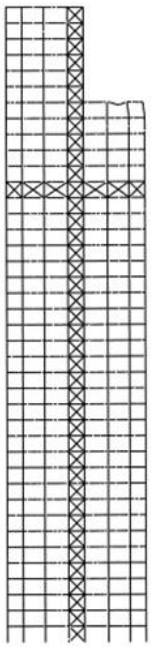	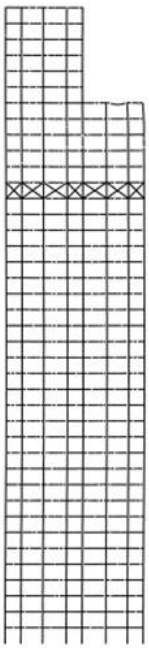	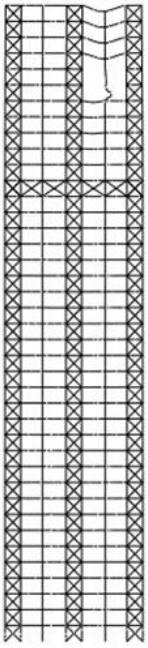	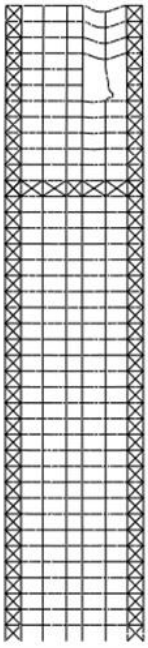
Column Collapse	700°C – 30 min	700°C – 30 min	700°C – 30 min	700°C – 30 min
Vertical Displacements (Point M)	-16.275	-15.826	-1.492	-1.590
Lateral Displacements (Point N)	-10.699	-11.175	-0.329	-0.3258
Progressive Collapse Susceptibility	YES	YES	NO	NO

Figure 10.20 - Effectiveness of braced walls

The frame without vertical braced systems (second configuration from left in Figure 10.20) shows the same behaviour of the original configuration (first configuration from left in Figure 10.20) and experiences the same type of collapse. The central braced system does not affect the mechanism or the extension of the collapse, which is limited to the lateral area of the building above the fire.

The insertion of the external vertical braced systems (third configuration from left in Figure 10.20) allows the establishment of another resistant mechanism that ensures better performance to the structure. In this case the collapse of the column remains a local phenomenon without implications for the entire structural system. A catenary effect can develop: the exterior columns can support the beams which are adjacent to the failed column. The same mechanism can occurs also in the frame with two vertical braced systems (fourth configuration from left in Figure 10.20).

10.7. CONCLUSIONS

In this chapter the behaviour of a high rise building in fire is investigated, with the aim of highlighting possible fire-induced failure mechanisms in high-rise buildings and of comparing the response of the building to fires at different heights.

The assumptions taken and the problems faced in the modelling have been discussed and some significant aspects concerning the definition of collapse condition and the interpretation of the outcomes have been highlighted. With specific reference to the case study considered, some outcomes are worth of being summarised in the following:

1. The structure is characterized by a stiff column -slender beams framed system. This characteristic is responsible of a high vulnerability to fire of the floor system, where early buckling failures of beams are triggered as a consequence of the fact that the beam thermal expansion is almost completely hindered by the stiff columns.
2. To the high vulnerability of the floor system counterpoises a relative high robustness of the building as a whole, as a consequence of the high critical temperature of the columns, which ensure a long resistance of the vertical bearing system, also when the beams buckle and do not provide horizontal restrains to the columns any longer.
3. The system seems more sensible to a fire in the upper part of the building, as shown by the comparison of the investigations carried on at the 5^{th} and 35^{th} floor: when a fire triggers at lower floor levels, where the difference in the stiffness of beams and columns is more pronounced, a vertical or horizontal propagation of the collapse seems unlikely, due to the very

modest redistribution of stresses on the column; however, in case of a fire at higher floors, both horizontal vertical propagation of the collapse seem possible.

4. The structure offers better performance when a system of outrigger at the top or external vertical bracing systems are provided.

From the results presented above, more general considerations can be derived. In particular, the failure mechanism of a steel framed beam-column system seems to be driven by:

1. the loading conditions of the structure;
2. the raise of eigenstresses as a consequence of restrained thermal expansion;
3. the possible loss of lateral restraints, which can induce a buckling failure in compressed elements;
4. the bracing system plays an important role in the development of progressive collapse.

It has to be noted that the consideration of the first two aspects is influenced by the current European regulations, which allow a significant reduction of the design loads in case of fire (EN 1991-1-2, 2004) and permit to neglect the effects of hindered thermal expansion in the verification of isolated elements, provided that the standard fire is used (EN 1993-1-2, 2005).

The third and the fourth aspects can only be evaluated by means of an advanced investigation, where the behaviour of the structure as a whole is considered and the response of the system is studied beyond the occurrence of the first failures directly induced by the fire. This aspect is particularly meaningful in the framework of ensuring a proportionate response also in case of unexpected circumstances, such as design errors, consequence of arsons, or other unexpected critical events not explicitly considered in the usual fire design. Even if it seems sensible to accept few local damages in case of rare abut severe events (LP-HC), the occurrence of major structural collapse should be avoided under all circumstances, as explicitly required nowadays by most codes and regulations (ASCE, 2002) (EN 1991-1-7, 2006). In case of fire in particular, it seems sensible to set the limit for a proportionate collapse on the basis of the area directly involved in the fire and avoid a propagation of the structural damages to elements outside the considered fire scenarios, i.e. elements where the temperatures do not play a significant role in the failure.

CONCLUSIONS

CONCLUSIONS

CONCLUSIONS

The thesis focuses on some aspects of fire safety. In particular attention is given on:

- Multi-physics nature of fire safety.

Fire safety requires a multi-disciplinary approach, as knowledge in fire dynamics, risk assessment, and numerical computational aspects are necessary. Both s CFD and FEM numerical analyses should be carried out in order to assess the fire resistance of a complex structure. Under fire conditions, a construction can be considered complex for reasons related to the fire action and to structural response.

- Large compartments in fire.

Current design fires for structural fire safety refer to post-flashover conditions, where a uniform distribution of the temperatures can be assumed within the compartment. These methods have been extensively tested and safely used in small compartment, which are typically densly furnished and present a reasonably uniform distribution of the combustibles along the floor area.

Large compartments, being typically less densely furnished, have a lower fuel load per square meter of floor area. Nevertheless, especially for building atria, where furniture can be concentrated only in a part of the compartment, and for industrial and storage halls as well, where goods can be piled up in small area of the floor, the assumption of a uniform distribution of the combustible materials may be unrealistic. In those cases, the use of a post-flashover design fire with a distributed fuel load density could lead to un-conservative results.

In this thesis a well-ventilated fire in a large compartment devoted to storage of wood pallets has been investigated. The outcomes of the investigations show that simplified analytical models may not represent with sufficient accuracy the element temperatures, either in case of a highly concentrated fuel load, as the temperatures of elements impinged from the flame can be strongly underestimated, and in case the combustible is spread along the compartment, the duration of the fire, which may travel along the compartment without developing a flashover, can be strongly underestimated.

- Progressive collapse susceptibility of a high-rise building.

Among buildings, high rise buildings can be particularly susceptible to fire, due to the possible vertical propagation of both the fire and the structural failures.

In this thesis, the behaviour of a steel high rise building in fire has been investigated, with the aim of highlighting possible failure mechanisms induced by a fire at different heights along the buildings and identify the role played by the different organization of the structural system in the development of local damages or global collapse. The outcomes of the study show that the stiff column-slender beams framed system is responsible of a high vulnerability to fire of the floors,, where the horizontal restrain provided by the stiff columns to the beams leads to an early buckling of the most slender beams. From the investigation results, some general considerations can be derived. In particular, the failure mechanism of a steel framed beam-column system seems to be driven by:

1. the initial load-to-resistance ration of the elements;
2. the raise of eigenstresses as a consequence of hindered thermal expansion;
3. the possible loss of lateral restraints, which can induce a buckling failure in the columns;
4. the bracing system plays an important role in the development of progressive collapse.

The latter aspect is particularly meaningful in the framework of ensuring a proportionate response also in case of unexpected circumstances, such as design errors or as a consequence of arson or other critical events not explicitly considered in the usual fire design. The occurrence of major structural collapse should be avoided under all circumstances, as explicitly required nowadays by most codes and regulations (ASCE, 2002) (EN 1991-1-7, 2006). In particular, with respect to fire-induced collapses, it seems important to avoid the propagation of failures to elements not directly affected by the fire, i.e. elements where the temperatures do not play a significant role in the failure.

INDICES AND LITERATURE

LIST OF FIGURES

LIST OF TABLES

REFERENCES

ABAQUS, 2010. *Abaqus Theory Manual.* [Online] Available at: www.simulia.com [Accessed October 2012].

Alvarez A & Meacham B. *Towards and Integrated Performance-Based Design Approach for Life Safety across Different Building Use Groups*, London, Interflam2010, 2010.

Anderberg Y. Modelling steel behaviour. *Fire Safety Journal,* 13(1), pp. 17-26, 1988.

Anderberg Y. *Assessment of fire-damaged concrete structures and the corresponding repair measures.* Cape Town, South Africa, 2nd International Conference on Concrete Repair, Rehabilitation and Retrofitting II (ICCRRR-2), 2009.

Annerel E & Taerwe L. *Techniques for the evaluation of concrete structures after fire.* Prague, Czech Republic, Proceedings of the International Conference on Applications of Structural Fire Engineering (ASFE 2011), 2011.

Arangio S. Reliability based approach for structural design and assessment. *International Journal Life-Cycle Performance Engineering*, 2012.

Arangio S & Bontempi F. Basis of the analysis and design for fire-induced collapses in structures. *International Journal Lifecycle Performance Engineering*, 2012.

Arangio S, Bontempi F & Ciampoli M. Structural integrity monitoring for dependability. *Journal of Structure and Infrastructure Engineering*, 2010.

ASCE. *Structural fire protection. Manual No 78*, Reston, 1992

ASCE. *Minimum design loads for buildings and other structure*, 2002

Ascenzi G. Villi G., Vulpiani G.: "Ingegneria della sicurezza antincendio - Guida all'utilizzo di FDS", Flaccovio Ed., 2010.

Avižienis I, Laprie JC & Randell B. *Dependability and its threats: a taxonomy.* 18th IFIP World Computer Congress, Building the Information Society, Kluwer Academic Publishers, 12, 91-120, 2004.

Babrauskas V. Heat release rate. In: 3rd, ed. *SFPE Handbook of fire protection engineering.* Quincy, MA, 2002.

Baum HR & McCaffrey B. *Fire-Induced Flow - Theory and Experiment.* Washington, 2nd International Symposium Fire Safety Science, 1989.

Best Practice Group. *CFD best practice (in Danish)*, Danish Building Regulations, 2009

Best Practice Gruppen. *CFD Best Practice*, Brandteknisk Selskab, 2009.

Beyler C, Beitel J, Iwankiw N & Lattimer B. *Fire Resistance Testing for Performance-Based Fire Design of Buildings,* Quincy MA, 2007.

Bong M W. *Ph.D. Thesis - Structural fire performance of steel portal frame buildings,* 2005.

Bontempi F, Crosti C, Giuliani L. & Petrini F, Principi fondamentali e applicazioni dell'approccio prestazionale (in Italian). *Antincendio,* Issue 5, pp. 106-119, 2009.

Bontempi F & Malerba P. The role of softening in the numerical analysis of R.C. structures. *Structural Engineering and Mechanics*, 5(6), pp. 785-801, 1997.

Bontempi F & Petrini F. *Fire-Induced Collapses in structures: Basis of the Analysis and Design.* Cape Town, SEMC, 2010.

Brando F, Cao L, Olmati P. & Gkoumas K. *Consequence-based robustness assessment of bridge structures.* Stresa, Lake Maggiore, Italy, Proceedings of the 6th International Conference on Bridge Maintenance, Safety Management, Resilience and Sustainability (IABMAS'12), 2012.

British Standards Institution. *BS 55-88-5 Fire Precautions in the design, construction and use of buildings - Part 5,* 2004.

British Standards Institution. *BS 476 (Parts 20-23) - Fire Tests on Building Materials and Structures,* 1987.

Buchanan AH. Fire engineering for a performance-based code. *Fire Safety Journal,* Volume 23, pp. 1-16, 1994.

Buchanan A H. *Structural Design for Fire Safety.* Chichester (England), Wiley, 2002.

Bystrom A, Cheng X, Wickström U, Veljkovic M. Measurement and calculation of adiabatic surface temperature in a full-scale compartment fire experiment. *Journal of Fire Science*, 2012.

Carstensen J, Jomaas G. & Pankaj P. Element size and other restrictions in finite element modelling of Reinforced Concrete at Elevate Temperatures. *Journal of Engineering Mechanics,* in press.

Catallo L. *Ph.D. - Progettazione prestazione nei sistemi complessi: fidatezza strutturale,* 2005.

Cervenka V, Pukl R & Eligehausen R. Computer Simulation of Anchoring Technique in Reinforced Concrete Beams. *Computer Aided Analysis and Design of Concrete Structures,* 1(1), pp. 1-21, 1990.

Concrete Society. *Assessment, design and repair of fire-damaged concrete structure, Technical Report no. 68,* Camberley, UK: Concrete Society, 2008.

Construction of European Community. *Construction Product Directive,* Brussels, 1988.

Construction of European Community. *Regulation (EU) No 305/2011,* Brussels, 2011.

Craighead G. *High-rise security and fire life safety.* 3rd ed. U.S.A, Elsevier, 2009.

Crosti C. *PhD. Thesis - Improving the safety of the steel bridges through more accurate and affordable modeling of the connection,* 2011.

Crosti C. Structural analysis of steel structures under fire loading. *Acta Polytechnica,* 49(1), pp. 21-28, 2009.

Crosti C. & Bontempi F. *Performance assessment of steel structures subject to fire action.* Athens, The Ninth International Conference on Computational Structures, 2008.

Crosti C, Giuliani L, Gentili F & Bontempi F. *Il ruolo della robustezza strutturale nella impostazione.* Pisa (Italy), VGR, 2012.

Danish National Annex to Eurocode 1. *EN 1991-1-2 DK NA - Danish National Annex to Eurocode1,* 2008.

DIANA. *User's Manual.* [Online] Available at: www.tnodiana.com, 2008 [Accessed October 2012].

Dominio sfantasticos, 2012. [Online] Available at: http://www.dominiosfantasticos. xpg.com.br/joelma48.jpg [Accessed October 2012].

Dorn J. Some fundamental experiments on high temperature creep. *J. Mech. Phys. Solids,* Volume 3, pp. 85-116, 1955.

Drysdale D. *An Introduction to Fire Dynamics.* 2nd ed. Chichester, West Sussex, England, Wiley, 1999.

DS411. *Norm for Betonkonsttruktioner (Code of practice for the structural use of concrete - in Danish),* s.l.: Danish Standard, 1999.

Duthinh, D, McGrattan K. & Khashkia A. Recent advances in fire-structure analysis. *Fire Safety Journal,* 43(2), pp. 161-167, 2008

EN 1990. *Basis of structural design,* Brussels: Comité Européen de Normalization CEN, 2002.

EN 1991-1-2. *General actions – Actions on structures exposed to fire,* Brussels: Comité Européen de Normalisation CEN2004.

EN 1991-1-7. *Actions on structures - General actions - Accidental actions,* Brussels: Comité Européen de Normalisation CEN, 2006.

EN 1992-1-1. *Design of concrete structures - Part 1-1: General rules and rules for buildings,* Brussels: Comité Européen de Normalization CEN, 2004.

EN 1992-1-2. *Design of concrete structures, Part 1-2: General rules - Structural Fire Design.* Brussels, Comité Européen de Normalisation CEN, 2004.

EN 1993-1-2. *Design of steel structures - Part 1-2 General rules - Structural fire design,* Brussels: Comité Européen de Normalisation CEN, 2005.

Eurocode 10027-1. *Designation systems for steel - Part 1: Steel names,* Brussels: Comité Européen de Normalization CEN, 2005.

Faber MH. Robustness of structures: an introduction. *Structural Engineering International SEI,* 16(2), 2006.

Faber, MH. *Risk and safety in civil engineering - Lecture notes.* Zurich: Swiss Federal Institute of Technology (ETH), 2007.

Faber MH & Steward MG. Risk assessment for civil engineering facilities: critical overview and discussion. *Reliability Engineering and System Safety,* Volume 80, pp. 173-184, 2003.

Feenstra P & De Borst R. Constitutive Model for Reinforced Concrete. *Journal of Engineering Mechanics* , 121(1), pp. 587-595, 1995.

FireFighter EMT. [Online] Available at: http://www.firefighteremt.com/archives/first-interstate-bank-fire-may-4-1988.php [Accessed October 2012], 2009.

Fletcher I, Borg A, Hitchen N & Welch S. *Performance Of Concrete In Fire: a review of the state of the art, with a case study of the Windsor Tower Fire.* Aveiro, 4th International Workshop in Structures in Fire, Universidade de Aveiro, 2006.

Fletcher I, Welch S, Capote JA, Alvear D, Lazaro M. *Model-Based Analysis of a concrete building subjected to fire.* Santander, Advanced Research Workshop on Fire Computer Modelling, 2007.

flickr, 2012. [Online] Available at: http://farm4.static.flickr.com/3583/3820288269_bb3eb6289a.jpg [Accessed October 2012].

Forsberg U & Thor J. *Brandbelastingsstatistik for skolor och hotel,* Stockholm, Stalbygnadsinstitutet, 1971.

Franssen JM, Kodur V & Zaharia R. *Designing steel structures for fire safety.* London: CRC Press, 2009.

Galambos TV. *Guide to stability design criteria for metal structures.* Wiley, Fifth Edition, New York, 1998.

Gann RG. *NIST NCSTAR 1A- Final Report on the Collapse of World Trade Centre Building 7,* Federal Building and Fire Safety Investigation of the World Trade Centre Disaster, 2008.

Gann RG. *NCSTAR 1-5 - Reconstruction of the Fires in the World Trade Center Towers,* NIST, 2005.

Gentili F, Crosti C & Giuliani L. *Performance based investigation of structural systems under fire.* Cape Town, SEMC 2010, 2010.

Gentili F, Giuliani L & Bontempi F. Structural response of high-rise buildings to fire: system characteristics and failure mechanisms. *Journal of Structural Fire Engineering,* Volume March, in press.

Gentili F, Giuliani L & Petrini, F. *Numerical investigation of the fire induced collapse of a single storey two span frame.* Budapest, Eurosteel, 2011.

Giuliani L. *Ph. D. Thesis - Structural integrity: robustness assessment and progressive collapse susceptibility,* 2008.

Giuliani L. Structural safety in case of extreme events. *International Journal Life-Cycle Performance Engineering,* 2012.

Giuliani L & Budny I. Different design approaches to structural fire safety. *International Journal Life-Cycle Performance Engineering,* 2012.

Giuliani L. *Lecture Notes of the course 11023 - Structural fire safety design,* Technical University of Denmark, 2011

Gkoumas K, Crosti C. & Bontempi F. *Risk Analysis and Modelling Techniques for Structural Fire Safety.* Athens, International Conference on Computational Structures Technology, 2008.

Guo Z. & Shi X. *Experiment and calculations of reinforced concrete at elevated temperatures.* Tsinghua University Press ed. ed. MA, USA: Elsevier Inc, 2011.

Gustaferro A. *Experiences From Evaluating Fire-Damaged Concrete Structures.* s.l.:American Concrete Institute (ACI), 1983.

Hadjisophocleous GV & McCartney CJ. *NRCC-47740 - Guidelines for the use of CFD simulations for fire and smoke modelling,* Canada: National Research Council, 2005

Hall J. *High-rise buildings fire,* NFPA, 2011.

Hamburger RO & Whittaker AS. *Considerations in performance-based blast resistant design of steel structures.* New York, AISC-SINY Symposium on Resisting Blast and Progressive Collapse, American Institute of Steel Construction, 2003.

Hammond JR. 9/11 and Skeptic Magazine's Science of Controlled Demolitions. *Foreign Policy Journal,* 2011.

Handling Exceptions in Structural Engineering, Rome, 2008.

Harmathy T. A comprehensive creep model. *Journal of Basic Engineering,* Volume 89, pp. 4996-502, 1967.

Hasemi Y & Tokunuga T. Flame geometry effects on buoyant plumes from turbulent diffusion flames. *Fire Science and Technology,* Volume 4, pp. 15-26, 1984.

Hertz KD. *Vejledning i dimensionering af bygningskonstruktioner for fuldt udviklet brand (in Danish),* Copenhagen, National Agency for Enterprise and Construction, 2006.

Hertz KD. Parametric Fires for Structural Design. *Journal of Fire Technology,* 2001.

Hertz K. *Simple temperature calculations of fire-exposed concrete construction,* Lyngby, Denmark: Technical University of Denmark, 1981.

Hertz KD. Limits of spalling of fire exposed concrete. *Fire Safety Journal,* 38(2), pp. 103-116, 2003.

Hertz KD. Concrete Strength for Fire Safety Design. *Journal of Magazine of Concrete Research,* 57(8), pp. 445-453, 2005.

Hertz K & Bagger A. *CO2 emissions from Super-light Structures.* London, UK, Proceedings of the International Association for Shell and Spatial Structures (IABSE-IASS) Symposium, 2011.

Hertz KD. *Assessment of Performance-Based Requirements for Structural Design.* s.l., International Symposium on Fire Safety Science (IAFSS05), 2005.

Hertz KD. *Guide for design for fully developed fire (in Danish),* Denmark: Danish Ministry of Industry. 2006.

Heskestad G. Fire Plumes. In: *SFPE Handbook of Fire Protection Engineering.* Quincy (MA): National Fire Protection Association, pp. 2-9, 1995.

http://911research.wtc7.net/, 2011. [Online] Available at: http://911research.wtc7.net/cache/wtc/analysis/compare/iklim_meridienplaza.html [Accessed October 2012].

http://911research.wtc7.net, 2012. [Online]. Available at: http://911research.wtc7.net/wtc/analysis/wtc7/index.html [Accessed October 2012].

ISO 15392. *Sustainability in building construction - General principles,* s.l.: International Standard Organization, 2008

ISO/FDIS 2394. *General principles on reliability for structures,* 1988.

ISO/PDTS 16773. *Fire Safety Engineering - Selection of design fire scenarios and design fires,* 2005

ISO/TR 13387-1. *Fire safety engineering - Part 1: Application of fire performance concepts to design objectives,* 1999.

ISO. *Fire resistance tests - Elements of building construction - Part 1: General requirements for fire resistance testing,* 1975.

Jayasree G, Lakshmipaty M. & Santhanaselvi S. Behaviour of R.C. beams under elevated temperatures. *Journal of Structural Fire Engineering,* 2(1), pp. 45-55, 2011.

Karlsson B & Quintiere J. *Enclosure Fire Dynamics.* Taylor&Francis , 2009.

Kodur V & Dwaikat M. Effect of high temperature creep on the fire response of restrained steel beams. *Materials and Structures,* Volume 43, pp. 1327-1341, 2010.

Krasner L. *Burning characteristic of wooden pallets as a test fuel,* Norwood, MA, Factory Mutual Research Corp., 1968.

La Malfa A & La Malfa S. *Approccio ingegneristico alla sicurezza antincendio (in Italian).* 5th ed., Legislazione Tecnica, 2009.

Law A, Stern-Gottfried J, Gillie M. & Rein G. The influence of travelling fires on a concrete frame. *Engineering Structures,* 33(5), pp. 1635-1642, 2011.

Leonardo Da Vinci Pilot Project, Handbook 5 – Design of buildings for the fire situation, Luxembourg, 2005

Lew, H. *NCSTAR 1-1 Design, Construction and Maintenance of Structural and Life Safety Systems,* NIST, 2005.

Los Angeles Fire Department, 1999. [Online] Available at: http://www.lafire.com/famous_fires/1988-0504_1stInterstateFire/050488_InterstateFire.htm [Accessed October 2012].

Luecke WE, Banovic SW & McColskey JD. *High temperature, tensile, constitutive data for World Trade Center steels,* s.l.: NIST, in press.

Meacham BJ, Park H, Engelhardt M, Kodur V, Van Straalen I, Maljaars J, Van Weeren K, De Feijter R & Both K. *Fire and Collapse, Faculty of Architecture Building, Delft University of Technology: Implications for Performance-Based Design.*. Bethesda, MD., 8th International Conference on Performance-Based Codes and Fire Safety Design Methods, SFPE, 2010.

Moss P, Dhakal R, Bong M. & Buchanan, AH. Design of steel portal frame buildings for fire safety. *Journal of Constructional Steel Research Research,* Volume 65, pp. 1216-1224, 2009.

National Institute for Land and Infrastructure Management (NILIM), 2005. *Report on the Windsor Building Fire in Madrid, Spain (in Japanese),* Japan: s.n.

NBC news, 2009. [Online] Available at: http://www.msnbc.msn.com/id/29099358/ns/world_news-asia_pacific/t/china-tv-sorry-fireworks-caused-blaze/#.UGBYSI3N_Lw [Accessed October 2012].

Newman G. *Fire and steel construction: the behaviour of steel portal frames in boundary consitions.* 2nd ed. UK, The Steel Construction Institute, 1990.

NFPA Journal, 2005. [Online] Available at: http://www.nfpa.org/journalDetail.asp?categoryID=961&itemID=23290&src=NFPAJournal&cookie_test=[Accessed October 2012].

NFPA, *NFPA 555: Gide on Methods for Evaluating Potential for Room Flashover* , 2009.

Nii D, Yamaguchi J, Mase R, Notake H, Ikehata Y, Tanaka T. *Risk-Based Selection of Design Fire Scenarios in Performance Based Evacuation Safety Designs of buildings.* Lund, International Conference on Performance-Based Codes and Fire Safety Design Methods, 2010.

NILIM. *Report on the Windsor Building Fire in Madrid, Spain (in Japanese),* Japan: National Institute for Land and Infrastructure Management, 2005.

Nilsson L. *Rapport R34 - Brandbelastning i bostadslagenheter (in Swedish).* Statens Institut for Byggnadsforskning, 1970.

NIST. *NCSTAR1-A Final report on the collapse of WTC building 7,* s.l.: NIST, 2008

NIST. *FDS - User guide - www.fire.nist.gov/fds*, Washington, 2009.

NIST. *Fire Dynamics Simulator (Version 5) - User guide - Special Publication,* Washington, 2009.

NTC 2008. *Nuove Norme Tecniche per le Costruzioni, (in Italian),* Italy, Ministero delle Infrastruttre, 2008.

NUREG 1824. *Verfication and validation of selected fire models for nuclear power plant applications vol.7,* s.l.: US Nuclear Regulatory Commission, 2007.

O'Meagher A, Bennetts I, Dayawansa P & Thomas I. Design of single storey industrial buildings for fire resistance. *Journal of Australian Institute of Steel Construction,* 26(2), 1992.

PBS, 2012. [Online] Available at: http://www.pbs.org/wgbh/amex/lasvegas/timeline/timeline2.html [Accessed October 2012].

PD 6688-1-2-2007. *Backgroud paper to the UK National Annex to BS EN1991-1-2*, 2007.

Perrow C. *Normal Accidents: Living with High-Risk Technologies.* New York, Basic Book, 1984.

Petrini F. Performance-based fire design of complex structures. *International Journal Life-Cycle Performance Engineering,* 2012.

Petrini F & Ciampoli M. Performance-based wind design of tall buildings. *Structure and Infrastructure Engineering: Maintenance, Management, Life-Cycle Design and Performance,* 2011.

Petterson, O, Magnusson SE & Thor J. *Fire Engineering design of steel structures.* Sweden: Bulletin 52, 1976.

Petterson O & Odeen K. *Brandteknisk dimensionering, principer, underlag, exempel (Fire safety design, principles, basis, exemples - in Swedish).* Stockholm, Sweden: Forlag Vallingby, 1978.

Pfeiffer U. *INCA2 v.2.8 - Interactive Nonlinear Cross-Section Analysis Biaxial.* Hamburg: Institute for Concrete Structures, Hamburg University of Technology (downloadable at www.tuhh.de/mb), 2011.

Poh K. Stress-strain-temperature relationship for structural steel. *Journal Material of Civil Engineering,* 13(5), pp. 371-379, 2001.

Portland Cement Association. *Assessing the Condition and Repair Alternatives of Fire-exposed and Masonry Members,* Illinois, USA, 1994: National Codes and Standards Council of the Concrete and Masonry Industries, 1994.

Purkiss, JA. *Fire Safety Engineering Design of Structures.* Burlington (USA), Butterworth-Heinemann, 2007.

Reason J. *Human Error.* s.l.:Cambridge University Press, 1990.

Rein Guillermo, Zhang Xun, Williams Paul, Hume Ben & Heise Alex. *Multi-storey fire analysis for high-rise buildings.* London, 11th Interflam, 2007

Research Fund for Coal and Steel of the European Community. *Multi-storey steel buildings - Part 6: Fire Engineering, Steel Building in Europe design manual, ,* 2008

Riggs HR, Robertson IN, Cheung KF, Pawlak G, Young YL, Yim SC. *Experimental simulation of tsunami hazards to buildings and bridges.* Knoxville, USA, NSF CMMI Engineering Research and Innovation Conference, 2008.

Robertson A & Ryan I. Proposed Criteria for Defining Loading Load Failure of Beams, Floors and Roof Constructions. *Journal of Research, National Bureau of Standards,* Volume 63c, 1959.

Schiermacher I. & Poulsen A. *Temperaturanalyse ved hjaelp af CAE/CAD (Temperature analysis by CAD - in Danish),* Denmark: Danish Academy of Civil Engineer DIA-B, 1987.

Schleich JB. Performance-based design for the fire situation. In: *Steel a new and traditional material for building.* Brasov: ICMS, pp. 553-560, 2006.

SEAOC. *A framework for performance Based Earthquake Engineering.* 1995.

SEI - Progressive Collapse Standards and Guidance Committee. *A PreStandard Prospectus: Robustness and collapse resistance for buildings,* 2007.

Sgambi L, Malerba P, Gotti G. & Ielmini D. The influence of degradation phenomena on collapse modes in prestressed concrete beams. *International Journal of Life-Cycle and Performance Engineering,* pp. 41-63, 2012.

Shanley FR. Inelastic Column Theory. Journal of the Aeronautical Sciences, Vol. 14, No. 5 1947. p. 261–268, 1947

SIA 260 Building Code. *Sicherheit und Gebrauchstauglichkeit von Tragwerken - Weisung des SIA an seine Kommissionen fur die Koordination des Normenwerk,* Swiss Society of Engineers and Architects ,1982

skyscrapercity, 2004. [Online] Available at: http://www.skyscrapercity.com/showthread.php?t=401028&page=2[Accessed October 2012].

Society of Fire Protection Engineers. *Guidelines for Designing Fire Design Safety in Very Tall Buildings - Draft,* Society of Fire Protection Engineers, 2012.

Song Y, Huang Z, Burgess I & Plank R. *The design of Pitched-Roof Steel Portal Frames Against Fire.* Singapore, International Conference on Advances in Steel Structures (ICASS07), 2007..

Song Y, Huang Z, Burgess I & Plank R. *A new design method for industrial portal frames in fire.* Prague, International Conference Application of Structural Fire Engineering (ASFE), 2009.

Starrosek U. Progressive Kollaps von Bauwerken (in German). In: *Betonkalender - Part VIII.* Berlin: Wiley, 2008.

Starrosek U. *Progressive Collapse of Structures.* London: Thomas Telford Publishing, 2009.

Stern-Gottfied J, Law A, Rein G & Torero J. *A performance based methodology using travelling fires for structural analysis.* Lund, Conference of Fire Protection Engineering (SPFPE'10), 2010.

The Council of the European Communities. *Interpretative Document No 2 - Safety in case of fire,* , 1994

The Institution of Structural Engineers. *Safety in tall buildings and other buildings with large occupancy,* London, 2002.

TU 2005. *Testo Unico - Norme tecniche per le costruzioni (in Italian),* Italy, Ministero delle Infrastrutture e dei Trasporti, 2005.

UFC, 2005. *Design of buildings to resist progressive collapse,* s.l.: Unified Facilies Criteria

Usmani A, Chung Y & Torero J. How did the WTC collapse: a new theory. *Fire Safety Journal,* 38(6), 2003.

Usmani AS O'Connor MA, Rotter JM, Elghazouli AY, Drysdale DD, Sanad AM. Gillie M & Lamont S. *Behaviour of Steel Framed Structures under Fire Conditions,* s.l.: DETR-PIT Project, 2000.

Vassart O, Cajot LG, Franssen JeanMarc, O'Connor M & Zhao B. *3D simulation of industrial hall in case of fire. Benchmark between ABAQUS, ANSYS and SAFIR.* Edinburgh, 10th International Fire Science & Engineering Conference INTERFLAM, 2004.

Wald F, Bosiljkov V, Da Silva L, De Matteis G, Haller P, Santiago A & Vila Real P. *Structural integrity of buildings under exceptional fire.* Lisbon, COST C12, 2002. .

Wang Y, Wald F, Vacha J. & Hajpal M. Fire damaged structures. In: *Urban Habitat Constructions Under Catastrophic Events.* London: Taylor&Francis, 2010.

Wickstrom U. Application of the standard fire curve for expressing natural fires for design purposes. *Fire Science: Science and Engineering, American Society for Testing and Materials ASTM,* 1985.

Williams-Leir G. Creep of structural steel in fire: analytical expressions. *Fire and Materials,* 7(2), pp. 73-80, 1983.

Wong S, Burgess I & Plank R. *Simplified Estimation of Critical Temperatures of Portal Frames in Fire.* Istanbul, International Conference on Steel Structures of the 2000s., 2000.

Yeoh G & Yuen K. *Computational Fluid Dynamics in Fire Engineering.* London, Butterworth Heinemann, 2009

911 Myths, 2012. *WTC 7.* [Online] Available at: http://www.911myths.com/html/ wtc7_fire.html [Accessed October 2012].

triposo, 2012. [Online] Available at: https://www.triposo.com/poi/Joelma_Building [Accessed October 2012].

University of Manchester, 2012. *Interstate Bank Building.* [Online] Available at: http://www.mace.manchester.ac.uk/project/research/structures/strucfire/CaseStudy/HistoricFires/BuildingFires/interstateBank.htm [Accessed October 2012].

University of Manchester, 2012. *Windsor Tower.* [Online] Available at : http://www.mace.manchester.ac.uk/project/research/structures/strucfire/CaseStudy/HistoricFires/ BuildingFires/default.htm [Accessed October 2012].

University of Nevada Las Vegas, 2012. *digital library unlv edu.* [Online] Available at: http://digital.library.unlv.edu/objects/sky/565 [Accessed October 2012].

Lista de desastres en torres y rascacielos. [Online] Available at: http://www.urbanity.es/foro/rascacielos-y-highrises-inter/1024-lista-de-desastres-en-torres-y-rascacielos-28.html [Accessed October 2012].

wikipedia,2007.[Online]. Available at: http://en.wikipedia.org/wiki/File:TVCC_Site_2007.jpg [Accessed October 2012].

wikipedia, 2008. *Andraus Building.* [Online] Available at: http://en.wikipedia.org/wiki/File:30-12-2008_017.(By_Felipe_Mostarda).JPG [Accessed October 2012].

wikipedia, 2012. [Online]. Available at: http://en.wikipedia.org/wiki/Joelma_fire [Accessed October 2012].

wikipedia, 2012. [Online] Available at: http://en.wikipedia.org/wiki/One_Meridian_Plaza [Accessed October 2012].

Wikipedia, 2012. *Andraus Building.* [Online] Available at: http://en.wikipedia.org/wiki/ /Andraus Building [Accessed October 2012].

wikipedia, 2012. *MGM Grand Fire.* [Online] Available at: http://en.wikipedia.org/ wiki/MGM_Grand_fire [Accessed October 2012].

wikipedia, 2012. *Seven World Trade Center*. [Online] Available at: http://en.wikipedia.org /wiki/7_World_Trade_Center [Accessed October 2012].

zetatalk, 2012. [Online] Available at: http://www.zetatalk.com/index/oct17g.htm [Accessed October 2012]

Dottorato in Ingegneria delle Strutture
XXV ciclo

SAPIENZA
UNIVERSITÀ DI ROMA

Multi-physics modelling for the safety assessment of complex structural systems under fire

The case of high-rise buildings

Filippo Gentili

e-mail: filippo.gentili@uniroma1.it

Advisor

Prof. Franco Bontempi

Co-Advisor

Prof. Luisa Giuliani

Ph.D. Candidate

Ph.D. Candidate at the Sapienza University of Rome. Thesis title: ***Multi-physics modelling for the safety assessment of complex structural systems under fire. The case of high-rise buildings***, advisor: Prof. F. Bontempi (Sapienza University of Rome), co-advisor Prof. L. Giuliani (DTU Technical University of Denmark).

Visiting Student at the BRE Centre for Fire Safety Engineering, University of Edinburgh, in Edinburgh, UK, in 2011 (3 months Jan-Mar), working with Dr. L. Bisby.

Visiting Student at the Department of Civil Engineering, Technical University of Denmark (DTU), in Lyngby, DK, in 2012 (6 months Jan-Jun), working with Prof. L. Giuliani.

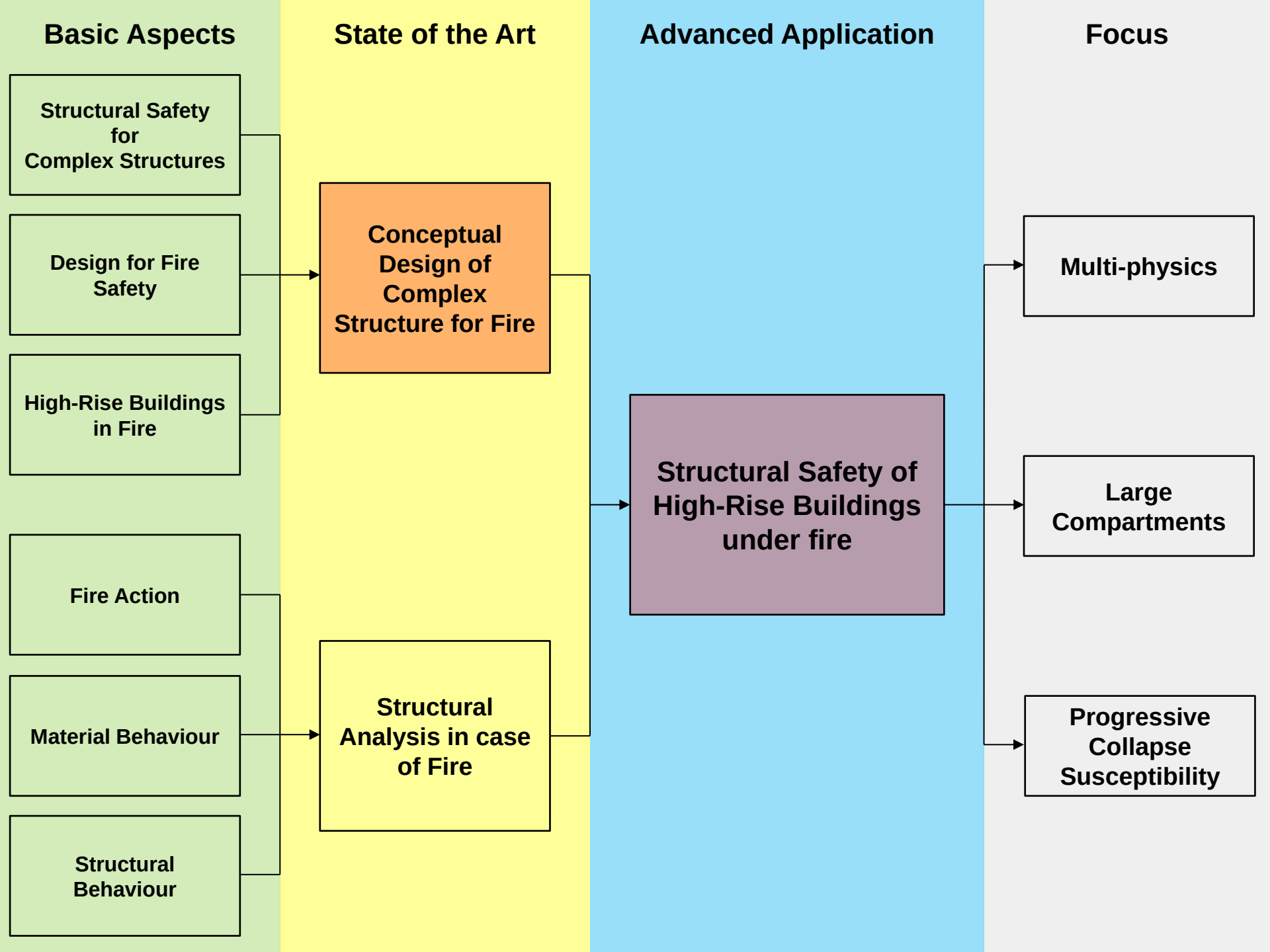
Basic Aspects
State of the Art
Advanced Application
Focus
Structural Safety for Complex Structures
Design for Fire Safety
High-Rise Buildings in Fire
Fire Action
Material Behaviour
Structural Behaviour
Conceptual Design of Complex Structure for Fire
Structural Analysis in case of Fire
Structural Safety of High-Rise Buildings under fire
Multi-physics
Large Compartments
Progressive Collapse Susceptibility

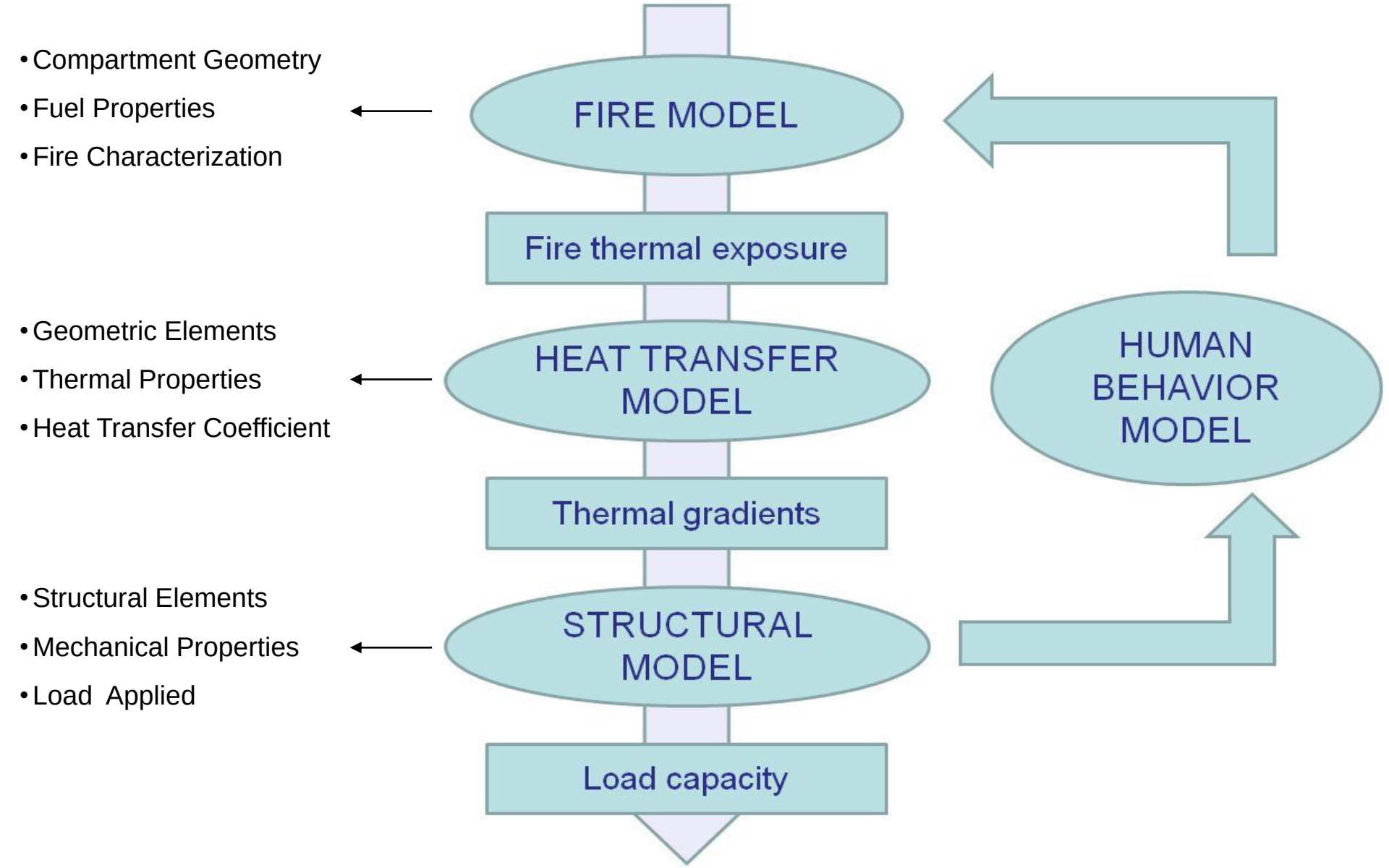
• Compartment Geometry
• Fuel Properties
• Fire Characterization
FIRE MODEL
Fire thermal exposure
• Geometric Elements
• Thermal Properties
• Heat Transfer Coefficient
HEAT TRANSFER MODEL
HUMAN BEHAVIOR MODEL
Thermal gradients
• Structural Elements
• Mechanical Properties
• Load Applied
STRUCTURAL MODEL
Load capacity

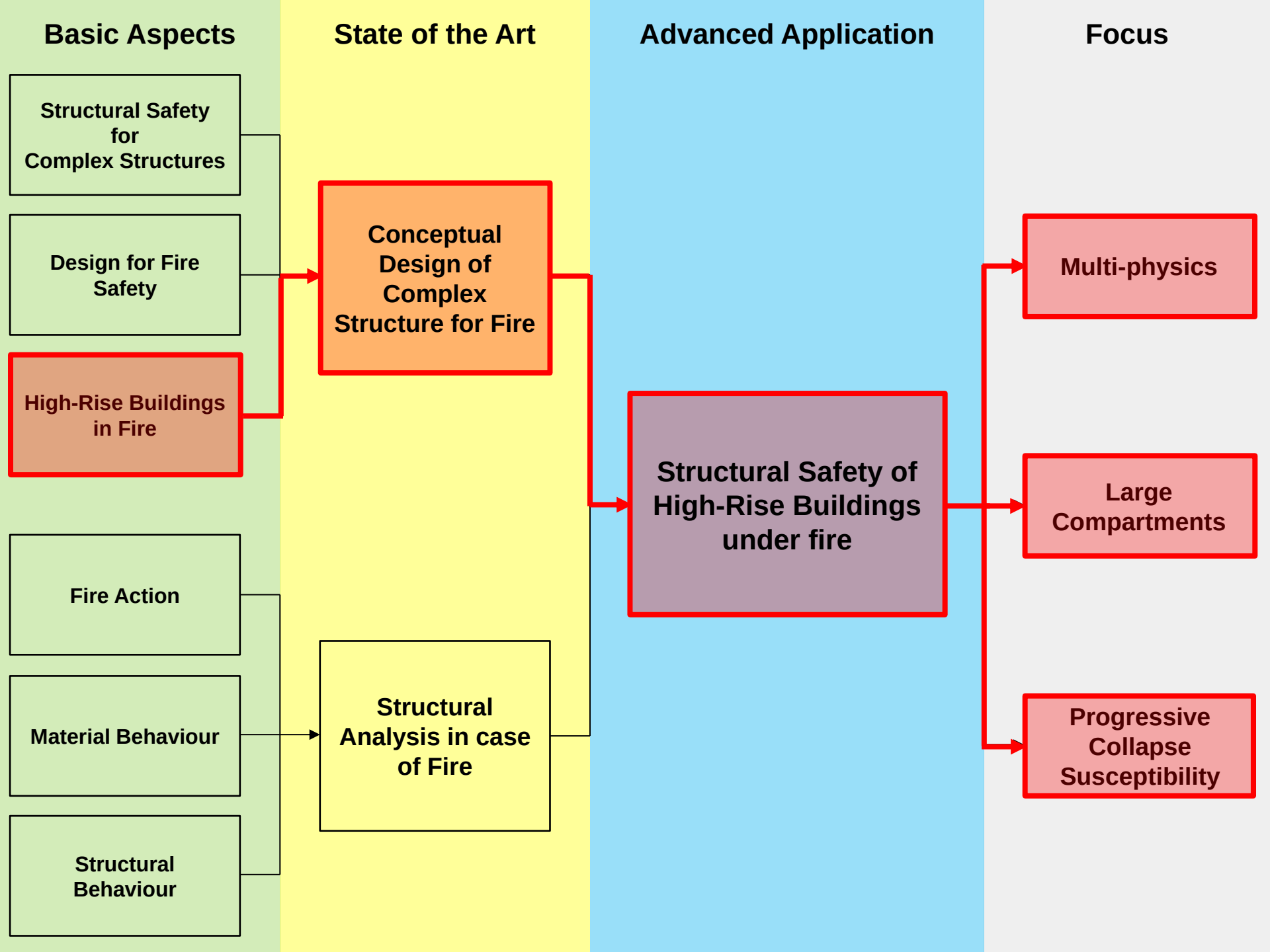
Basic Aspects
State of the Art
Advanced Application
Focus
Structural Safety for Complex Structures
Design for Fire Safety
High-Rise Buildings in Fire
Fire Action
Material Behaviour
Structural Behaviour
Conceptual Design of Complex Structure for Fire
Structural Analysis in case of Fire
Structural Safety of High-Rise Buildings under fire
Multi-physics
Large Compartments
Progressive Collapse Susceptibility

Introduction

Part I

Part II

Conclusions

Ph.D. Thesis Background

Fire Action

Structural Behaviour

Conclusive evaluations

Motivations

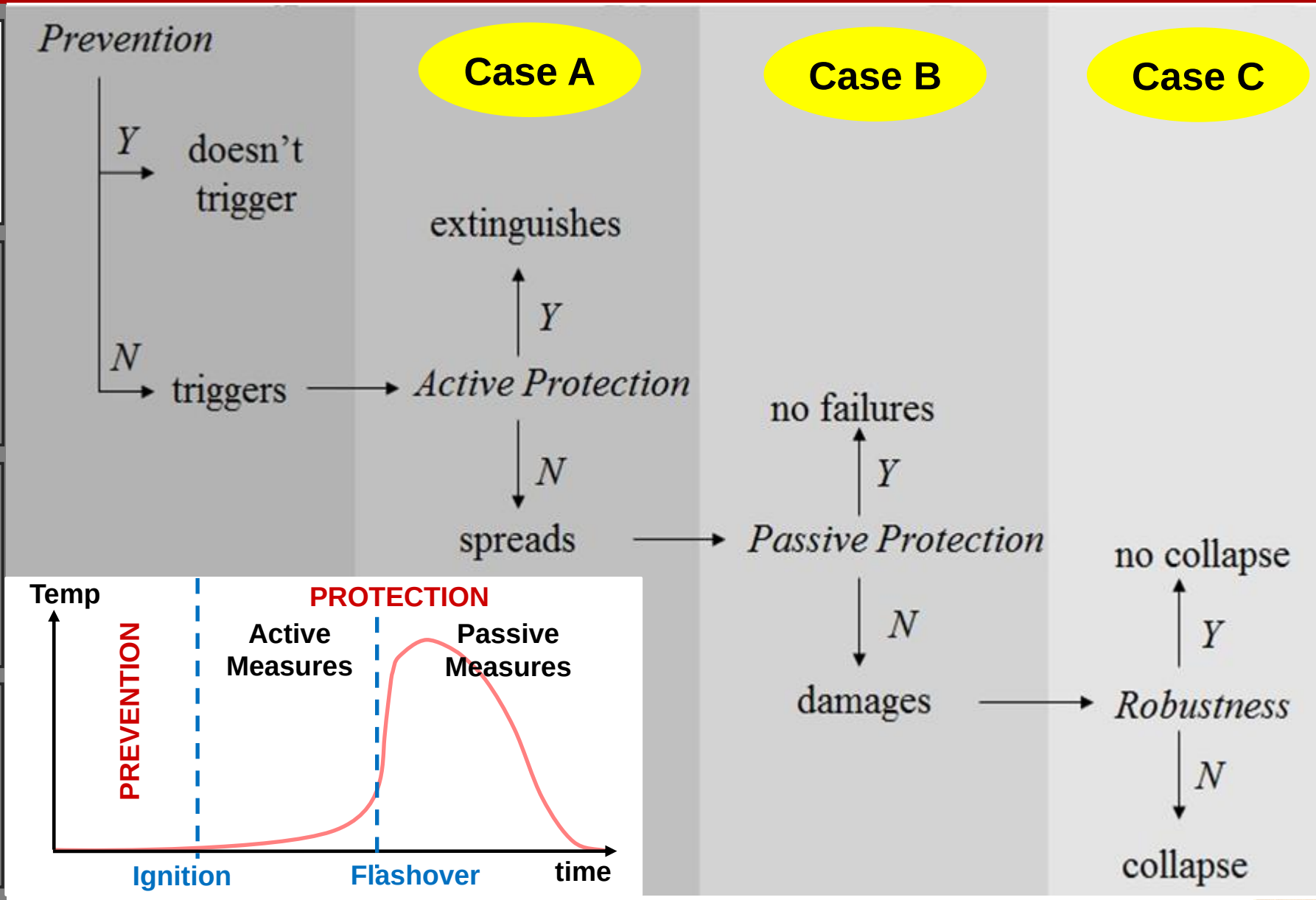

Case A

Fires without structural damages

Joelma Building, Sao Paulo (1974)

Built: 1971

Height: 25-story building

Structure: reinforced fire-resistant concrete

Fire: The fire spread externally up 13 storeys on two of the facades to the top of the building.

Cause: A short-circuit in a faulty air-conditioner on the 12th floor. The building had no emergency exits, fire alarms or fire sprinkler systems installed

Injuries: 179 fatalities, 300 people injured.

Duration: 2 hours

Damages: 4 years for reconstruction

Case B

Fires with structural damages

Mandarin Oriental Hotel, Beijing (2009)

Built: under construction
Height: 44 floors, 158 m
Use: hotel, not occupied yet
Structure: steel-framed with concrete core
Fire: triggered at roof, spread downwards
Cause: unauthorized firework
Duration: 5 hours
Injuries: 1 casualty (fireman), 7 injuries
Damages: many floors, no frame, ca. $100mil

Case C

Fires with structural collapses

Windsor Tower, Madrid (2005)

Built: 1979, fire protection under construction

Height: 106 m, 32 floors

Use: office building

Structure: concrete core and steel columns

Fire: triggered at 21st, vertical spread

Cause: short-circuit/arson? - partial insulation

Duration: 24 hours

Injuries: 7 firemen, no casualties

Damages collapse of upper part, collapse standstill

Method

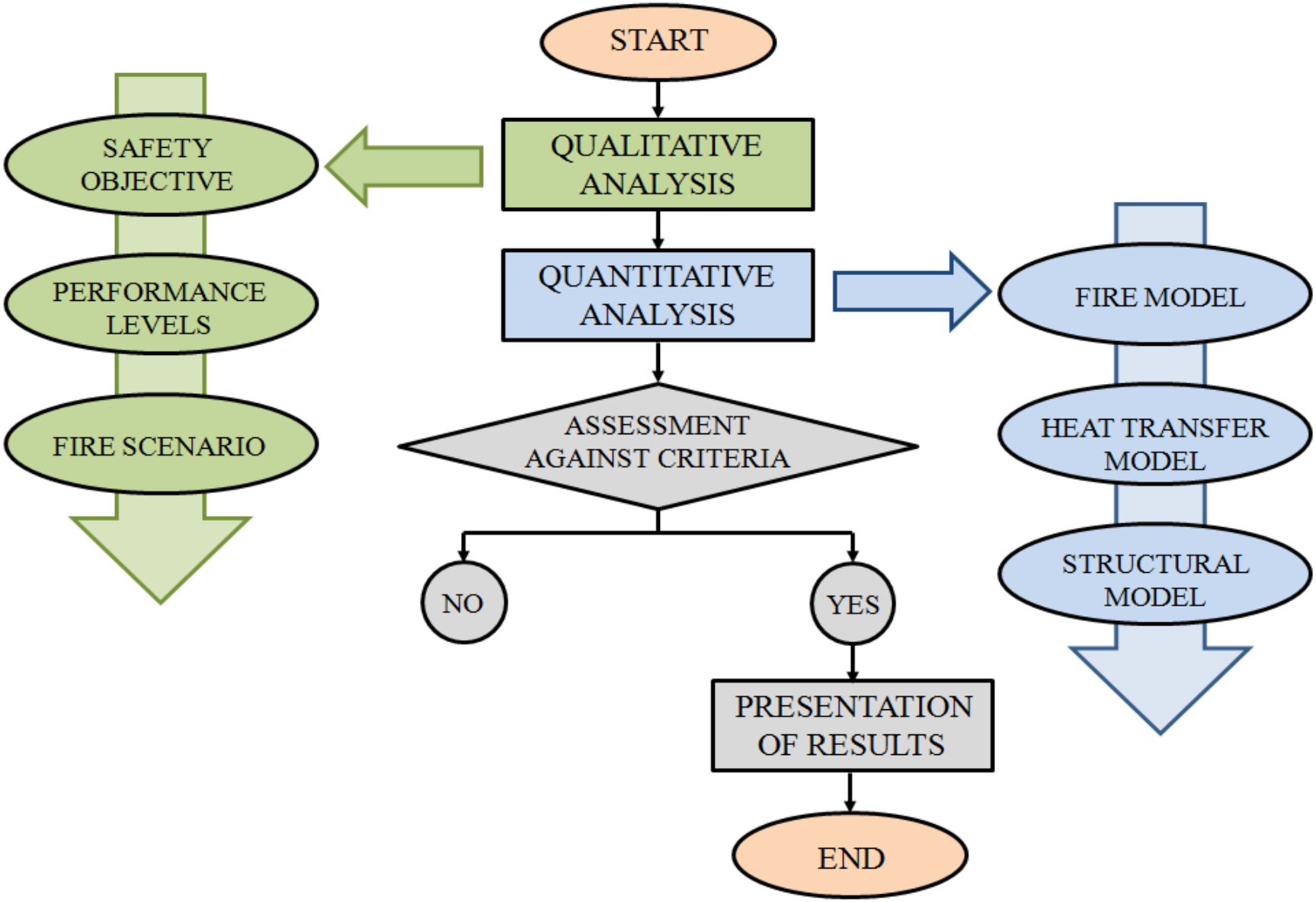
START
QUALITATIVE ANALYSIS
SAFETY OBJECTIVE
PERFORMANCE LEVELS
FIRE SCENARIO
QUANTITATIVE ANALYSIS
FIRE MODEL
HEAT TRANSFER MODEL
STRUCTURAL MODEL
ASSESSMENT AGAINST CRITERIA
NO
YES
PRESENTATION OF RESULTS
END

Essential Literature (I)

Fire Action

- Drysdale D. **An Introduction to Fire Dynamics,** Second Edition, Wiley, 1999.
- SFPE. **The SFPE Handbook of Fire Protection Engineering**, 3rd ed., National Fire Protection Association (NFPA), Quincy MA, 2002.
- Karlsson B, Quintiere JG. **Enclosure Fire Dynamics**, CRC Press, London, 1999.

Structural Behaviour

- Usmani AS, Rotter JM, Lamont S, Sanad AM and Gillie M. **Fundamental principles of structural behaviour under thermal effects**, Fire Safety Journal, Volume 36, Issue 8, Pages 721-744, November 2001.
- Buchanan AH. **Structural Design for Fire Safety**, Wiley, 2002.
- Pettersson O, Magnusson SE, Thor J. **Fire Engineering design of steel structures**, Bulletin 52, Sweden, 1976.
- Starossek U. **Progressive collapse of structures**, Thomas Telford Publishing, London, 2009.
- Gillie M. **Analysis of heated structures: Nature and modeling benchmarks,** Fire Safety Journal, 44, pp.673-680, 2009.
- Jayasree G, Lakshmipathy M, Santhanaselvi S. **Behaviour of RC beams at elevated temperature**, Journal of structural fire safety, 2(1), 45-55, 2011.

Essential Literature (II)

High Rise Building

- **Guidelines for Designing Fire Safety in Very Tall Buildings,** Society of Fire Protection Engineers, 2012.
- Usmani AS, Chung YC, Torero JL. **How Did the WTC Collapse: A New Theory,** Fire Safety Journal, 38, 6, 501-591, 2003.
- **MSB-6, Multi-storey steel buildings - Part 6: Fire Engineering**, Steel Building in Europe design manual, Research Fund for Coal and Steel of the European Community, 2008.
- Craighead G. **High-rise security and fire life safety,** Elsevier Science, U.S., 2003.
- Stern-Gottfried J, Rein G. **Travelling fires for structural design-Part I: Literature review,** Fire Safety Journal, Volume 54, November 2012, Pages 74–85
- Stern-Gottfried J, Rein G. **Travelling fires for structural design-Part II: Design methodology,** Fire Safety Journal, Volume 54, November 2012, Pages 96–112
- Flint GR. **Fire Induced Collapse of Tall Buildings**, PhD thesis, University of Edinburgh, 2005.
- Federal Emergency Management Agency, **World Trade Center Building Performance Study: Data Collection, Preliminary Observations and Recommendations**", FEMA, 2003.
- COWI. **Vejledning om brandsikkerhed i høje bygninger**, Energistyrelsen, Draft May 2012 (in Danish)

MULTIPHYSICS MODELLING FOR THE SAFETY ASSESSMENT OF COMPLEX STRUCTURAL SYSTEMS UNDER FIRE.
THE CASE OF HIGH-RISE BUILDINGS

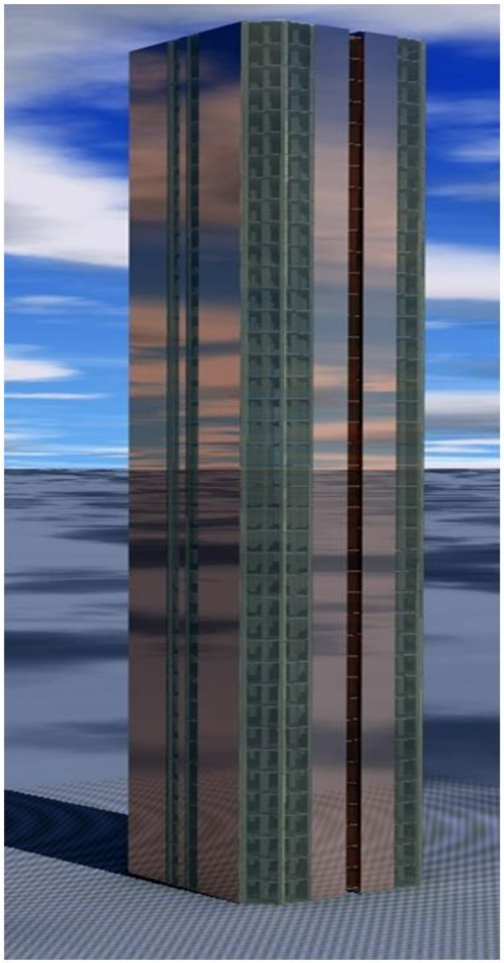

Fire Action

- ✓ Fire Scenario
- ✓ Temperature-time Curves
- ✓ Large Compartments

Structural Response

- ✓ Non-linearities
- ✓ Local and global collapse
- ✓ Substructures

✓ Fire scenario

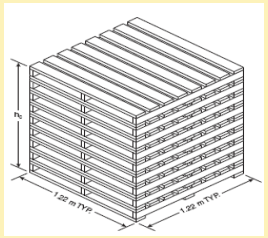

Height	3.05m
Size	1.2m x 1..2m
Weight of one pallets	15 kg
Weight of one stack of pallets	300 kg
Weight of all stacks	5400 kg
$HRR_{s,max}$	6810 Mw/m^2
t_g	80 s

floor plan

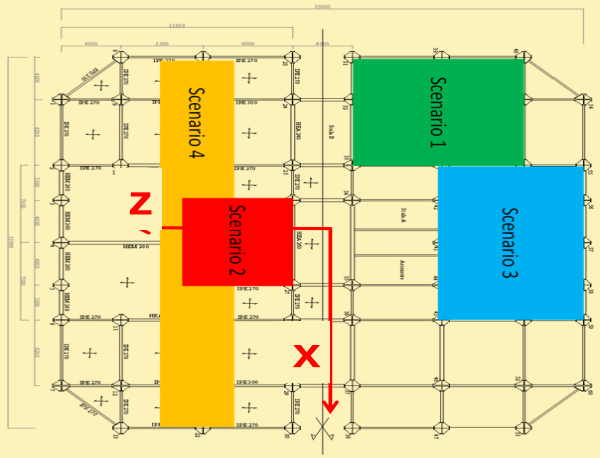

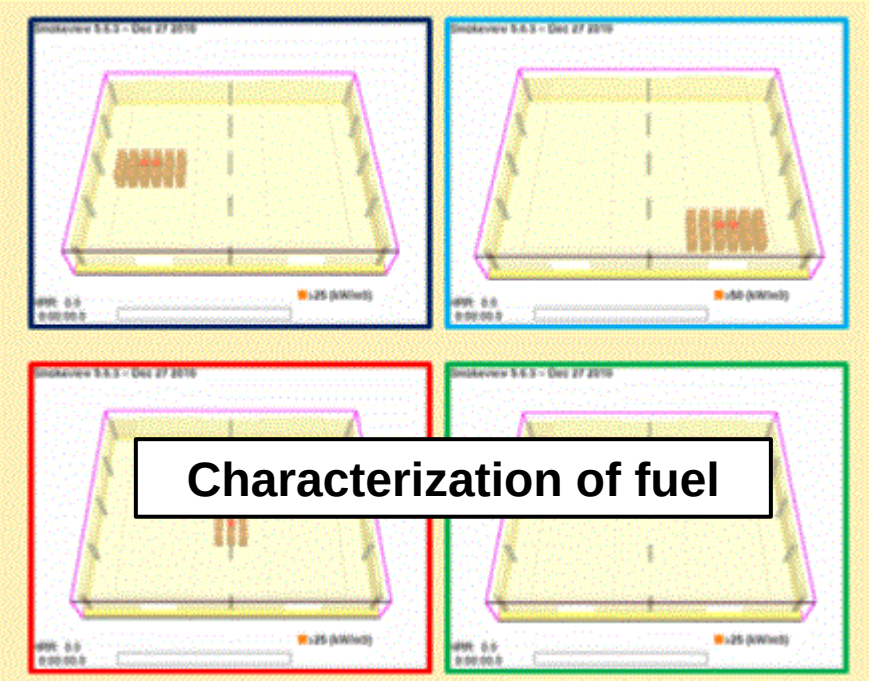

Characterization of fuel

lateral *central* *lateral* *transversal*

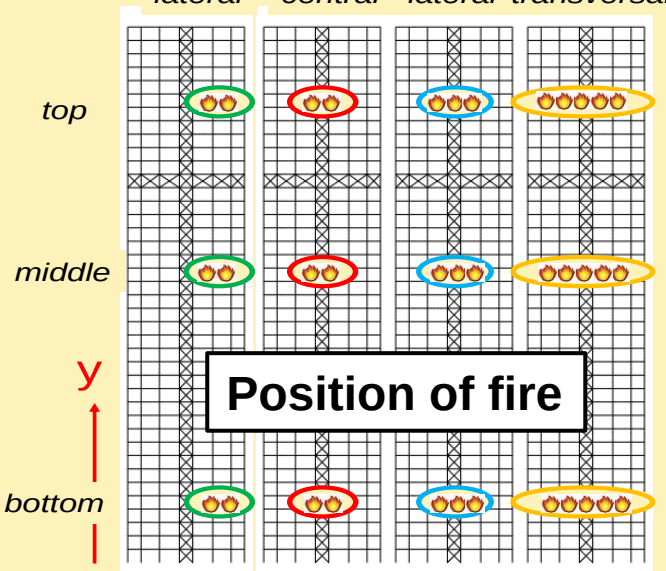

Position of fire

✓ Temperature-time curves

Nominal ISO 834

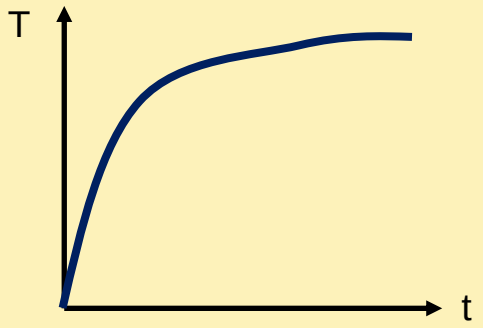

- Only post-flashover
- Monotonically increasing
- Fire test
- Given expressions

Natural Parametric

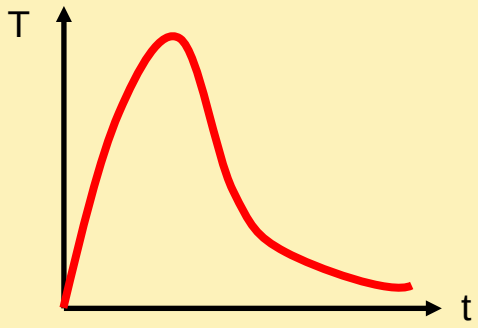

- Only post-flashover
- Cooling phase
- Analytic model
- Fuction of fuel and comparment

Natural Advanced

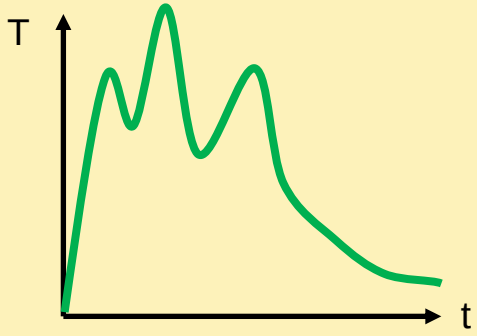

- Pre/post-flashover
- Realistic
- Computational
- Fuction of fuel, comparment and variation in time

✓ Large Compartments

Picture from
http://www.fotothing.com/Osamadaoud1950/

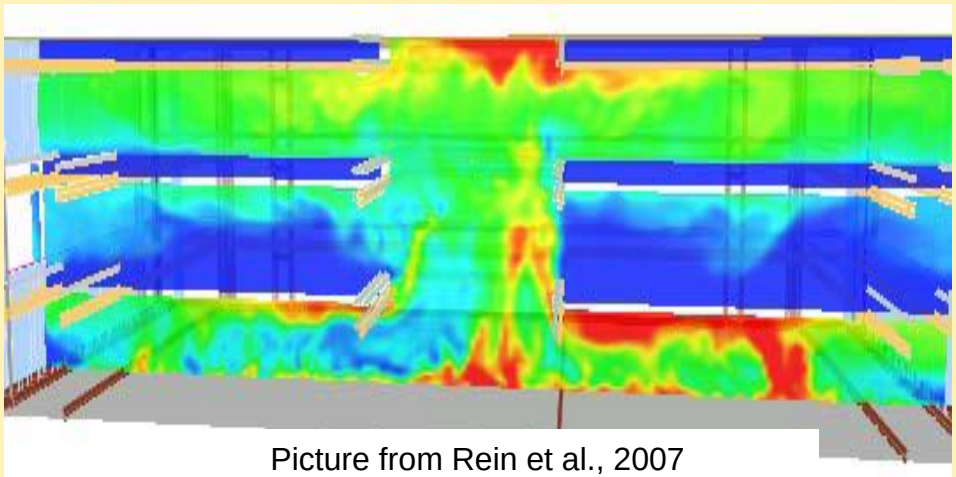

Picture from Rein et al., 2007

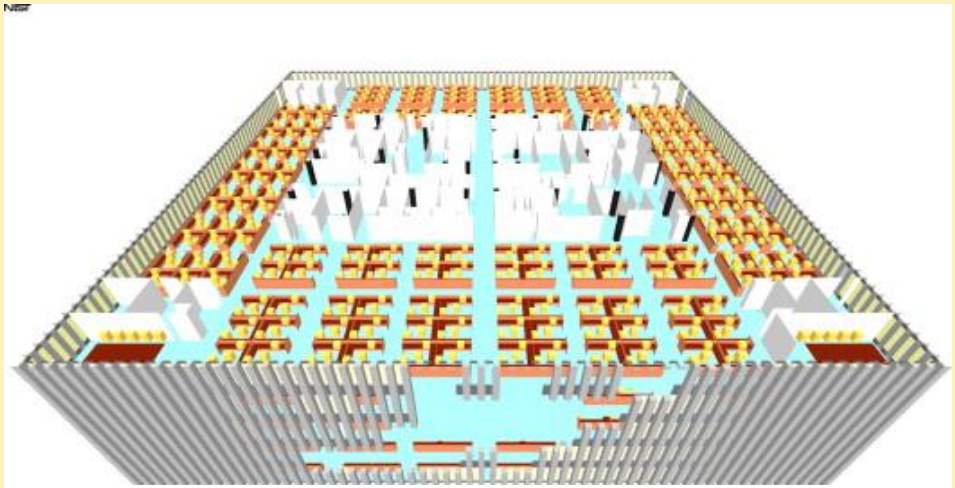

Picture from
http://www.nist.gov/el/disasterstudies/wtc/wtc_finalreports.cfm

✓ Non - linearities

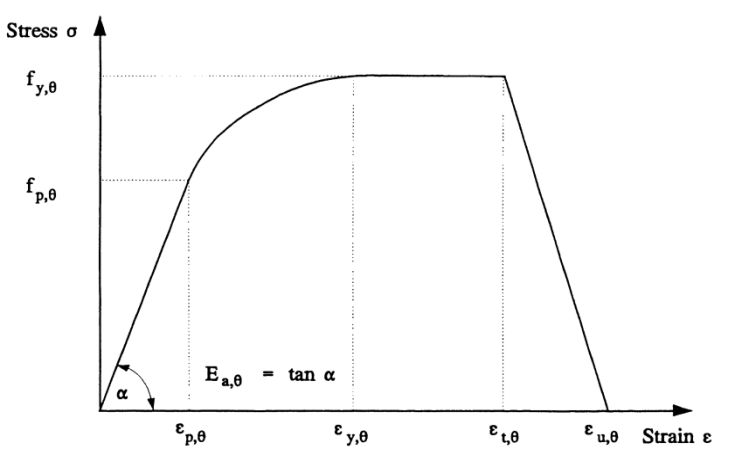

Buchanan, 2002

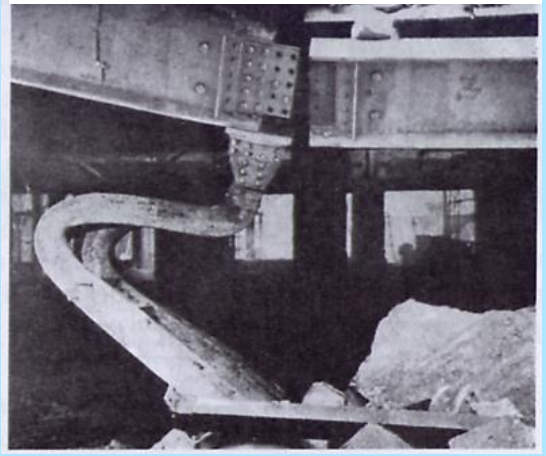

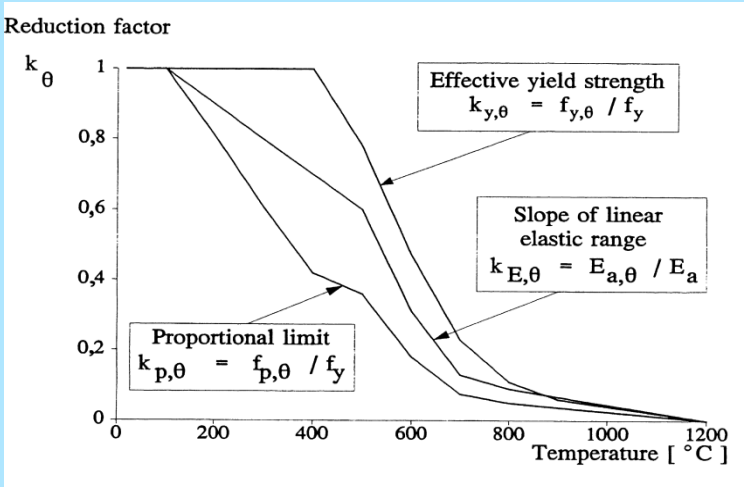

Picture from
http://www.era.lib.ed.ac.uk

Structural Response

✓ Local and global collapse

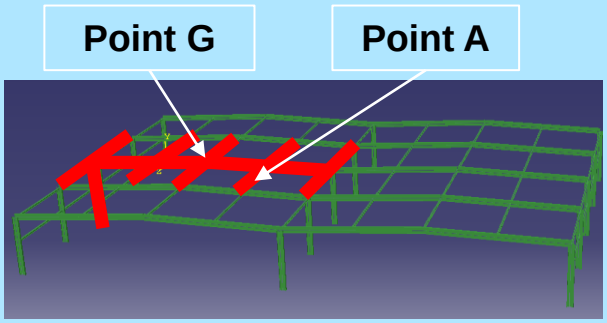

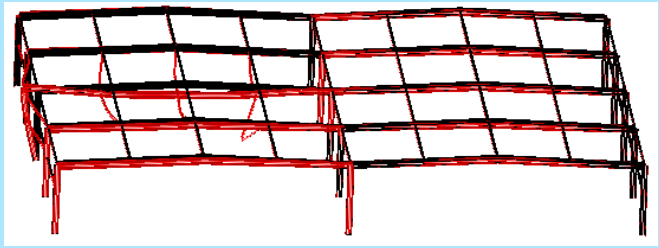

Local Collapse
Time: 18 min
(Scale Factor 5)

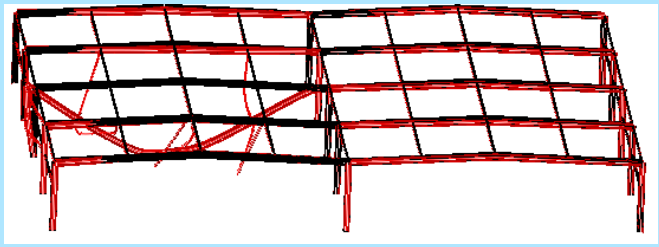

Global Collapse
Time: 22 min
(Scale Factor 5)

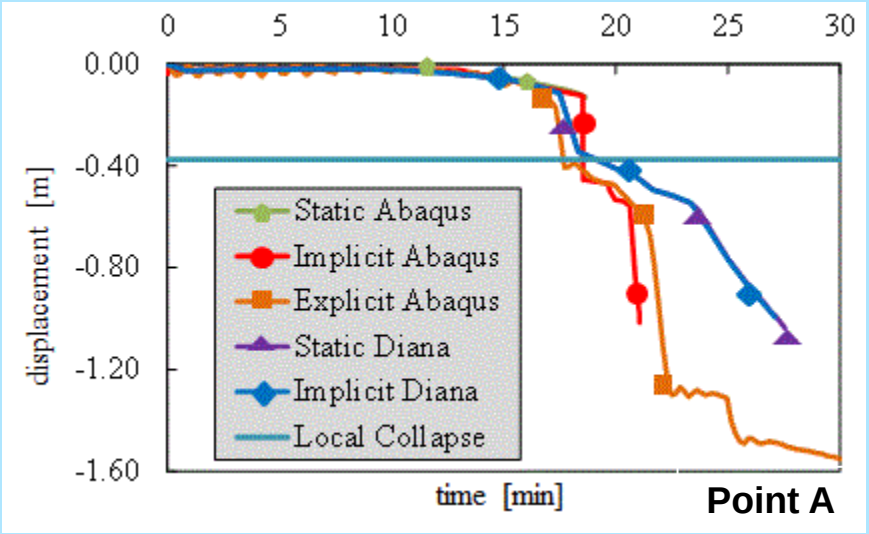

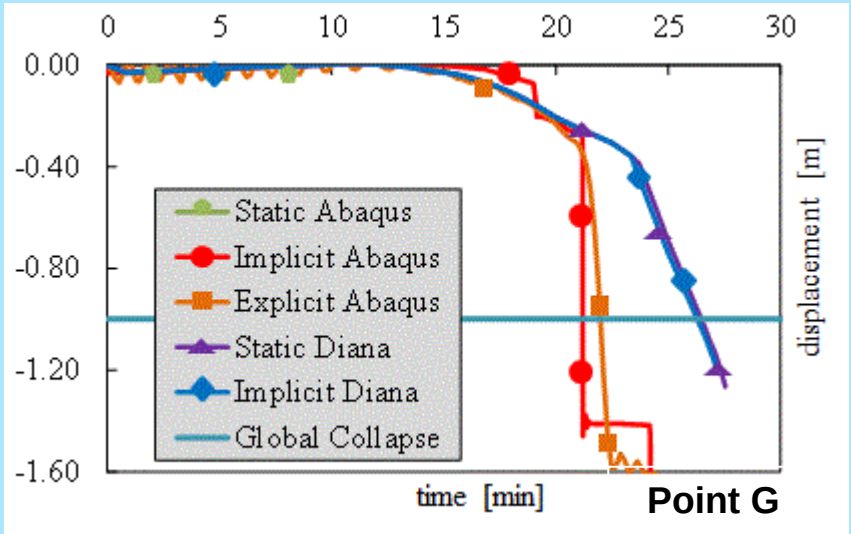

Structural Response

- ✓ **Substructures**

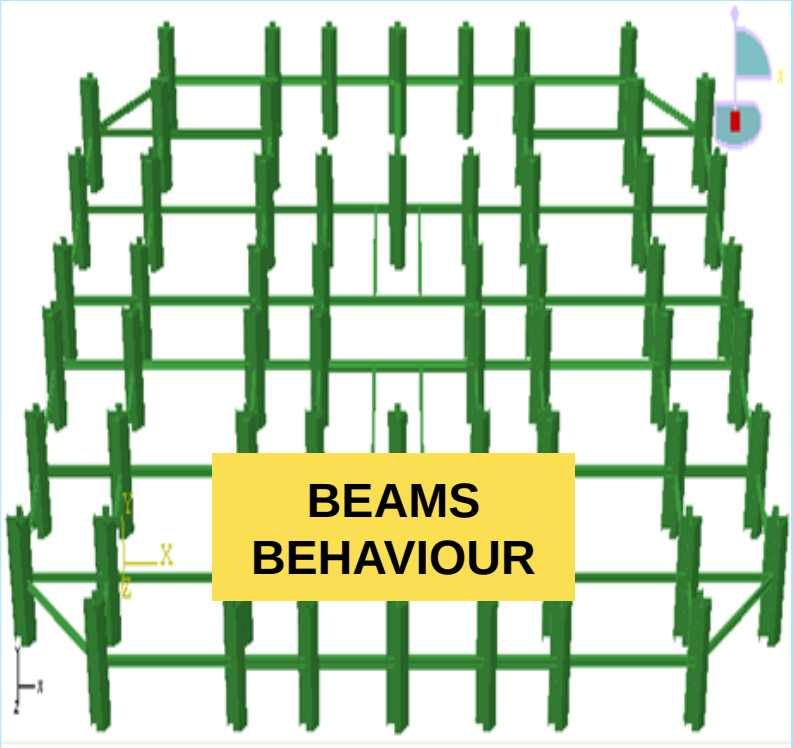

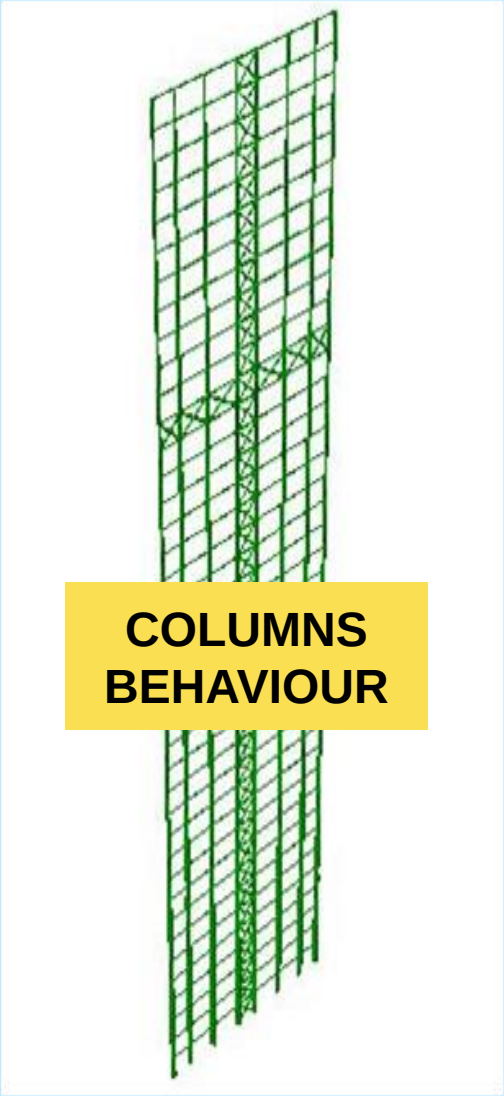

Introduction

Part I

Part II

Conclusions

Ph.D. Thesis Background

Fire Action

Structural Behaviour

Conclusive evaluations

Case Study I

Floor area		
A_f	1200	m^2
Enclosure area		
A_t	3135	m^2
Opening factor		
O	0.055	$m^{0.5}$
Thermal Inertia		
b	1017	$W \cdot s^{0.5}/(K \cdot m^2)$

Fuel load density (enclosure)		
q	30	MJ/m^2
Fuel load density (floor)		
q_f	79	MJ/m^2
Total fuel load		
Q	94500	MJ
Fire growing rate		
α	0.156	kJ/s^3

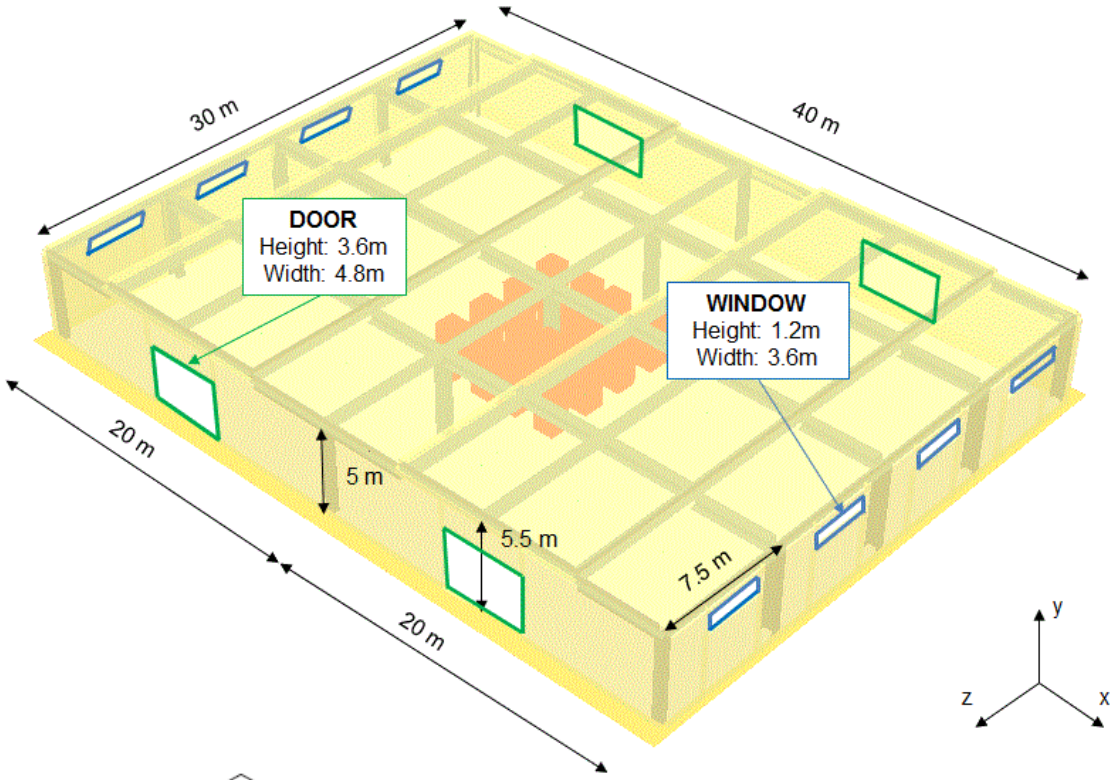

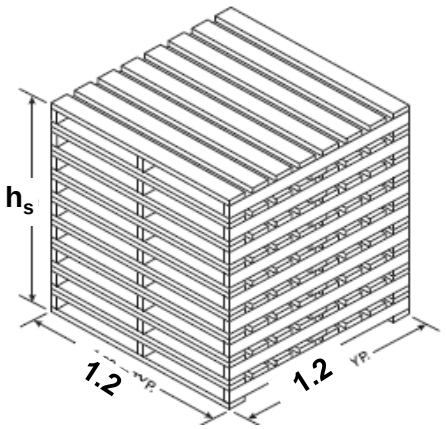

Stack height	3.0	m
No. of pallets in a stack	20	---
HRR_{max} of a stack	6.81	MW
No. stacks in the hall	18	---
$HRR_{max,\ tot}$	176	MW

FDS: Solver

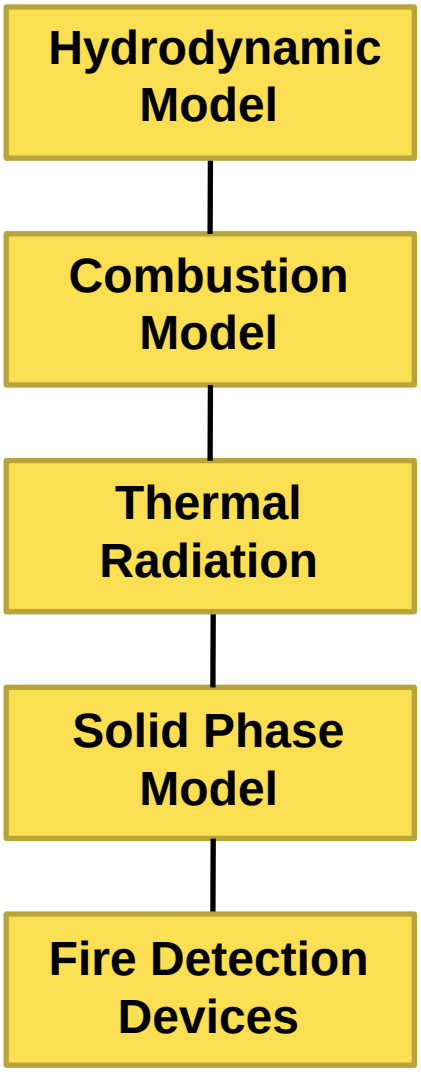

Notes:

- The partial derivatives of the conservation equations of mass, momentum and energy are approximated as finite differences.
- The solution is updated in time on a three-dimensional, rectilinear grid.
- Thermal radiation is computed using a finite volume technique on the same grid as the flow solver.
- Lagrangian particles are used to simulate smoke movement, sprinkler discharge, and fuel sprays.

http://code.google.com/p/fds-smv/

Fire Model – Fuel locations

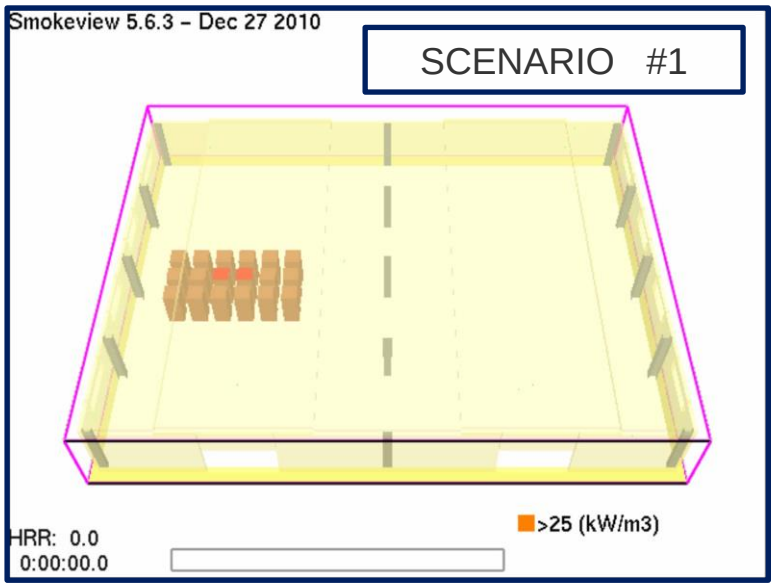

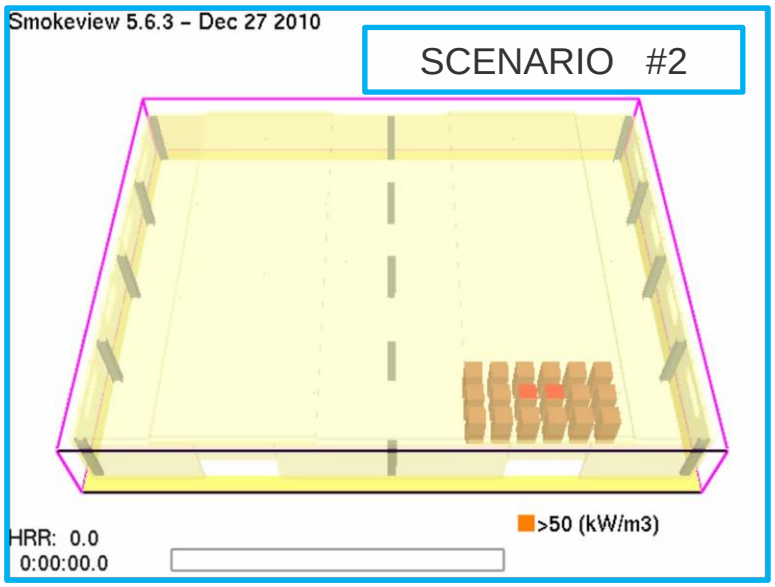

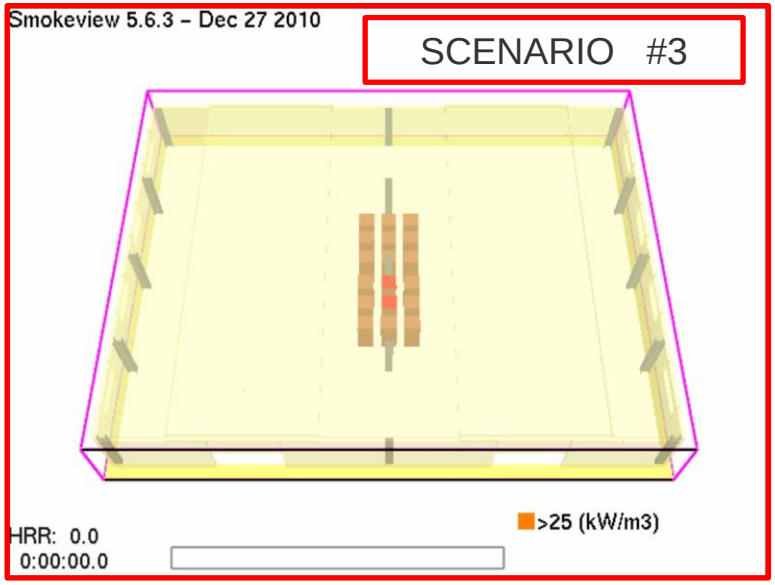

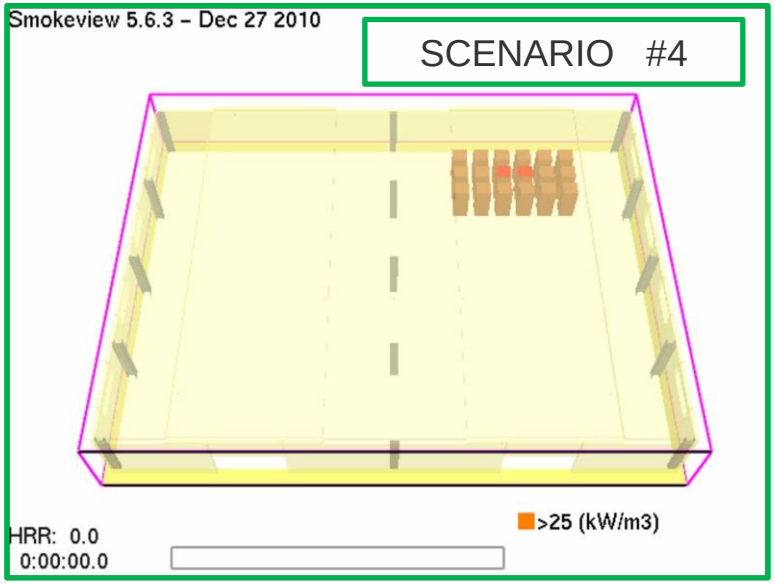

Fire Model – Ventilation conditions

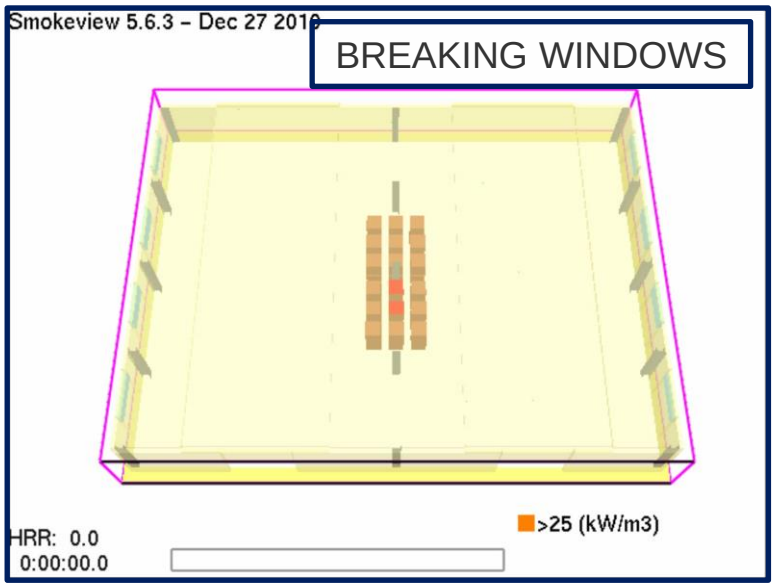

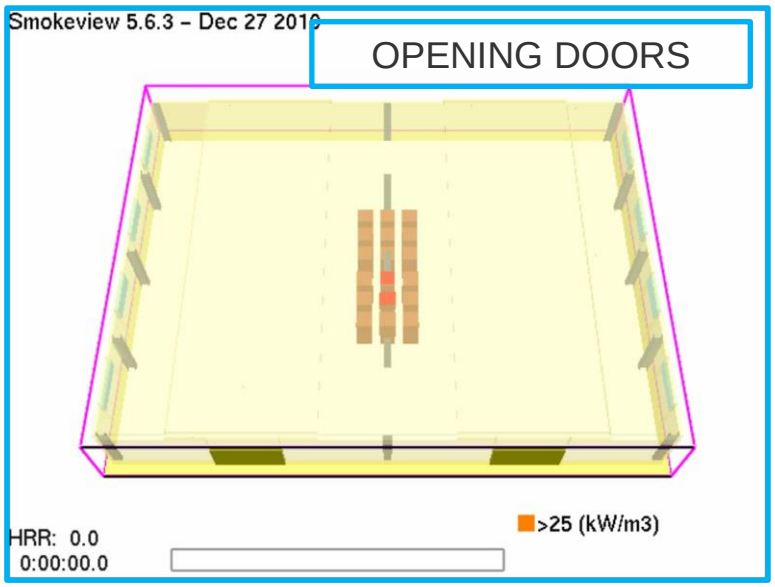

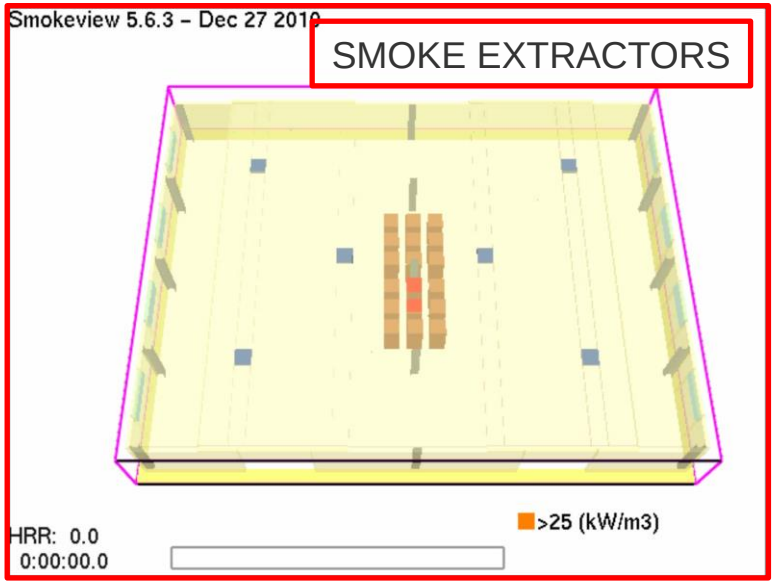

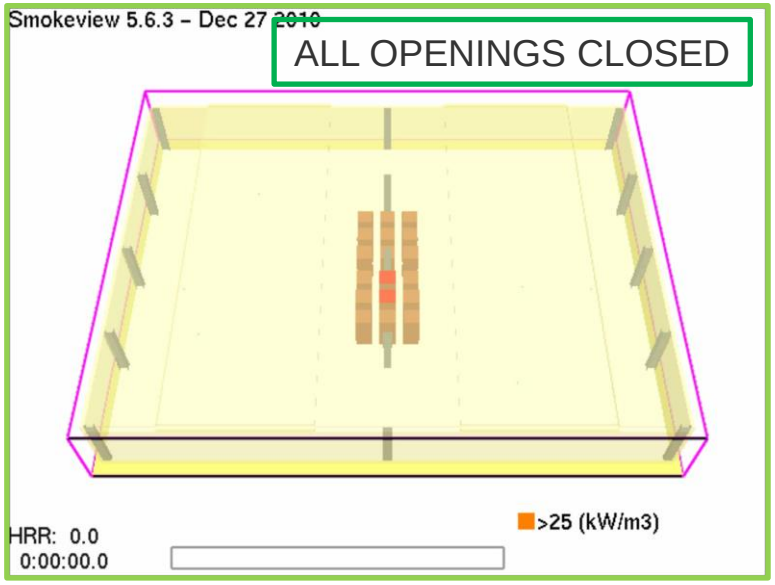

Fire Model

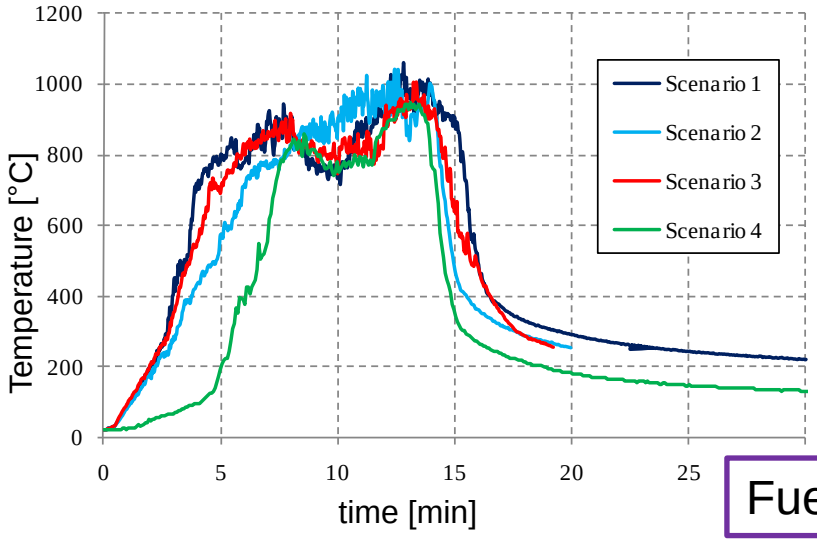

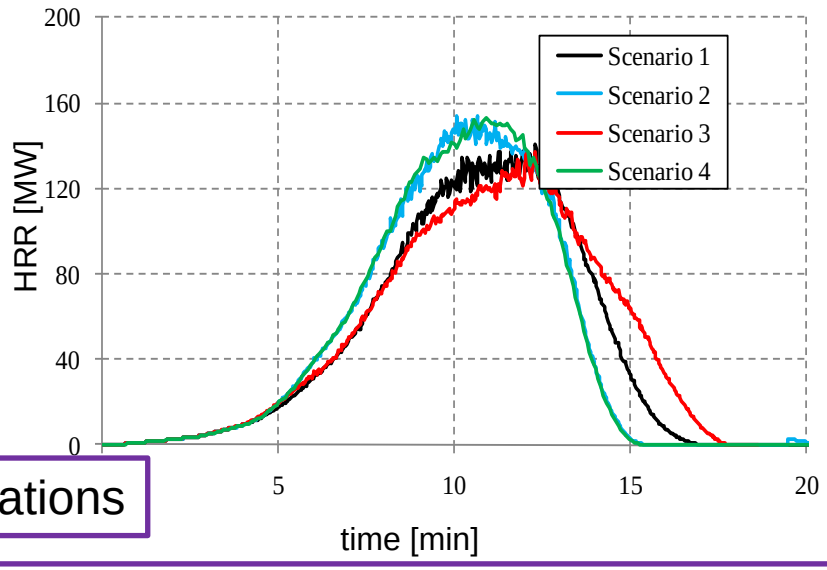

Fuel Locations

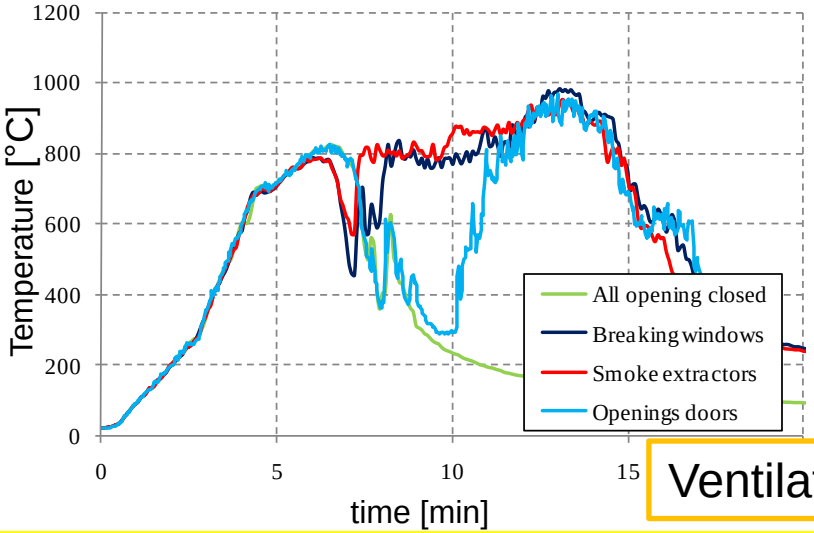

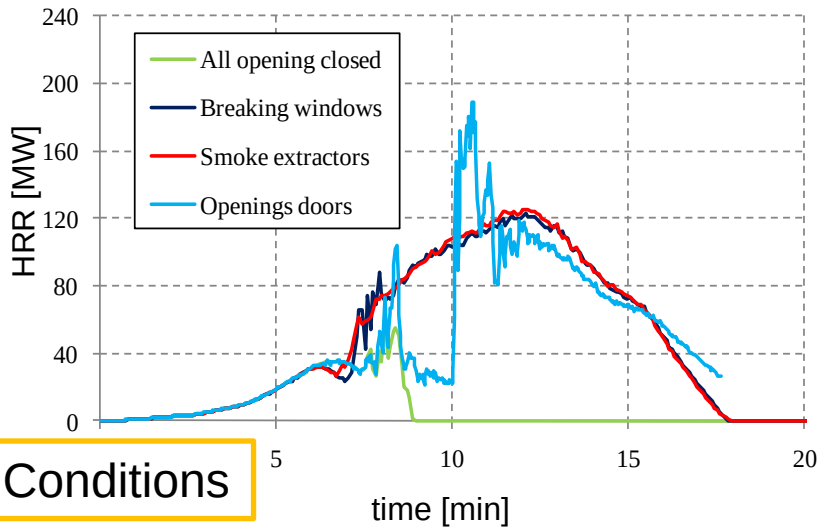

Ventilation Conditions

Fire Model – Mesh optimization

dx	%D*	D*/Dx	Number of cells
0.3	0.039	25.31	298080
0.4	0.052	18.98	126360
0.5	0.065	15.18	64512
0.6	0.075	12.65	38880

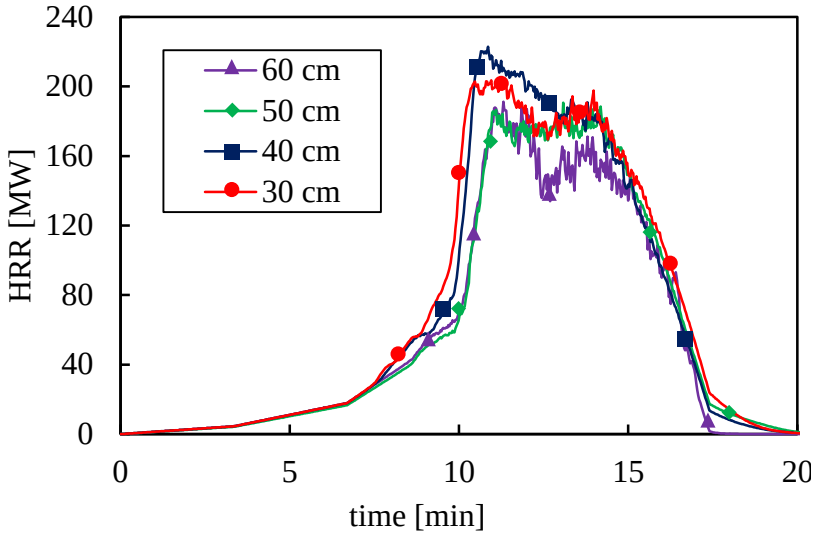

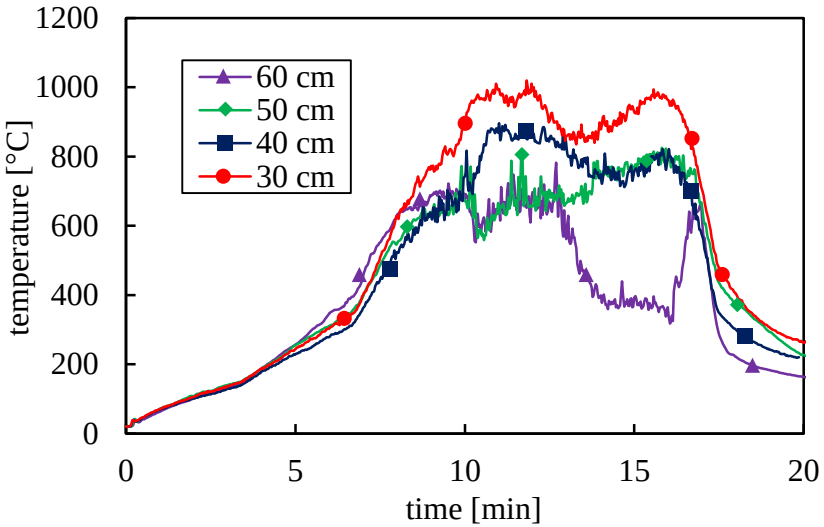

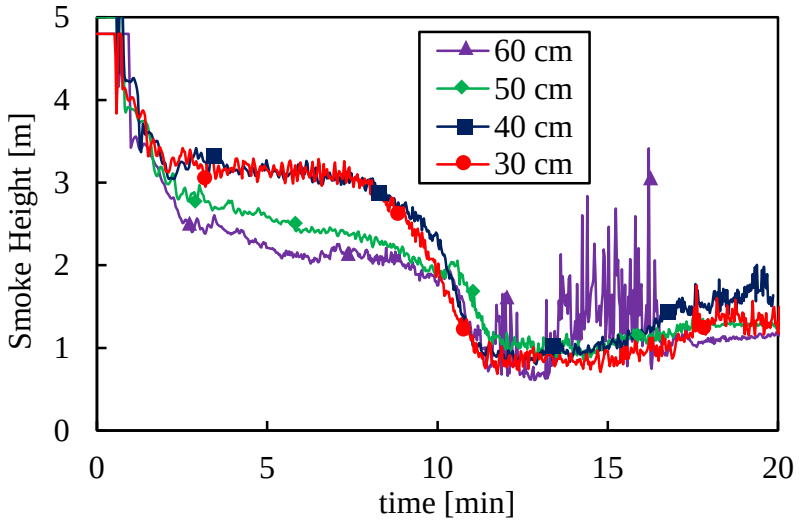

Fire Model – Fuel involvement

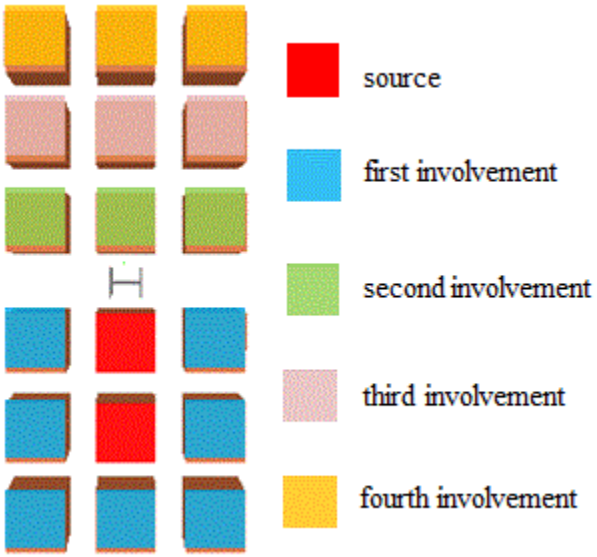

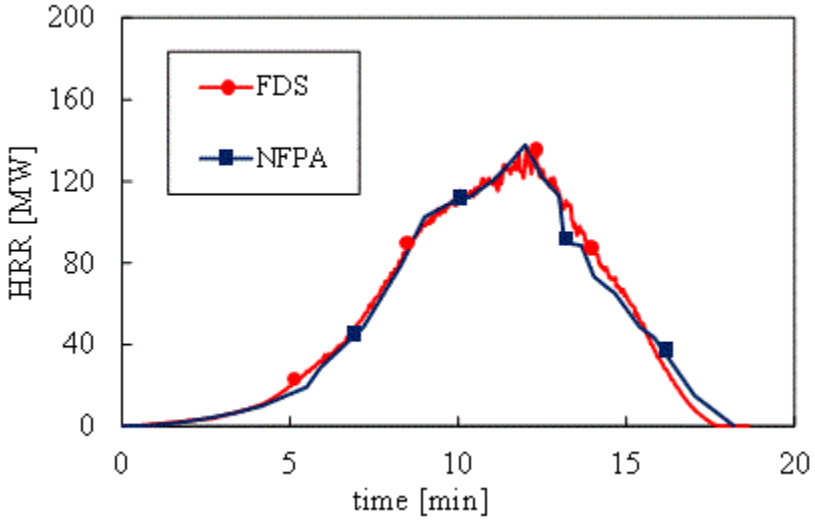

NFPA CRITERION — Heat Release Rate

$$HRR_{\min} = 30 \cdot \frac{(d + 0.05)}{0.019}$$

FDS CRITERION — Temperature

$$T_{\min} = 275°C$$

Structural Response – Scenario 1

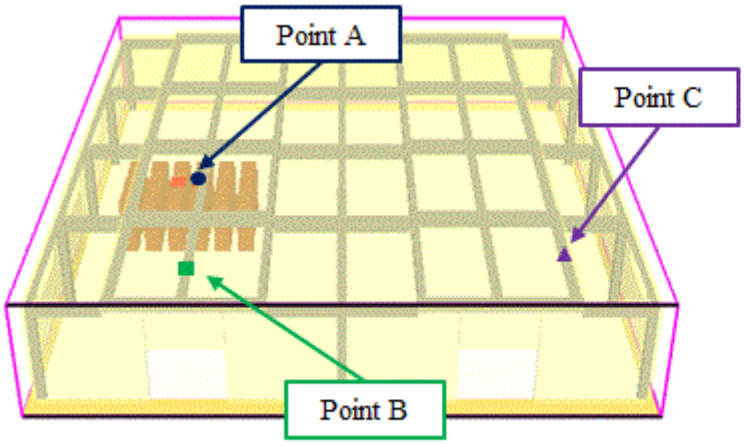

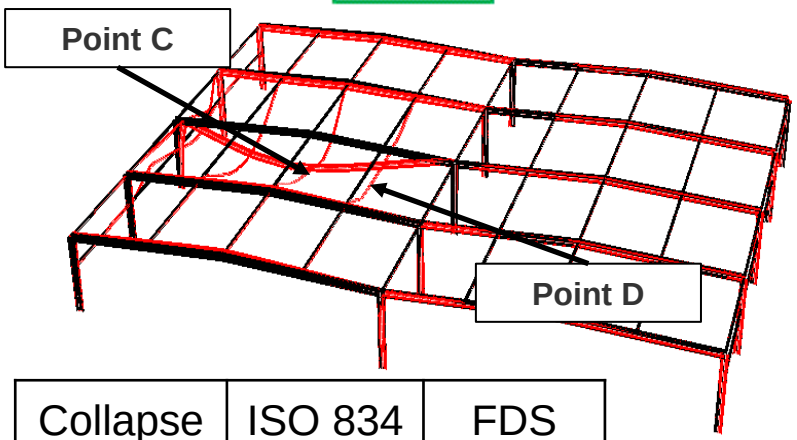

Collapse	ISO 834	FDS
Local	18 min	9 min
Global	22 min	9 min

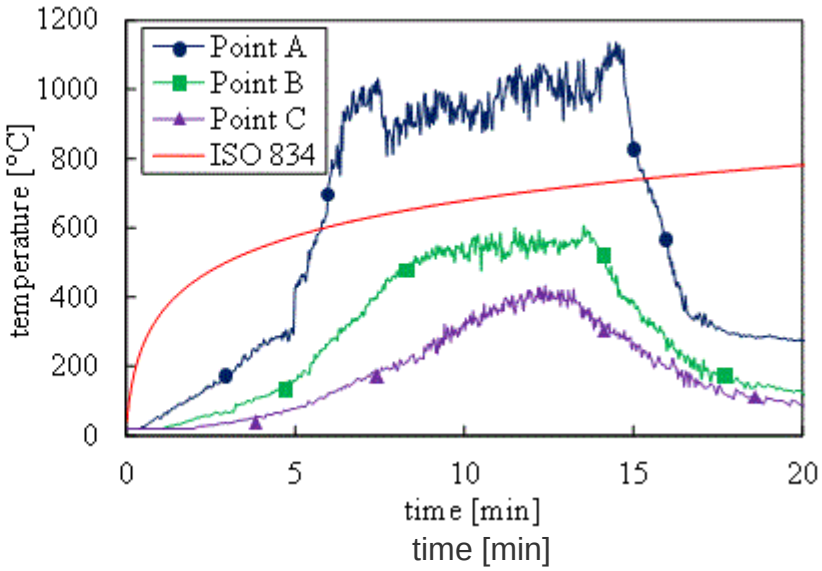

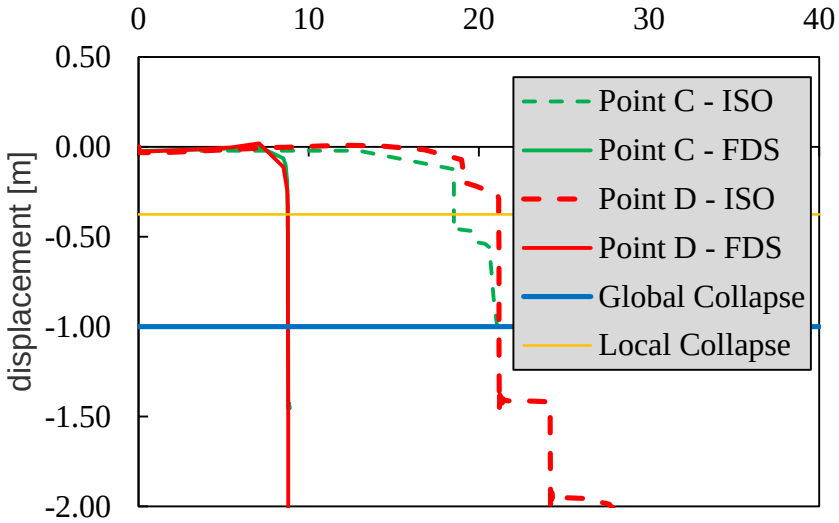

Gentili F. (in press), *Advanced numerical analyses for the assessment of steel structures under fire*, International Journal of Lifecycle Performance Engineering, Special Issue on Fire Safety Design and Robustness Considerations in Structural Engineering, Inderscience.

Case Study II

Floor area		
A_f	1200	m^2
Enclosure area		
A_t	3135	m^2
Opening factor		
O	0.055	$m^{0.5}$
Thermal Inertia		
b	1017	$W \cdot s^{0.5}/(K \cdot m^2)$

Fuel load density (enclosure)		
q	27	MJ/m^2
Fuel load density (floor)		
q_f	70	MJ/m^2
Total fuel load		
Q	84000	MJ
Fire growing rate		
α	0.156	kJ/s^3

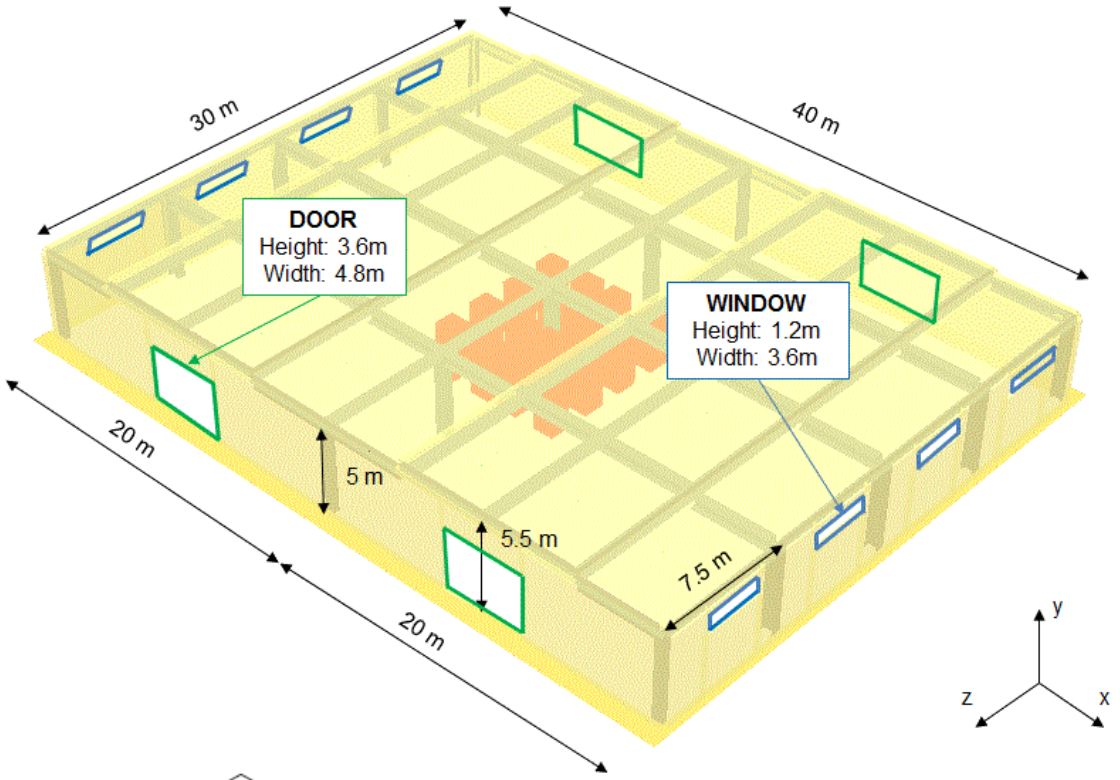

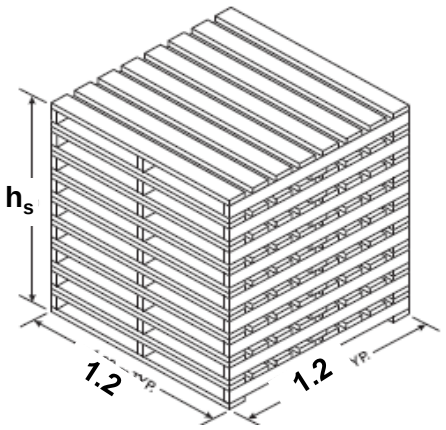

Stack height	3.0	m
No. of pallets in a stack	20	---
HRR_{max} of a stack	6.81	MW
No. stacks in the hall	16	---
$HRR_{max, tot}$	157	MW

Partial vs Complete Model

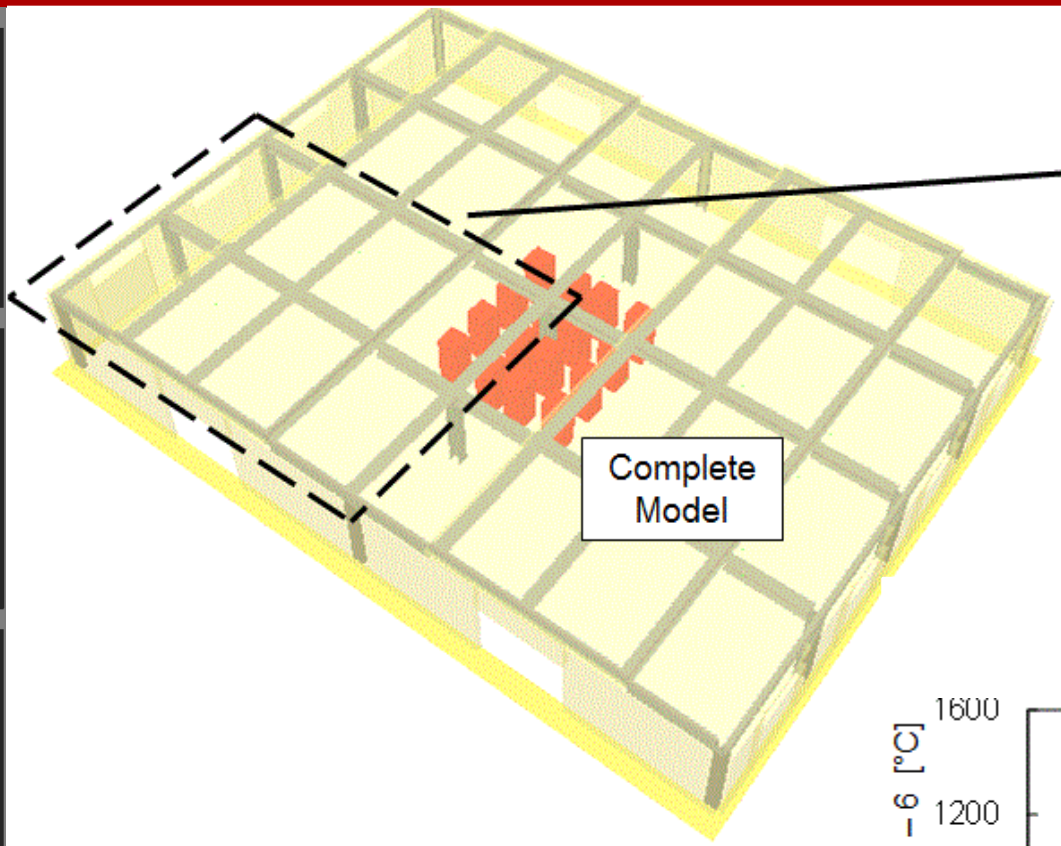

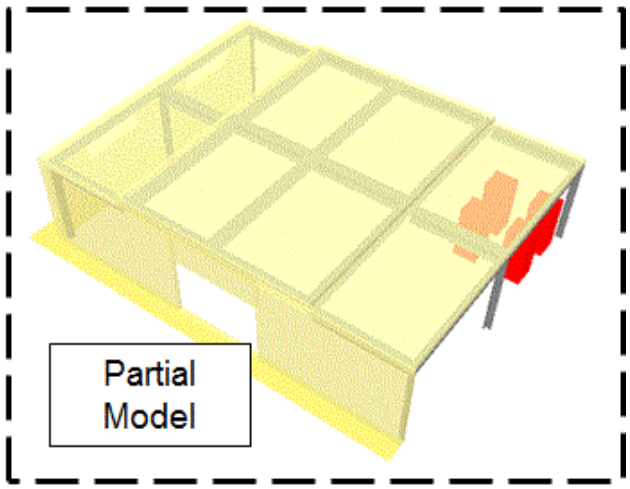

Model	Dimensions		
	X	Y	Z
Complete	40	30	6
Partial	20	15	6

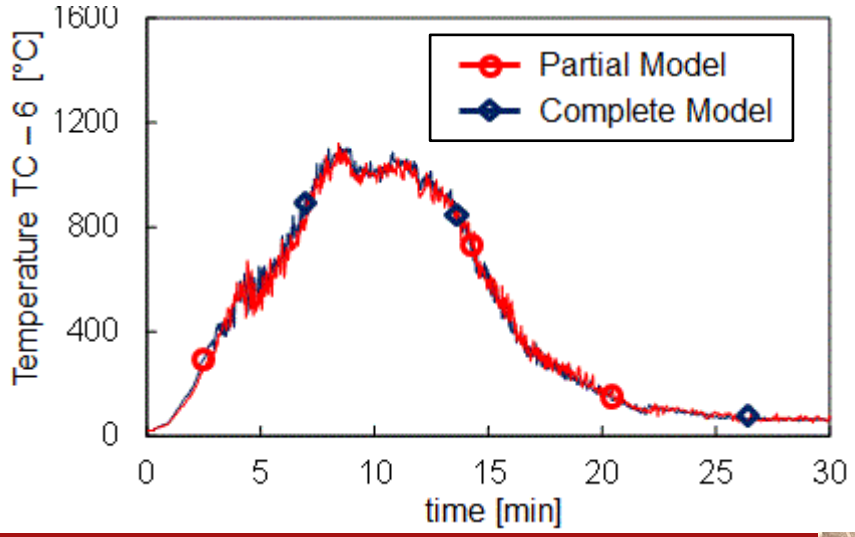

Combustible stacking

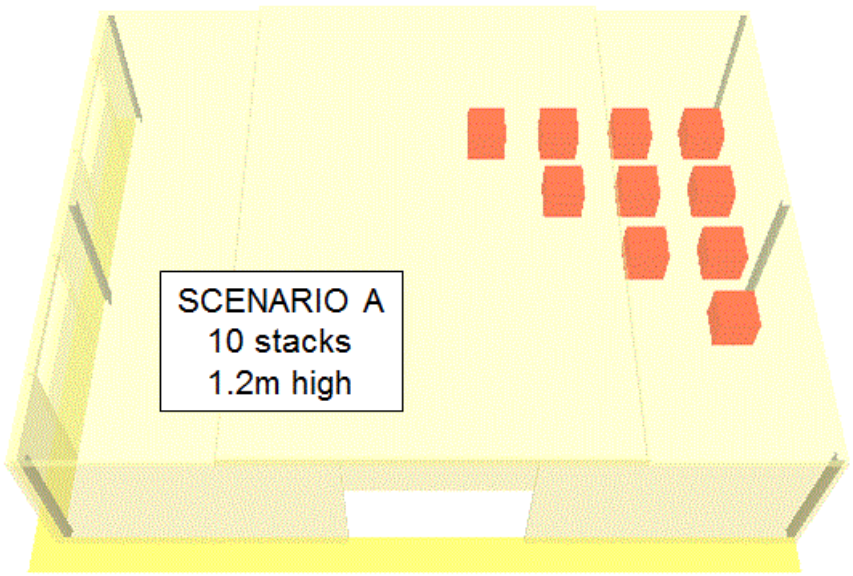

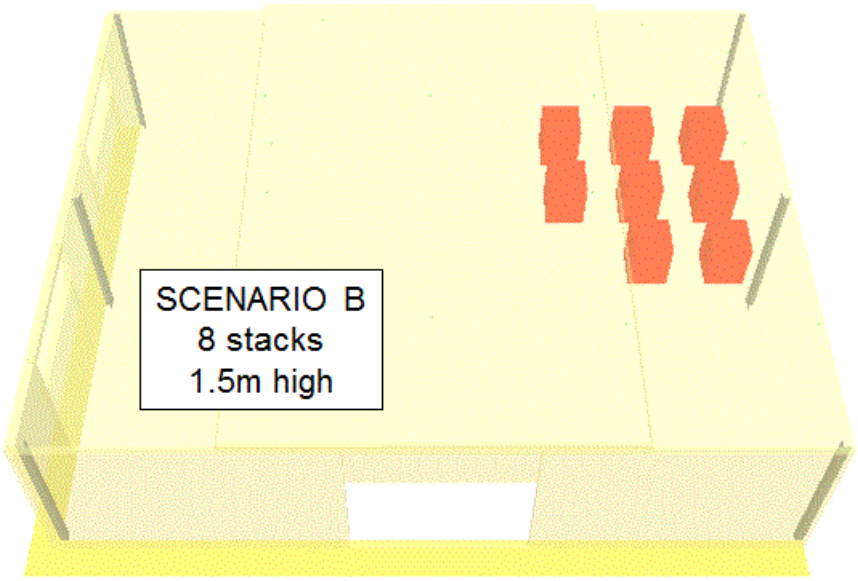

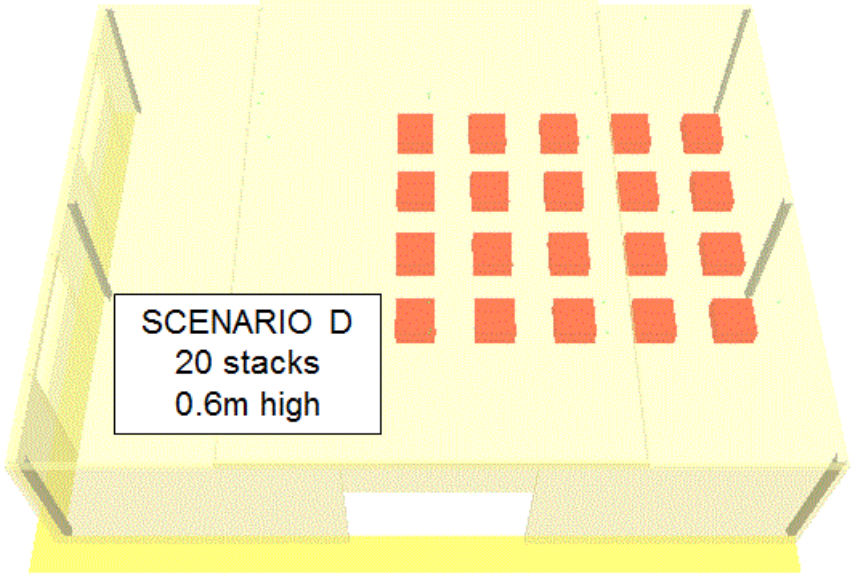

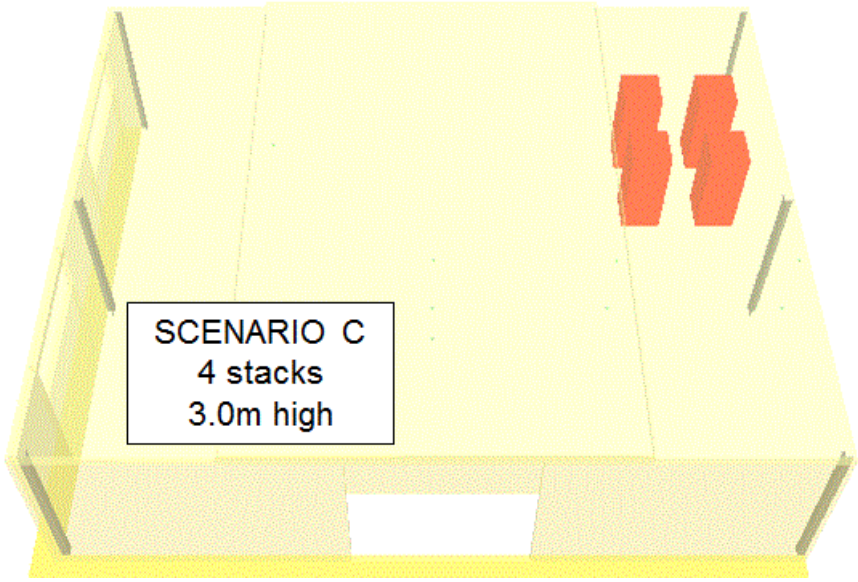

Combustible stacking

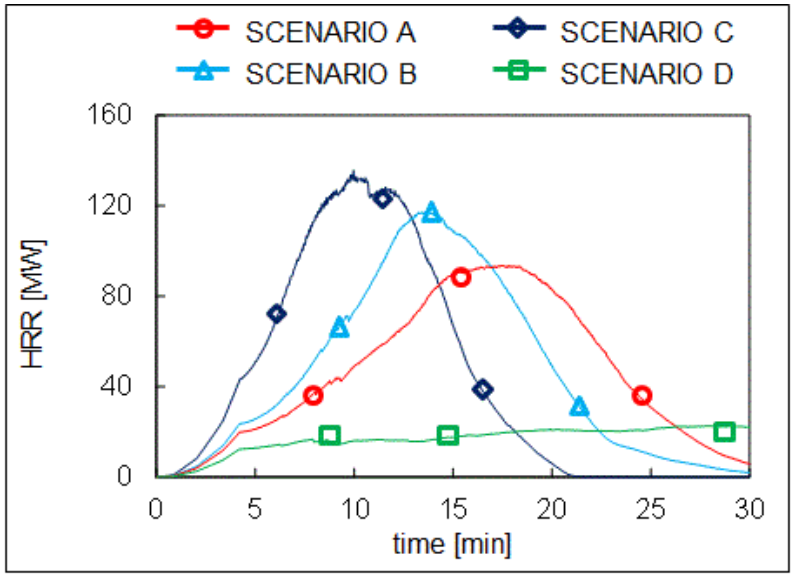

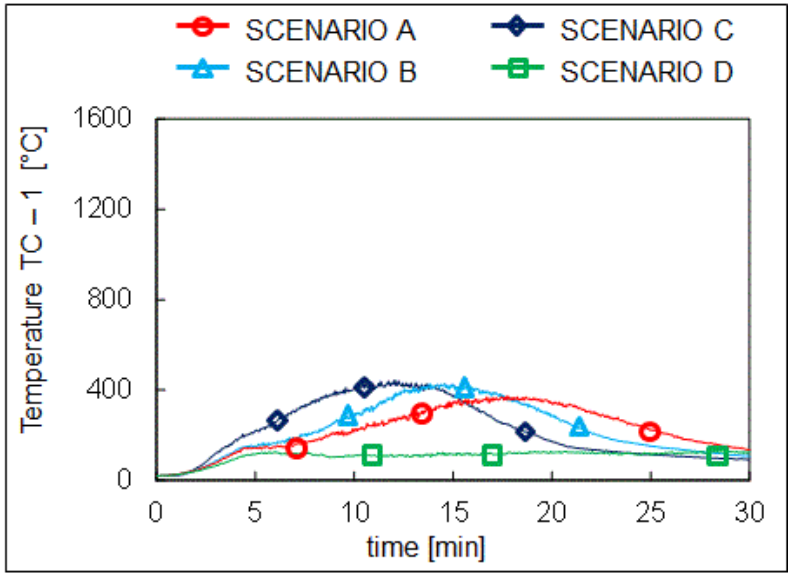

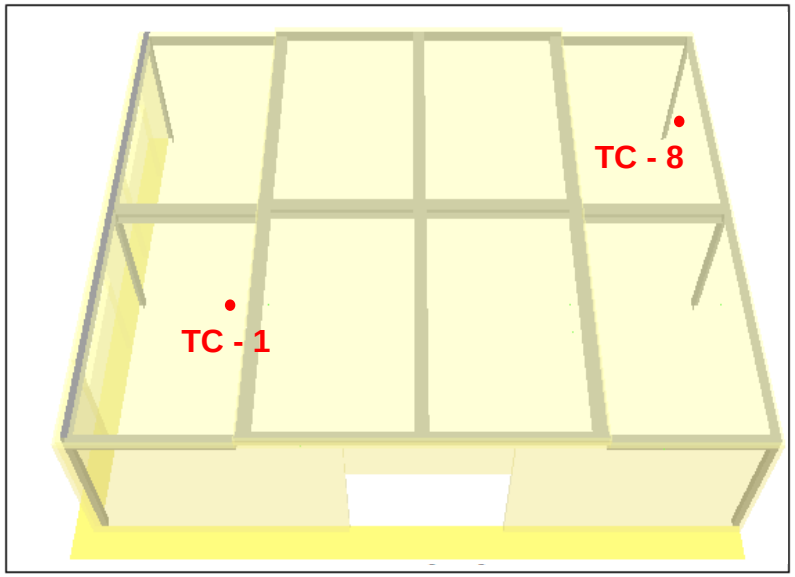

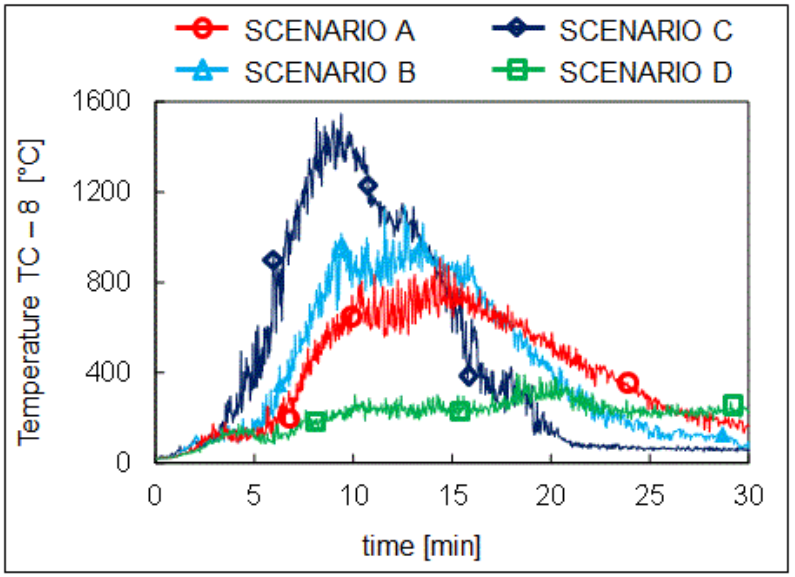

Travelling Fire (I)

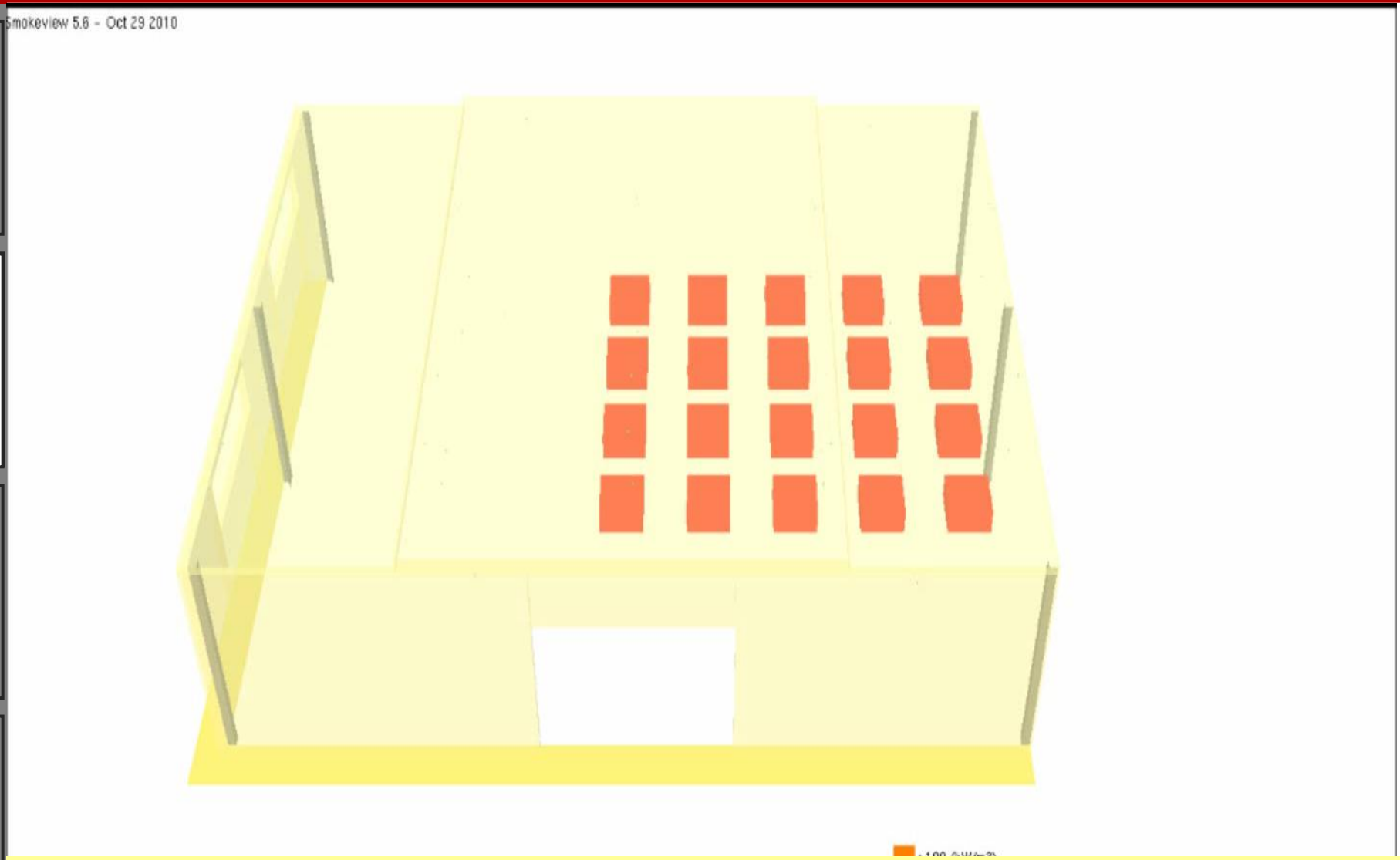

Gentili F, Giuliani L, Bontempi F. (in press), *Effects of combustible stacking in large compartments*, Journal of Structural Fire Engineering

Travelling Fire (II)

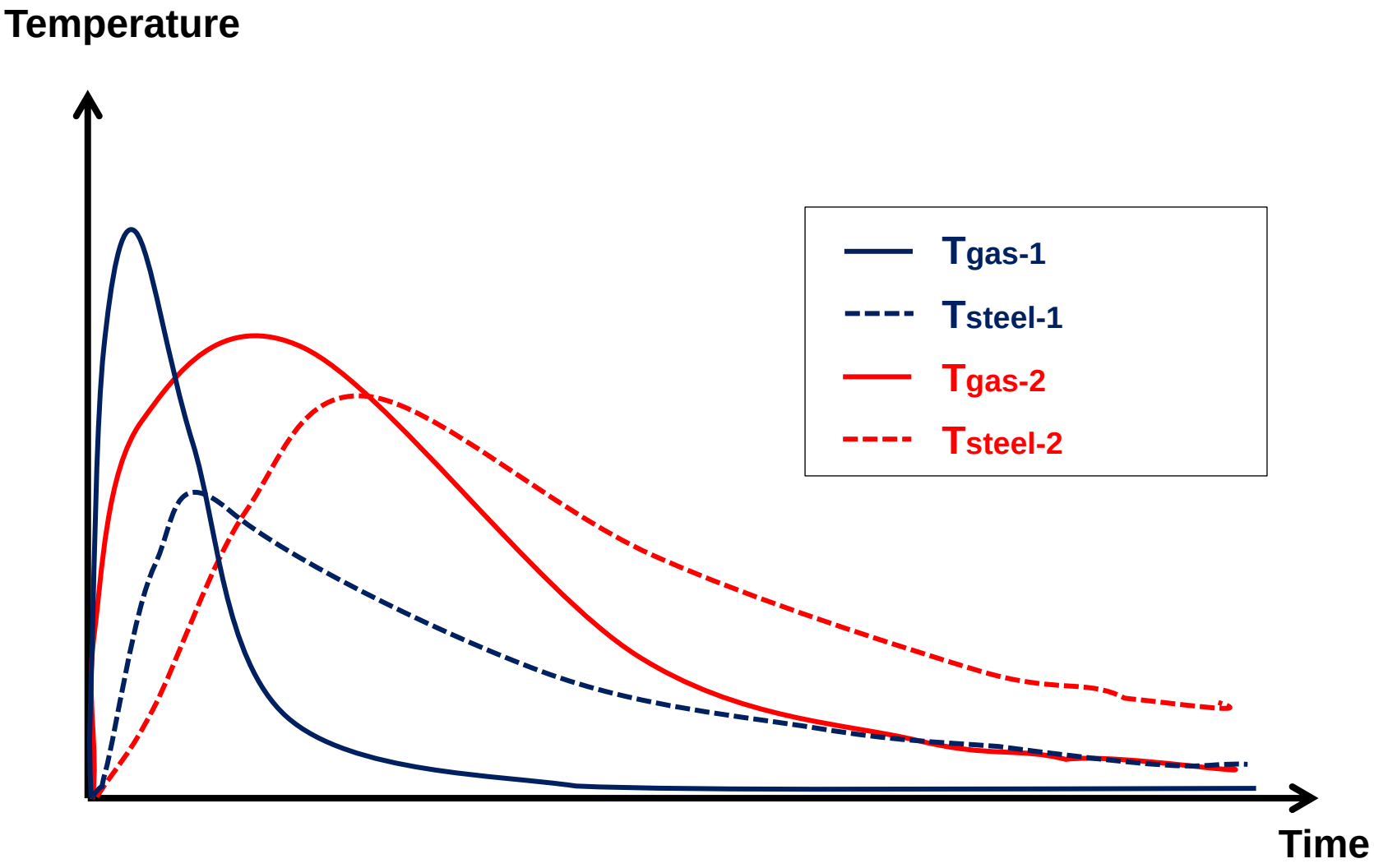

Introduction

Part I

Part II

Conclusions

Ph.D. Thesis Background

Fire Action

Structural Behaviour

Conclusive evaluations

Case study: 40 floors, 160 m heigth, 35 m x 35 m floor, office building

RENDERING

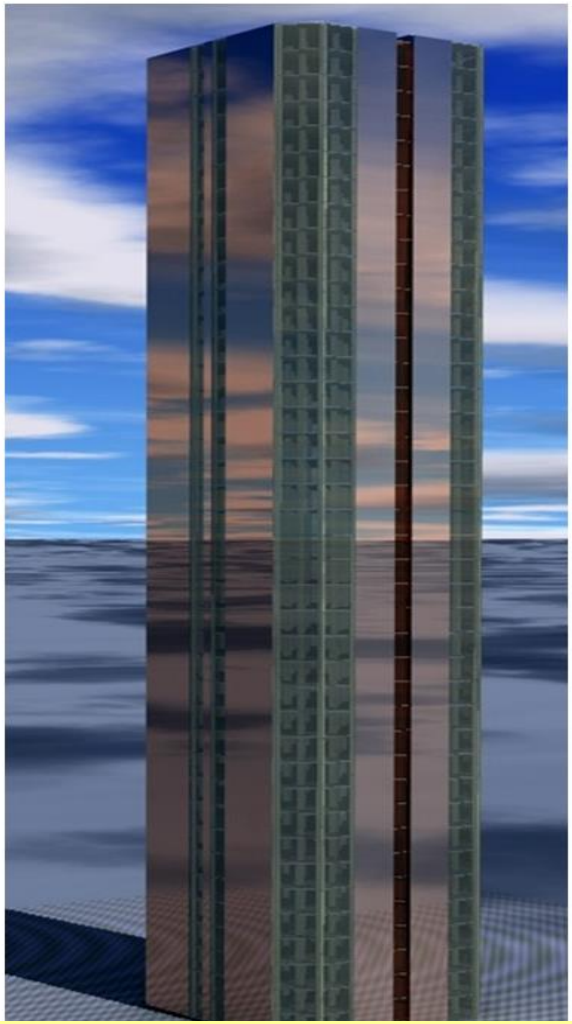

STRUCTURAL SYSTEM

FEM MODEL

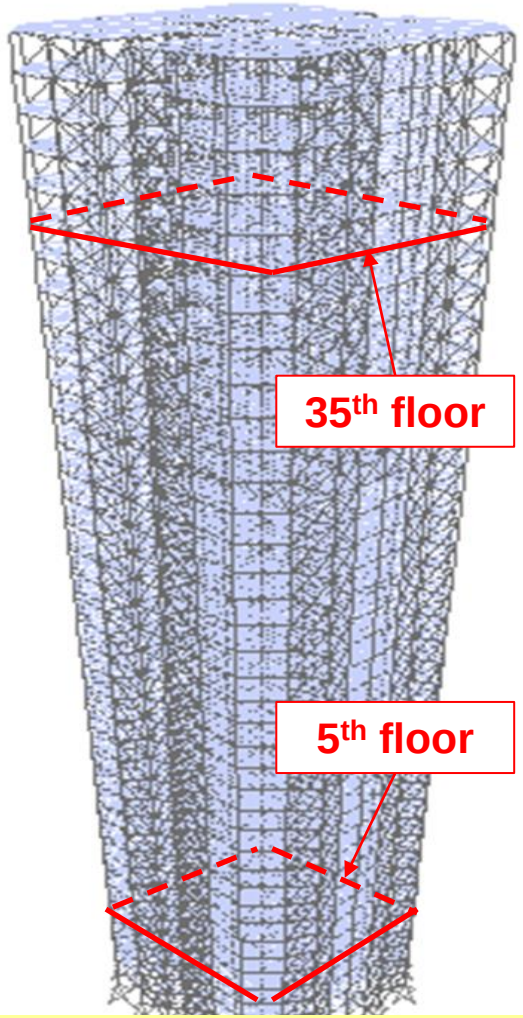

Gentili F, Giuliani L, Bontempi F. (in press), *Structural response of steel high rise buildings to fire: system characteristics and failure mechanisms*, Journal of Structural Fire Engineering

Case study: 40 floors, 160 m heigth, 35 m x 35 m floor, office building

Bracing System

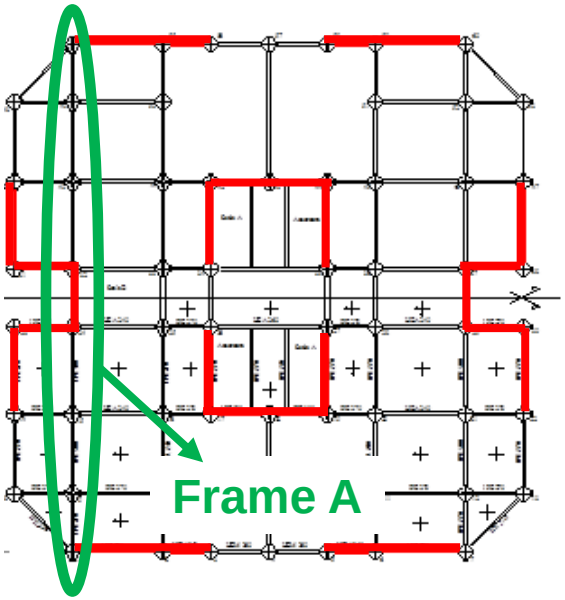

Outrigger

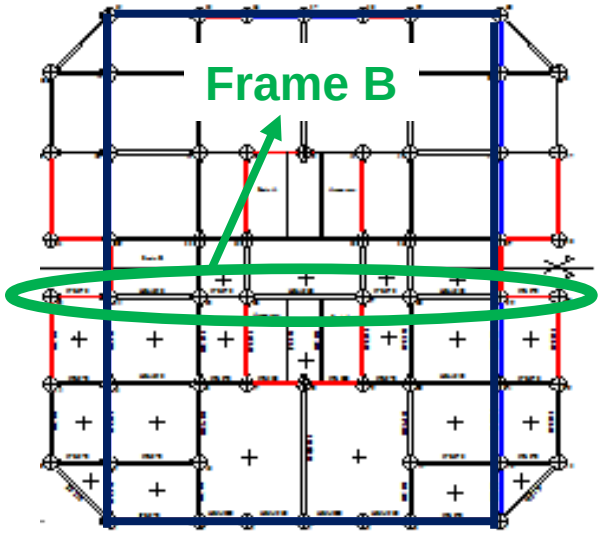

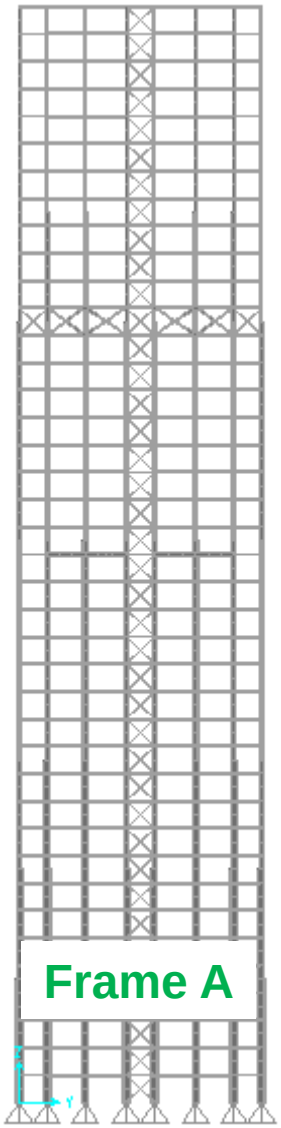

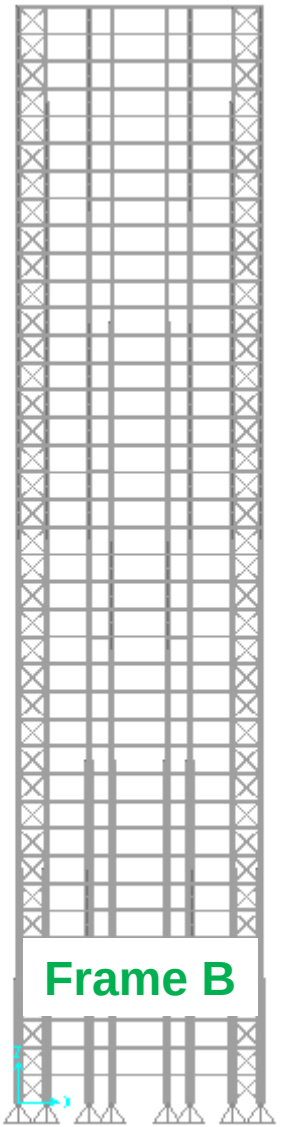

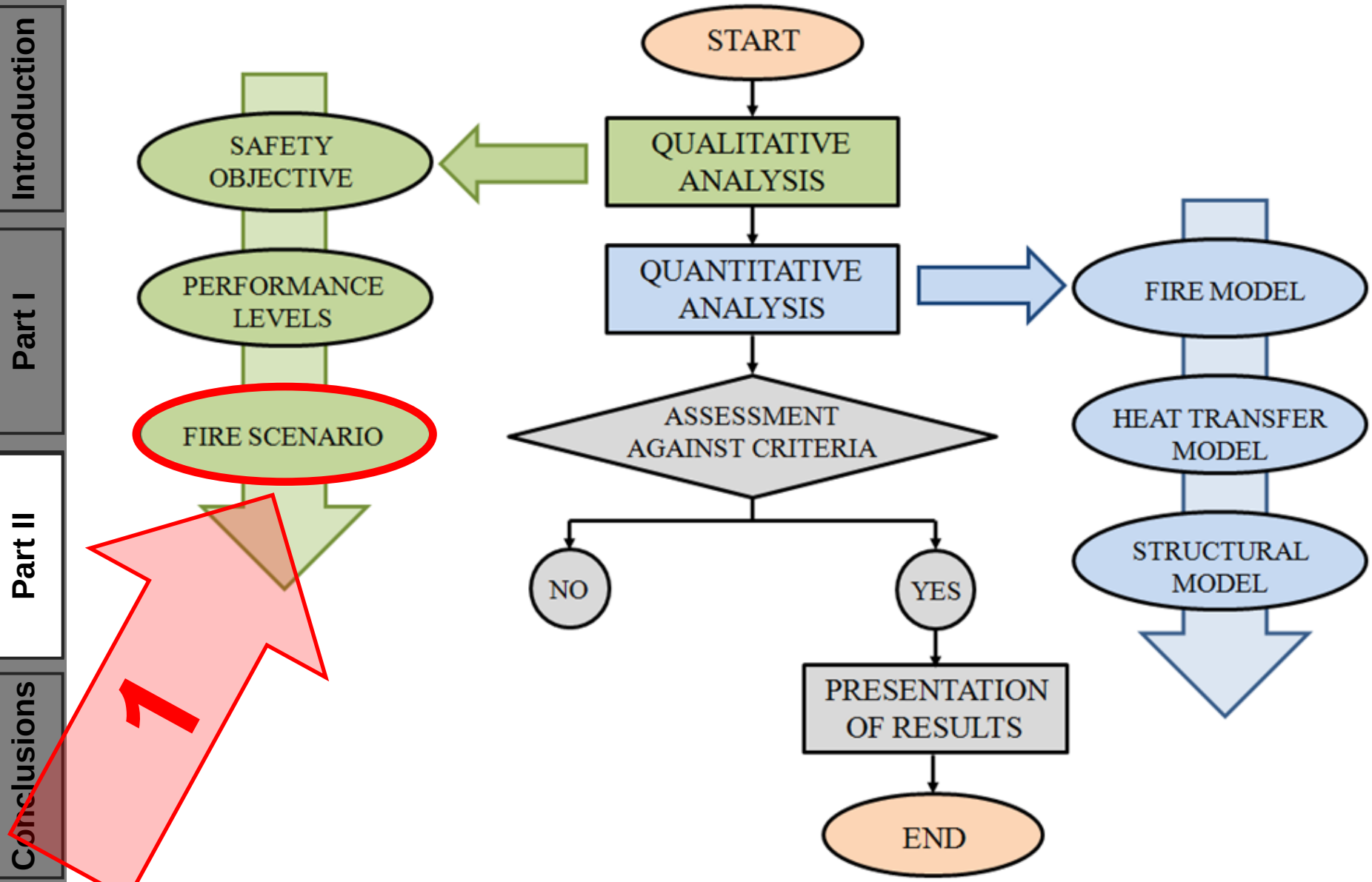
START
QUALITATIVE ANALYSIS
SAFETY OBJECTIVE
PERFORMANCE LEVELS
FIRE SCENARIO
QUANTITATIVE ANALYSIS
FIRE MODEL
HEAT TRANSFER MODEL
STRUCTURAL MODEL
ASSESSMENT AGAINST CRITERIA
NO
YES
PRESENTATION OF RESULTS
END
1

1 – Fire Scenarios: floors and height locations

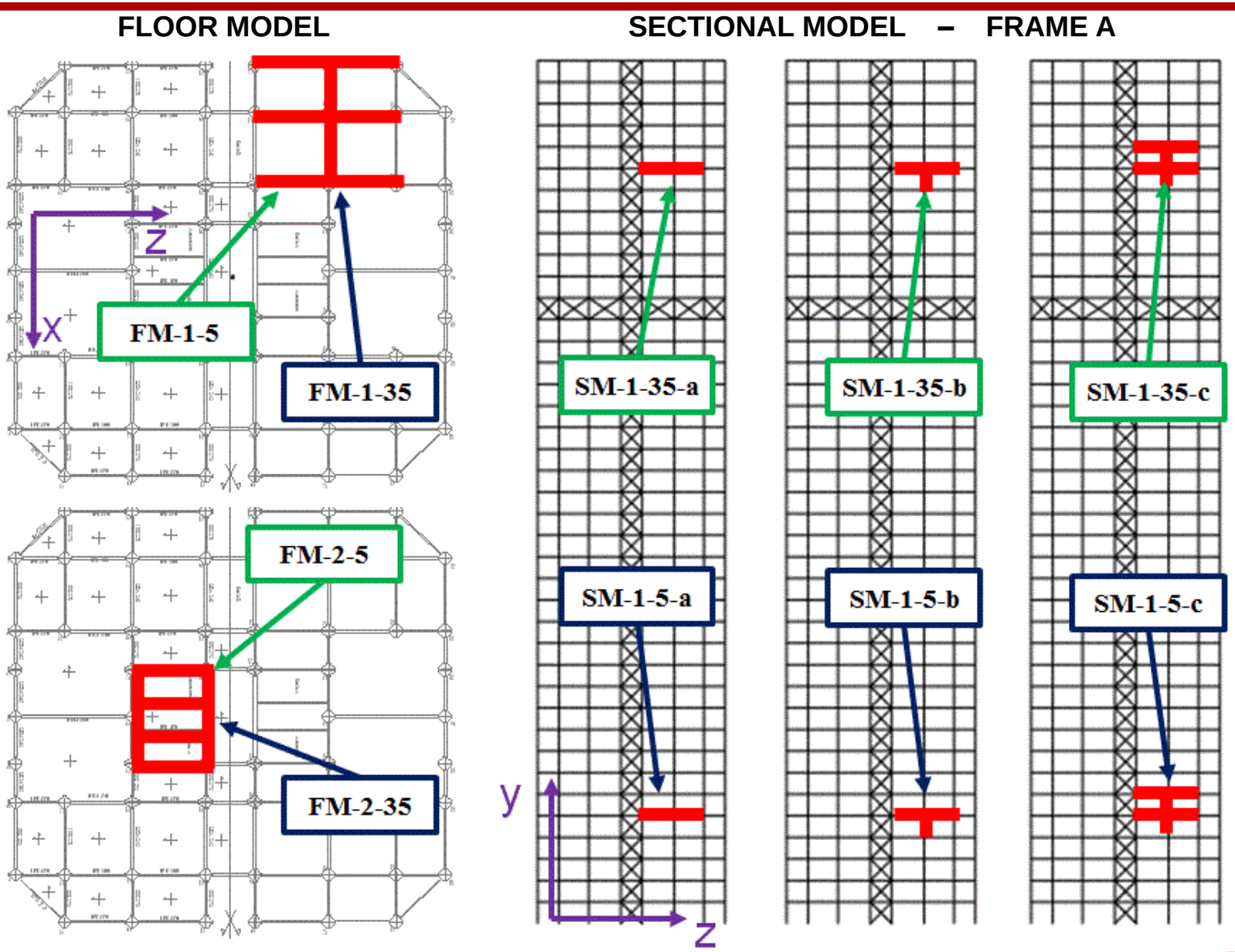

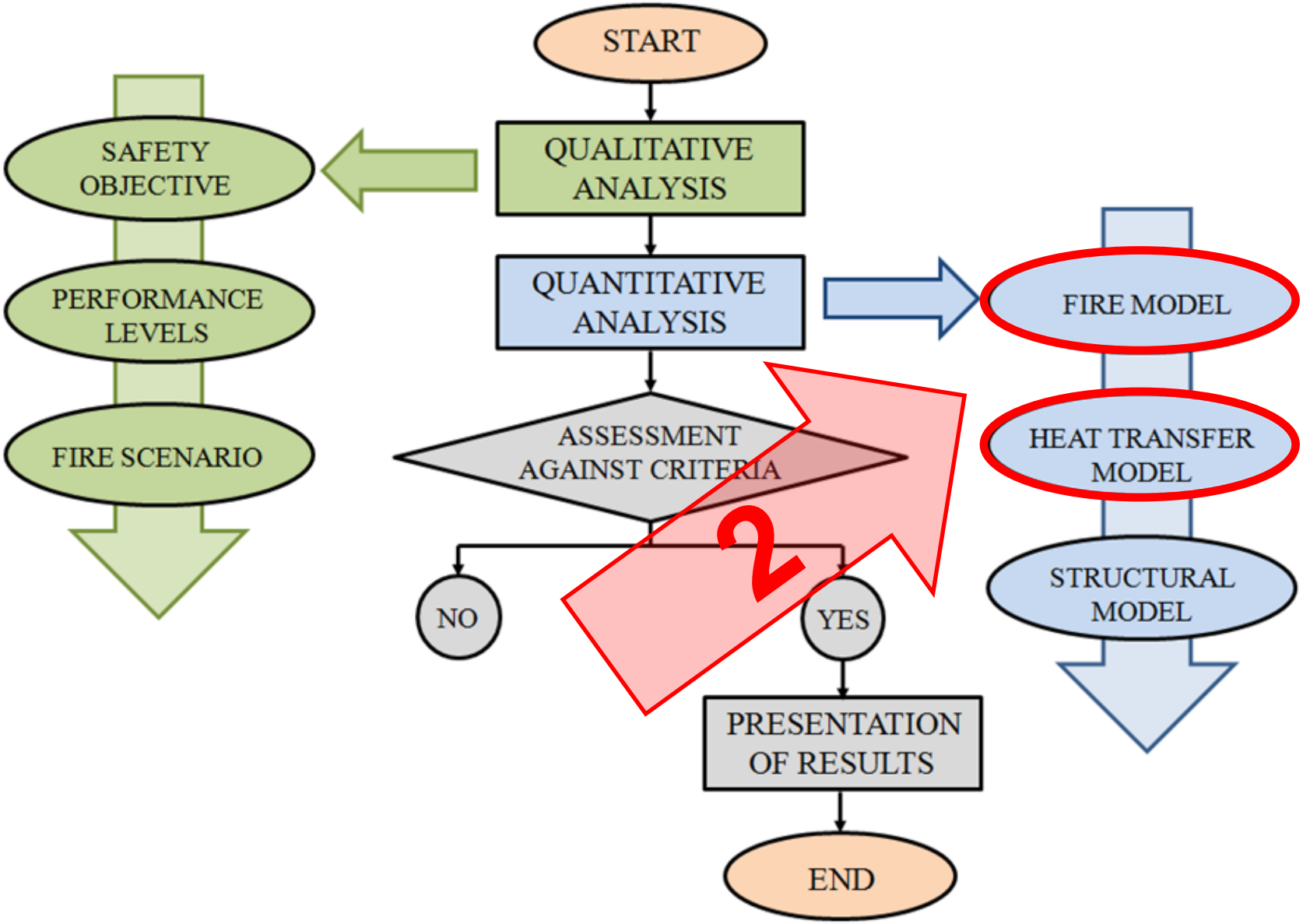
START
QUALITATIVE ANALYSIS
SAFETY OBJECTIVE
PERFORMANCE LEVELS
FIRE SCENARIO
QUANTITATIVE ANALYSIS
FIRE MODEL
HEAT TRANSFER MODEL
STRUCTURAL MODEL
ASSESSMENT AGAINST CRITERIA
NO
YES
2
PRESENTATION OF RESULTS
END

2 – Fire model and heat transfer model

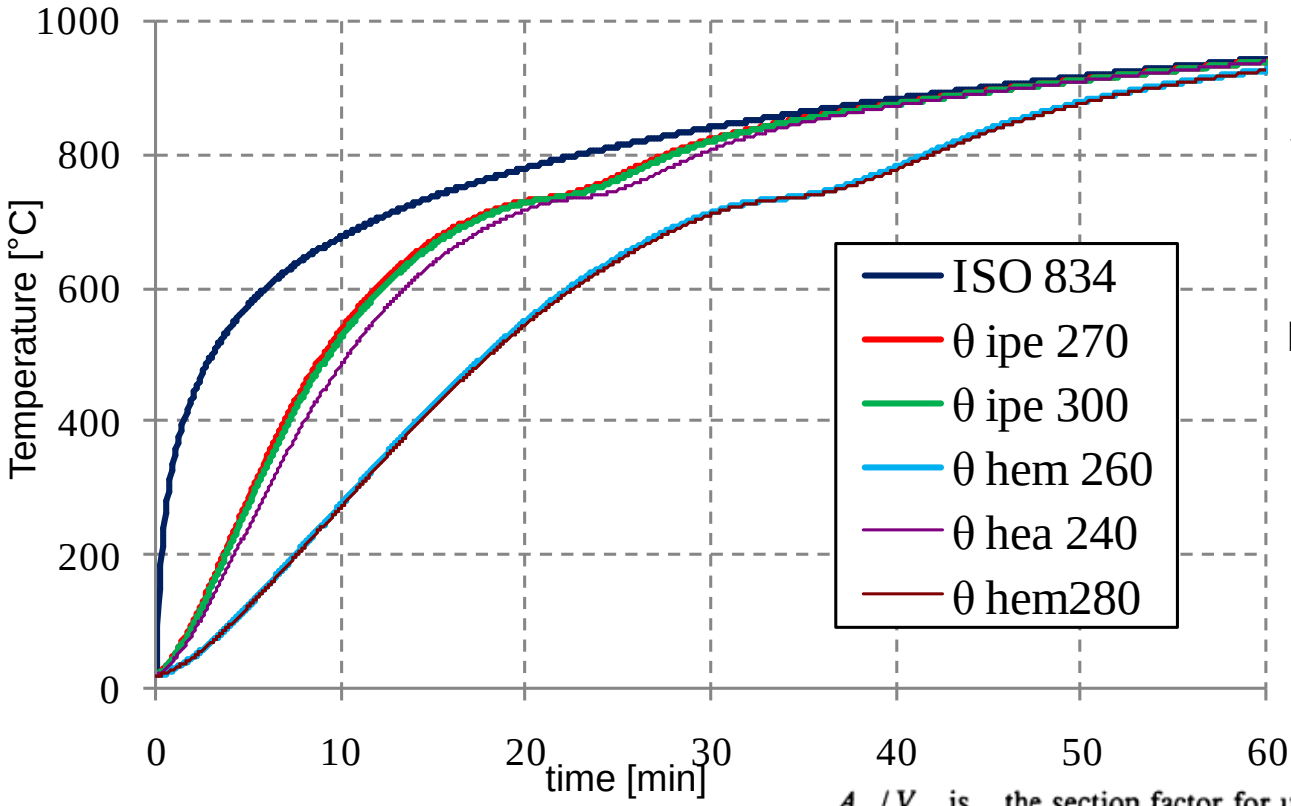

STEEL TEMPERATURE FOR UNPROTECTED BEAM
ENV 1993 – 1 – 2 : 1995

$$\Delta\theta_{a,t} = \frac{A_m/V}{c_a \cdot \rho_a} \cdot \dot{h}_{net,d} \cdot \Delta t$$

A_m / V	is	the section factor for unprotected steel members;
A_m	is	the exposed surface area of the member per unit length;
V	is	the volume of the member per unit length;
c_a	is	the specific heat of steel, from 3.3.1.2 [J/kgK];
$\dot{h}_{net,d}$	is	the design value of the net heat flux per unit area [W/m^2];
Δt	is	the time interval [seconds];
ρ_a	is	the unit mass of steel, from 3.2.2(1) [kg/m^3].

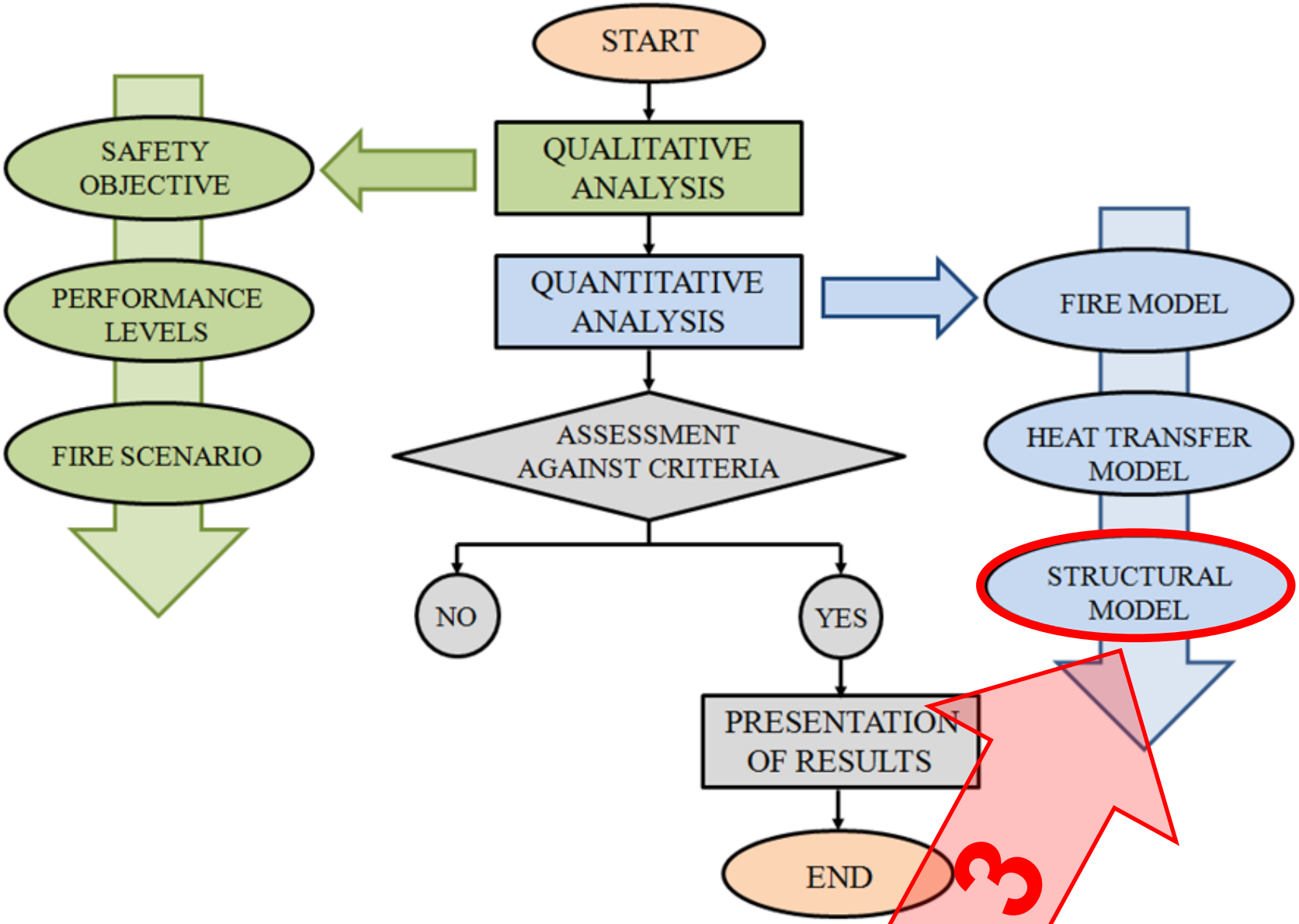
START
QUALITATIVE ANALYSIS
QUANTITATIVE ANALYSIS
ASSESSMENT AGAINST CRITERIA
NO
YES
PRESENTATION OF RESULTS
END
SAFETY OBJECTIVE
PERFORMANCE LEVELS
FIRE SCENARIO
FIRE MODEL
HEAT TRANSFER MODEL
STRUCTURAL MODEL
3

3 – Structural models: horizontal and vertical slice substructures

		Nodes	Elements	D.O.F.	
Model #1	**Floor model Single Storey**	2358	954	9556	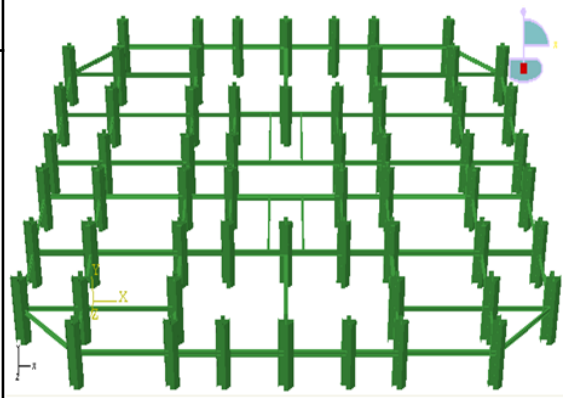
Model #2	**Sectional Model All Storeys**	**11477**	**3536**	**22638**	

		Nodes	Elements	D.O.F.	
Model #1	**Floor model Single Storey**	2358	954	9556	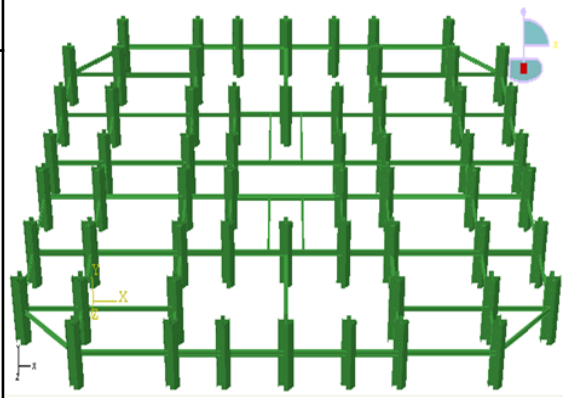

Scenario #2 – Beams

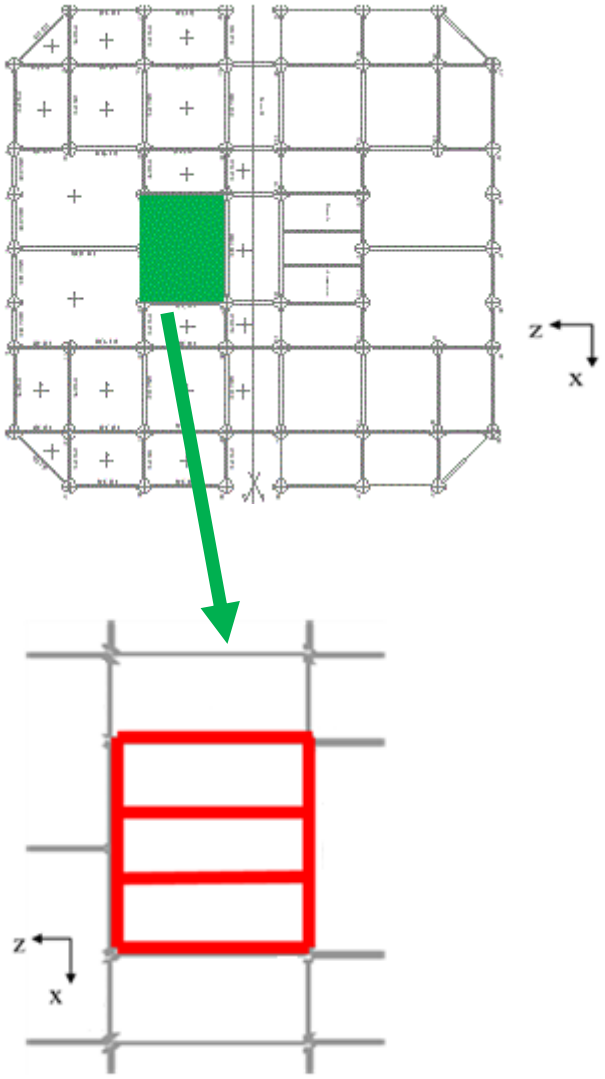

Deformed configuration: at 5th floor

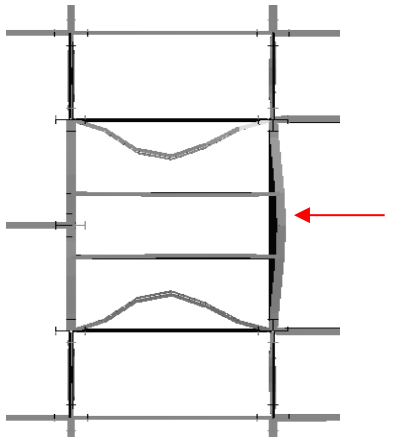

Deformed configuration at 35th floor

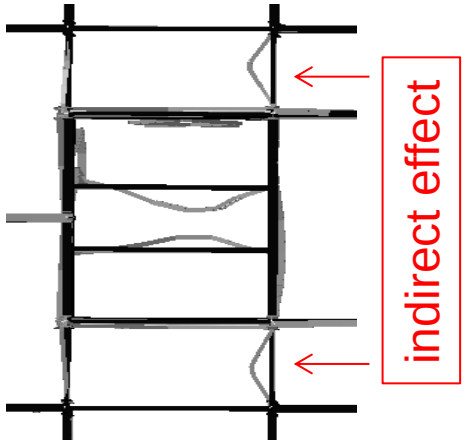

Progressive Collapse

Scenario #2 – Beams

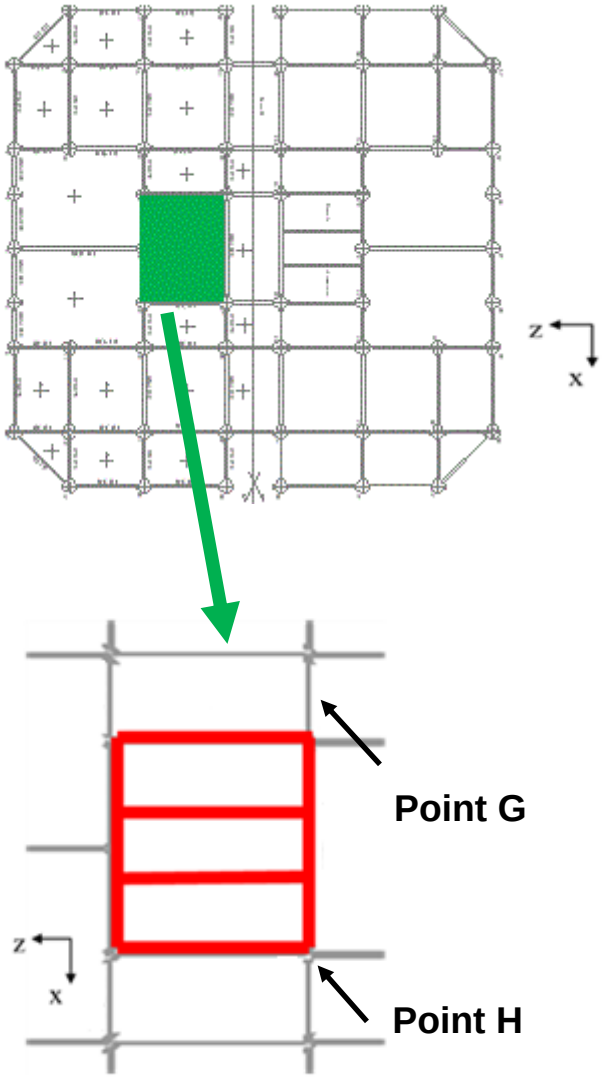

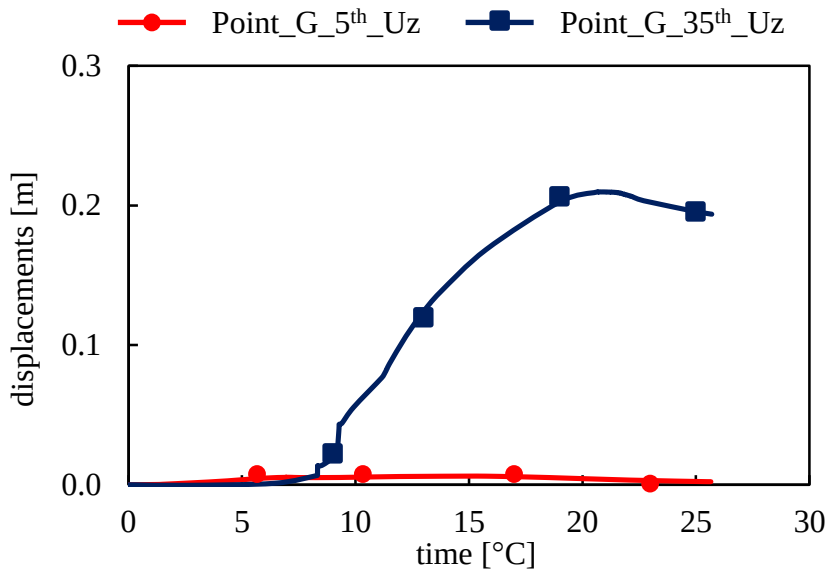

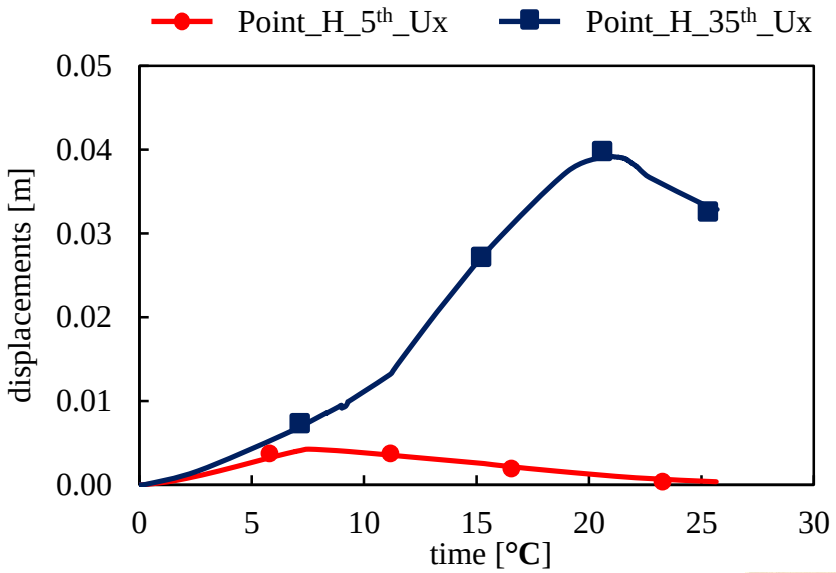

		Nodes	Elements	D.O.F.	
Model #2	Sectional Model All Storeys	11477	3536	22638	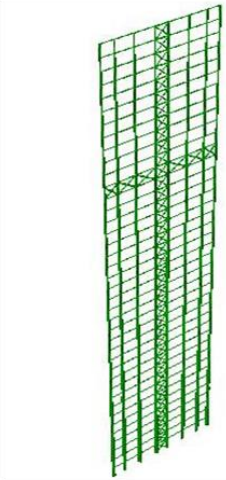

Fire involving one floor

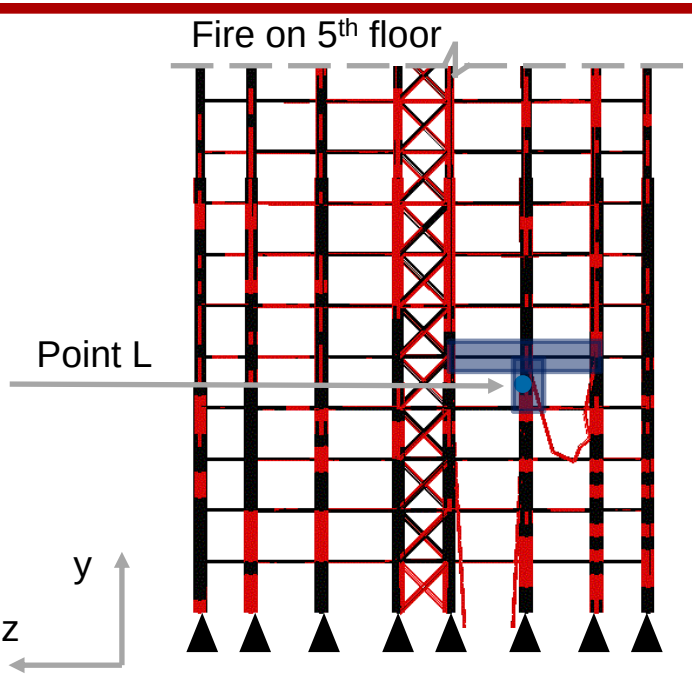

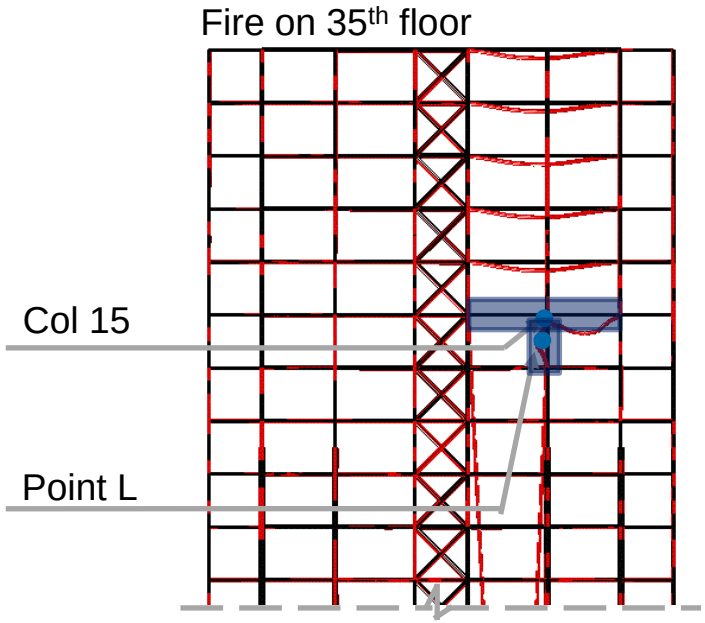

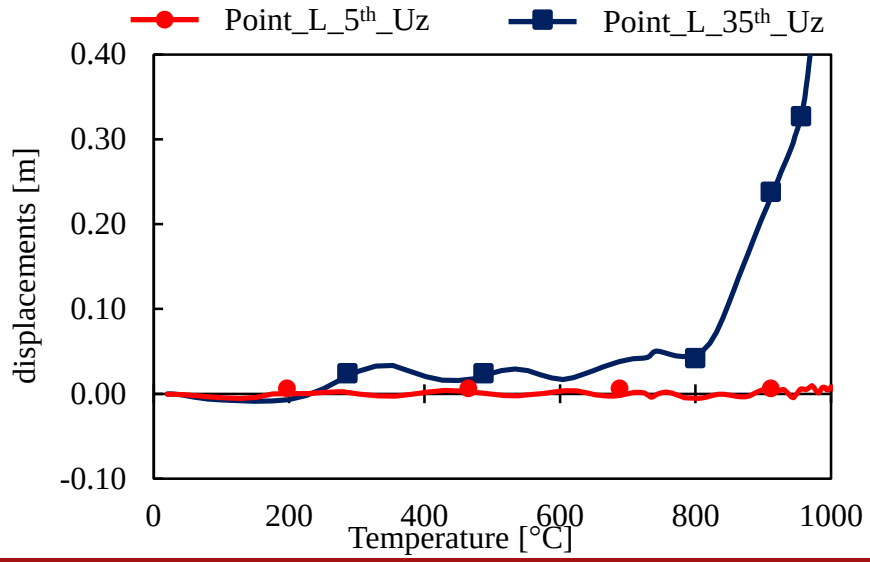

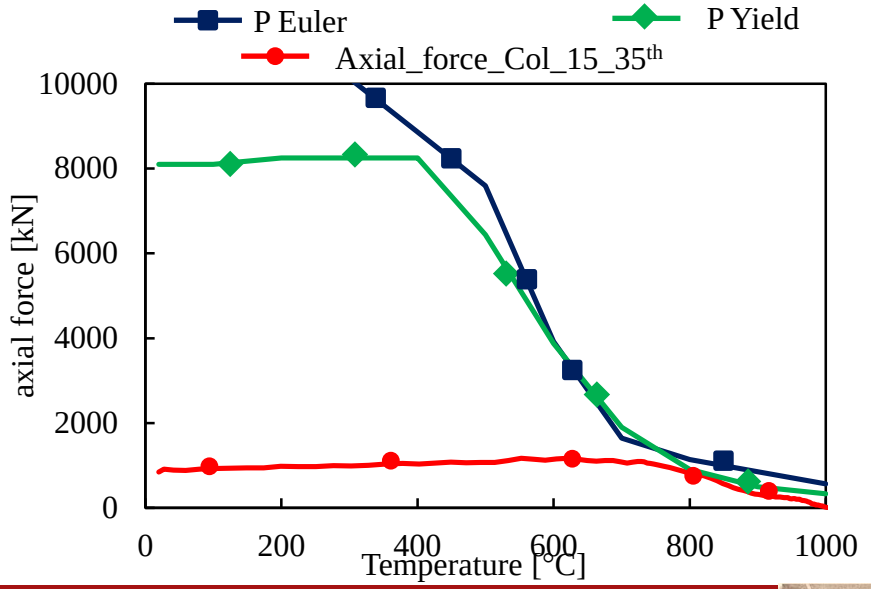

Fire involving one floor

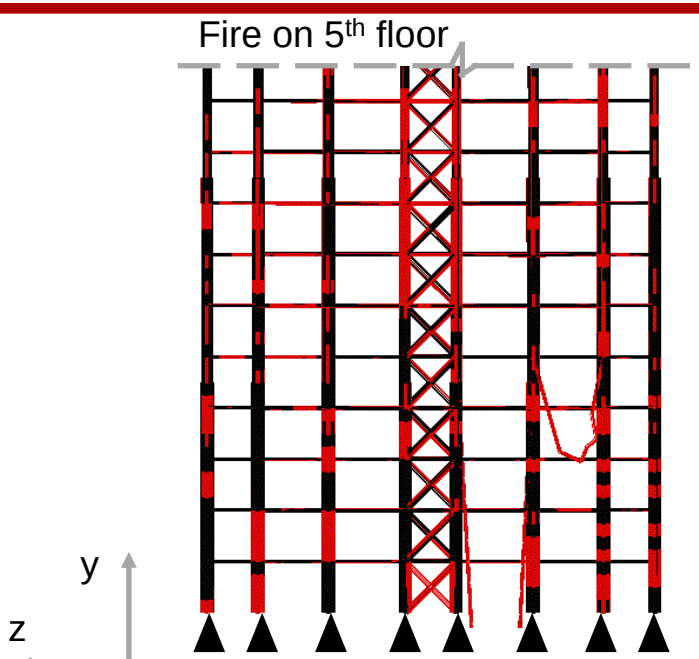

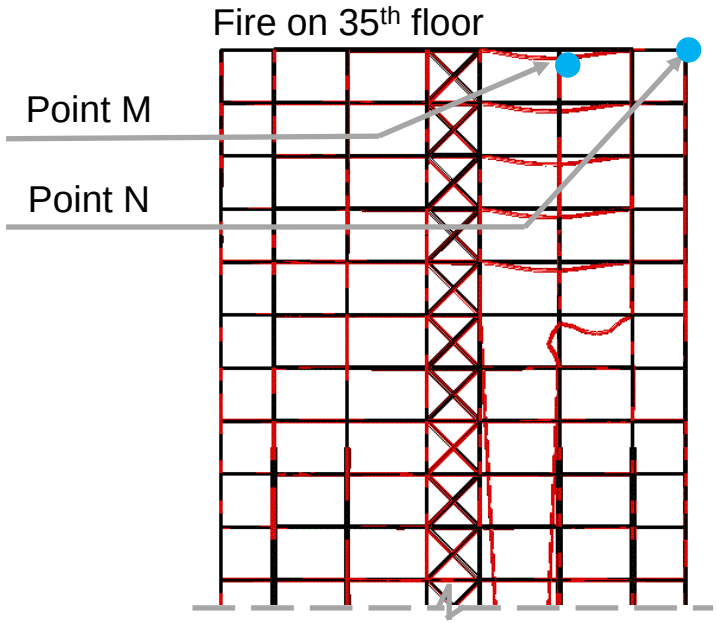

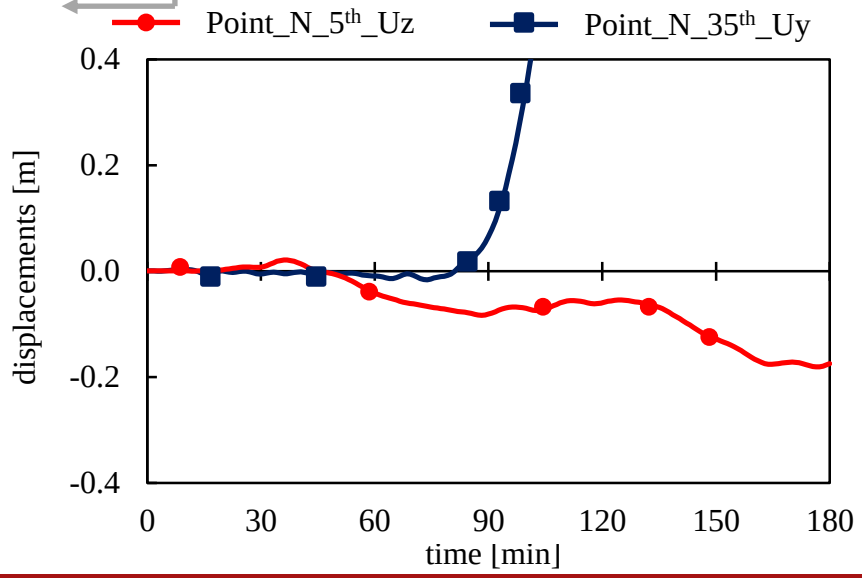

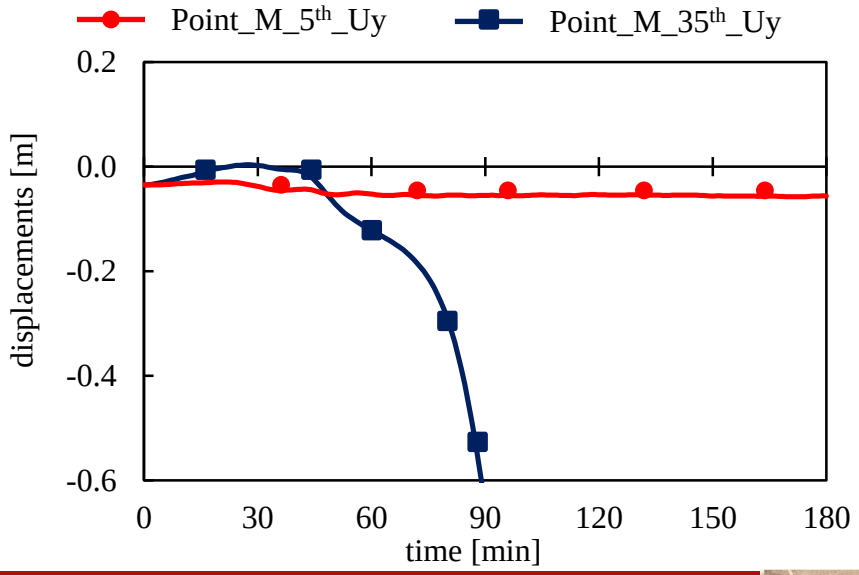

Fire involving two floors

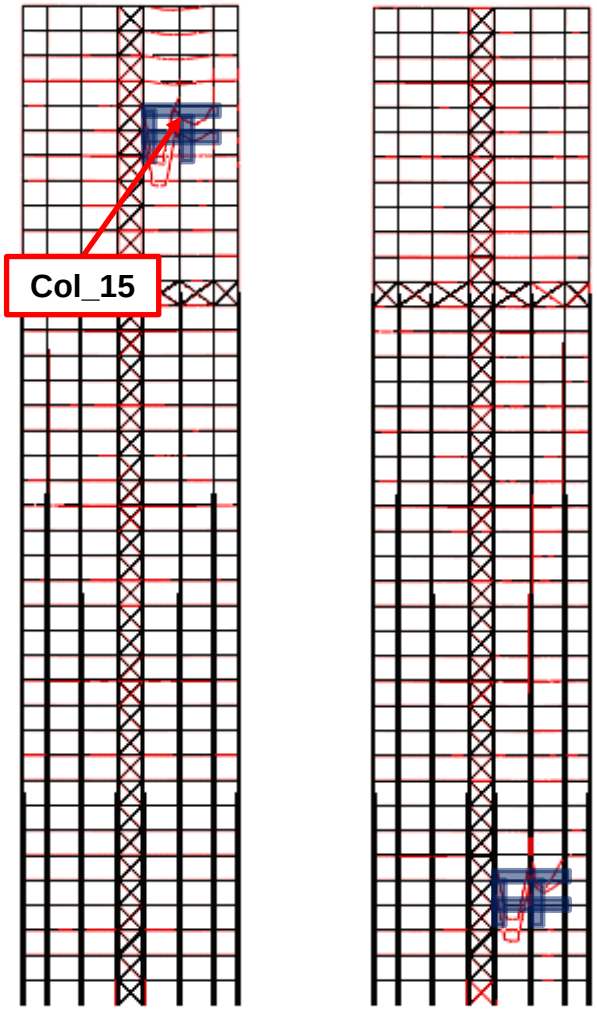

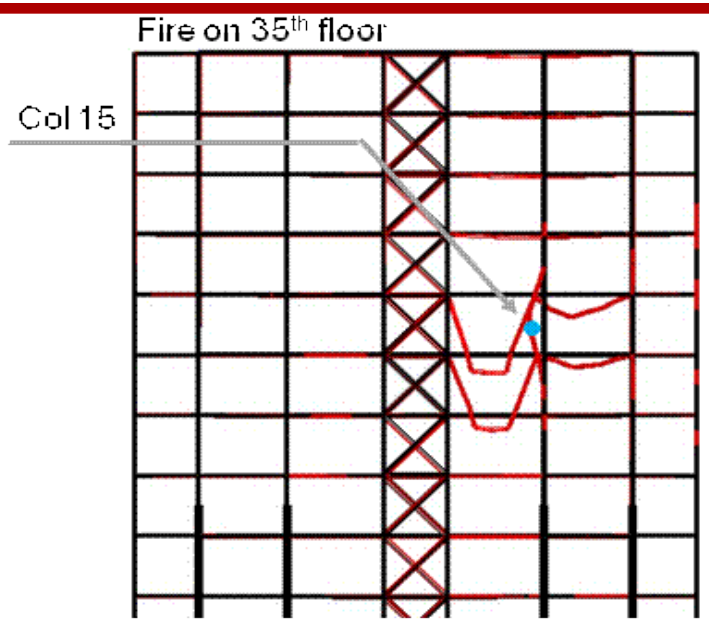

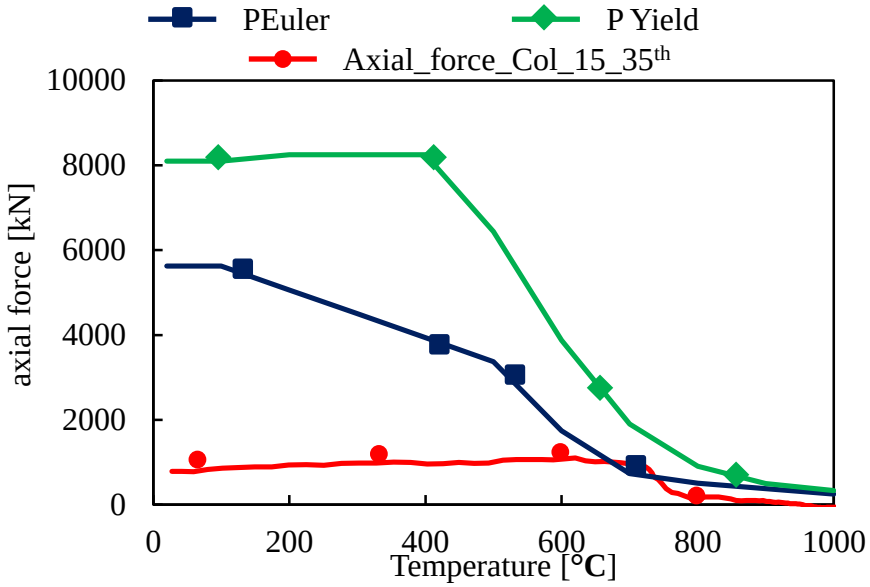

Collapse Mechanism

Isolated element

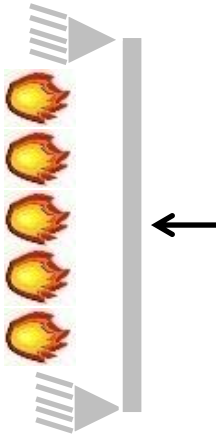

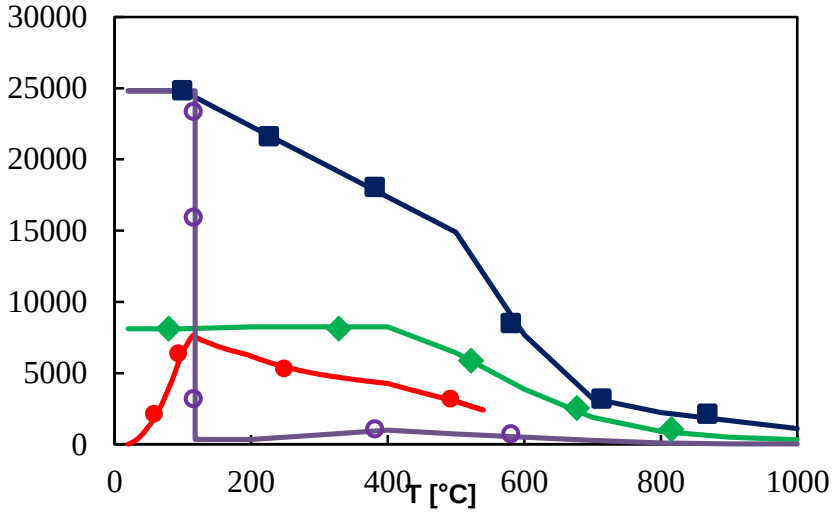

One floor

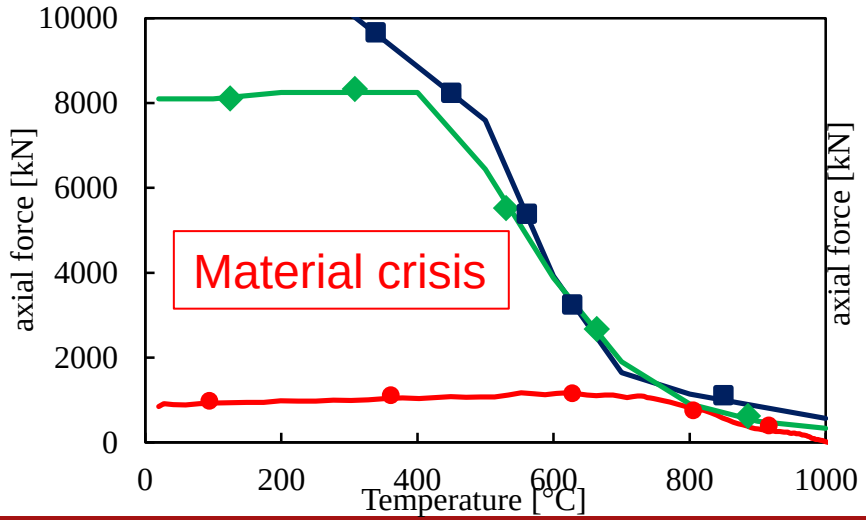

Two floors

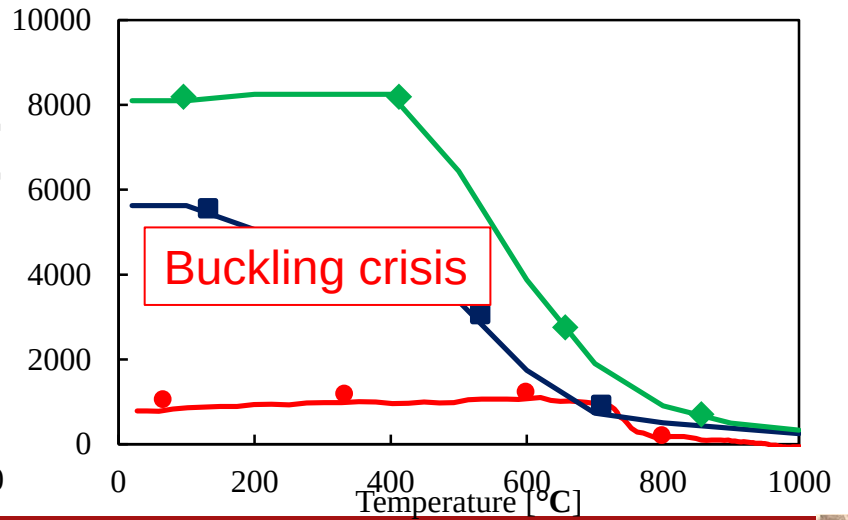

Collapse Mechanism

Combinations of actions for persistent or transient design situations

$$F_d = 1.3 \cdot G_1 + 1.5 \cdot G_2 + 1.5 \cdot Q_1 + 1.5 \cdot \psi_{0i} \cdot Q_2$$

↓

0.6 for wind

Combinations of actions for accidental design situations

$$F_d = 1 \cdot G_1 + 1 \cdot G_2 + \psi_{2i} \cdot Q_1 + \psi_{2i} \cdot Q_2$$

↓

0.0 for wind

COLUMNS OF HIGH-RISE BUILDING HAVE A LOW RATE OF WORK

Frame A

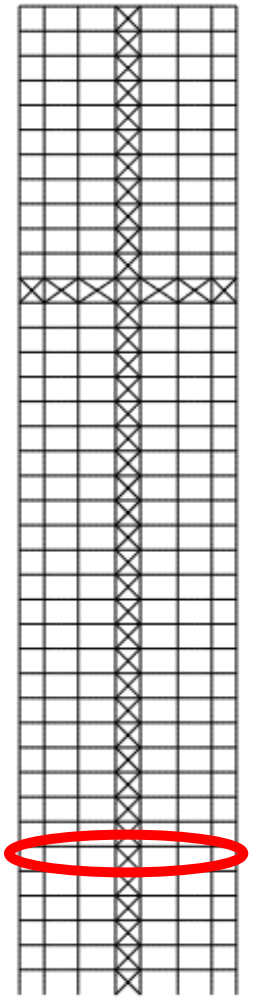

Assumption

- Collapse for displacement of 1 meter on the top
- Exposure to 180 minutes of ISO Curve

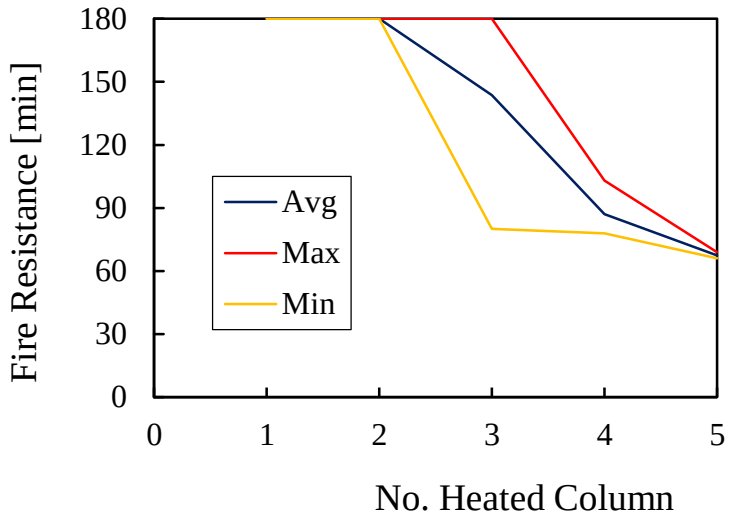

No. Heated Columns		1	2	3	4	5
Cases		8	8	6	6	4
Fire Resistance	Avg	180	180	143.6	87	67.5
	Min	180	180	80	78	66
	Max	180	180	180	103	69

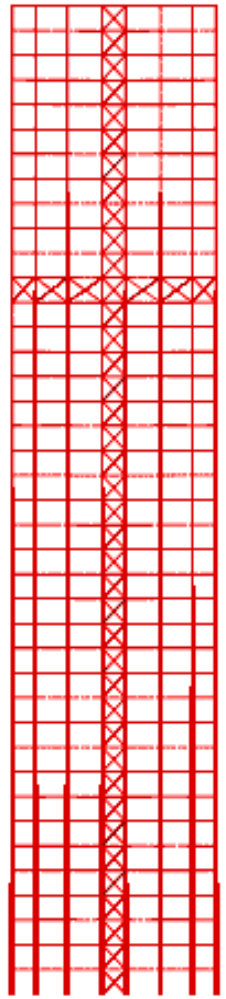

Progressive Collapse

1 Heated Column	2 Heated Columns	3 Heated Columns	4 Heated Columns	5 Heated Columns
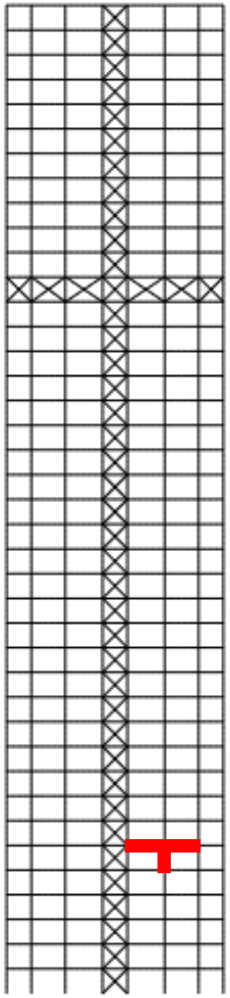	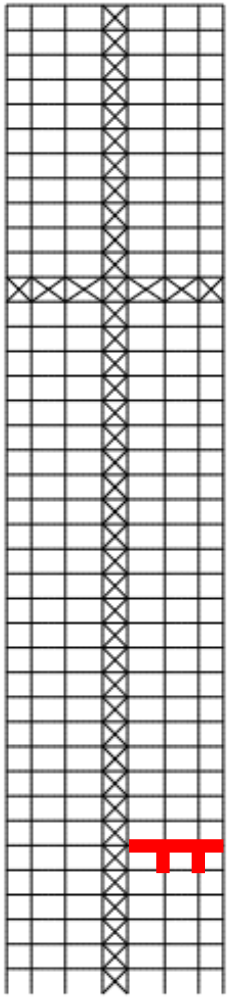	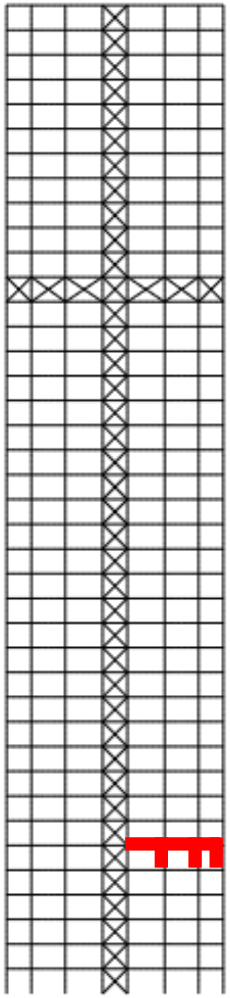	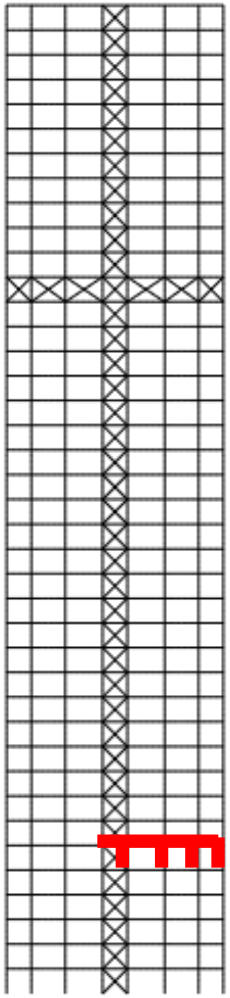	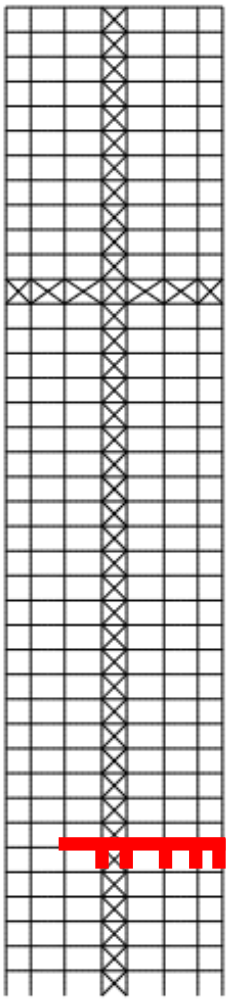
29 min - 688°C	28 min - 680°C	28 min - 680°C	27 min - 680°C	28 min - 688°C

Progressive Collapse

1 Heated Column	2 Heated Columns	3 Heated Columns	4 Heated Columns	5 Heated Columns
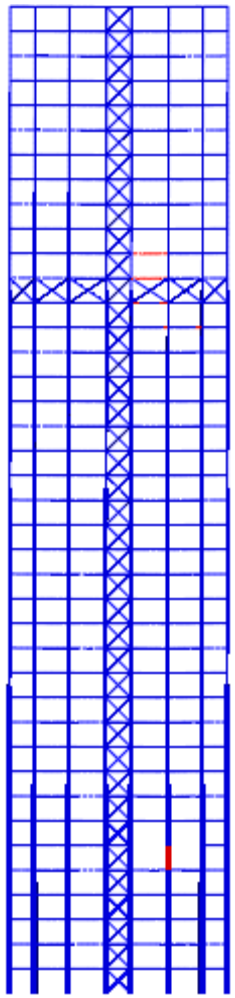	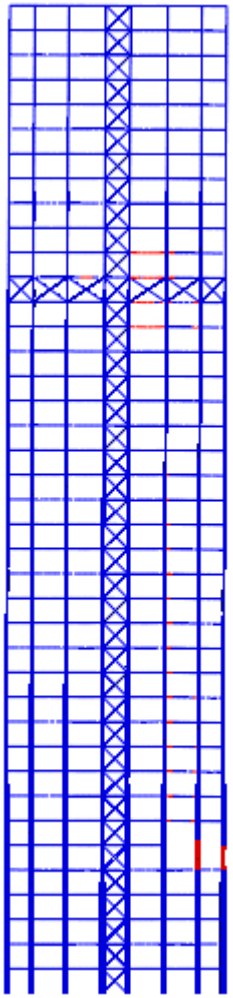	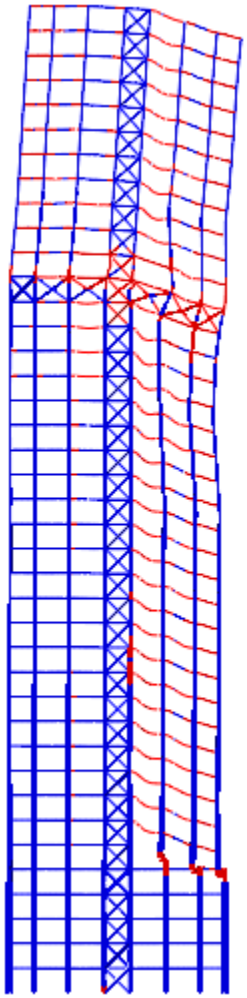	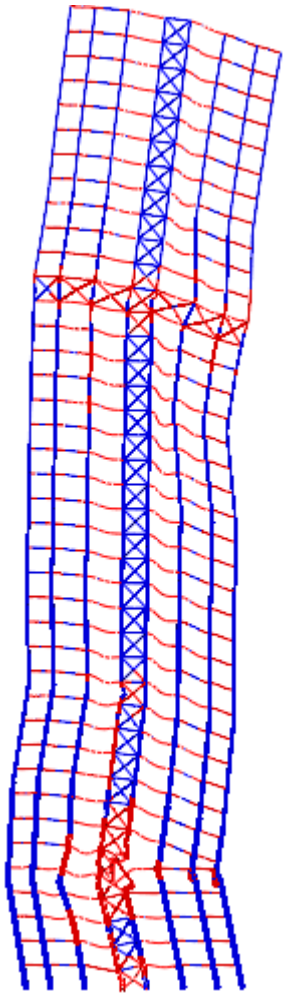	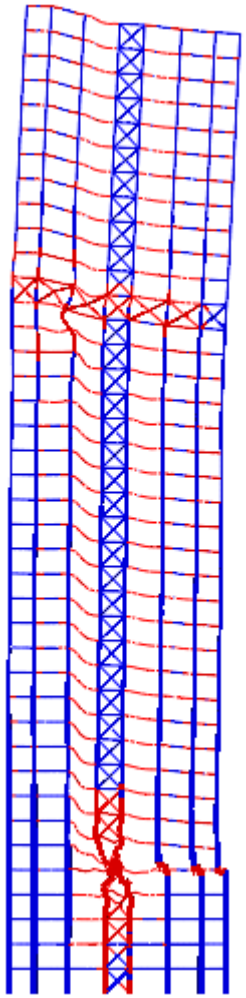
After 180 min	After 180 min	After 126 min	After 144 min	After 100 min

Progressive Collapse

	VMises 235 195 156 117 78 39 0	Deformation plastic elastic
Without Fire	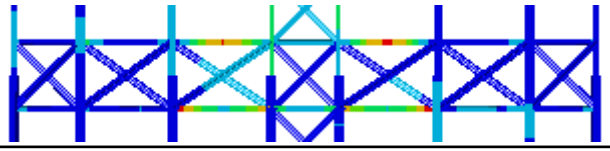	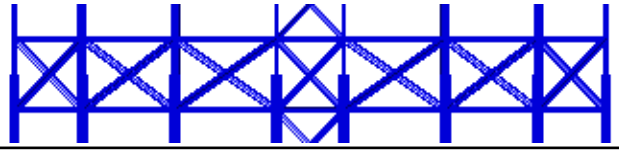
1 Heated Column	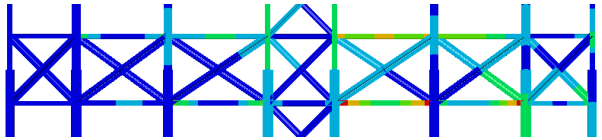	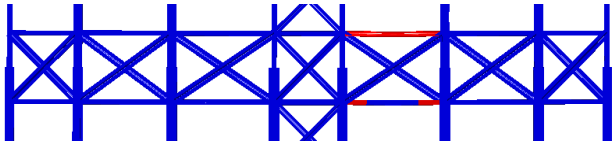
2 Heated Columns	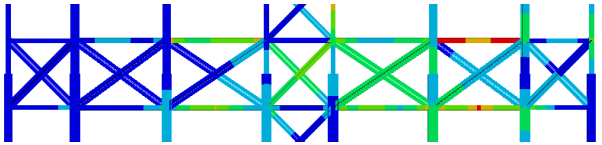	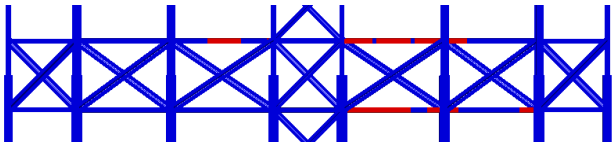
3 Heated Columns	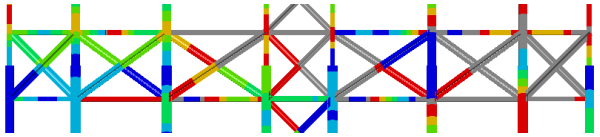	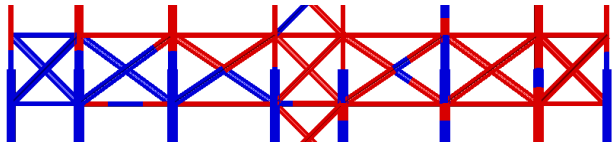
4 Heated Columns	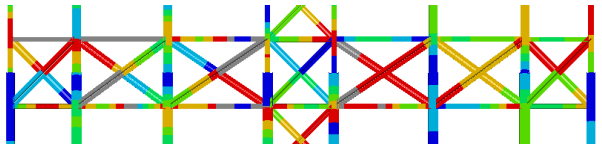	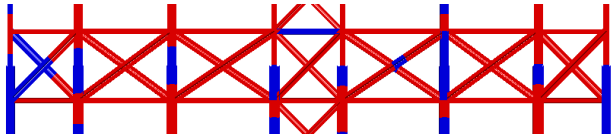
5 Heated Columns	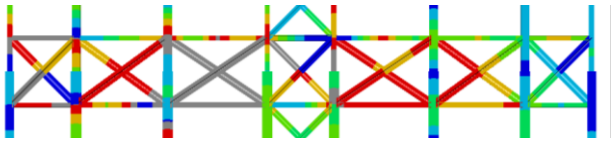	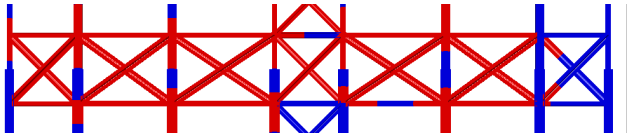

Frame B

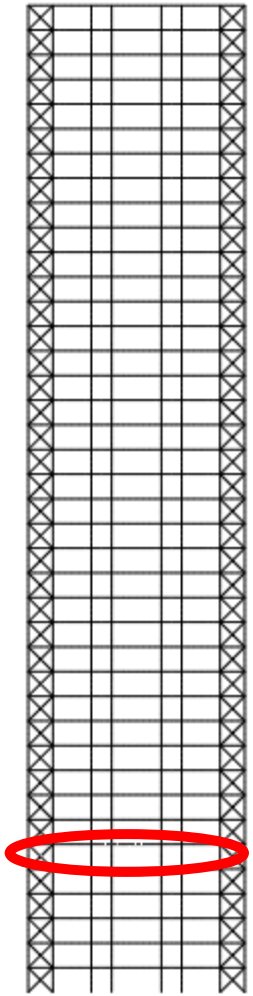

Assumption

- Collapse for displacement of 1 meter on the top
- Exposure to 180 minutes of ISO Curve

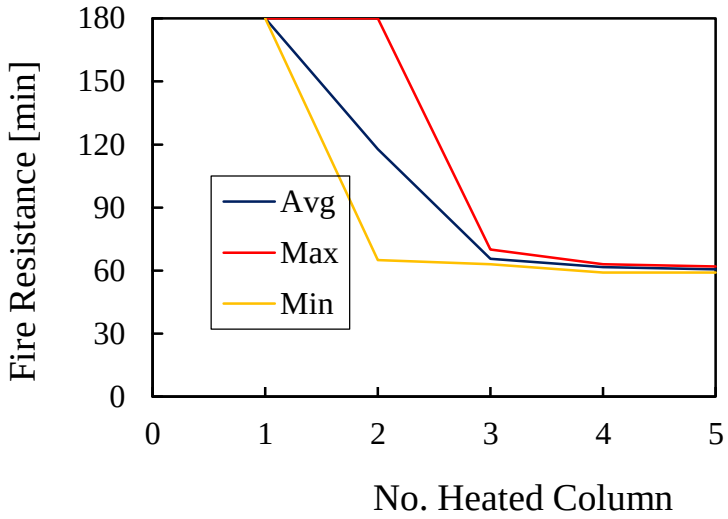

No. Heated Columns		1	2	3	4	5
Cases		8	8	6	6	4
Fire Resistance	Avg	180	117.7	65.6	61.6	60.5
	Min	180	65	63	59	59
	Max	180	180	70	63	62

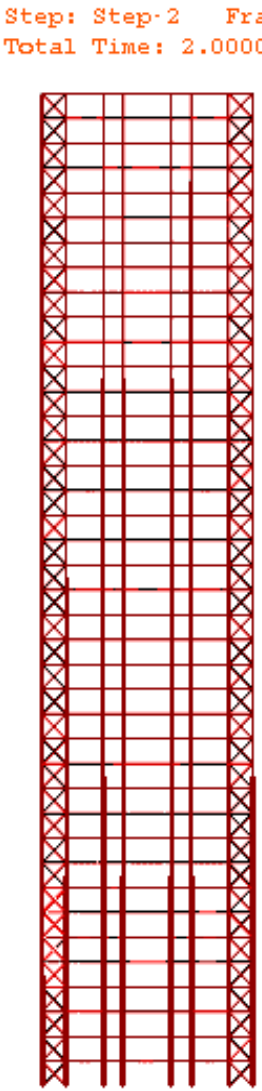

Progressive Collapse

1 Heated Column	2 Heated Columns	3 Heated Columns	4 Heated Columns	5 Heated Columns
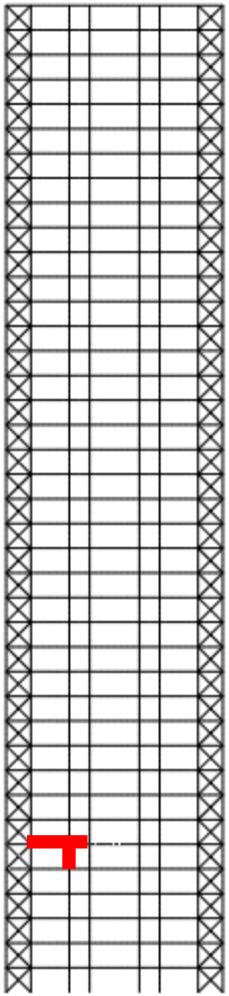	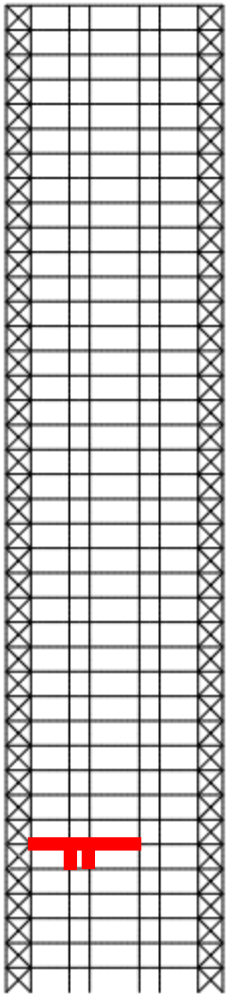	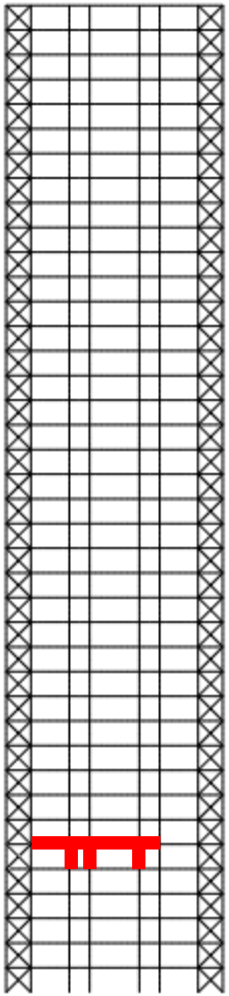	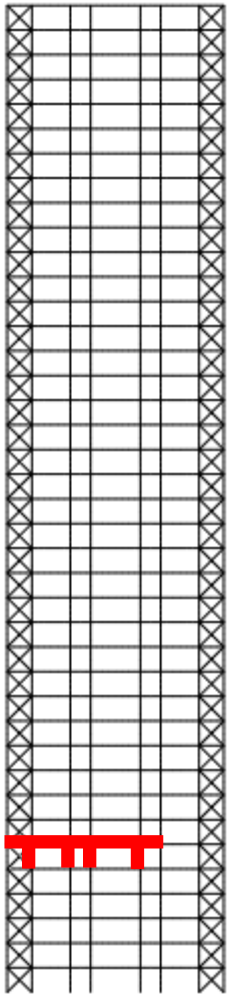	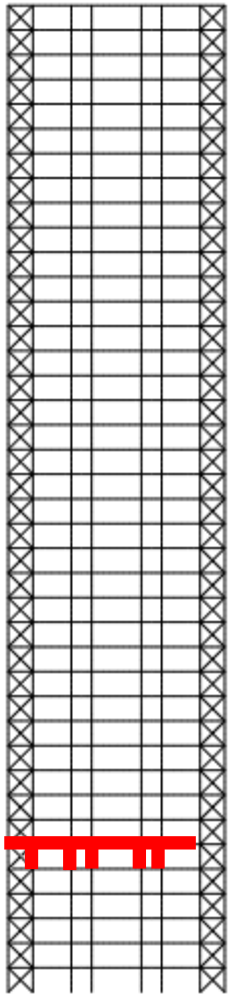
29 min - 688°C	29 min - 704°C	30 min - 696°C	27 min - 680°C	29 min - 696°C

Progressive Collapse

1 Heated Column	2 Heated Columns	3 Heated Columns	4 Heated Columns	5 Heated Columns
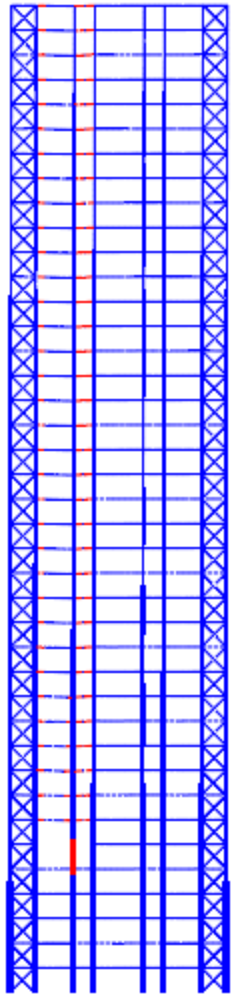	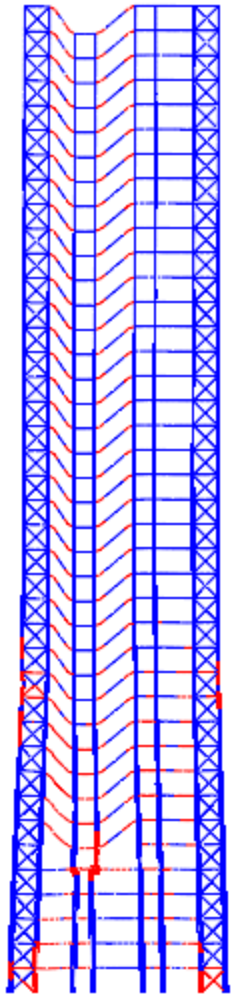	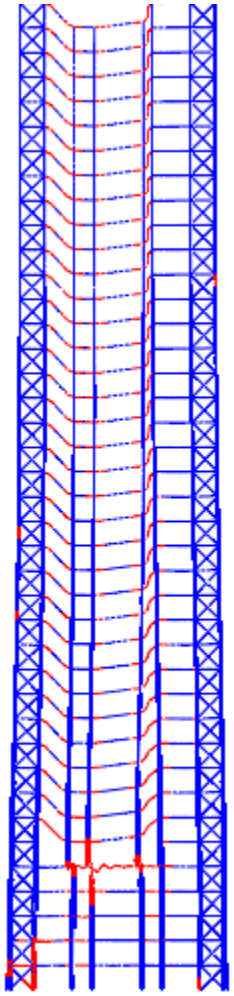	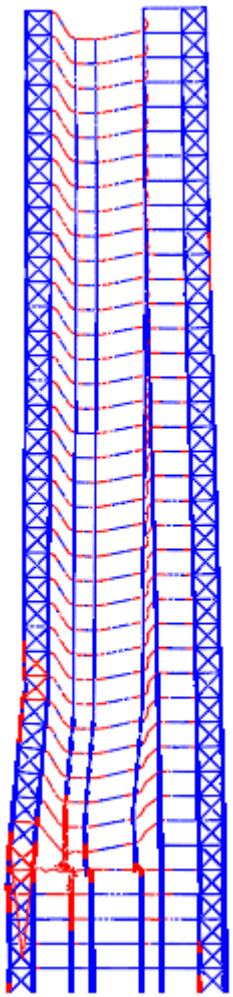	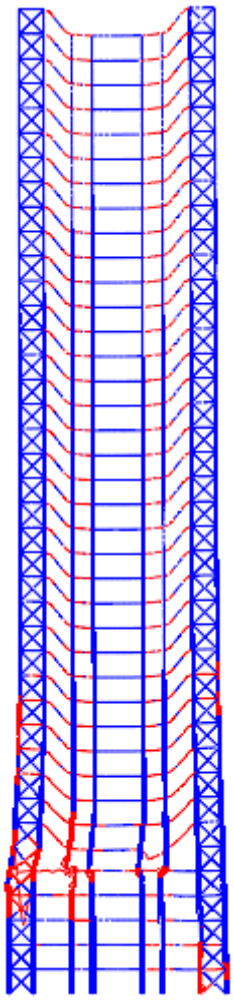
After 180 min	After 107 min	After 93 min	After 102 min	After 87 min

Progressive Collapse

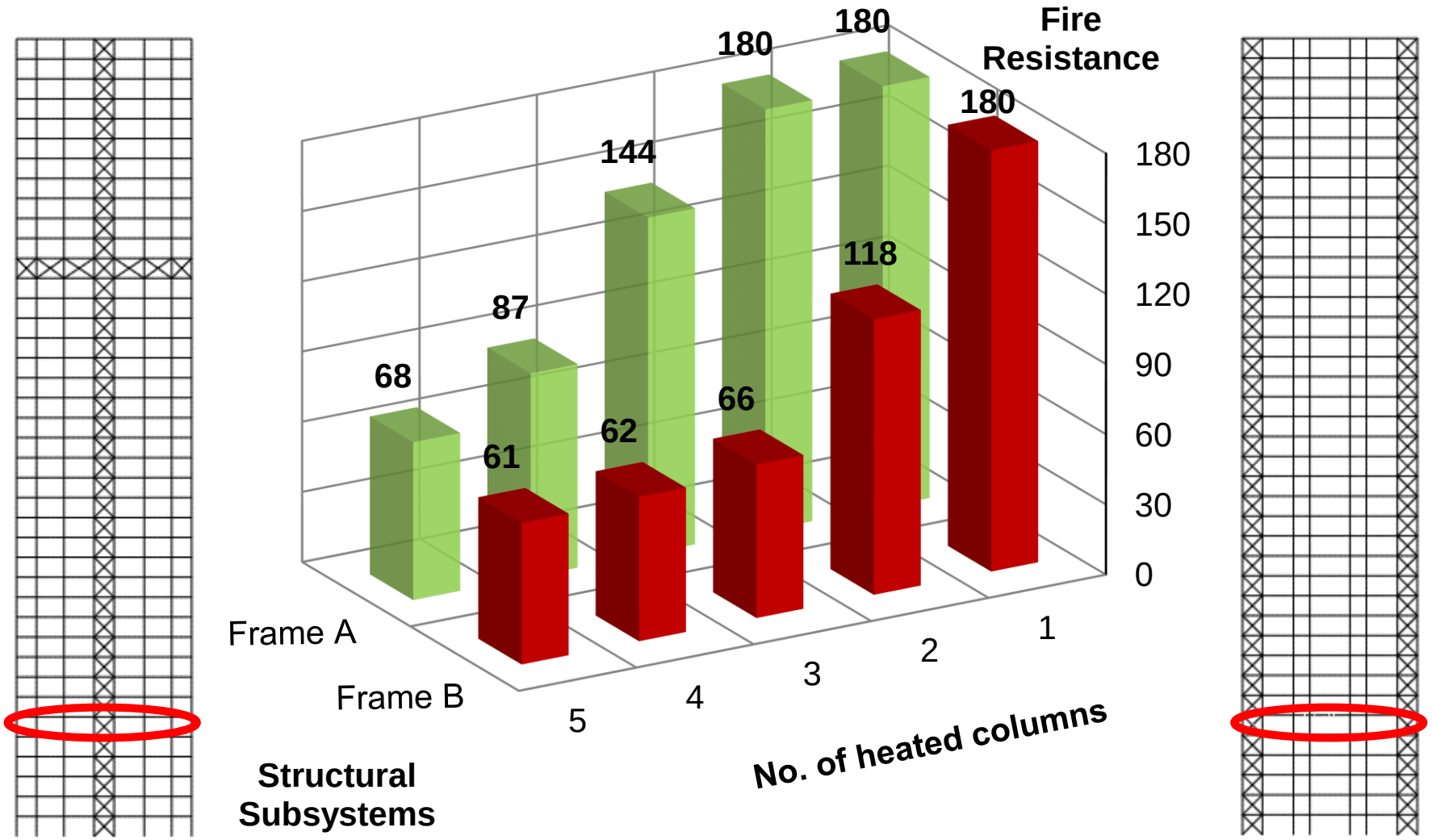

Effectiveness of bracing systems: outrigger

	Original Solution	Configuration A	Configuration B	Configuration C
Structural Configuration	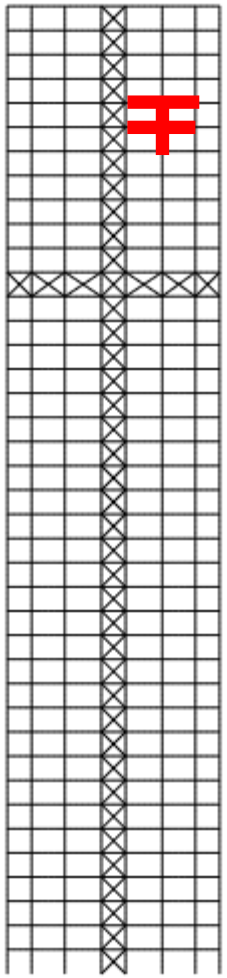	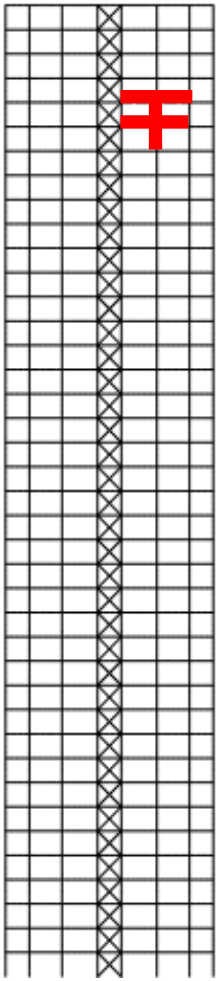	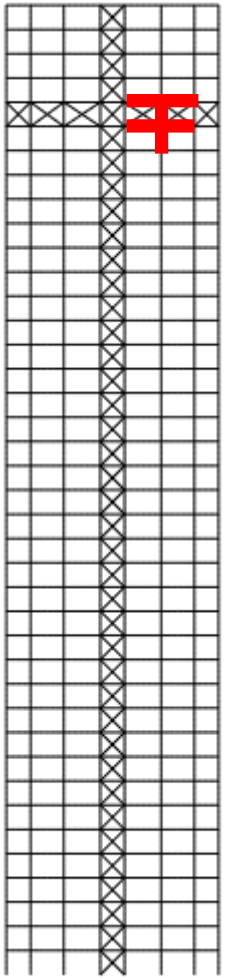	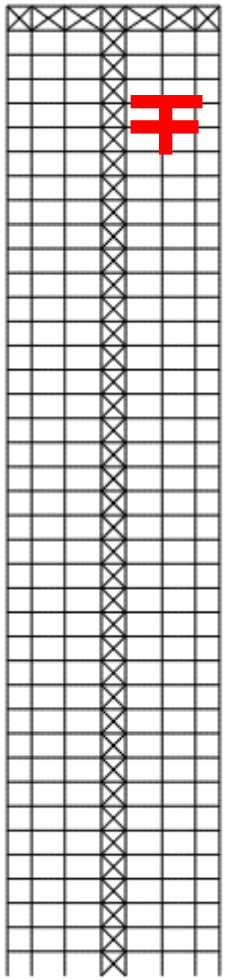
Column Collapse	700°C – 30 min	700°C – 30 min	687°C – 29 min	400°C – 15 min

Effectiveness of bracing systems: outrigger

	Original Solution	Configuration A	Configuration B	Configuration C
Deformed Configuration	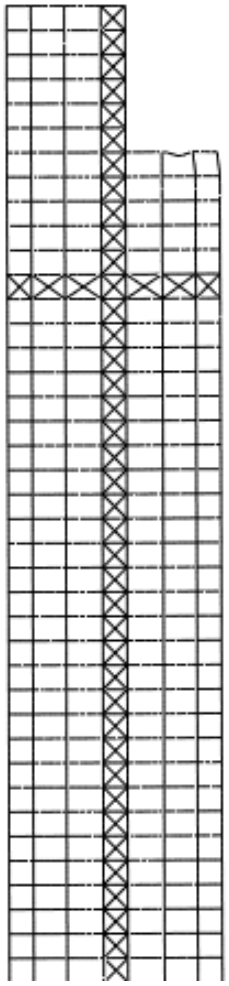	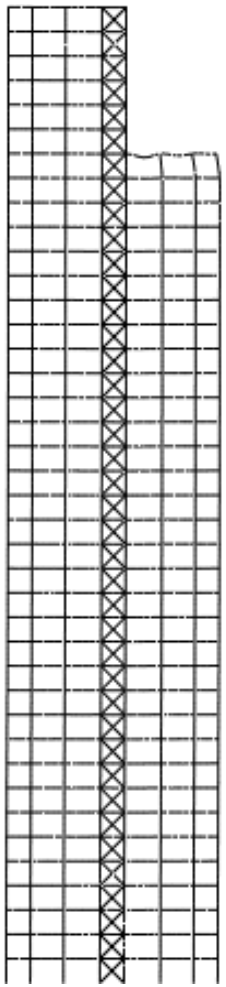	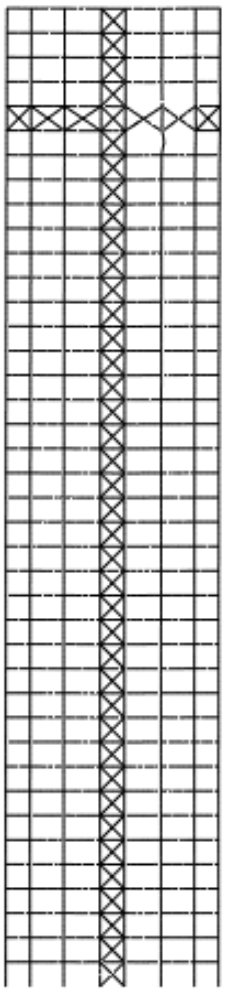	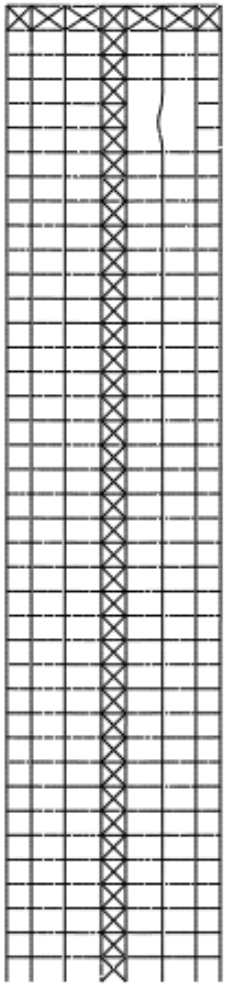
Progressive Collapse Susceptibility	YES	YES	NO	NO

Effectiveness of bracing systems: tube

	Original Solution	Configuration D	Configuration E	Configuration F
Structural Configuration	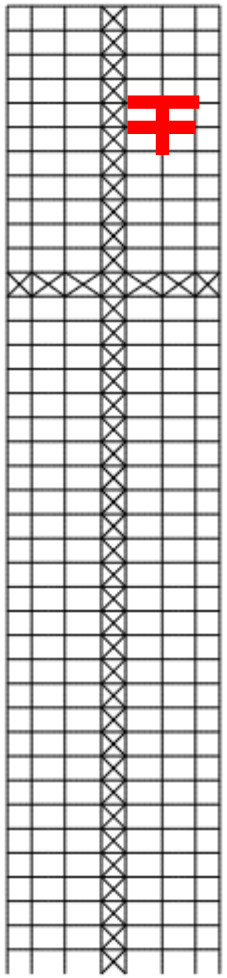	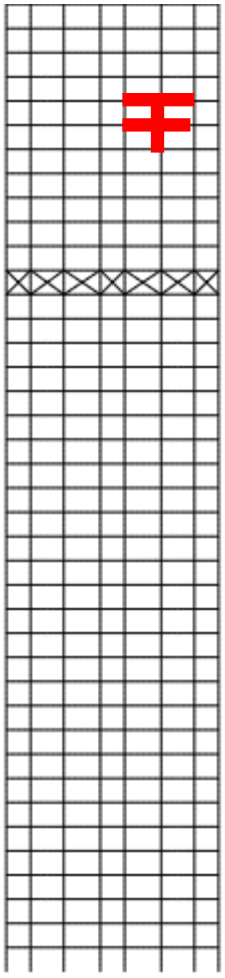	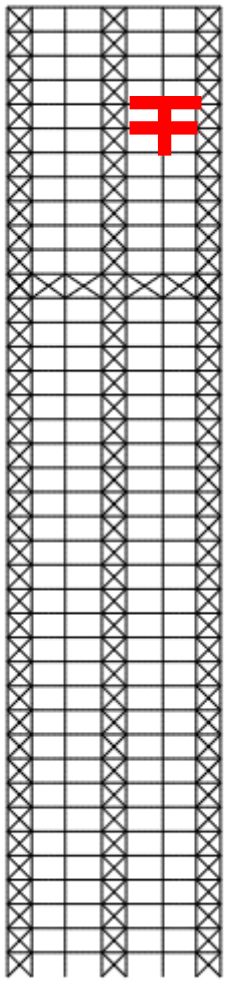	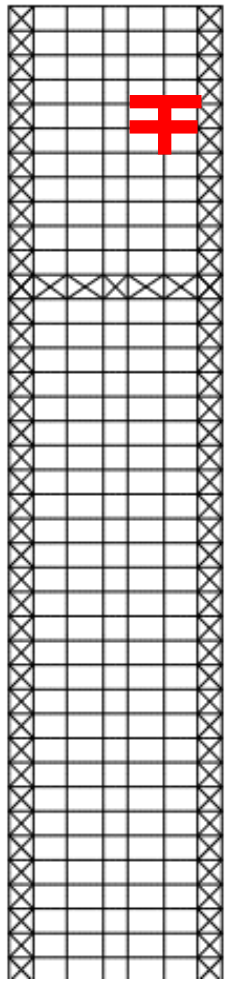
Column Collapse	700°C – 30 min	700°C – 30 min	700°C – 30 min	700°C – 30 min

Effectiveness of bracing systems: tube

	Original Solution	Configuration D	Configuration E	Configuration F
Deformed Configuration	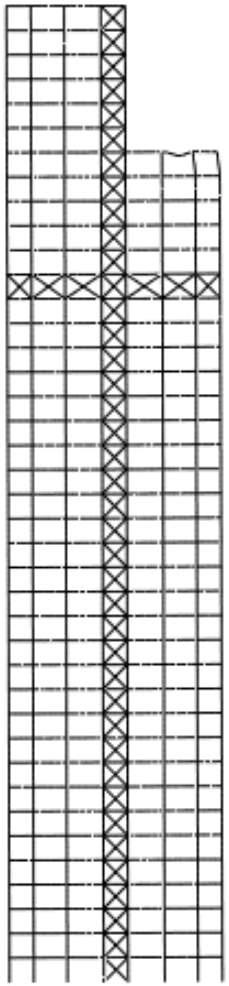	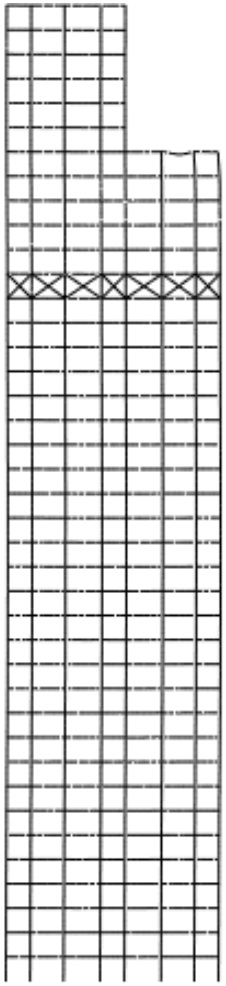	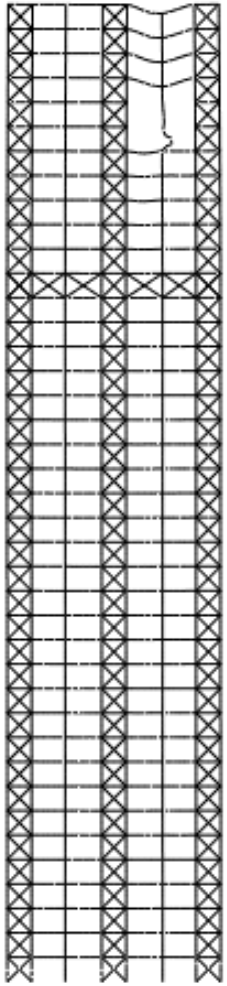	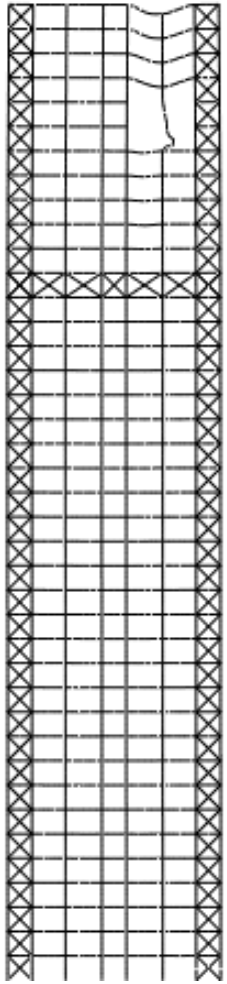
Progressive Collapse Susceptibility	YES	YES	NO	NO

Multi-physics Approach

Fire Safety Assessment

of High-Rise Buildings

CFD

FEM

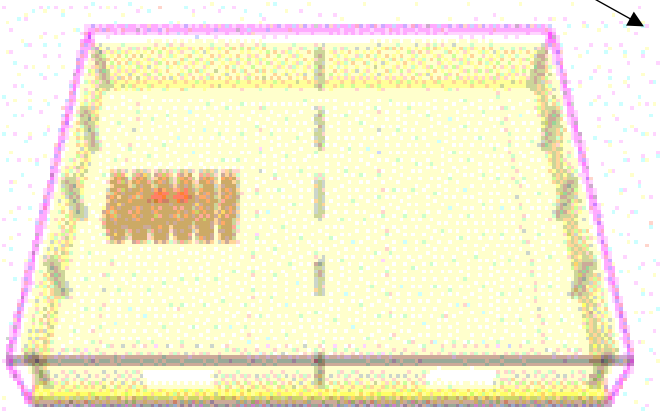

Multi-Physics

Modelling

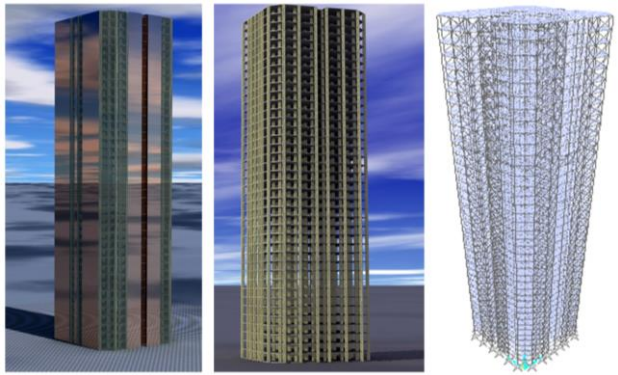

Fire Action

Fuel Stacking in **Large Compartments**

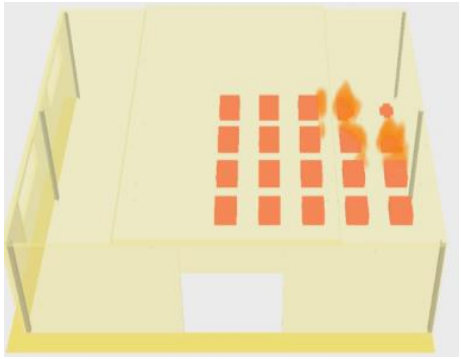

High Concentration

Local temperatures **much higher** than those predicted by a flashover fire

Low Concentration

Possible **Travelling Fire**

Structural Behaviour

Progressive Collapse Analysis

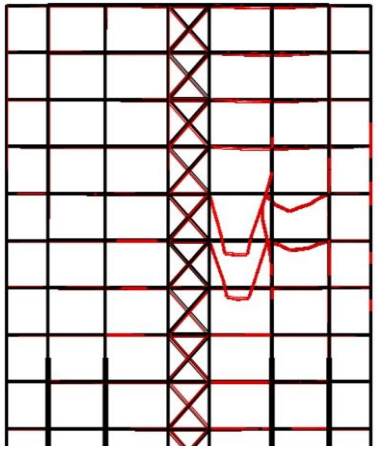

Beam – Column

Stiffness Ratio

Bracing systems

Different behaviour at different height

Constrained Thermal Expansion

Direct and **indirect** effect

Failure mode

Fire **Resistance**

Constrained Thermal Expansion

Failure mode

Curriculum Vitae

Personal information

First name(s) / Surname(s)	**Filippo GENTILI**
Address(es)	24, via San Martino, 00015, Monterotondo (RM), Italy
Telephone(s)	+39 0644585072 Mobile: +39 3474720047
Fax(es)	+39 0648844852
E-mail	filippo.gentili@uniroma1.it, filippo.gentili@francobontempi.org
Website	http://www.francobontempi.org/persone.html, http://www.researcherid.com/rid/C-6563-2011 http://uniroma1.academia.edu/FilippoGentili, http://it.linkedin.com/pub/filippo-gentili/24/271/700
Nationality	Italian
Date of birth	08 June 1983
Gender	Male

Work experience

Dates	2013
Occupation or position held	Consultant engineer
Main activities and responsibilities	Analysis and optimization of precast elements
Name and address of employer	StroNGER S.r.l., Rome, Italy
Type of business or sector	Structural engineering
Dates	2009-2013
Occupation or position held	PhD
Main activities and responsibilities	Study and research on structural engineering Title of thesis: *Multi-physics modelling for the safety assessment of complex structural systems under fire*, advisor Prof. Franco Bontempi (Sapienza University of Rome), co-advisor Prof. Luisa Giuliani (DTU Technical University of Denmark).
Name and address of employer	Sapienza University of Rome, Rome, Italy
Type of business or sector	Structural engineering
Dates	2009
Occupation or position held	Consultant engineer
Main activities and responsibilities	Analysis of fire resistance of slabs
Name and address of employer	Grossi, Camplone & Pierdomenico Studio associato di ingegneria di impianti, Rome, Italy
Type of business or sector	Structural engineering

Education and training

Dates	2011
Title of qualification awarded	Fire Protection Certification (National Fire Protection Registry / art. 1 818/84)
Principal subjects/occupational skills covered	Specialization course in fire prevention (100 hours)
Name and type of organisation providing education and training	Sapienza University of Rome, Rome, Italy and The National Fire Corps, Italy
Date	2010
Title of qualification awarded	Registered Professional Engineer in Rome

Dates	2009
Title of qualification awarded	Construction site safety coordinator
Principal subjects/occupational skills covered	Specialization course in work safety – Construction site safety (120 hours)
Name and type of organisation providing education and training	Sapienza University of Rome, Rome, Italy
Dates	2006-2009
Title of qualification awarded	Master of Science in Civil Engineering (Laurea specialistica in Ingegneria Civile)
Principal subjects/occupational skills covered	Thesis Title: *Simulation of fire of a complex structure for the performance-based design,* advisor Prof. Franco Bontempi), co-advisor Dr. Chiara Crosti (in Italian *Simulazioni di incendi in una struttura complessa per la progettazione prestazionale)*.
Name and type of organisation providing education and training	Sapienza University of Rome, Rome, Italy
Dates	2002-2006
Title of qualification awarded	Bachelor of Science in Civil Engineering (Laurea triennale in Ingegneria Civile)
Principal subjects/occupational skills covered	Thesis Title: *Design of a Steel Structure with Sap2000 Software*, advisor Prof. Franco Bontempi co-advisor Dr. Stefania Arangio (in Italian *Calcolo automatico delle strutture in acciaio con il codice di calcolo Sap2000)*
Name and type of organisation providing education and training	Sapienza University of Rome, Rome, Italy
Dates	1997-2002
Title of qualification awarded	High school diploma (diploma di scuola superiore)
Name and type of organisation providing education and training	Liceo Classico Catullo, Monterotondo (RM), Italy

Teaching Experience

Dates	September 2012 – December 2012 September 2011 – December 2011 March 2011 – April 2011 March 2010 – April 2010
Name and address of employer	Sapienza University of Rome Department of Structural and Geotechnical Engineering
Main activities and responsibilities	Teaching assistant of Course of Fire Structural Design held by Prof. Franco Bontempi
Dates	December 2010
Name and address of employer	Sapienza University of Rome Department of Structural and Geotechnical Engineering
Main activities and responsibilities	Teaching assistant of Course of Metal Construction held by Prof. Franco Bontempi
Dates	December 2009
Name and address of employer	Sapienza University of Rome Department of Structural and Geotechnical Engineering
Main activities and responsibilities	Teaching assistant of Course of Structural Analysis held by Prof. Franco Bontempi

Scientific activity

Research periods abroad	- Visiting Researcher (January 2012 – June 2012) Research on the structural behaviour of high buildings in fire conditions under the supervision of Prof. Luisa Giuliani. Attended the course of *Fire Dynamics* (Prof. A. Dederichs). DTU – Department of Civil Engineering DK-2800 Kgs. Lyngby (DK).

- Visiting Researcher (January 2011 – April 2011)

  Experimental test on shear strength of reinforced concrete elements at high temperatures under the supervision of Dr. Luke Bisby. Attended courses of *Quantitative Methods in Fire Safety Engineering* (Prof. J.Torero), *Fire Dynamics Laboratory* (Dr. S. Welch), *Fire Resistance of Structures* (Dr. M. Gillie).

  BRE Centre for Fire Safety Engineering, University of Edinburgh (UK).

Session organizer in International Conferences

- Special Session: The Role of Collapse Safety in the Design of Sustainable Structures, SEMC 2013: The Fifth International Conference On Structural Engineering, Mechanics And Computation, Cape Town, South Africa, September 2-4, 2013, Chairs: Prof. Luisa Giuliani, Mr. Filippo Gentili

Personal skills and competences

Mother tongue(s) **Italian**

Other language(s)

Self-assessment	Understanding				Speaking				Writing	
European level (*)	Listening		Reading		Spoken interaction		Spoken production			
English	B2	Independent user	C1	Proficient user	B2	Independent user	B2	Independent user	B2	Independent user
French	A2	Basic user	A2	Basic user	A2	Basic user	A2	Basic user	A2	Basic user

(*) Common European Framework of Reference for Languages

Research Topics: Fire safety engineering – Finite element analysis – Multi-physics

Computer skills and competences:
Finite Element (FE) linear and non-linear analysis (ABAQUS ®, DIANA ®, STRAND7 ®, SAP2000 ®)
Computational Fluid Dynamic (CFD) analysis (FDS)
Linux Ubuntu
Microsoft Office ®
Autocad

Driving licence: B

Annexes

ANNEX 1: LIST OF PUBLICATIONS
ANNEX 2: LAYOUT OF PH.D. THESIS
ANNEX 3: PARTICIPATION AT CONFERENCES AND SEMINARS
ANNEX 4: MSC THESES CO-ADVISOR

ANNEX 1: LIST OF PUBLICATIONS

INTERNATIONAL JOURNALS (3 DOCUMENTS)

1. Gentili F, Giuliani L, Bontempi F. *Structural response of steel high rise buildings to fire: system characteristics and failure mechanisms*, Journal of Structural Fire Engineering, p. 9-26, Volume 4, Number 1, 2013.
2. Gentili F, Giuliani L, Bontempi F. *Effects of combustible stacking in large compartments*, Journal of Structural Fire Engineering, in press.
3. Gentili F. *Advanced numerical analyses for the assessment of steel structures under fire*, International Journal of Lifecycle Performance Engineering, Special Issue on Fire Safety Design and Robustness Considerations in Structural Engineering, Inderscience, in press.

INTERNATIONAL CONFERENCE PROCEEDINGS (10 DOCUMENTS)

4. Monti A, Pariciani T, Gentili F, Petrini F. *No-sway collapse of steel frames under fire conditions: a parametric investigation*, Proceedings of The Fifth International Conference on Structural Engineering, Mechanics and Computation (SEMC2013), Cape Town (South Africa), 2-4 September 2013, submitted.
5. Gentili F, Petrini F. *Evaluation of structural risk for bridges under fire*, Proceeding of 6th International Conference On Bridge Maintenance, Safety And Management (IABMAS 2012), Stresa, Lake Maggiore, Italy, 8-12 July 2012.
6. Crosti C, Olmati P, Gentili F. *Structural response of bridges to fire after explosion*, Proceeding of 6th International Conference On Bridge Maintenance, Safety And Management (IABMAS 2012), Stresa, Lake Maggiore, Italy, 8-12 July 2012.
7. Giuliani L, Crosti C, Gentili F. *Vulnerability of bridges to fire*, Proceeding of 6th International Conference On Bridge Maintenance, Safety And Management (IABMAS 2012), Stresa, Lake Maggiore, Italy, 8-12 July 2012.
8. Gentili F, Giuliani L, Bontempi F. *Investigation of fire-induced collapse scenarios for a steel high-rise building*, Proceedings of The 2011 International Conference on Advances in Structural Engineering and Mechanics (ASEM'11), Seoul (South Korea), 18-22 September 2011.
9. Gentili F, Giuliani L, Petrini F. *Numerical investigation of fire induced collapse of a single storey two span frame*, Proceedings of Eurosteel, 6th European Conference on Steel and Composite Structures, Budapest (Hungary), 31 August - 2 September 2011.
10. Gentili F, Grossi L, Bontempi F. *Role of CFD in the quantitative assessment of structural performance in fire scenarios*, Proceedings of Applications of Structural Fire Engineering (ASFE), Prague (Czech Republic), 29-30 April 2011.
11. Gentili F, Giuliani L. *Simulation of the structural behavior of steel-framed buildings in fire*, Proceedings of Applications of Structural Fire Engineering (ASFE), Prague (Czech Republic), 29-30 April 2011.
12. Gentili F, Crosti C, Giuliani L. *Performance based investigations of structural systems under fire*, Proceedings of The Fourth International Conference on Structural Engineering, Mechanics and Computation (SEMC2010), Cape Town (South Africa), 6-8 September 2010.
13. Gentili F, Crosti C, Gkoumas K. *Fire safety assessment of long tunnels*, Proceedings of The Fourth International Conference on Structural Engineering, Mechanics and Computation (SEMC2010), Cape Town (South Africa), 6-8 September 2010.

NATIONAL CONFERENCE PROCEEDINGS (5 DOCUMENTS)

14. Crosti C, Giuliani L, Gentili F, Bontempi F. *The role of the structural robustness in fire safety* (in Italian: *Il ruolo della robustezza strutturale nella impostazione ingegneristica della sicurezza antincendio*), Proceedings of Valutazione e Gestione del Rischio negli Insediamenti Civili ed Industriali, Pisa, Italy, 3-5 October 2012 (in Italian).
15. Arangio S, Gentili F. *Role of the creep deformation in the fire induced collapse of a steel structure*, Proceedings of XXIII Congresso CTA, Ischia (NA), Italy, 9-12 October 2011.
16. Gentili F, Giuliani L, Bontempi F. *Modeling of the structural response to fire of a high-rise steel building*, Proceedings of XXIII Congresso CTA, Ischia (NA), Italy, 9-12 October 2011.
17. Gkoumas K, Giuliani L, Petrini F, Gentili F. *Fire safety assessment of tunnel structures*, Proceedings of 7th National Conference on Steel Structures, Volos (Greece), 29-30 September - 1 October 2011.
18. Gentili F, Grossi L. *Numerical simulation for fire safety in industrial hall*, Proceedings of Handling Exceptions in Structural Engineering: Structural Systems, Accidental Scenarios, Design Complexity (HE10), DOI:10.3267/HE 2010, Rome, Italy, 8-9 July 2010.

PAPER OF TECHNICAL JOURNAL (3 DOCUMENTS)

19. Bontempi F, Gentili F, Petrini F. *Numerical simulation for performance – based design of complex structures subject to fire action*, Enginsoft Newsletter, vol. 1, 2010, p. 24-28.

20. Gentili F, Petrini F, Bontempi F. *Aspetti elementari della modellazione dell'azione incendio tramite codici di calcolo automatico*, Antincendio - parte 1, vol. 3, 2013.
21. Gentili F, Petrini F, Bontempi F. *Aspetti elementari della modellazione dell'azione incendio tramite codici di calcolo automatico*, Antincendio - parte 2, vol. 4, 2013.

PAPER OF TECHNICAL JOURNAL (2 DOCUMENTS)

22. Gentili F, Carstensen JV, Giuliani L. Comparison of the performances of two concrete floor slabs in the case of fire
23. Gentili F. The role of the outrigger systems in the robustness enhancement of tall buildings

ANNEX 2: LAYOUT OF PH.D. THESIS

Keywords

Structural Fire Safety Design – Performance Based Design – Multi-physics – Fire modelling – Structural integrity – Progressive collapse susceptibility – Computational Fluid Dynamic – Nonlinear response of structures – Vulnerability of structures to fire

Thesis outline

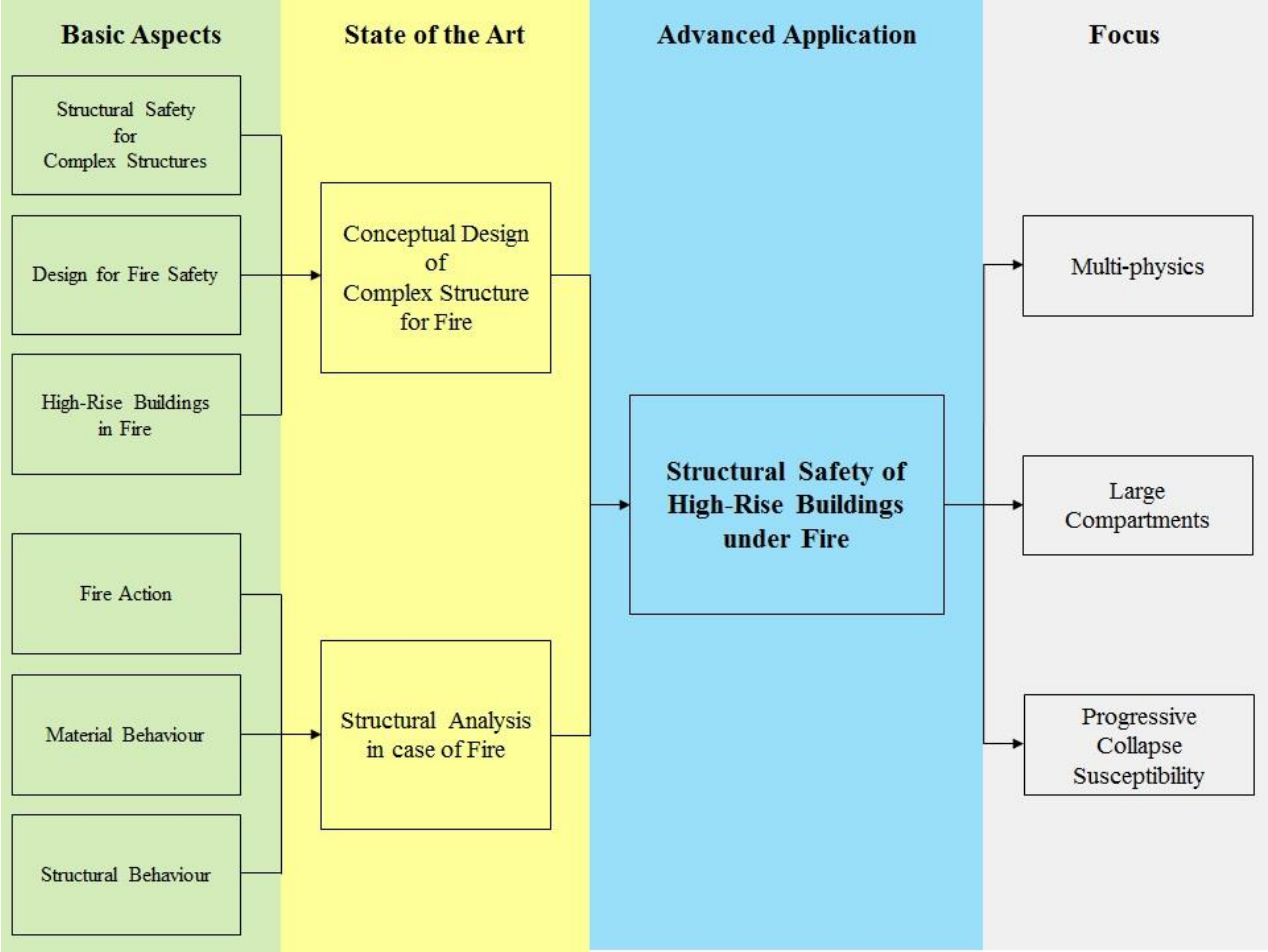

Synthesis

Among all structures, high-rise buildings pose specific design challenges with respect of fire safety for a number of reasons, in particular the evaluation of both the fire development (fire action) and response of the structural system to fire (structural behaviour).

In relation to the fire action, large compartments and open hallways often present in modern high-rise buildings don't let themselves to be designed within compliance to current codes and standards. A comprehensive analysis of the fire environment is required to understand the fire dynamics in these cases. A Computational Fluid Dynamic (CFD) model allows a quite accurate representation of realistic fire scenarios, because it takes into account the distribution of fuel, the geometry, the occupancy of individual compartments and the temperature rise in structural elements that are located outside the tributary area of fire scenario.

In relation to the structural behaviour under fire, the passive fire resistance of structural elements and the intrinsic robustness of the system are the only measures to rely on in order to maintain the structural integrity of the building during and after the fire and avoid major economic losses due to structural failures and prolonged inoperability of the premises. Disproportionate damages induced by fire can be avoided with a proper design of the structure, aimed at reducing the vulnerability of the elements to fire (i.e. their sensitivity to fire) or at increasing the robustness of the structural system (i.e. its sensitivity to local damages).

The topic of this thesis is the evaluation of the structural safety in case of fire by means of advanced multi-physics analyses with direct reference to the modern Performance-Based Fire Design (PBFD) framework. A fundamental aspect is how some basic

failure mechanisms can be triggered or modified by the presence of fire on a part of a structural system, such as three hinge mechanism, bowing effects, catenary action, thermal buckling and snap-through, sway and non-sway collapse. High rise buildings, which are expected to be susceptible to fire-induced progressive collapse, will be investigated. Critical elements will be identified in the system and countermeasure for enhancement of structural integrity will be suggested. The investigation of the response of such a complex structures subjected to fire scenarios requires the use of CFD and Finite Element (FE) models for a realistic evaluation of the fire action and of the structural response respectively.

Thesis content

INTRODUCTION

1. Structural safety of high-rise buildings under fire

SECTION I: Complex structures in fire

2. Structural safety
3. Design for fire safety
4. High-rise buildings in fire

SECTION II: Background aspects for structural fire safety

5. Fire action
6. Material behaviour
7. Structural behaviour

SECTION III: Applications

8. Advanced numerical analyses for the assessment of steel structures under fire
9. Fire action in a large compartment
10. Progressive collapse susceptibility of a high-rise building

CONCLUSIONS

ANNEX 3: CONFERENCE PRESENTATIONS AND SEMINAR

July 2012	Sapienza Università di Roma, Dipartimento di Ingegneria Civile e Geotecnica 16 July 2012. Title of presentation: *Multi-physics modelling for safety assessment in complex structural system under fire*.
July 2012	6th International Conference On Bridge Maintenance, Safety And Management (IABMAS 2012), Session SS05 Vulnerability of bridges to fire and explosions, Stresa, Lake Maggiore, Italy, 8-12 July 2012. Title of presentation: *Evaluation of structural risk for bridges under fire.*
June 2012	DTU – Department of Civil Engineering (Denmark), 25 June 2012. Title of presentation: *Multiphysics modelling for safety assessment in complex structural system under fire*.
April 2012	Fire Safety Day, Lund University (Sweden), 18 April 2012. Title of presentation: Analysis of a steel high-rise building in case of fire.
February 2012	DTU – Department of Civil Engineering (Denmark), 9 February 2012. Title of presentation: Multi-physics modelling for safety assessment in complex structural system under fire: the case of high-rise building.
November 2011	Sapienza Università di Roma, Dipartimento di Ingegneria Civile e Geotecnica, 4 November 2011. Title of presentation: Multi-physics modelling for safety assessment in complex structural system under fire: the case of high-rise building.
October 2011	XXIII Conference Collegio dei Tecnici dell'Acciaio (CTA), Ischia (NA), Italy, 9-12 October 2011. Title of presentation 1: *Modelling of the structural response to fire of a high-rise steel building*. Title of presentation 2: *Role of the creep deformation in the fire induced collapse of a steel structure*.
September 2011	6th European Conference on Steel and Composite Structures (Eurosteel), Budapest, Hungary, 31 August-2 September 2011. Title of presentation**:** *Numerical investigation of fire induced collapse of a single storey two span frame*.
April 2011	Applications of Structural Fire Engineering (ASFE 2011), Prague, Czech Republic, 29 April 2011. Title of presentation: *Role of CFD in the quantitative assessment of structural performance in fire scenarios.*
October 2010	15 Incontri di Informazione Tecnica organizzato dalla DEI al SAIE 2010, Bologna, 29 October 2010. Title of presentation: *Sicurezza strutturale in caso di incendio*.
September 2010	*The Fourth International Conference on Structural Engineering, Mechanics and Computation* (SEMC 2010), Cape Town, South Africa, 6-8 September 2010. Title of presentation: *Performance based investigations of structural system under fire.*
July 2010	Workshop *Handling Exceptions in Structural Engineering: Sistemi Strutturali, Scenari Accidentali, Complessità di Progetto*, Sapienza University of Rome, Rome, Italy, 8 – 9 July 2010. Title of presentation: *Numerical simulation for fire safety in industrial hall.*
June 2010	Corso di formazione Progettazione di strutture in acciaio in accordo alle vigenti normative nazionali ed europee, Milano, 30 June 2010. Title of presentation: *Sicurezza strutturale in caso di incendio.*

ANNEX 4: MSC THESES CO-ADVISOR

1. Gigante Giuseppe, A.Y. 2011/2012, Title: *Gli effetti del travelling fire nell'analisi strutturale in caso di incendio*, advisor Prof. F. Bontempi (in English: *The effects of travelling fire in the structural analysis in case of fire*), on-going, Master of Science of the Safety Engineering Education, Sapienza University of Rome.
2. Romanelli Maddalena, A.Y. 2011/2012, Title: A*nalisi degli effetti della temperatura su elementi in cemento armato e cemento armato precompresso*, advisor Prof. F. Bontempi (in English: *Analysis of temperature effects on elements in reinforced concrete and prestressed concrete)*, Master of Science of the Civil Engineering Education, Sapienza University of Rome.
3. Monti Adriano, A.Y. 2011/2012, Title: *Valutazione dell'influenza del danno sismico sulla resistenza al fuoco di strutture intelaiate in acciaio*, advisor Prof. F. Bontempi (in English: *Assessment of the influence of seismic damage on the fire resistance of steel framed structures)*, Master of Science of the Civil Engineering Education, Sapienza University of Rome.
4. Lucci Maurizio, A.Y. 2011/2012, Title: *Modellazione della risposta al fuoco di strutture in acciaio*, advisor Prof. F. Bontempi, co-advisor Dr. L. Giuliani (DTU) (in English: *Modelling of the structural response of steel structures under fire*), Master of Science of the Civil Engineering Education, Sapienza University of Rome.
5. Carli Stefano, A.Y. 2010/2011, Title: *Analisi comportamentale all'incendio di un edificio industriale con struttura in acciaio*, advisor Prof. F. Bontempi (in English: *The fire structural analysis of an industrial hall in steel)*, Master of Science of the Safety Engineering Education, Sapienza University of Rome.
6. Tomaselli Stefano, A.Y. 2010/2011, Title: *Analisi comportamentale all'incendio di un edificio industriale in cemento armato,* advisor Prof. F. Bontempi (in English: *The fire structural analysis of an industrial hall in concrete)*, Master of Science of the Safety Engineering Education, Sapienza University of Rome.
7. Brigante Biagio, A.Y. 2010/2011, Title: *Modellazione fluidodinamica di una galleria stradale ai fini della valutazione della sollecitazione strutturale dovuta all'incendio,* advisor Prof. L. Grossi (in English: *Fluid dynamics modelling of a road tunnel for the evaluation of structural stress due to fire)*, Master of Science of the Safety Engineering Education, Sapienza University of Rome.
8. Brigante Nicola, A.Y. 2010/2011, Title: *Analisi di una galleria stradale: aspetti strutturali correlati alla sollecitazione di incendio,* advisor Prof. F. Bontempi (in English: *Analysis of a road tunnel: structural aspects related to the stress of fire)*, Master of Science of the Safety Engineering Education, Sapienza University of Rome.
9. Marsicola Tommaso, A.Y. 2010/2011, Title: *Influenza del comportamento umano sotto stress nei confronti dell'utilizzo delle vie di esodo*, advisor Prof. F. Bontempi (in English: *Influence of human behaviour under stress with respect to the use of escape routes)*, Master of Science of the Safety Engineering Education, Sapienza University of Rome.
10. Salciccia Roberto, A.Y. 2010/2011, Title: *Scenari d'incendio nelle gallerie stradali. Analisi delle condizioni termo fisiche,* advisor Prof. L. Grossi (in English: *Fire scenarios in road tunnels. Analysis of thermo physical conditions)*, Master of Science of the Safety Engineering Education, Sapienza University of Rome.
11. Di Maria Sebastiano, A.Y. 2010/2011, Title: *Scenari d'incendio nelle gallerie stradali. Analisi strutturale*, advisor Prof. L. Grossi (in English: *Fire scenarios in road tunnels. Structural analysis)*, Master of Science of the Safety Engineering Education, Sapienza University of Rome.
12. Pisaneschi Ernesto, A.Y. 2010/2011, Title: *Scenari di incendio in galleria. Panorama normativo. Gestione e sviluppo dei software CFD*, advisor Prof. L. Grossi (in English: *Fire scenarios in road tunnels. Regulatory landscape. Management and development of CFD software)*, Master of Science of the Safety Engineering Education, Sapienza University of Rome.